THE UNIVERSITY OF WARWICK

# Library Declaration and Deposit Agreement

## 1. STUDENT DETAILS

*Please complete the following:*

Full name: ……

University ID number: ……

## 2. THESIS DEPOSIT

2.1 I understand that under my registration at the University, I am required to deposit my thesis with the University in BOTH hard copy and in digital format. The digital version should normally be saved as a single pdf file.

2.2 The hard copy will be housed in the University Library. The digital version will be deposited in the University's Institutional Repository (WRAP). Unless otherwise indicated (see 2.3 below) this will be made openly accessible on the Internet and will be supplied to the British Library to be made available online via its Electronic Theses Online Service (EThOS) service.
[At present, theses submitted for a Master's degree by Research (MA, MSc, LLM, MS or MMedSci) are not being deposited in WRAP and not being made available via EthOS. This may change in future.]

2.3 In exceptional circumstances, the Chair of the Board of Graduate Studies may grant permission for an embargo to be placed on public access to the hard copy thesis for a limited period. It is also possible to apply separately for an embargo on the digital version. (Further information is available in the *Guide to Examinations for Higher Degrees by Research*.)

2.4 *If you are depositing a thesis for a Master's degree by Research, please complete section (a) below. For all other research degrees, please complete both sections (a) and (b) below:*

(a) Hard Copy

I hereby deposit a hard copy of my thesis in the University Library to be made publicly available to readers (please delete as appropriate) EITHER immediately OR after an embargo period of ……..... months/years as agreed by the Chair of the Board of Graduate Studies.

I agree that my thesis may be photocopied. YES / NO (*Please delete as appropriate*)

(b) Digital Copy

I hereby deposit a digital copy of my thesis to be held in WRAP and made available via EThOS.

Please choose one of the following options:

EITHER My thesis can be made publicly available online. YES / NO (*Please delete as appropriate*)

OR My thesis can be made publicly available only after…..[date] (Please give date)
YES / NO (*Please delete as appropriate*)

OR My full thesis cannot be made publicly available online but I am submitting a separately identified additional, abridged version that can be made available online.
YES / NO (*Please delete as appropriate*)

OR My thesis cannot be made publicly available online. YES / NO (*Please delete as appropriate*)

## 3. GRANTING OF NON-EXCLUSIVE RIGHTS

Whether I deposit my Work personally or through an assistant or other agent, I agree to the following:

Rights granted to the University of Warwick and the British Library and the user of the thesis through this agreement are non-exclusive. I retain all rights in the thesis in its present version or future versions. I agree that the institutional repository administrators and the British Library or their agents may, without changing content, digitise and migrate the thesis to any medium or format for the purpose of future preservation and accessibility.

## 4. DECLARATIONS

(a) I DECLARE THAT:

- I am the author and owner of the copyright in the thesis and/or I have the authority of the authors and owners of the copyright in the thesis to make this agreement. Reproduction of any part of this thesis for teaching or in academic or other forms of publication is subject to the normal limitations on the use of copyrighted materials and to the proper and full acknowledgement of its source.

- The digital version of the thesis I am supplying is the same version as the final, hard-bound copy submitted in completion of my degree, once any minor corrections have been completed.

- I have exercised reasonable care to ensure that the thesis is original, and does not to the best of my knowledge break any UK law or other Intellectual Property Right, or contain any confidential material.

- I understand that, through the medium of the Internet, files will be available to automated agents, and may be searched and copied by, for example, text mining and plagiarism detection software.

(b) IF I HAVE AGREED (in Section 2 above) TO MAKE MY THESIS PUBLICLY AVAILABLE DIGITALLY, I ALSO DECLARE THAT:

- I grant the University of Warwick and the British Library a licence to make available on the Internet the thesis in digitised format through the Institutional Repository and through the British Library via the EThOS service.

- If my thesis does include any substantial subsidiary material owned by third-party copyright holders, I have sought and obtained permission to include it in any version of my thesis available in digital format and that this permission encompasses the rights that I have granted to the University of Warwick and to the British Library.

## 5. LEGAL INFRINGEMENTS

I understand that neither the University of Warwick nor the British Library have any obligation to take legal action on behalf of myself, or other rights holders, in the event of infringement of intellectual property rights, breach of contract or of any other right, in the thesis.

---

*Please sign this agreement and return it to the Graduate School Office when you submit your thesis.*

Student's signature: .....…… Date: .....

# Interaction of Translocase MraY with the Antibacterial E Protein from Bacteriophage ΦX174

**Maria Teresa Rodolis**

Thesis submitted in partial fulfillment of the requirements for the degree of Doctor of Philosophy in Chemistry

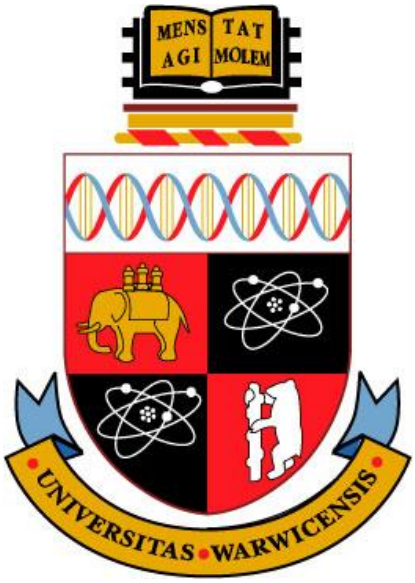


**University of Warwick**
**Department of Chemistry**

**September 2013**

# Contents

# Abbreviations

| | |
|---|---|
| °C | degrees Celcius |
| aa | Amino acid |
| $Ac_2O$ | Acetic anhydride |
| Ala | Alanine |
| Arg | Arginine |
| *B. subtilis* | *Bacillus subtilis* |
| Boc | *t*-butyloxycarbonyl |
| BSA | Bovine Serum Albumin |
| Bu | Butyl |
| $C_{35}$-P | Heptaprenyl phosphate |
| $C_{55}$-P | Undecaprenyl phosphate |
| $C_{55}$-P | Undecaprenyl pyrophosphate |
| Ca | Calcium |
| CFU | Colony forming units |
| $CHCl_3$ | Chloroform |
| COOH | Carboxyl |
| DIC | *N*,*N*´-diisopropylcarbodiimide |
| DCC | *N*,*N*´-dicyclohexylcarbodiimide |
| DCM | Dichloromethane |
| DIPEA | *N*,*N*´-Diisopropylethylamine |
| DMF | Dimethylformamide |
| DMAP | 4-dimethylamino pyridine |
| DMSO | Dimethyl Sulphoxide |
| DTT | Dithiothreitol |
| *E. coli* | *Escherichia coli* |
| EA | Activation Energy |
| ECL | Electrochemiluminescence |
| EDCI | 1-ethyl-3-(3-dimethylamino-propyl)carbodiimide |
| EDT | Ethanedithiol |
| EDTA | Ethylenediaminetetraacetic acid |
| ESBL | Extended spectrum β-lactamases |
| ESI-MS | ElectroSpray Ionisation Mass Spectroscopy |
| $Et_2O$ | Diethyl ether |
| EtOAc | Ethyl acetate |
| Fmoc | Fluorenylmethyloxycarbonyl |

| | |
|---|---|
| GlcNAc | *N*-acetylglucosamine |
| Gln | Glutamine |
| Glu | Glutamic acid |
| Gly | Glycine |
| GT | Glycosyltransferases |
| HATU | 2-(7-Aza-1*H*-benzotriazole-1-yl)-1,1,3,3-tetramethyluronium Hexafluorophosphate) |
| HEPES | 4-(2-hydroxyethyl)-1-piperazineethanesulfonic acid |
| Hex | Hexane |
| His | Histidine |
| HOBt | 1-hydroxybenzotriazole |
| HPLC | High-Performance Liquid Chromatography |
| HRMS | High Resolution Mass Spectrometry |
| HRP | Horse Radish Peroxidase |
| Ile | Isoleucine |
| IPTG | Isopropyl β-D-1-thiogalactopyranoside |
| LB | Luria Broth |
| Lys | Lysine |
| K | Kelvin |
| $IC_{50}$ | Half maximal inhibitory concentration |
| Lac | Lactate |
| Leu | Leucine |
| Lipid I | $C_{55}$-PP-MurNAc-pentapeptide |
| LPS | Lipopolysaccharide |
| *m/z* | Mass to charge ratio |
| *m*-DAP | *meso*-diaminopimelic acid |
| *m*-Tyr | *meta*-Tyrosine |
| MDR | Multidrug Resistant Bacteria |
| MeOH | Methanol |
| Met | Methionine |
| MIC | Minimal Inhibitory Concentration |
| *M. flavus* | *Micrococcus flavus* |
| MM | Master mix |
| MraY | Phoshpo-MurNAc-pentapeptide translocase, translocase I |
| mRNA | Messenger Ribonucleic acid |
| MRSA | Methicillin resistant *S. aureus* |
| MurNAc | N-acetylmuramic acid |

| | |
|---|---|
| MurG | Undecaprenyldiphospho-muramoylpentapeptide beta-N-Acetylglucosaminyltransferase |
| $N^{\varepsilon}$-Dns | 5-(dimethylamino)naphthalene-1-sulfonyl |
| NMM | *N*-Methylmorpholine |
| NMR | Nuclear Magnetic Resonance |
| NOESY | Nuclear Overhauser Effect Spectroscopy |
| NPN | 1-*N*-phenylnaphthylamine |
| OD | Optical density |
| *P. aeruginosa* | *Pseudomonas aeruginosa* |
| *P. putida* | *Pseudomonas putida* |
| PBP | Penicillin binding proteins |
| Phe | Phenylalanine |
| PMC | 2,2,5,7,8-pentamethyl-chroman-6-sulphonyl |
| Pro | Proline |
| PyBOP | Benzotriazol-1-yl-oxytripyrrolidinophosphonium hexafluorophosphate |
| *S. aureus* | *Staphylococcus aureus* |
| SACA | Stacked arrangement of carboxylates over aromatics |
| Ser | Serine |
| SlyD | Sensitive to lysis D |
| $S_N^1$ | Unimolecular nucleophilic substitution |
| $S_N^2$ | Bimolecular nucleophilic substitution |
| SPPS | Solid phase peptide synthesis |
| tBu | *t*-Butyl |
| TEA | Triethylamine |
| TES | Triethylsilane |
| TFA | Trifluoroacetic acid |
| THF | Tetrahydrofuran |
| TIPS | Triisopropylsilyl |
| TLC | Thin Layer Chromatography |
| TLR | Toll-Like Receptors |
| TMS-Cl | Trimethylsilyl chloride |
| TP | Transpeptidases |
| Trityl | Tripheylmethyl |
| tRNA | Transfer Ribonucleic acid |
| Trp | Tryptophan |
| Trt | Tripheylmethyl |
| TFA | Trifluoroacetic Acid |

| | |
|---|---|
| Tyr | Tyrosine |
| UDP | Uridine diphosphate |
| UMP | Uridine monophosphate |
| UPA | Uridyl peptide antibiotics |
| UppP | Undecaprenyl pyrophosphatase |
| UppS | Undecaprenyl pyrophosphate synthase |
| UV | Ultraviolet |
| Val | Valine |
| VRE | Vancomycin Resistant Enterococci |
| WT | Wild-type |

# List of Figures

# List of Tables

# Declaration

The experimental work reported in this thesis is original research carried out by the author, unless otherwise stated, in the Department of Chemistry, University of Warwick, between October 2010 and September 2013. No material contained herein has been submitted for any other degree, or at any other institution.

Results from other authors are referenced in the usual manner throughout the text.

_____ Date: _____

Maria Teresa Rodolis

# Acknowledgments

Firstly, I would like to thank my supervisor Professor Timothy D.H. Bugg for his help in all aspects of research and team building. Special thanks to Agnes Mihalyi for all her hard work optimising the continuous fluorescence assay and the radiochemical assay. In addition, I'd like to thank MOAC project student Amy O'Reilly for construction of the MraY mutant plasmids and MChem student Justinas Slikas for his assistance in the synthesis of pentapeptides.

I'm extremely grateful to Dr. Dhar who encouraged me to pursue a career in chemistry and for being an absolutely brilliant life mentor. You've impacted my life in ways you could never imagine. You are without a doubt my biggest inspiration. I'd like to thank Dr. Stacie Nunes, Reena Depaolo and the entire $AC^2$ family for their endless support and guidance throughout my academic career. I would also like to thank NSF GRFP for funding my PhD research project.

I would like to thank all members of the Bugg research group for all their support and entertainment in the laboratory. I would also like to thank the Challis group for the many helpful discussions regarding chemistry. Many thanks to the NMR, Mass spectroscopy and QuBic research technicians for their assistance in my research project.

I would also like to thank the Salsa dancing society for giving me a fantastic outlet to express myself and unwind. Thanks for reconnecting me with my Latina roots and allowing me to develop such fruitful friendships.

Finally, I would like to thank all my family and friends for their support. Jason for your understanding, patience and love over the years. Kerri, Baker, Ging and Gia for being my rock. I love you all dearly.

# Abstract

The widespread use of antibiotics has played a significant role in the emergence of resistant bacteria. It is of great interest and need to develop novel, effective and safe antimicrobial therapeutics. The biosynthesis of bacterial cell wall peptidoglycan is an intricate process that has become a popular target for antibiotics. Lytic protein E of Bacteriophage ΦX174 was found to inhibit peptidoglycan biosynthesis via an unknown interaction with integral protein MraY. Genetic studies have revealed that E-mediated lysis is dependent on the interaction between Phe288 of MraY and the transmembrane segment of protein E.

We have constructed an α-helical model for the predicted transmembrane interactions between protein E and MraY and shown that favourable interactions can be formed between Phe288 and the RWXXW motif of protein E. In this thesis, analogues of the RWXXW motif were synthesised in solution and via solid phase peptide synthesis using 2-chlorotrityl chloride resin as the polymeric support. The inhibitory activity of these analogues was determined on a continuous fluorescence assay against membrane bound MraY. Inhibition studies on site-directed mutants of *E. coli* MraY were also conducted. Testing the inhibitory activity of RWXXW analogues provided compelling information on the importance of protein E residues for the inhibition of MraY. Peptides which contained a tryptophan residue were especially good inhibitors of MraY presumably due to their interaction with Phe288. Mutation of Phe288 caused a dramatic decrease or complete loss to the inhibitory activity of peptides containing an aromatic residue.

Some analogues also contained antibacterial activity across multiple strains of bacteria including *E. coli*, *B. subtilis* and *P. putida* with MIC values as low as 8μg/mL. To confirm if MraY was the target enzyme, *E. coli* cells overexpressing MraY were treated with RWXXW analogues. An increase in the MIC of RWXXW analogues signified that the MraY was the lysis target.

In the course of the project, we noticed that members of the UPA class of natural products contained some structural features that are also found in the RWXXW motif. These natural products were tested for activity against site-directed mutants of *E. coli* MraY. Results showed that Phe288 plays some role in the inhibition of MraY by pacidamycin. This work identifies a promising target for the development of novel antimicrobial agents that is located on the outer face of the cytoplasmic membrane.

# Chapter 1: Introduction

The application of antibiotics into human medicine has had an enormous effect on the treatment of infectious diseases, the advances in medical procedures and the evolution of cells. Prior to Alexander Fleming's discovery of Penicillin in 1928, simple wounds and infections were left untreated, often leading to death[1]. At the time of his discovery, bacterial infections such as tuberculosis, pneumonia, enteritis and nephritis plagued the lives of over 388,790 people in the United States[2]. Bacterial infections remained one of the top leading causes of death in the United States until the 1950's when penicillin was mass produced, increasing the life expectancy to 68 years[3]. The mass production and affordability of antibiotics had a tremendous impact on the success of invasive medical procedures such as surgery and chemotherapy[4], however, with the discovery, affordability and success of such powerful drugs looms overconsumption, dependence and abuse.

Antibiotics are often administered as default measures for treatment of minor and/or irrelevant illnesses. Some infections such as bronchitis will resolve on its own with sleep, plentiful fluids, aspirin and deep inhalations in 1-2 weeks without leaving any permanent damage[5]. Even so, many bronchitis patients are misprescribed antibiotics to ease the suffering and shorten the length of illness. Such over consumption and generalized use of any drug will inevitably result in antibiotic resistance.

## 1.1 Resistance

After multiple exposures to the same class of antibiotics, bacteria have developed an extraordinary ability to recognize, export and even modify antibiotic compounds. Resistant genes usually arise by random genetic mutation, which can produce a new resistance trait or strengthen an existing one. These resistant genes are then readily spread to neighbouring bacteria through horizontal gene transfer such as conjugation, transformation and transduction[6].

To ward off destruction, resistant genes can eliminate cellular entry ports, code for efflux pumps that eject antibiotics out of the cell or code for enzymes that degrade or chemically alter the antibiotics or the target so that it is resistant to the antibiotic (Figure 1.1)[7]. In addition to these methods, bacteria also produce enzymes which correct the damages done by antibiotics.

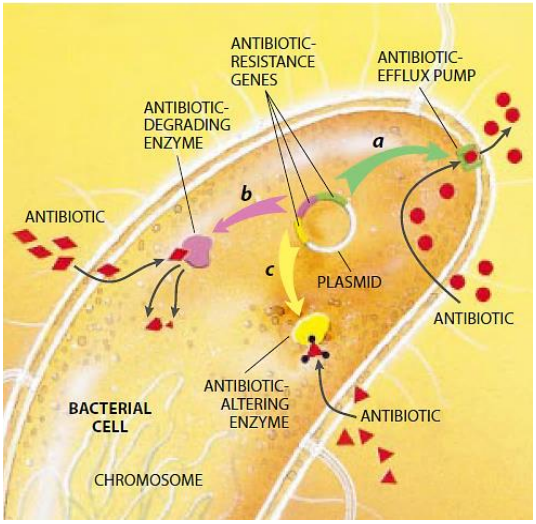


**Figure 1.1: Bacterial resistance to antibiotics[7].** The production of (a) Efflux pumps (b) Degrading enzymes and (c) Chemically altering enzymes are various modes of resistance.

The first example of resistance to an antibiotic was observed in the early 1940's, 12 years after the discovery of penicillin, when an increase in the MIC for *S. aureus* was observed[8]. Within 20 years, over 80% of *S. aureus* clinical isolates were resistant to

penicillin[9]. This resistance evolved from the production of penicillinase, a group 2 β-lactamase[10] capable of hydrolysing penicillin at the β-lactam ring[11,12] (Figure 1.2).

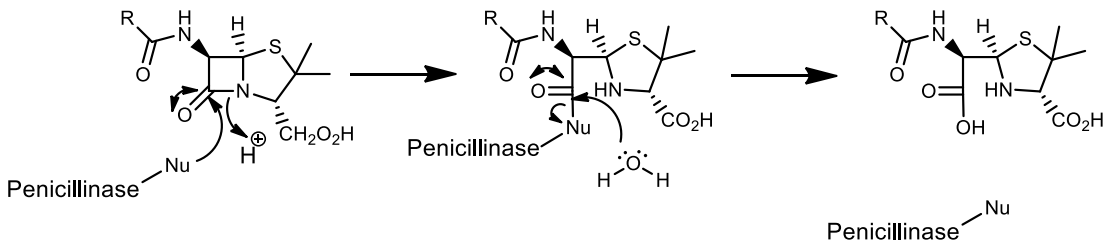


**Figure 1.2: Penicillinase activity in β-lactam ring opening**

To counter act the activity of β-lactamases, a new class of penicillin antibiotics was introduced; the antistaphylococcal penicillins. This class evolved from the treatment of penicillin with penicillin acylase which removed the natural phenyl acetyl group, followed by chemical acylation which attached various bulky side chains. These bulky side chains function to sterically hinder the antistaphylococcal penicillin molecules from β-lactamases[13]. This group of penicillins include methicillin, oxacillin, nafcillin, cloxacillin and dicloxacillin[14]. In 1961, British scientist Patricia M. Jevons isolated the first strain of methicillin resistant *S. aureus* bacteria, MRSA[15]. Resistance to methicillin was reported to be mediated by the expression of *secA* which codes for a novel penicillin-binding protein (PBP2´) with low binding affinity for β-lactam antibiotics such as penicillin, amoxicillin, oxacillin, methicillin, and others[16-17]. In 1968 the first human case of MRSA was reported in Boston, Massachusetts, United States[18]. By 2002, CDC reported that 2.3 million persons were infected with MRSA in the United States[19].

For the treatment of severe MRSA, natural product vancomycin is typically used. Vancomycin is a haloorganic glycopeptide antibiotic made by the soil bacterium Actinobacteria *Amycolatopsis orientalis* (Figure 1.3).

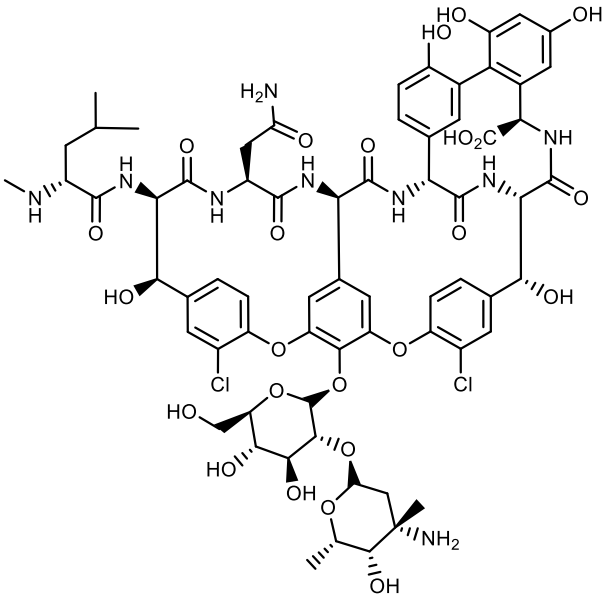

**Figure 1.3: Structure of Vancomycin**

Vancomycin was an effective and powerful antibiotic against *S. aureus* and *Pseudomembranous enterocolitis* for nearly 40 years before the evolution of resistance[20]. Vancomycin forms hydrogen bonds with the D-Ala-D-Ala motif of peptidoglycan intermediates, preventing crosslinking and ultimately the formation of peptidoglycan (Figure 1.4). Vancomycin Resistant Enterococci (VRE) were first reported in the United States and Europe in 1987[21].

Currently, seven resistance patterns have been reported (VanA-VanG), however less is known about VanD, Vane E and VanG type resistance[21]. The mechanism of resistance is best understood for the *vanA* cluster of genes. In this mechanism, Vancomycin acts as an inducer, activating transcription of the *vanA* cluser[21]. Translation of these genes produces a 38kDa membrane associated protein VanA. VanA was found to have sequence similarity to the D-Ala-D-Ala ligases responsible for the synthesis of the D-Ala-D-Ala dipeptide in the assembly of peptidoglycan[22-23] (Chapter 1.3). However, VanA was found to have modified substrate specificity in comparison to the Gram-negative D-Ala-D-Ala ligases. VanA is able to synthesise

various peptide and depsipeptide products including D-Ala-D-Lac, D-Ala-D-Met, and D-Ala-D-Phe in preference to D-Ala-D-Ala[24]. These alternative dipeptides can still be incorporated into peptidoglycan but cannot be recognized by vancomycin due to a missing hydrogen bond (Figure 1.4)[22,25]. As a result, crosslinking can still proceed.

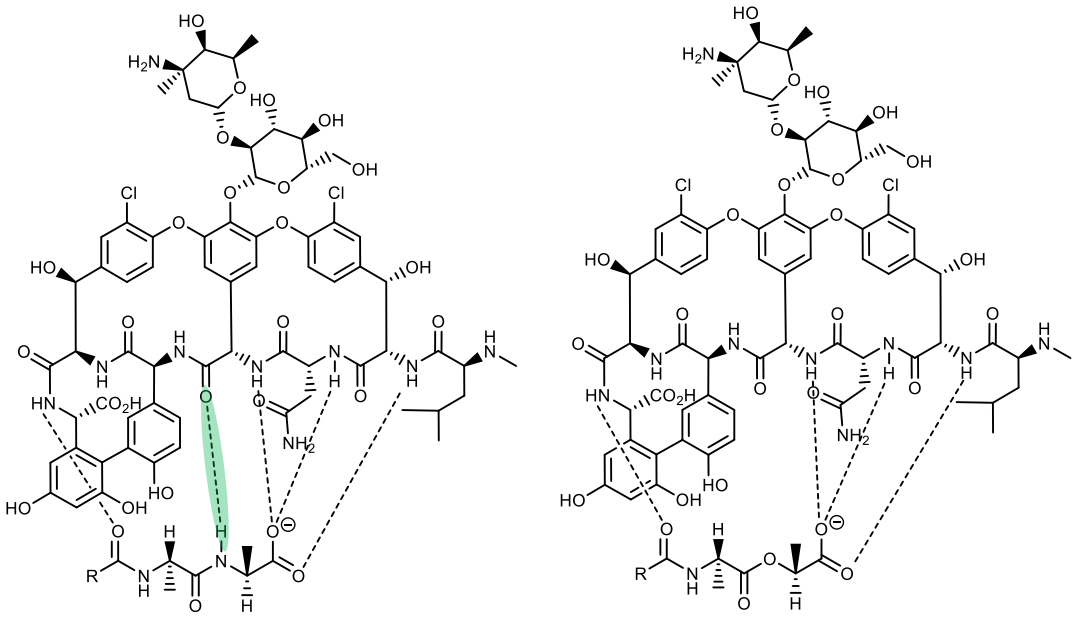

**Figure 1.4: Structures of the Vancomycin complexes with D-Ala-D-Ala (left) and D-Ala-D-Lac (right)[25].** Vancomycin is unable to recognise the D-Ala-D-Lac due to a missing hydrogen bond. As a result polymerisation of peptidoglycan proceeds.

VRE has become a serious concern to the scientific community given that only a limited amount of antibiotics are effective in treating this infection. The greatest concern about VRE is its potential to spread to other pathogens such as *S. aureus* or even Gram-negative bacteria[24].

Several Gram-negative bacteria have already acquired various forms of resistance. *E. coli*, *K. pneumoniae*, *P. aeruginosa*, and *A. baumannii* are opportunistic pathogens which are typically only dangerous to persons with comprised immune systems. However, recently these pathogens have evolved resistance *to* β-lactam antibiotics via the production of plasmid-mediated extended spectrum β-lactamases (ESBL)[26-27]. ESBL leads to resistance of third generation cephalosporins (e.g, cefotaxime,

ceftriaxone, ceftazidime) and monobactams (e.g. aztreonam)[28]. The evolution of multiple mechanisms of resistance including efflux pumps, impermeability and enzymatic inactivation have generated multidrug resistant bacteria (MDR) such as *Pseudomonas aeruginosa* MDR and *Klebsiella pneumoniae* MDR[29].

Resistance to commercially available antibiotics has increased so drastically that it is now considered an epidemic. Therefore, there is an urgent need for the development of new, effective and safe antimicrobial therapeutics that can target these increasingly dangerous Gram-negative and Gram-positive bacteria.

## 1.2 Antimicrobial Peptides

Over the past 40 years there have only been three new classes of antibiotics developed; lipopeptides, oxazolidinones and streptogramins which are all geared for the treatment of Gram positive bacteria[30]. The lipopeptide, daptomycin is a cyclic 13-member amino acid polypeptide with a decanoyl side-chain (Figure 1.5). It is proposed that in the presence of $Ca^{2+}$, daptomycin oligomerizes on the cytoplasmic membrane creating a channel that excretes important intracellular ions[31].

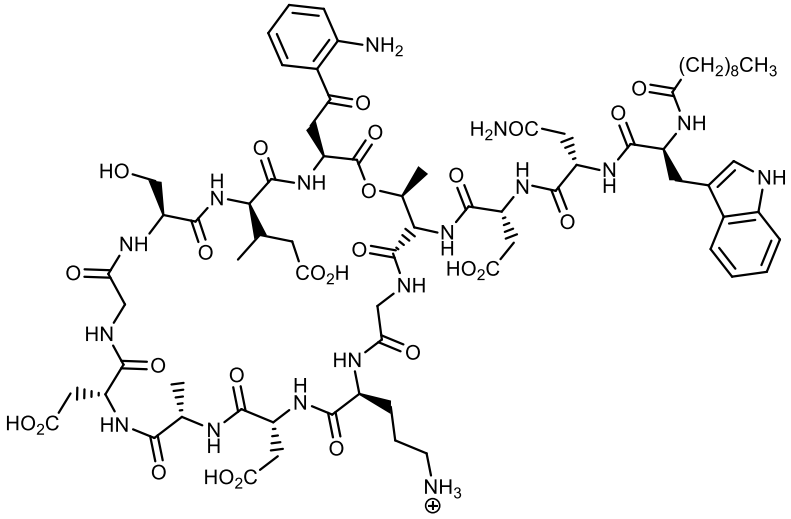

**Figure 1.5: Structure of Daptomycin**

The oxazolidinone class (Figure 1.6) of antibiotics work by inhibiting protein synthesis. The exact mechanism of action remains unknown. However, research has shown that it does not inhibit formation of initiator tRNA or block peptide elongation. Instead it has been proposed to be involved in the binding of mRNA to the 30S ribosomal subunit[32].

The streptogramins class are natural products produced by *Streptomyces pristinaespiralis* and *Streptomyces virginiae* (Figure 1.6). Streptogramins bind to the P-site of the ribosome effectively blocking protein translation[33].

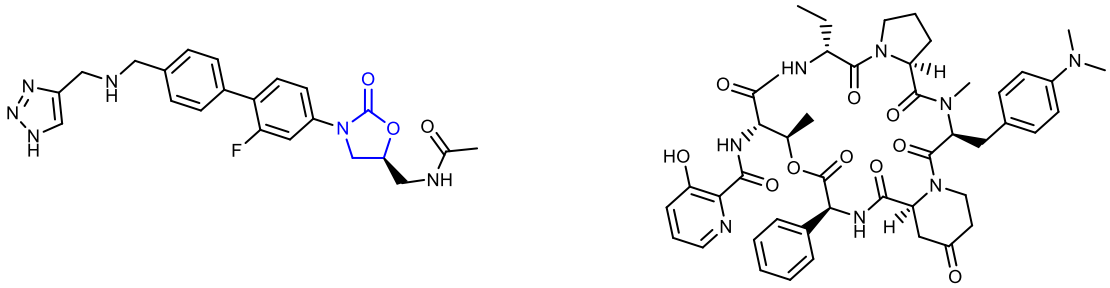

**Figure 1.6: Structure of the oxazolidinone Radezolid (left) and Streptogramin B (right)**

The effectiveness of streptogramins and oxazolidinones has been compromised by resistance. Conversely, the lipopeptide daptomycin has experienced <0.2% resistance *in vitro* and in Phase II and III clinical trials[31]. The success and near absence of resistance to lipopeptides has sparked the scientific community with great interest in the development of novel antimicrobial peptides.

There are many advantages of peptides over conventional antibiotics. While most antibiotics target Gram-positive bacteria, antimicrobial peptides are effective against both Gram-negative and Gram-positive bacteria. Some peptides have even been found to have activity against protozoa, including trypanosomes, malaria, and nematodes[4].

Antimicrobial peptides have very diverse potential application. They can be used as a single antimicrobial, synergistically with other antibiotics or as an immunomodulator.

Without directly acting on the bacteria, peptides are capable of encouraging the host's natural defences to fight off the infection. For instance, synthetic peptide IMX00C1 was found to have no antimicrobial activity *in vitro* (MIC ≥128 μg/ml), however when injected in an *in vivo* infection model the bacterial load was significantly reduced[34].

Another immunomodulatory property of antimicrobial peptides is their ability to neutralize sepsis and endotoxemia, which is a common and dangerous complication in systematic antibacterial drug administration[30]. Sepsis is antagonized by the overstimulation of the innate immunity which occurs when bacterial signature molecules (for example, lipopolysaccharide) bind to Toll-Like Receptors (TLRs)[35]. To avoid sepsis, peptides moderate the TLR signalling response to a proactive level. Its ability to moderate immunity responses while simultaneously promoting angiogenesis and wound healing responses is quite impressive.

The most notable advantage of peptides over conventional antibiotics is its invulnerability to bacterial resistance. It takes 30 passages of *P. aeruginosa* in a sub-MIC peptide to increase its resistance by two- to four-fold. Under the same conditions, resistance to the aminoglycoside gentamicin increases by 190-fold[30]. The lack of diversity in the sequence and in the targets of conventional antibiotics renders it susceptible to resistance. Conventional antibiotics target a specific enzyme or function of the cell. Peptides, on the other hand, have multiple targets and consequently multiple modes of causing cell lysis. For resistance to emerge, modifications would be necessary at every site of action of the peptide. Furthermore, as peptides are made of naturally occurring compounds, antimicrobial peptides can easily assimilate with other essential peptides. As a result, a resistance mechanism such as proteolysis could mistakenly target essential peptides, leading to cell death.

Even if an elegant mode of resistance were to evolve, the peptides attempt to enter the cell may still cause cell lyses (i.e. insertion via carpet model).

## 1.3 Entrance into the bacterial cell

An enormous amount of work has been invested in determining the mechanism of action of cationic peptides. The first obstacle peptides encounter is entrance into the bacterial cell. For a peptide to successfully enter the cell it must be stable, contain 50% hydrophobic residues in order to insert into the membrane, and capable of adopting an amphipathic secondary structure[36]. The first site of interaction occurs at the outer membrane or the cellular envelope.

To cross the outer membrane of a Gram-negative bacteria, cationic peptides interact with the negatively charged glycolipid lipopolysaccharide (LPS) surface, displacing the magnesium ions which normally neutralize them[4]. This electrostatic interaction distorts the outer membrane, allowing the peptides to insert and migrate across the bilayer. Hancock (1997) termed this interaction as "self-promoted uptake" (Figure 1.7). This interaction is believed to be energetically favourable, as the binding affinity of LPS for a typical peptide is three times stronger than that for a divalent cation.[37]

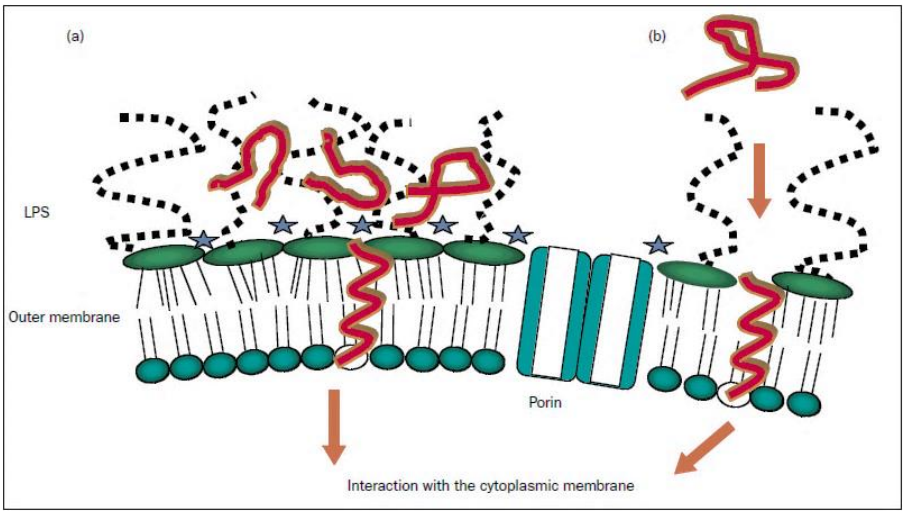


**Figure 1.7:Self-promoted uptake of cationic peptides[4].** Electrostatic interaction between cationic peptides and LPS can create a gap in the membrane which peptides can use to cross the bilayer.

The initial interaction between cationic peptides and Gram-positive bacteria is very similar even in the absence of an outer membrane or LPS. The cellular envelope is rich in negatively charged teichoic and teichuronic acids. The basic residues of cationic peptides are able to form an electrostatic interaction with these acids, then enter the cell via self-promoted uptake[37].

There is much controversy over the fate of antimicrobial peptides after crossing the outer membrane barrier. Once it traverses the outer membrane or cellular envelope, the peptide enters a second stage of membrane interaction referred to as the threshold concentration[37]. The threshold concentration is heavily influenced by the peptide's concentration and its ability to multimerise. The composition, fluidity and size of the phospholipid heads groups in the cytoplasmic membrane are also very important[38]. These factors facilitate different modes of insertion into the cytoplasmic membrane. Three distinct methods have been proposed.

### *1.3.1 The Barrel-Stave Mechanism*

In this model, peptides are positioned in a barrel-like ring structure to form an aqueous pore. Initially, peptide binding at the membrane surface occurs. This forces the polar phospholipid head groups to dislocate[37]. The thinned membrane is then permeated by α-helical peptides that assemble in a barrel-like ring structure. In this assembly, hydrophilic residues face the centre of the pore and hydrophobic residues face the outside of the pore. The hydrophobic interactions between the nonpolar residues of the cationic peptides and the nonpolar tail of phospholipids stabilise the assembly[39] (Figure 1.8). For the barrel-stave model, an even distribution of hydrophobic and hydrophilic residues in cationic peptides is critical to the threshold

concentration. In addition, membrane fluidity and low protein composition is favourable.

Fungal peptide antibiotic Alamethicin utilises the barrel-stave mechanism to cross the membrane. This was confirmed by oriented dichroism, neutron scattering and synchrotron-based X-ray scattering[40]. The open alamethicin transmembrane pore can contain 3-11 parallel helical molecules with a diameter of up to ~40nm[41].

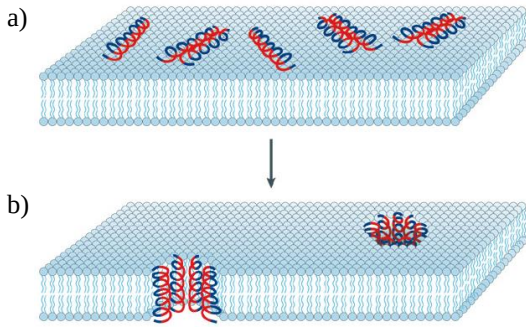


**Figure 1.8: Barrel-Stave Mechanism**[39] a) Cationic peptides bind to the phospholipid head groups causing the head groups to dislocate b) α-helical peptides permeate the thinned membrane and assemble a barrel-like ring structure with hydrophobic residues (blue) facing the phospholipidis and hydrophilic residues (red) facing the centre of the pore.

### *1.3.2 The Toroidal pore*

In this model, lipids are intercalated with antimicrobial peptides to form a disordered pore. Initially, cationic peptides are oriented parallel to the cytoplasmic membrane as it binds to the polar head groups of phospholipids[37]. After having aggregated, one or two peptides begin to embed deeper into the interface causing large deviations from planarity in the phospholipids[42]. The pore begins to form when the most deeply embedded peptide connects with the other interface forming a water pore. The water pore is relaxed into a toroidal shape as peptides and lipid molecules move across the membrane (Figure 1.9). To assist this model, the peptides must be amphiphatic.

In 2012, Bertelsen *et al* used $^{13}P$ oriented solid-state NMR to investigate the interaction between antimicrobial peptide Novicidin and lipids. At high peptide concentrations, it was found that Novicidin forms toroidal pores with substantial perturbation to the lipid bilayer[43].

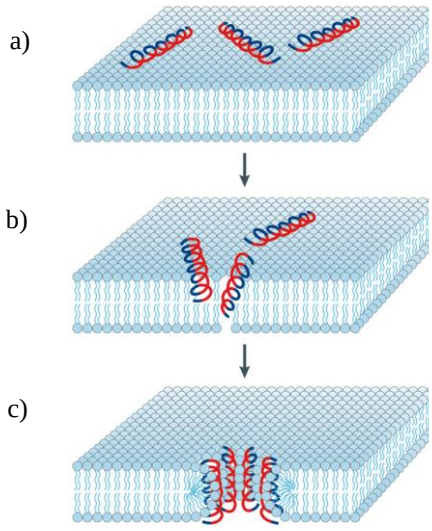


**Figure 1.9: A schematic of magainin pores in a lipid bilayer crystallized into a regular hexagonal lattice[38].** a) Cationic peptide orient parallel to the phospholipids and bind to the polar head groups b) peptides start to embed deeper into the interface causing great deviation from planarity c) a water toroidal pore is formed when cationic peptides reach the cytoplasmic side of the membrane.

### *1.3.3 The Carpet Model*

In this model, antimicrobial peptides cause a catastrophic break down of membrane integrity[4]. This process is initiated by the formation of an extensive layer or carpet of high density peptides on the membrane surface (Figure 1.10). When the threshold concentration is exceeded, the peptides disrupt the bilayer in a detergent-like-manner forming toroidal transient holes[44]. At such critical threshold concentrations, the membrane is subjected to unfavourable energetics causing it to disintegrate and form micelles[37].

There is much debate over whether pore formation is the killing mechanism of antimicrobial peptides. Before the collapse of the membrane, the formation of

transient holes may enable the passage of peptides or other small molecules into the cell[45]. It is plausible that inhibition of an intracellular target by these peptides or small molecules proceeds and influences membrane disintegration.

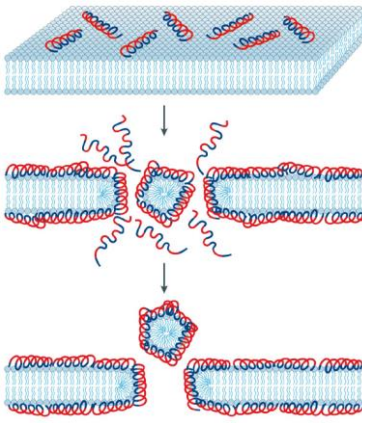

**Figure 1.10: The carpet model of antimicrobial-induced killing [44].** High concentration of cationic peptides on the membrane surface disrupts the cytoplasmic membrane in a detergent-like manner.

For some peptides that are known to act on intracellular targets such as Indolicidin, Histatin-5 and Pyrrhocoricin[46], crossing the membrane is only the first of many obstacles; peptides still have the challenge of finding their intracellular targets while simultaneously avoiding degradation by proteases[35]. To overcome these additional barriers, the dosage may have to be altered in order to make sure a sufficient quantity of peptides reach its target and infection can cease. Though sensible, this may lead to a toxicity problem, which poses a greater dilemma as peptide-mediated toxicity is not well understood[30]. This problem could be entirely avoided if the peptides' target was in the intramembrane region. For such peptides, only insertion into the cytoplasmic membrane will be necessary. Once inserted, the peptides can interact with its membrane bound targets. Fortunately there are many vital membrane-bound enzymes that, if targeted, can lead to bacterial cell death. Among these enzymes include MraY

and MurG which catalyze two membrane-bound steps in the biosynthesis of peptidoglycan.

## 1.4 Peptidoglycan

Peptidoglycan or murein is an important bacterial heteropolymer that protects the cell against the lethal effects of internal osmotic pressure. Peptidoglycan is also responsible for preserving the characteristic shape of the cell and is intimately involved in the process of cell division[47]. This cellular protective coat is composed of long glycan chains made up of alternating units of N-acetylmuramoyl-peptides (MurNAc-peptides) and N-acetylglucosamine (GlcNAc) connected by a β-(1,4)-glycosidic bond and further cross-linked through peptide chains[48] (Figure 1.11).

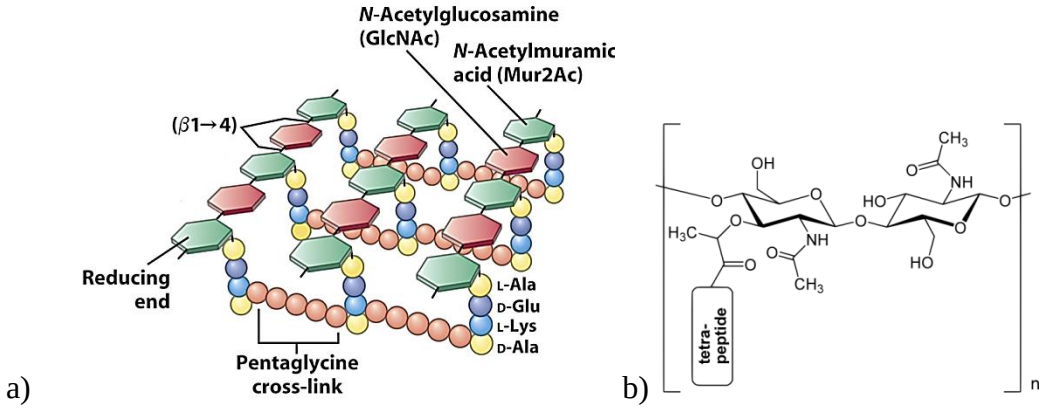


**Figure 1.11: a) Simplified schematic of peptidoglycan in gram positive bacteria b) β-(1,4) linked N-Acetylmuramoyl-peptide and N-Acetylglucosamine-peptide**

Peptidoglycan biosynthesis is highly conserved in bacteria, making it an excellent target for the development of broad spectrum antibiotics[49]. The biosynthesis of peptidoglycan can be divided into three stages[50]: (I) cytoplasmic biosynthesis of substrates, (II) formation of monomeric building blocks and (III) polymerisation (Figure 1.12).

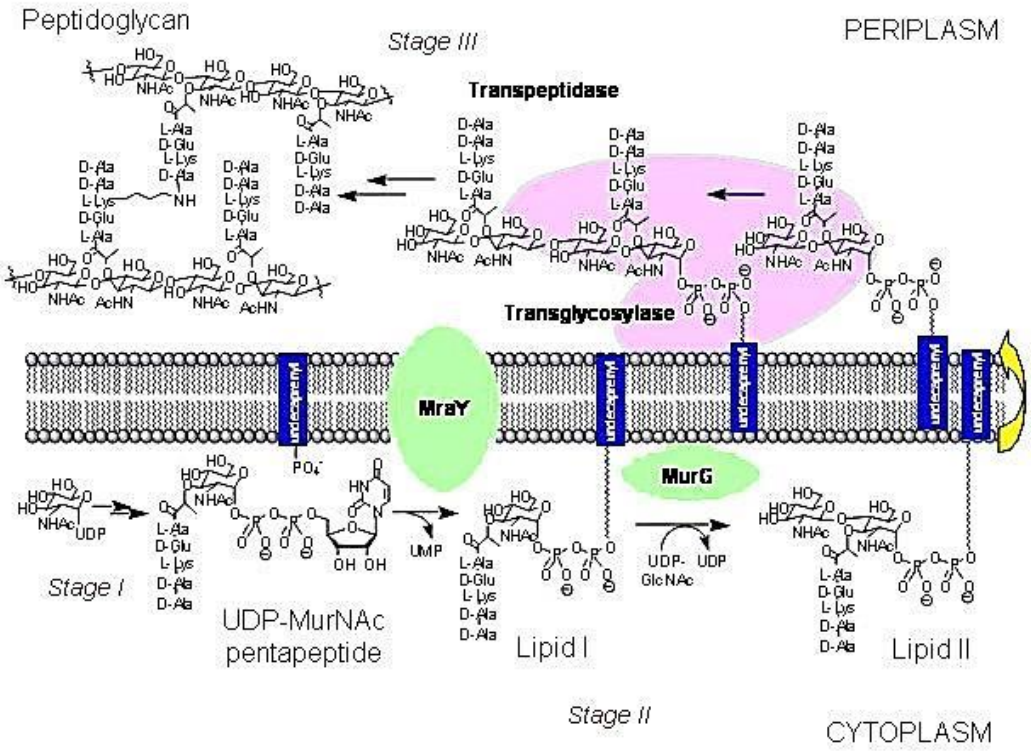


**Figure 1.12: Peptidoglycan biosynthesis**[51]**.** Stage I corresponds to the formation of lipid carrier undecaprenyl phosphate and MraY substrate UDP-MurNAc-pentapeptide. In stage II, MraY and MurG catalyse the formation of monomeric building blocks. Stage III occurs at the periplasm and involves the polymerisation of peptidoglycan monomers by Penicillin Binding Proteins.

### *1.4.1 Cytoplasmic Biosynthesis of Peptidoglycan Substrates*

The biosynthesis of peptidoglycan begins in the cytosol or near the cytosolic face of the plasma membrane where a series of enzymes catalyse the synthesis of Undecaprenyl phosphate and UDP-MurNAc-pentapeptide[48,52,53,54].

Undecaprenyl phosphate ($C_{55}$-P) is a 55 carbon isoprenoid (Figure 1.13). It is the only known lipid carrier in bacteria that facilitates the translocation of hydrophilic intermediates across the hydrophobic cellular bilayer[55].

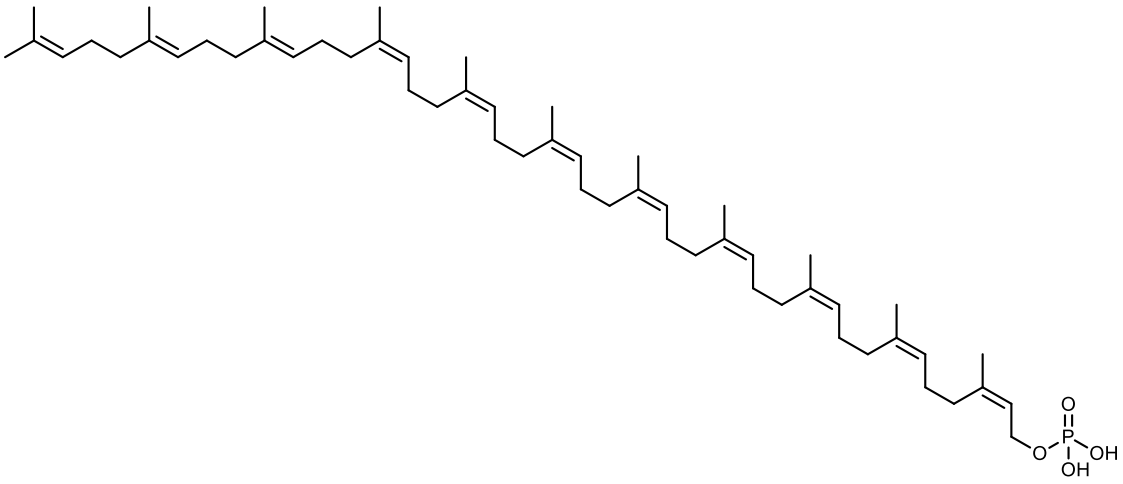


**Figure 1.13: Structure of $C_{55}$-P**

Undecaprenyl pyrophosphate ($C_{55}$-PP) is synthesized by cytoplasmic enzyme undecaprenyl pyrophosphate synthase (UppS)[56]. UppS catalyzes the addition of eight ($C_5$) isopentenyl pyrophosphate units onto a ($C_{15}$) farnesyl pyrophosphate unit forming new *cis* double bonds[57]. The product $C_{55}$-PP is delivered to the cytoplasmic membrane where undecaprenyl pyrophosphatase (UppP) dephosphorylates it producing $C_{55}$-P[52,58].

Natural product bacitracin (Figure 1.14) from *Bacillus subtilis* has been found to bind to $C_{55}$-PP in the presence of a divalent metal ion[59]. This in turn prevents the substrate from interacting with UppP leading to the arrest of bacterial peptidoglycan biosynthesis and ultimately cell death[60]. Overconsumption of bacitracin has inevitably led to resistance and contributed greatly to the emergence of MRSA strain ST8:USA300[61-62].

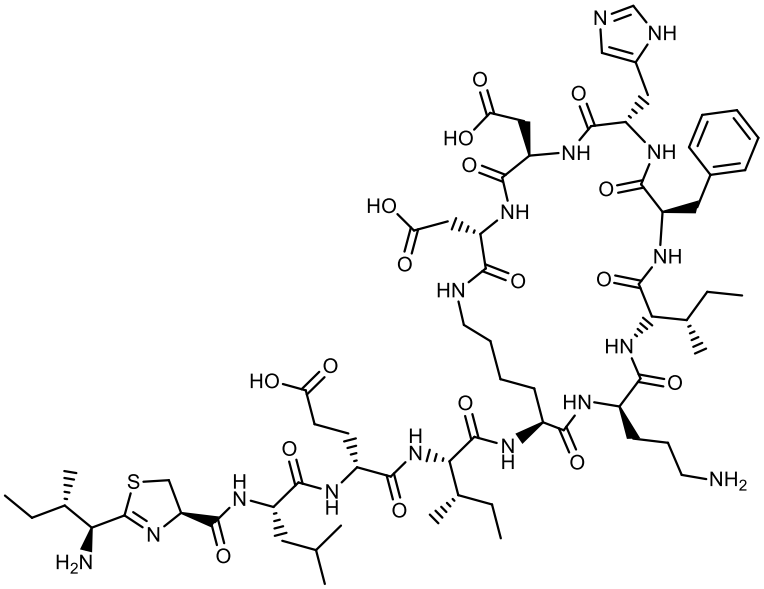

**Figure 1.14: Structure of Bacitracin**

The synthesis of UDP-MurNAc-pentapeptide is catalysed by a series of Mur enzymes. MurA to MurF are essential and highly conserved proteins in bacteria[63](Figure 1.15). The first committed step in the pathway is catalysed by enolpyruvyl transferase MurA. MurA transfers an enolypyruvate moiety from phosphoenolpyruvate (PEP) to C-3 UDP-N-acetylglucosamine[64] forming UDP-N-acetylglucosamine 3-enolpyruvyl ether (UDP-GlcNAc-EP)[65].

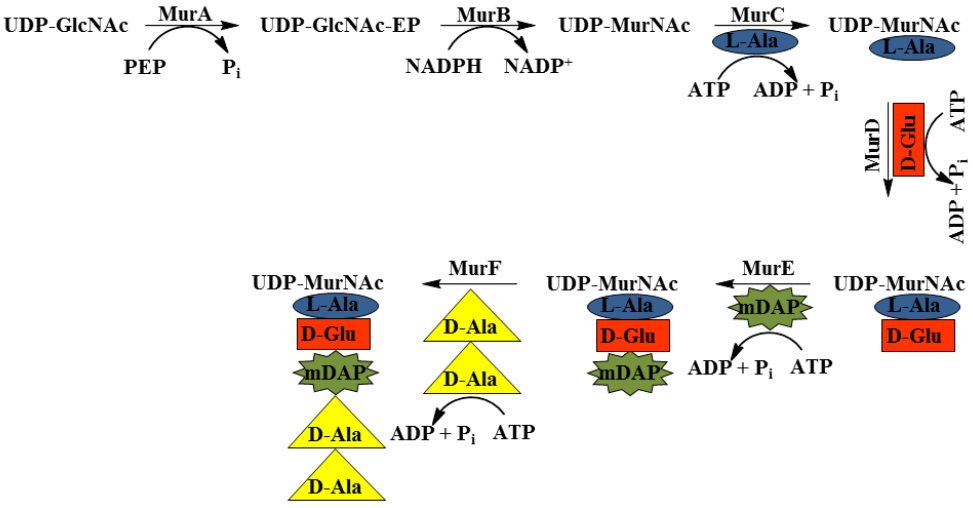


**Figure 1.15: The biosynthesis UDP-MurNAc-pentapeptide.** MurA catalyses the transfer of an enolpyruvyl unit onto UDP-GlcNAc. MurB reduces the enolpyruvyl unit producing UDP-MurNAc. MurC-MurF ligases attach five amino acids to the lactyl side chain of UDP-MurNAc.

MurA is the target of natural product fosfomycin (Figure 1.16). Fosfomycin irreversibly alkylates active site Cys115 preventing the acid/base catalysis necessary for the formation of UDP-GlcNAc-EP[66-67].

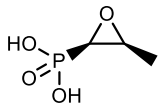


**Figure 1.16: Structure of Fosfomycin**

Following MurA, MurB catalyses the reduction of the enolpyruvate moiety of UDP-GlcNAc-EP to D-lactate, producing UDP-N-acetylmuramate (UDP-MurNAc)[54,63].

The addition of the pentapeptide moiety to UDP-MurNAc is performed by ATP-dependent ligases MurC, MurD, MurE and MurF[47]. These ligases are responsible for the consecutive additions of L-alanine, D-glutamic acid, *meso*-diaminopimelic acid (*m*-DAP) or L-lysine and D-alanyl-D-alanine to the lactyl side chain of UDP-MurNAc[68]. The final product, UDP-MurNAc-pentapeptide (Figure 1.17), is then delivered to the membrane where stage II of peptidoglycan biosynthesis commences.

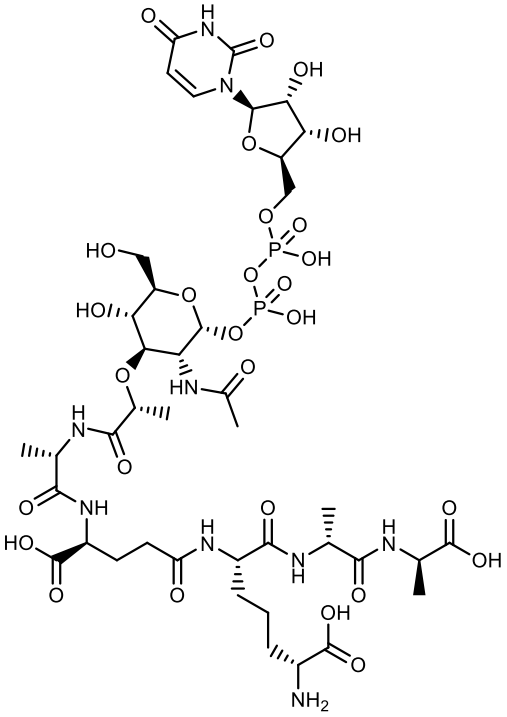

**Figure 1.17: Structure of UDP-MurNAc pentapeptide**

### *1.4.2 Biosynthesis of monomeric building blocks*

The biosynthesis of monomer GlcNAc-β-(1,4)-MurNAc-pentapeptide is catalysed by membrane bound proteins MraY and MurG[48,69-70].

Phospho-MurNac-pentapeptide translocase (MraY) couples UDP-MurNAc-pentapeptide to $C_{55}$-P to give undecaprenyl diphospho-MurNAc-pentapeptide (Lipid I) and uridine 5'-monophosphate (UMP)[69,71]. Attachment to the $C_{55}$-P lipid carrier is crucial as it facilitates transfer of the monomer to the periplasmic side of the membrane at a later stage[55].

MraY is the target of various of antibiotics including tunicamycin, mureidomycin A, amphomycin, pacidamycin, muraymycin and liposidomycin B[69,72-73]. Tunicamycin and amphomycin are unsuitable as novel drugs as they have mammalian toxicity due to preferential inhibition of the mammalian dolichyl phosphate pathway[74]. MraY will be discussed in further detail later (Chapter 1.4).

The addition of *N*-acetylglucosamine (GlcNAc) to the lipid I intermediate is catalysed by glycosyltransferase MurG[48-49]. MurG transfers a GlcNAc moiety from UDP-GlcNAc to the C4 MurNAc hydroxyl group of lipid I yielding lipid II, GlcNAc-β-(1,4)-undecaprenyl-pyrophosphoryl-MurNAc-pentapeptide (Figure 1.18), and uridine diphosphate (UDP)[75].

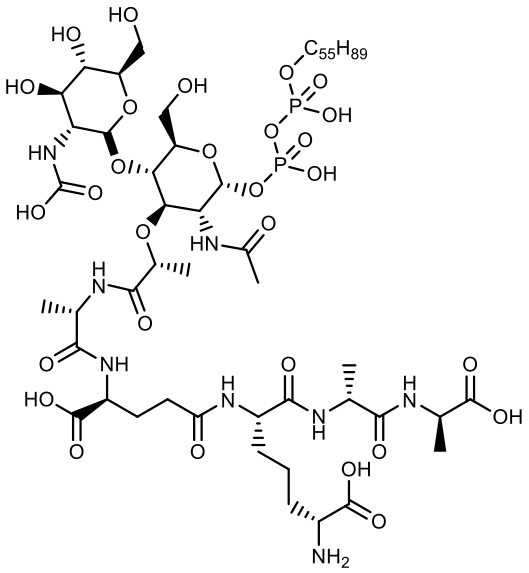


**Figure 1.18: Structure of Lipid II, GlcNAc-β-(1,4)-undecaprenyl-pyrophosphoryl-MurNAc-pentapeptide**

Lipid II is then transferred across the hydrophobic membrane to the periplasm, where Penicillin Binding Proteins (PBPs) polymerise lipid II to form the peptidoglycan layer[48]. The exact mechanism of transfer across the membrane is believed to catalysed by a putative flippase enzyme[47,64,74]. In 2011, Mohammadi *et al* provided the first biomedical evidence supporting Matsuhashi's (1994) and Höltje's (1998) hypothesis that FtsW, an essential division protein of the SEDS family (shape, elongation, division and sporulation), is a transporter of lipid II[76,77,78].

### *1.4.3 Polymerisation*

The final stage of peptidoglycan biosynthesis involves polymerisation of lipid II monomer units and the binding of that polymer to the cell wall. Polymerisation involves the formation of glycan chains and peptide cross-links, which are catalysed by glycosyltransferases (GT) and transpeptidases (TP), respectively[48]. GT and TP enzymes may be present as bifunctional proteins such as Penicillin Binding Protein 2 (PBP2) (Figure 1.19) or as monofunctional proteins[79].

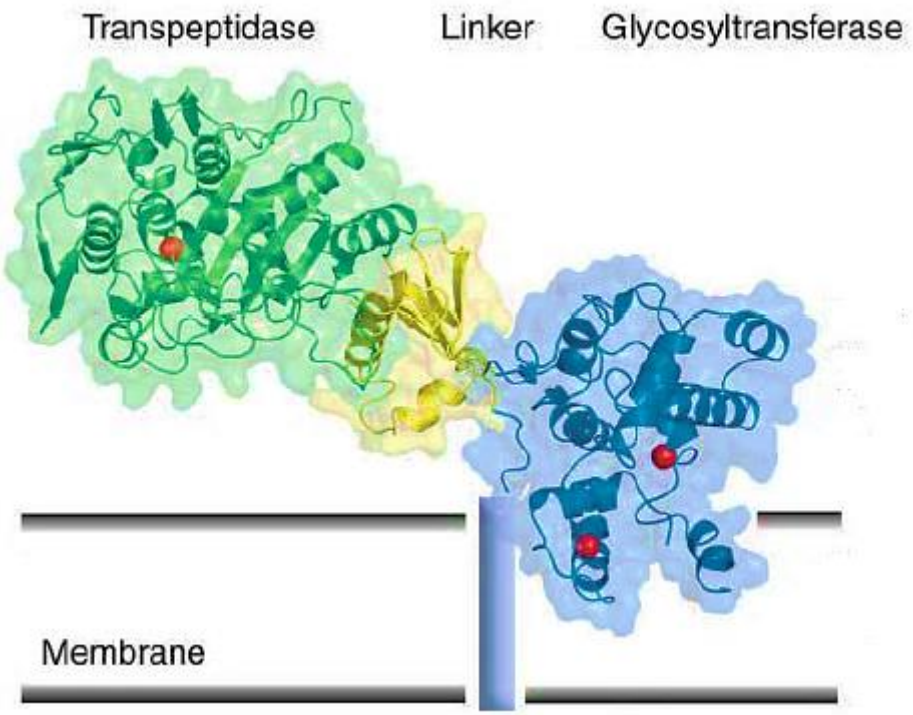


**Figure 1.19: Overall structure of PBP2 (PDB code 2OLU)[79]**

The condensation of glycan chains occurs at the active site of GT enzymes. Lovering *et al* (2007) proposed that active site residue E114 acts as a base and deprotonates the C-4 hydroxyl group of the acceptor lipid II, which concurrently attacks C-1 of the donor lipid II molecule in an $S_N^2$ manner (Figure 1.20)[79]. This produces a β-(1,4) linkage between the adjacent lipid II monomers and releases $C_{55}$-PP. This process

repeats as additional monomers are flipped to the periplasm. The released $C_{55}$-PP can then be recycled and used in stage I of peptidoglycan biosynthesis (Chapter 1.4.1). Alternatively, it is possible for the transglycosylation reaction to proceed in an $S_N1$ manner. The hemiacetal oxygen can stabilise the anomeric carbon facilitating the removal of the good leaving group, undecaprenyl pyrophosphate. The C-4 hydroxyl of the acceptor group could then attack the C-1 of the donor lipid II molecule to form the β-(1,4) linkage.

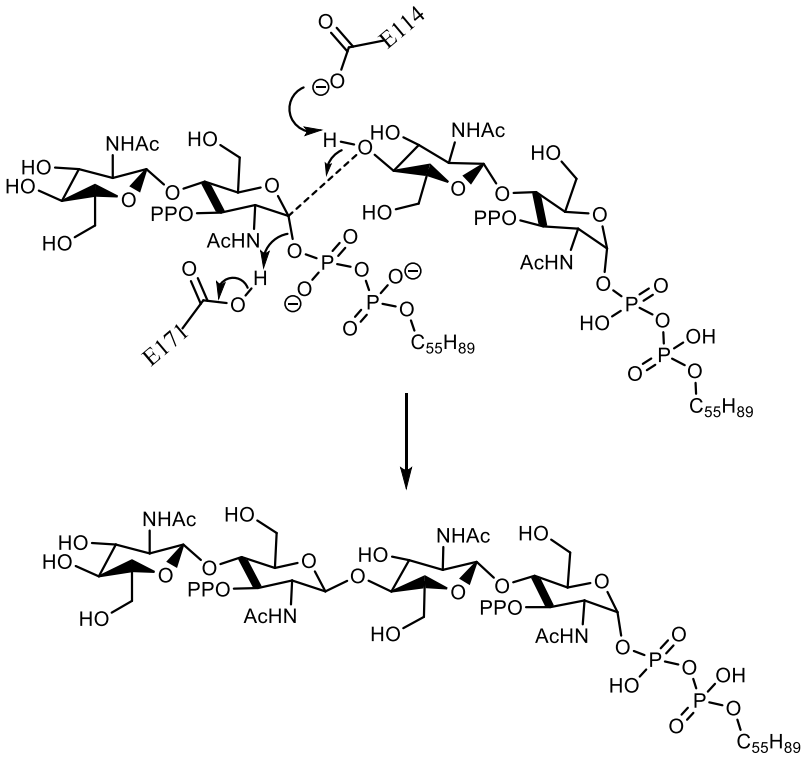


**Figure 1.20: Lovering *et al* proposed an $S_N2$ mechanism for the transglycosylation of lipid II.** In this scheme PPO is used in place of the lactyl-pentapeptide. Active site residue E114 acts as a base and deprotonates the C-4 hydroxyl group of the acceptor lipid II, which concurrently attacks C-1 of the donor lipid II producing a β-(1,4) linkage.

The natural product moenomycin is a potent antibiotic that directly inhibits peptidoglycan glyosyltransferase. Though potent, (MIC values ranging from 1ng/mL to 100ng/mL)[80], the suboptimal pharmacokinetic properties of this natural product prevents development as a novel drug[81].

Transpeptidation is the ultimate enzymatic reaction in the biosynthesis of peptidoglycan. TP enzymes cross-link neighbouring monomers via its pentapeptide chain providing strength and rigidity to the overall structure of peptidoglycan.

Cross linking is species-specific and is the most variable component of peptidoglycan[82]. In most Gram-negative bacteria the cross link is between an *m*-DAP and the D-Ala at position 4 of the neighbouring pentapeptide chain[83]. In *E. coli*, an *m*-DAP-*m*-DAP cross link can also be formed from the linkage of two *m*-DAP residues[84]. In Gram-positive bacteria, neighbouring pentapeptide chains are cross-linked via a peptide bridge containing 1-5 glycine residues[83]. These varying cross linkages are illustrated in Figure 1.21.

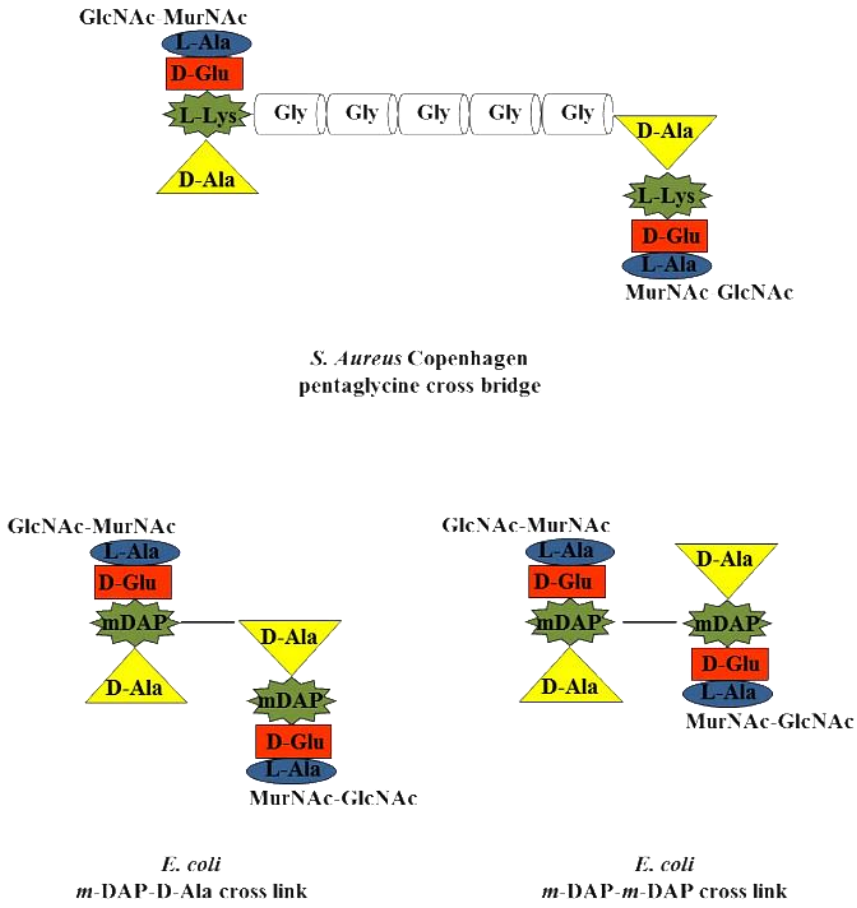


**Figure 1.21: Peptidoglycan cross links.** Gram-positive bacteria, neighbouring pentapeptide chains are cross-linked via a peptide bridge containing 1-5 glycine residues. In Gram-negative bacteria the cross link can be formed from two *m*-DAP residues or between *m*-DAP and D-Ala.

The transpeptidation reaction has been extensively studied in PBPs. PBPs utilize an active site serine residue to nucleophilically attack the carbonyl of D-Ala at position 4 which results in the cleavage of D-Ala at position 5 and yields an enzyme-substrate complex[85]. This enzyme-substrate complex enhances the electrophilicity of D-Ala and promotes a nucleophilic attack by the *m*-DAP or L-Lys of the neighbouring pentapeptide chain (Figure 1.22).

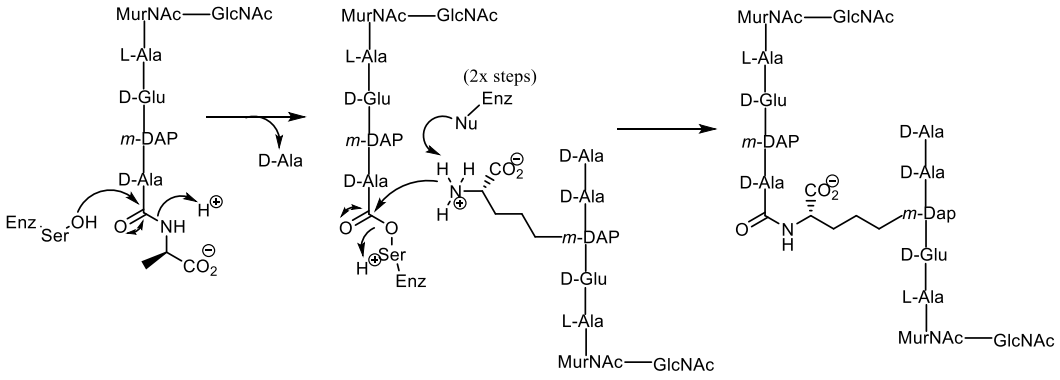


**Figure 1.22: Transpeptidation reaction for Gram-negative bacteria**

The transpeptidation reaction of peptidoglycan biosynthesis is the target of β-lactam antibiotics which include penicillin, cephalosporin and other related compounds. β-lactam antibiotics are structural analogues of the D-Ala-D-Ala linkage which competes and binds to PBPs preventing transpeptidation[86]. Several forms of resistance to β-lactam antibiotics have evolved. Bacteria can produce altered versions of PBPs which have a reduced affinity for β-lactam drugs (e.g. PBP2′ in MRSA), and are therefore able to crosslink peptidoglycan[16-17,87]. Bacteria can also produce β-lactamases, enzymes which hydrolyse the β-lactam ring effectively deactivating the antibiotic[88]. Production of β-lactamase has become more prevalent in Gram-negative bacteria.

The majority of antibiotics target the cytoplasmic and periplasmic reactions of peptidoglycan biosynthesis (Figure 1.16)[54]. This project will aim to identify a novel

antibacterial target for the membrane bounds steps of peptidoglycan biosynthesis, specifically MraY.

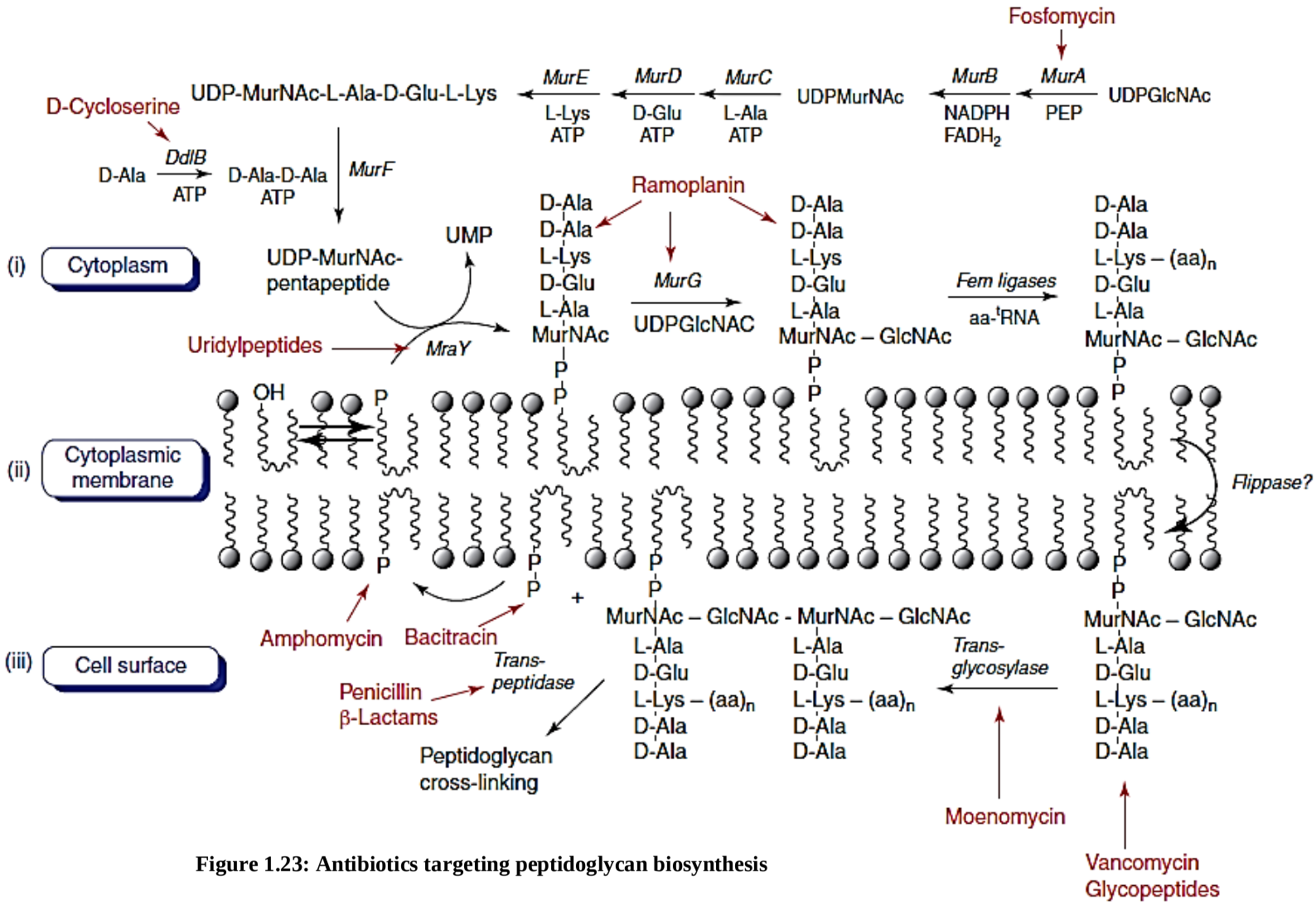


**Figure 1.23: Antibiotics targeting peptidoglycan biosynthesis**

## 1.5 MraY

Phospho-MurNAc-pentapeptide translocase (MraY) is essential for bacterial life, and at least one copy of the *mraY* gene is found in every bacteria[89]. This 40kDa protein is so important, that in its absence the cell cannot grow or reproduce, leading to swelling and ultimately cell lysis[53]. Its strong impact on viability (confirmed in *E. coli* and *Streptococcus pneumonia*)[90] and its accessibility from the periplasm makes this protein a very promising antimicrobial target.

The primary structure of MraY is composed of alternating hydrophobic and hydrophilic segments which suggests that MraY is an integral membrane protein that spans the cytoplasmic membrane several times[91]. Furthermore, Weppner and Neuhaus (1979) showed that a lipid microenvironment was required for the catalytic activity of MraY[92].

The secondary protein structure of *E. coli* and *S. aureus* MraY was predicted using β-lactamase fusion experiments[93], which revealed a common topological model consisting of ten transmembrane helices with four periplasmic loops and five cytoplasmic sequences[94]. In this model, the cytoplasmic and periplasmic loops correspond to the hydrophilic segments of the primary protein structure while the transmembrane helices correspond to the hydrophobic segments, as expected[47]. This model was confirmed in August 2013 by Chung and colleagues whom solved the crystal structure of MraY from thermophile *Aquifex aeolicus* (Figure 1.24).

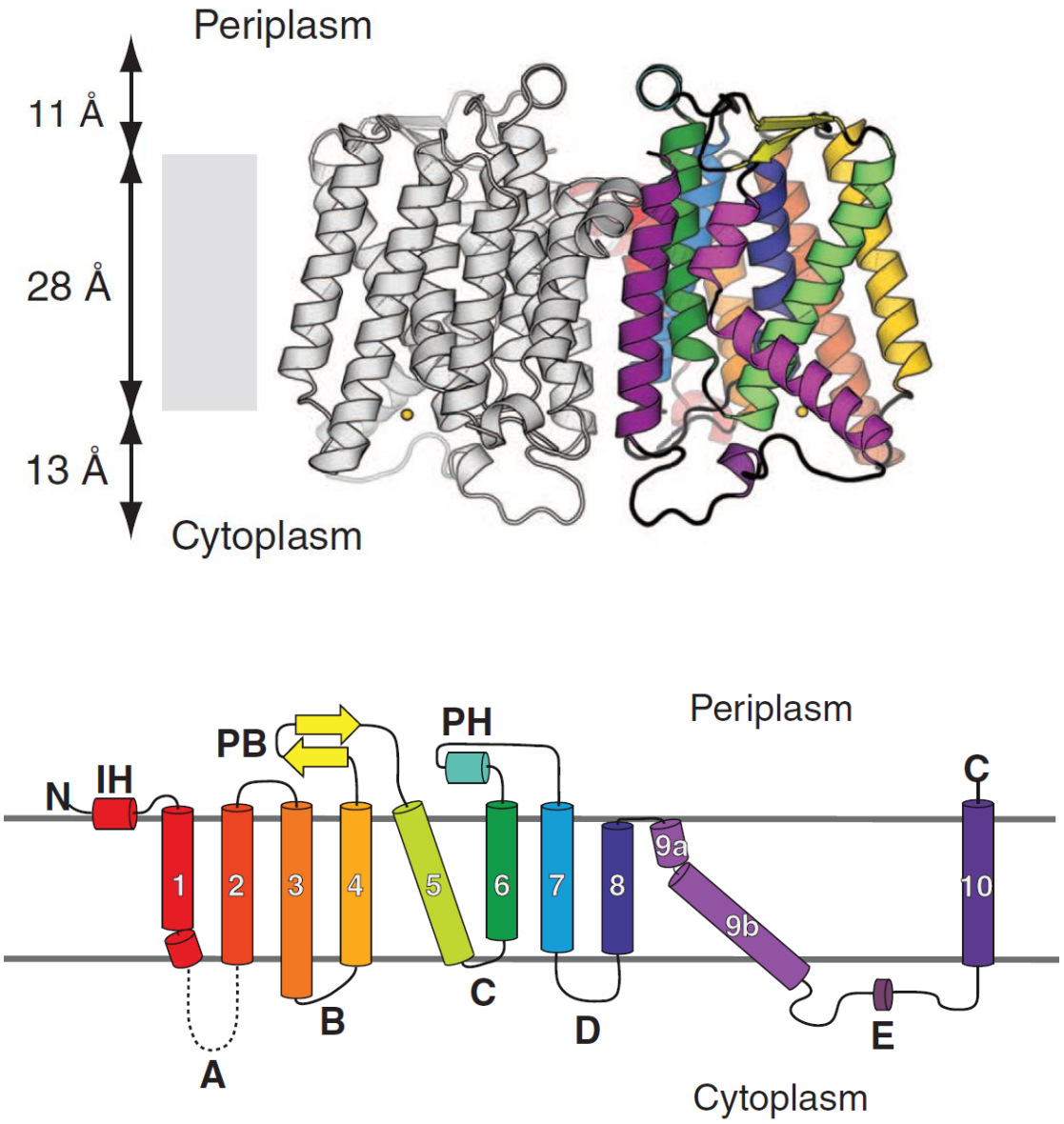


**Figure 1.24: Crystal structure of *A. aeolicus* MraY[95].** a) View from within the membrane. Each protomer contains 10 transmembrane helices, an interfacial helix (IH), a periplasmic β-hairpin (PB), a periplasmic helix (PH), and five cytoplasmic loops (loop A to loop E) The yellow sphere is $Mg^{2+}$. The overall dimensions of the dimer are about 72 x 55 x 52 Å. b) Topology diagram of MraY illustrating the individual helixes and loops.

MraY is a member of the polyprenyl-phosphate *N*-acetylhexosamine 1-phosphate transferase superfamily[96]. Sequence homology has been found at the predicted cytoplasmic loops of MraY, WecA, WbcO and RgpG[96]. Nineteen polar residues appeared as invariant in the sequences of these MraY orthologues, some of which are also conserved in the whole superfamily[97]. Conserved aspartic acid residues 115, 116 and 267 were found to be essential for activity in *E. coli* MraY[47,71]. Chung *et al*

reported that in addition to these aspartic acid residues, invariant histidine residues located at position 324, 325 and 326 in *A. aeolicus*, are also crucial for enzyme activity. The crystal structure of *A. aeolicus* MraY revealed that these conserved residues are located in a cleft formed by the cytoplasmic and inner-leaflet membrane regions of TM3, TM4, TM8, and TM9b. The composition and location of these conserved residues suggest that this region is the active site of MraY[95].

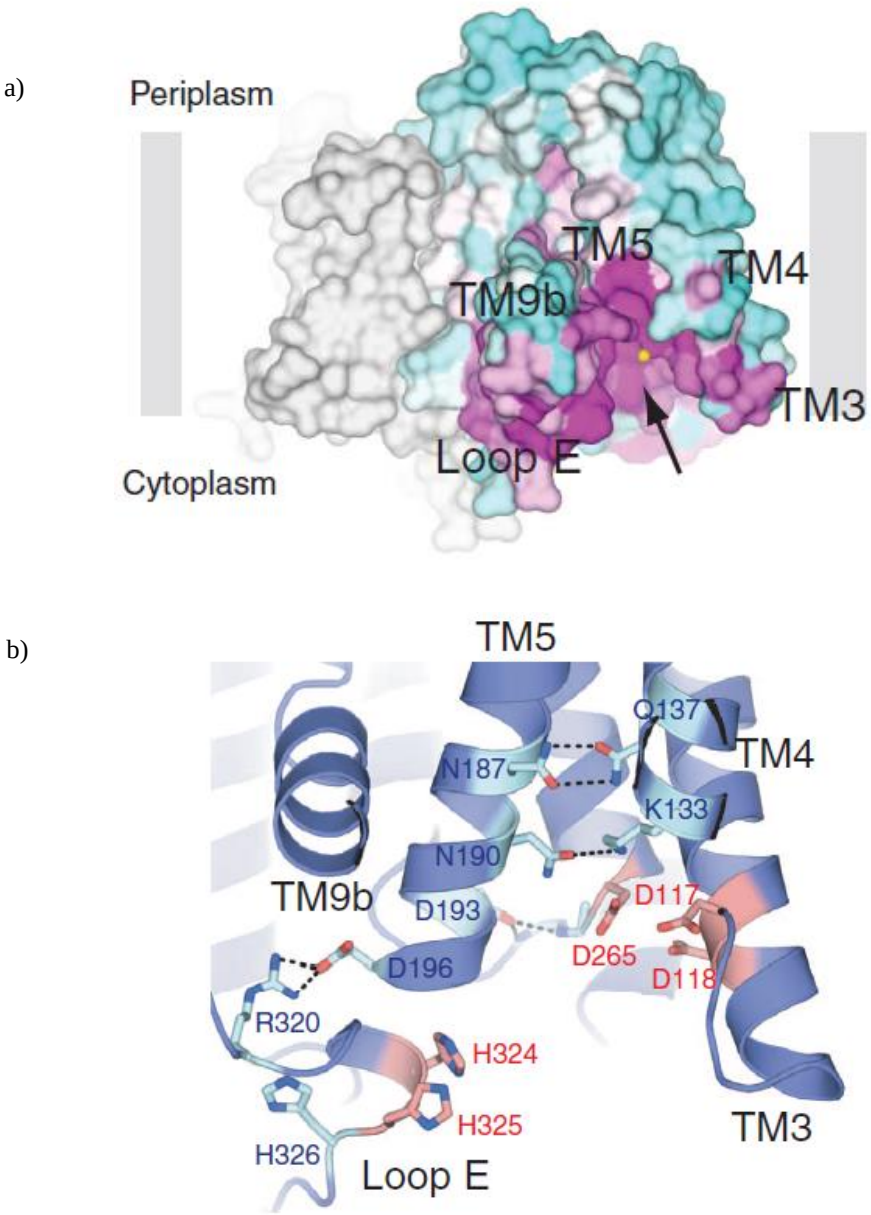


**Figure 1.25: The active site of *A. aeolicus* MraY[95].** a) Conservation mapping of one protomer of $MraY_{AA}$. Highlighted in purple are highly conserved residues. The arrow indicates the location of the active site cleft. b) Zoomed in view of the active site. Residues important for catalysis and structural maintenance of the active site are highlighted in pink and cyan, respectively.

As previously mentioned, MraY plays an important role in the biosynthesis of peptidoglycan. Two possible catalytic mechanisms have been proposed. Heydanek *et al* (1969) proposed a two-step mechanism for the formation of lipid I by MraY. In this two-step mechanism, a nucleophilic residue of MraY attacks the β-phosphate from UDP-MurNAc-pentapeptide displacing UMP. Following this step, the phosphate group in $C_{55}$-P attacks the same β-phosphate, releasing the bound MraY protein and forming lipid I (Figure 1.26)[98]. Lloyd *et al* (2004) proposed that D267 in *E. coli* MraY plays the role of the nucleophile in this two-step mechanism. D115 and D116 are believed to be involved in $Mg^{2+}$ chelation. Several observations support the two-step mechanism. In 1972, Pless and Neuhaus conducted isotope exchange experiments to determine the dependence of phosphatides for *S. aureus* MraY activity. In the absence of $C_{55}$-P, MraY was found to catalyse the exchange of [$^3$H]-uridine monophosphate with the UMP moiety of UDP-MurNAc-pentapeptide[98-99]. This indicates that the enzyme-substrate complex, MraY-Phospho-MurNAc-pentapeptide, is formed first. The addition of [$^3$H]-UMP pushes the reaction in the reverse direction generating the substrate, [$^3$H]-UDP-MurNAc-pentapeptide and free enzyme. The addition of $C_{55}$-P was found to reactivate the enzyme and allow formation of Lipid I. However, the addition dodecylamine or Triton X-100 inhibited the synthesis of lipid I, indicative of an apparent antagonistic relationship between the detergent and $C_{55}$-P[47,99].

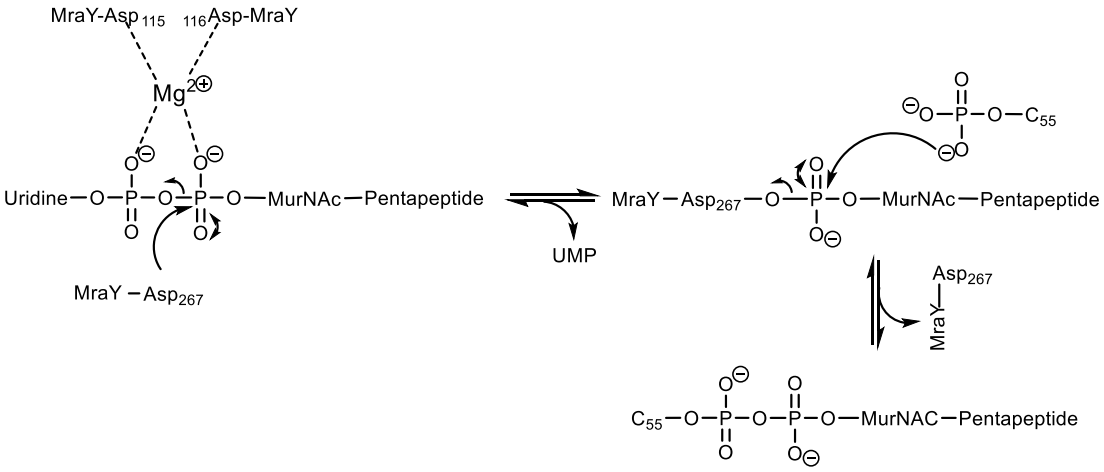


**Figure 1.26: MraY two-step catalytic mechanism**

Pless and Neuhaus's experiment was criticised due to the use of nonpurified MraY[97]. The observations made by Pless and Neuhaus could have been attributed to the presence of endogenous $C_{55}$-P or contaminating enzymes in the preparations used[47]. An alternative one-step mechanism has also been proposed, consisting in a direct attack by the phosphate oxyanion of $C_{55}$-P onto the β-phosphate of UDP-MurNAc-pentapeptide (Figure 1.27)[47]. In 2008, site-directed mutagenesis conducted by Al-Dabbagh *et al* supported this one-step mechanism. In this study, enzyme activity was severely altered by mutation of D115, D116 and D267 but was not completely abolished which may be consistent with a direct attack mechanism[97].

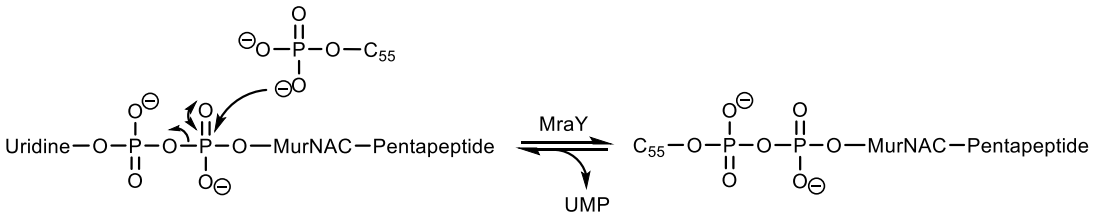


**Figure 1.27: MraY one-step catalytic mechanism**

The *mraY* gene located at minute 2 on the chromosome map of *E. coli*[100], can be amplified and cloned into several expression vectors including pTrc99A, pET52b and pET28b[91,94,101]. Previous reports have shown that the use of detergents such as *n*-

dodecyl-β-D-maltoside, N-lauroyl-sarcosine, Triton X-100 or CHAPS, can facilitate extraction of MraY from various cell membranes[71-72, 94]. However, attempts to purify *E. coli* MraY has been unsuccessful even as a $His_6$ tag fusion protein[94]. As a result, previous reports have used only partially pure or membrane bound MraY in enzymatic assays[47]. In 2004, Bouhss *et al.* described the high-level overexpression and purification of *B. subtilis* MraY. *B. subtilis* MraY was purified to homogeneity in milligram quantities with a specific activity of 1,900 units/mg of protein[94].

Initially, the activity of MraY was determined using a radiochemical assay which monitored the conversion of phospho-MurNAc-[$^{14}$C]pentapeptide to [$^{14}$C]lipid I by TLC or scintillation counter[102]. Alternatively, MraY activity can be determined using a fluorescence enhancement assay which monitors the conversion of fluorescently tagged UDP-MurNAc-pentapeptide to Lipid I[72,92]. UDP-MurNAc-pentapeptide is fluorescently tagged with a dansyl group at *m*-DAP or L-Lys at position 3. In this assay a fluorescence enhancement of 1.5-2 fold[71] is observed upon conversion to Lipid I. This change in fluorescence is a direct response to the insertion of the dansyl group from an aqueous environment to the hydrophobic membrane. The radiochemical assay and the fluorescence enhancement will be discussed in more detail in Chapter 3.

### *1.5.1 MraY Inhibitors*

MraY is the target of various natural products including tunicamycin, mureidomycin A, liposidamycin B and muraymycin. The potencies of these peptidyl nucleoside antibiotics have sparked the scientific community with great interest in investigating the structure-activity relationships of nucleoside antibiotics as MraY inhibitors (Chapter 4)[72,103-17].

Mureidomycin A, isolated from *Streptomyces flavidovirens* SANK 60486[104], consists of a 3'-deoxyuridine nucleoside linked to a modified peptide chain via an enamide linkage (Figure 1.28b)[103]. Mureidomycin A prevents peptidoglycan biosynthesis by selectively inhibiting MraY. Mureidomycin A was not found to inhibit mammalian glycoprotein biosynthesis and is therefore non-toxic[105].

Tunicamycin, isolated from *Streptomyces lysosuperificus,* is a fatty acyl nucleoside which reversibly inhibits MraY (Figure 1.28a)[72]. Tunicamycin has been reported to also inhibit eukaryotic GlcNAc-1-P-transferase, preventing mammalian glycoprotein biosynthesis[106]. GlcNAc-1-P-transferase is analogous to bacterial glycosyltransferase MurG. Tunicamycin has antibacterial activity against Gram-positive bacteria with MIC values ranging from 0.2-50μg/mL[107]. A concise synthesis of tunicamycin and some analogues were reported in 1994[108].

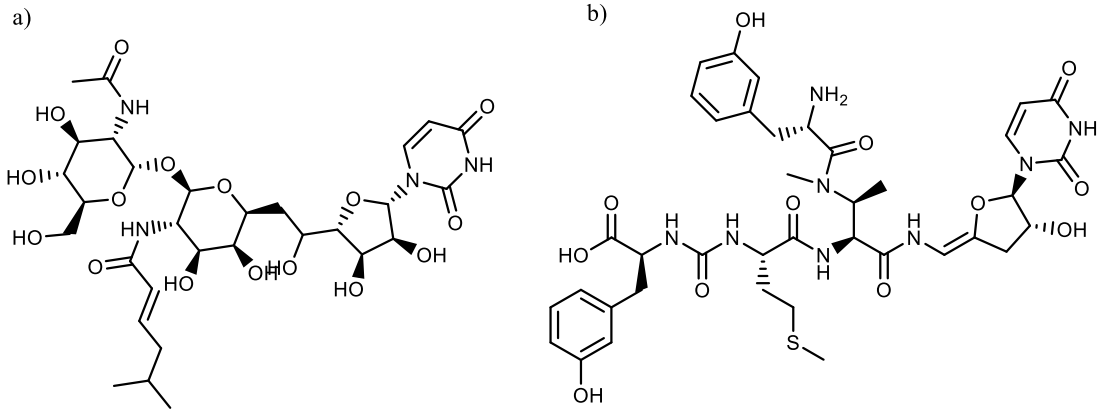


**Figure 1.28: Structure of Tunicamycin and Mureidomycin A**

Liposidomycin B, isolated from *Streptomyces griseosporus*[109], is a nucleoside antibiotic containing a uracil, fatty acid, sulfated amino sugar and a 7-membered heterocycle (Figure 1.29). Liposidomycin B is a strong inhibitor of MraY ($IC_{50}$ 0.03μg/mL) and MurG ($IC_{50}$ ~1μg/mL)[110]. Unlike tunicamycin, liposidomycin does not stimulate a toxic response in mice at 180mg/kg[111].

Muraymycin, produced by *Streptomyces sp.* NRRL 30471, is a potent inhibitor of *in vitro* MraY ($IC_{50}$ 0.027μg/mL)[112]. Muraymycin is an uridyl lipopeptide antibiotic whose activity is highly influenced by the nature of its lipophilic side chain (Figure 1.29)[73,113] McDonald *et al* (2002) reported antibacterial activity against *S. aureus* (MIC 2-16μg/mL), *Enterococci* (MIC 16–64 μg/mL) and Gram-negative bacteria (MIC 16–64 μg/mL)[112]. A previous report found that some members of the muraymycin family are able to protect mice from *S. aureus* infections ($ED_{50}$ 1.1mg/kg), the highest *in vivo* activity of this group of compounds[47].

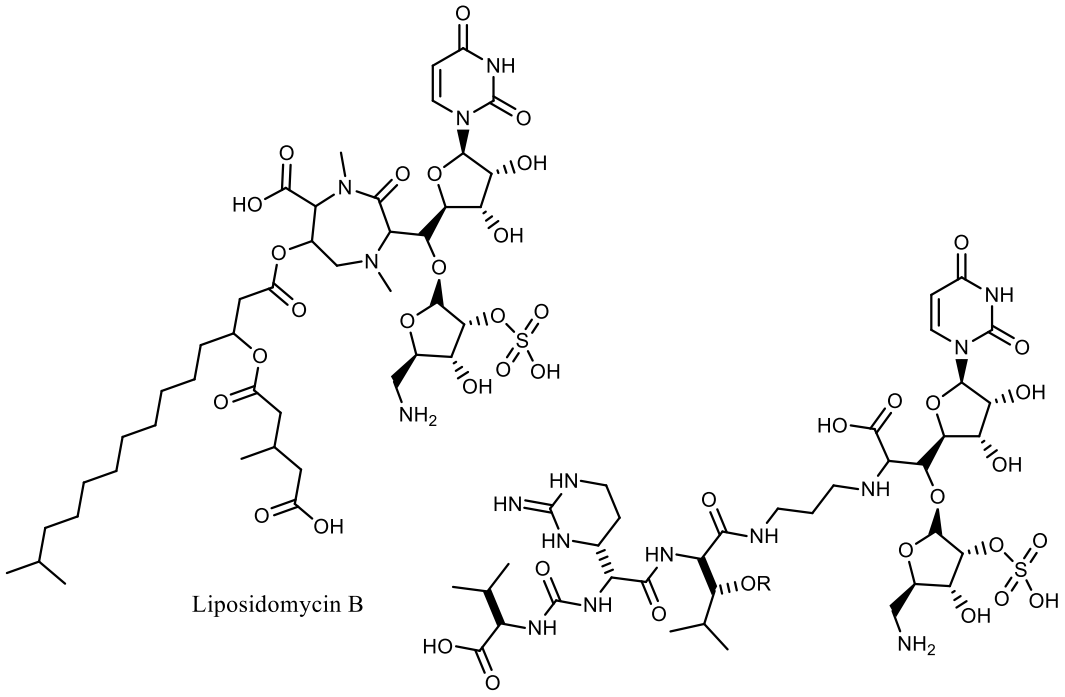


**Figure 1.29: Structure of Liposidomycin B and Muraymycin A1/A3**

## 1.6 Bacteriophage Protein E

In 2000 whilst investigating the different strategies of bacteriophage host cell lysis, Young *et al* came upon an interesting interaction between viral protein E and *E. coli*. In the case of Bacteriophage ΦX174, lytic protein E was found to cause host cell lysis

via inhibition of peptidoglycan[64,114]. Bacteriophage ΦX174 is a 5386bp phage that infects *E coli*. After replication of viral DNA, lysis of the *E. coli* host pursues via lytic proteins including protein E.

Viral protein E has had a major role in the history of molecular biology. It was the first gene to be subjected to site-directed mutagenesis[115], which is a critical and common procedure in research. It was also the first gene discovered to be overlapped within another gene in a different reading frame[116]. The complete DNA sequence of bacteriophage ΦX174 was determined in 1978 using the plus-and-minus method and the terminator method[116]. Gene E encodes a 91-amino-acid protein which activates endogenous autolytic membrane processes in *E. coli*[114]. No enzymatic activity has been observed for protein E itself[117]. Protein E is believed to be localised in the cytoplasmic membrane by its putative N-terminal transmembrane domain[118]. In 1997, Witte *et al* confirmed this by fusing protein E with a streptavidin moiety to produce hybrid protein E-FXa-StrpA. This hybrid protein was then recognised by α-streptavidin antibodies in membrane fractions[119].

The mechanism of E-mediated lysis is controversial and many models have been proposed to explain its function.

E-mediated lysis was observed to be strikingly similar to penicillin-mediated lysis[120]. This was confirmed by light and electron microscopy which revealed that lysis by protein E and penicillin both result in lesions at the cell septum[121-122-123]. These observations suggested that protein E targets and inhibits cell wall biosynthesis.

Unlike the holin-endolysin system which systematically digests peptidoglycan after a programmed amount of time[124], protein E has not been associated with cell wall degrading activity,[64] instead it has been proposed to target a host protein causing cell lysis. Two proteins have been implicated as protein E targets, SlyD and MraY[125].

### *1.6.1 SlyD and Protein E*

In 1985, Maratea *et al* isolated recessive mutations in the host gene *slyD* which blocks the lytic effects of protein E. Fusion experiments were conducted to determine if *slyD* mutants conferred resistance to protein E by preventing expression of gene *E*. Interestingly enough *EΦlacZ* fusions were still able to lyse *slyD* mutants, suggesting that these E fusions bypassed the step in which the wild-type *slyD* participates in E-mediated lysis[126]. Maratea *et al* concluded that the *slyD* gene product may potentially serve as an initial recognition target, not the final lysis target. Bernhardt *et al* supported this hypothesis and suggested that lysis prevention by *slyD* mutants is associated with the inability of E to accumulate in the membrane due to improper folding[120].

In 1997, Hottenrott *et al* identified SlyD as a cytoplasmic metal ion-regulated peptidyl-prolyl *cis/trans* isomerase (PPIase) with chaperone-like properties[127]. Chaperones assist in protein folding by binding to hydrophobic patches of polypeptide chains, preventing aggregation[128]. Proteomic analysis of *E. coli* BL21 showed an increase in the levels of SlyD after heat shock or membrane protein overexpression, implicating its role in protein folding[129-130].

The crystal structure of *Thermus thermophiles* SlyD (TtSlyD) was solved by Löw *et al* in 2010. The PPIase domain of TtSlyD has over 50% sequence similarity to *E. coli* SlyD and was co-crystallised with a prolyl-containing peptide structure (Figure 1.30). The active site is rich in hydrophobic residues which are believed to assist in binding and folding of polypeptides. Given the presence of multiple proline residues in the sequence of E peptide, it is plausible that SlyD assists in folding of the E protein.

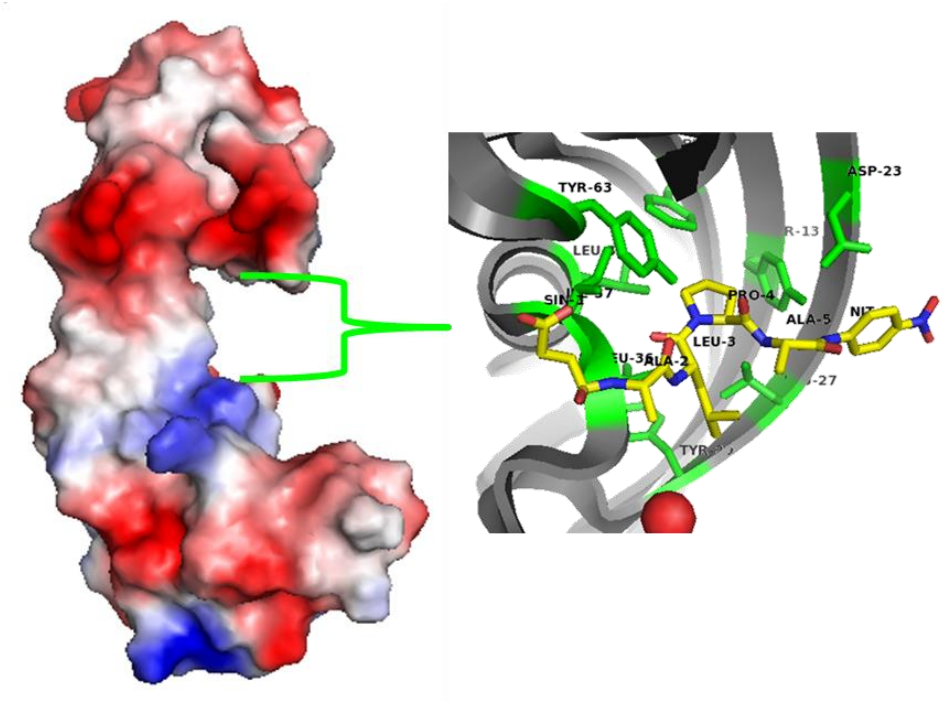


**Figure 1.30: Crystal Structure of TtSlyD co-crystallized with a prolyl-containing peptide substrate (PDB: 3LUO).** Electrostatic map (left) shows the hydrophobic centre (white). Active site residues (green) are located in the hydrophobic pocket. The substrates proline is oriented in the centre of the active site where *cis/trans* isomerisation can occur.

Further evidence that SlyD is not the lethal target for E-mediated lysis was reported by Bernhardt *et al* (2000). An *Epos* mutant of the E gene which contains two point mutation, R3H and L19F, was isolated on a *slyD*-null lawn[120]. This *Epos* mutant was found to be bacteriolytic in the absence of SlyD, suggesting that SlyD is an accessory protein in cell lysis, not the ultimate target[125]. It is possible SlyD may serve as a transport vessel, shielding protein E's hydrophobic residues and protecting it from proteolysis until it reaches its membrane bound target[125] (Figure 1.31).

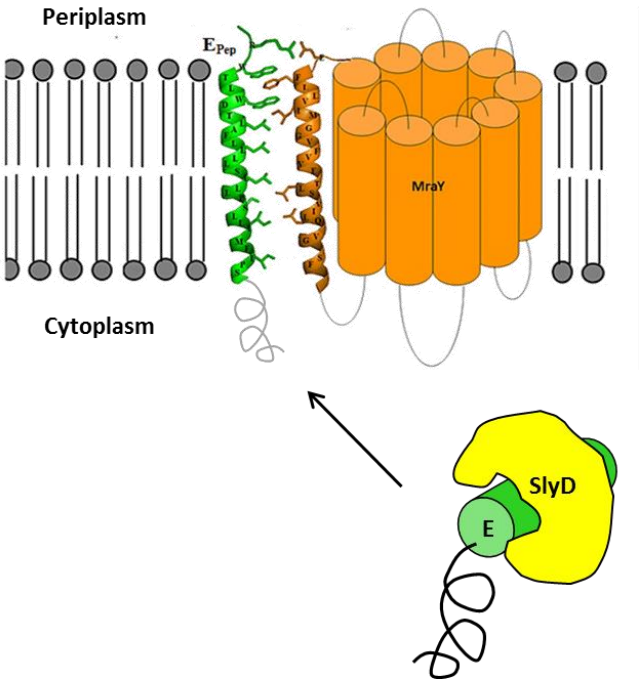


**Figure 1.31: SlyD as a protein E transport vessel.** SlyD may serve as a transport vessel, shielding protein E's hydrophobic residues and protecting it from proteolysis until it reaches its membrane bound target.

### *1.6.2 MraY and Protein E*

To identify the final target of protein E, host mutants conferring resistance to *Epos*, *slyD* and WT phage infections were isolated by Bernhardt *et al*. High-frequency recombination (Hfr) and P1 mapping localised the mutations to minute 2 on the *E. coli* chromosome map[120]. As previously mentioned, this is the location of the *mraY* gene. Sequence analysis revealed that the surviving *mraY* mutants contained mutation F288L which is located at the predicted transmembrane helix 9[120] (Figure 1.25). Further experimental analysis showed that in the presence of epitope-tagged $E_{myc}$ protein, the activity of MraY was found to decrease by 75% with an accumulation of the UDPMurNAc-pentapeptide precursor[64].

These findings have motivated the TDHB research group at the University of Warwick to probe the structural and chemical properties of protein E in the hope of identifying a novel antimicrobial site.

Gene fusion experiments have shown that only 35 amino acids are necessary for lysis. This was further confirmed by the isolation of E amber mutants which were able to produce the wild-type phage within the host cell but could not activate lysis[131]. These 35 amino acids are believed to encompass the putative transmembrane domain and will be referred to as Epep in this text[114,132]. The protein sequence of Epep is shown in Figure 1.32

| 5 | 10 | 15 | 20 | 25 | 30 | 35 |
|---|---|---|---|---|---|---|
| MVRWT | LWDTL | AFLLL | LSLLL | PSLLI | MFIPS | TFKRP |

**Figure 1.32: Sequence of Lytic E peptide.** Shaded green are residues predicted to interact with MraY. Shaded yellow are residues located in the transmembrane region

Epep was found to inhibit particulate *E. coli* MraY ($IC_{50}$ = 0.8μM), but no inhibition of solubilised MraY was observed[125]. This suggests that rigidity, provided by the membrane, is important for the interaction of protein E with MraY. These experiments led to the hypothesis that protein E inhibits MraY via a protein-protein interaction in the membrane, which prevents interaction of MraY with other cell division proteins.

## 1.7 Putative interaction between MraY and lytic E protein

To determine the site of interaction between two proteins, structural and mutational studies are necessary. In the case of MraY and protein E, genetic studies have shown that MraY mutation F288L causes resistance to protein E suggesting that Phe-288 is involved in binding protein E[120,133]. Utilising this information, we have constructed an α-helical model for the predicted transmembrane interactions between protein E and MraY, shown in Figure 1.33.

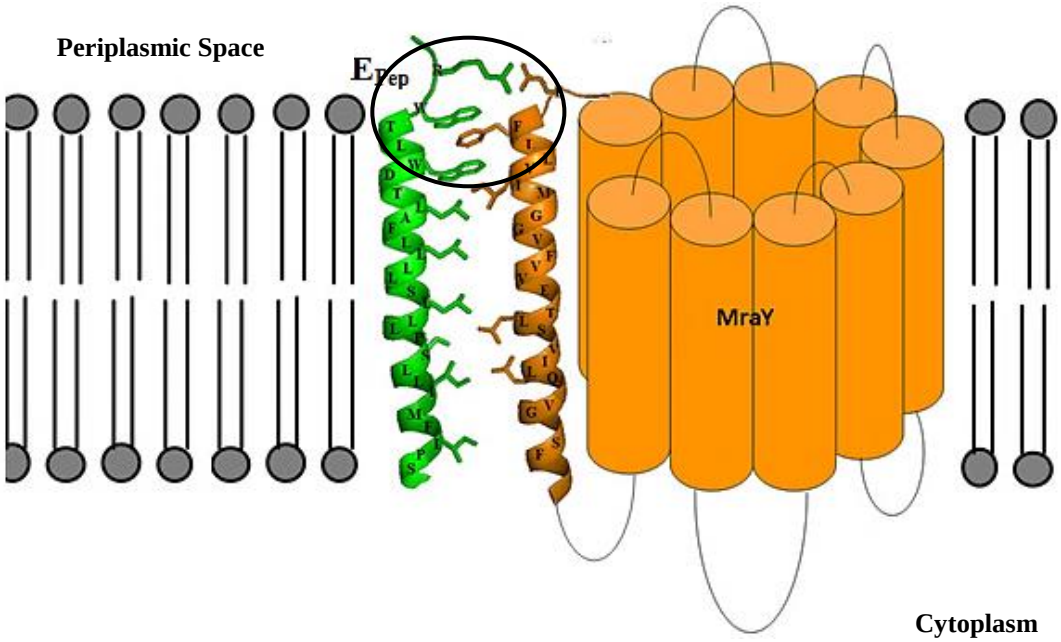


**Figure 1.33: Predicted transmembrane interactions between Protein E and MraY translocase.** The ten transmembrane helices, four periplasmic loops and five cytoplasmic sequences of MraY are shown. F288 in transmembrane helix 9 interacts with protein E in the transmembrane region

Optimal protein interaction can occur between Phe-288 of helix 9 and Trp-4 and Trp-7 of protein E, in which favourable aromatic interactions can be formed. Trp-4 and Trp-7 of protein E can participate in π-π stacking with Phe-288. π-π stacking is an attractive interaction that occurs between the π-clouds of aromatics in a parallel orientation[134]. π- π stacking interactions are prevalent in proteins and have been detected in the complexes of medicinal drugs and the targeted enzymes[135]. The parallel displaced orientation, in particular, is the most stable and energetically favourable orientation in proteins[135,136,137]. In this proposed model, it is plausible to form either a parallel-displaced orientation or a parallel-sandwich orientation (Figure 1.34).

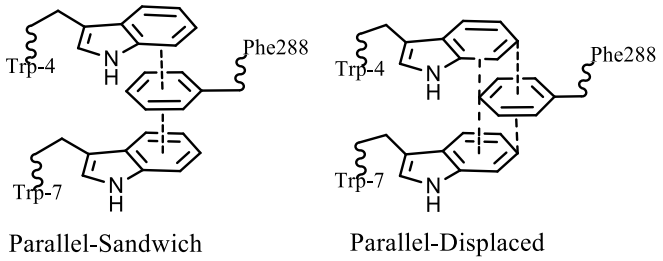


**Figure 1.34: Parallel π-π stacking orientations**

A salt bridge can also be formed between MraY's Glu-287 and Arg-3 of protein E. A salt bridge is a combination of hydrogen bonding and electrostatic interactions which can be formed between the carboxylate of glutamic acid and the cationic ammonium from arginine[137]. Salt bridges have been previously shown to contribute greatly to protein stability, folding and binding[138]. Through this salt bridge it is possible for protein E and MraY to bind more tightly.

Several protein X-ray crystal structures have shown a consistent pattern of salt bridges or charged residues stacked over aromatic interactions[139]. This structural motif has been termed cation-π interactions or SACA (Stacked Arrangement of Carboxylates over Aromatics)[139]. Cation–π interactions have been shown to be important for membrane insertion, substrate binding, catalysis and ion channel activity[140]. Entry into the transmembrane region is particularly difficult for charged amino acids such as arginine. However by associating with tryptophan, arginine can shield its positively charged side chain from the hydrophobic bilayer upon entry[141-142]. In the case of protein E, Trp-4 can shield Arg-3 during membrane diffusion. Once Arg-3 reaches the periplasmic side of the membrane, the combination of cation-π interactions and van der Waals forces can be used to align arginine's side chain to bind MraY via a salt bridge with Glu-287[140,143]. Together, these residues provide an Arg-Trp-X-X-Trp motif that could interact with MraY.

Within the transmembrane region there are also possible Leu-Ile and Leu-Val contacts, and a possible polar interaction between Ser-303 of MraY and Ser-17/Ser-22 of $E_{pep}$. This model provides a good basis for a detailed study of the Protein E-MraY interaction.

### *1.7.1 Mutational Studies on Protein E*

A variety of genetic studies on protein E have identified several mutations which are unable to cause lysis[119,133,144-145]. Mutational studies conducted by Witte *et al*, showed that mutations P29G, P29S, P29V and P65G, P65S and P65V delayed lysis by 10-15 minutes while mutations P21G, P21A, P21S and P21V completely abolished lysis[119]. The importance of P21 *in vivo* was further confirmed by Yu *et al*, Zheng *et al* and Tanaka and Clemons[133,144-145]. P21 is located in the membrane near the cytosolic surface and may be important for creating a helical kink. Helical kinks mediated by proline residues have been previously shown to allow for tightly packed structures in transmembrane helices[146-147]. Alternatively, P21 may be important for protein folding by SlyD. However, none of these studies have used SlyD mutants to confirm this.

In 2012, Tanaka and Clemons demonstrated that in addition to Pro21, Trp7 was also essential for E-mediated lysis. Mutation W7A inhibited lysis in a similar manner to mutation P21A[133(Fig S2A)]. W7A corresponds to the 2$^{nd}$ Trp residue of the RWXX**W** motif that we hypothesise is important for interaction with MraY.

### *1.7.2 Known antimicrobial peptides containing the RWXXW motif*

The RWXXW motif is very peculiar as it involves two of the bulkiest natural amino acids; one being very polar and basic and the other being the most hydrophobic. Cherkasov *et al* (2008) used Quantitative Structure Activity Relationship (QSAR) to

relate the structural characteristics of a molecule to biological activity. Interestingly enough, arginine and tryptophan were recorded to be prevalent amino acids in antimicrobial peptides[148] (Figure 1.35). The physical properties of Arg and Trp side-chains are expected to contribute greatly to this finding[149].

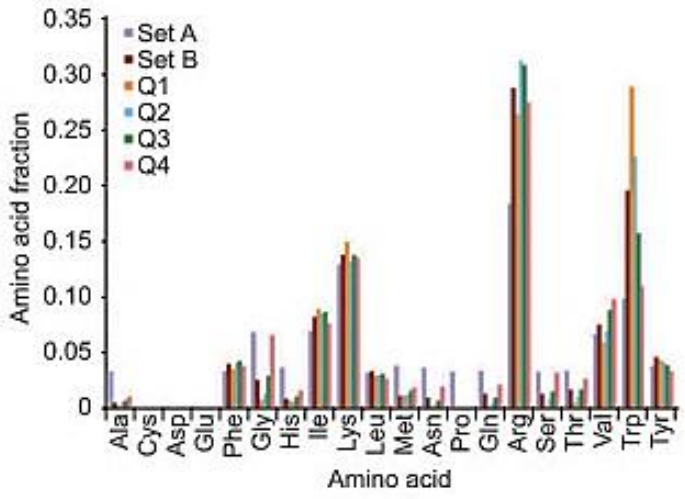


**Figure 1.35: Occurrence of amino acids in QSAR data sets[148].** Set A and B have antimicrobial activity. Q1-Q4 are samples predicted to have activity.

Remarkably, the RWXXW motif is also present in several known cationic peptides including Indolicidin[150] and CP-11[151] which show antibacterial activity against *S. aureus* and *E. coli*. The protein sequence of several antimicrobial peptides in comparison to protein E is given in Table 1.1. The sequence of indolicidin, isolated from bovine neutrophils[152], contains RWPWW starting at position 2 relative to the C-terminus. Derivatives of indolicidin such as Kai26 also contain the RWXXW motif. The N-terminal sequence of cecropin A contains the related KWKSF in which Lys-1 and Phe-5 replace chemically equivalent Arg-1 and Trp-5 of the RWXXW motif, respectively. It is documented that the Trp-2 residue in this sequence is essential for activity[153]. Similarly, the C-terminal sequence of tritrpticin also contains a related sequence, RFPWW[154]. Lactoferricin B contains RWQW starting at position 5. It has

been demonstrated that Trp-6 and Trp-8 of this peptide are both essential for antimicrobial activity[155].

**Table 1.1: Amino acid sequence alignment of ΦX174 E protein with other known antimicrobial peptides**

| Antimicrobial peptides | Sequence | PDB file | Ref |
|---|---|---|---|
| E peptide | N-MV**RW**TL**W**DTLAFLLL-C | | [114] |
| MX226 | N-IL**RW**PWPWRRK-C<br>C-KR**RW**PWPWRLI-N | | [150] |
| Kai26 | C-K**RW**KW**W**RFKWKIF-N | | [150] |
| Indolicidin | C-R**RW**PW**W**PWKWPLI-N | 1G89,<br>1G8C | [150] |
| CP-11 | C-KR**RW**PW**W**PWKKLI-N | 1QXQ | [151] |
| CycloCP-11 | C-K$C_1$R**RW**PW**W**PWKK$LC_1$I-N | 1QX9 | [156] |
| Sub6 | N-**RW**WKIWVIRWWR-C | | [150] |
| Kai50 | N-ILRWKW**RW**WR**W**WRR-C | | [150] |
| HHC-10 | N-K**RW**WK**W**IRW-C | | [148] |
| HHC-36 | N-K**RW**WK**W**WR-C | | [148] |
| HHC-8 | C-RK**RW**WW**W**IK-N | | [150] |
| HHC-45 | C-**RW**KK**W**WRKW-N | | [150] |
| Lactoferricin B | N-EKCR**RW**QWRMKKLG-C | 1LFC | [155-157] |
| Cecropin A | N-**KW**KL**F**KKI….-C | 1D9J | [153, 158] |
| Tritrpticin | N-VR**RF**PW**W**WPFLRR-C | 1D6X | [154] |
| 1002 | N-VQ**RW**LIVWRIRK-C | | [150] |
| 1020 | N-VRLRI**RW**WVLRK-C | | [150] |

Although cationic antimicrobial peptides are known to insert and form pores in bacterial membranes (Chapter 1.2), they are thought to have multiple cellular targets, so the appearance of the same motif suggests a possible link with the protein E mechanism of bacterial cell lysis.

### *1.7.3 Protein E analogues across ΦX174-like bacteriophages*

There are three groups of ΦX174-like bacteriophages[159-160] which contain variations on the RWXXW motif. In group 1, of which ΦX174 is the principal member, the RWXXW motif is well conserved (though not entirely) in protein E homologues. In

group 2 (type field by phage α3) and group 3 (type field by phage G4), an additional Glu-2 residue is conserved and in some cases Arg-3 is often replaced by His (Figure 1.36).

Like arginine, histidine is a very polar amino acid that is commonly involved in the active sites or binding sites of proteins. In addition, histidine has a $pK_a$ near to the physiological pH which allows its side chain to alternate between a neutral and positive charge[161]. Given its similarities, it is plausible that histidine can interact in a similar manner to arginine to form similar interactions as we proposed WT protein E forms with MraY.

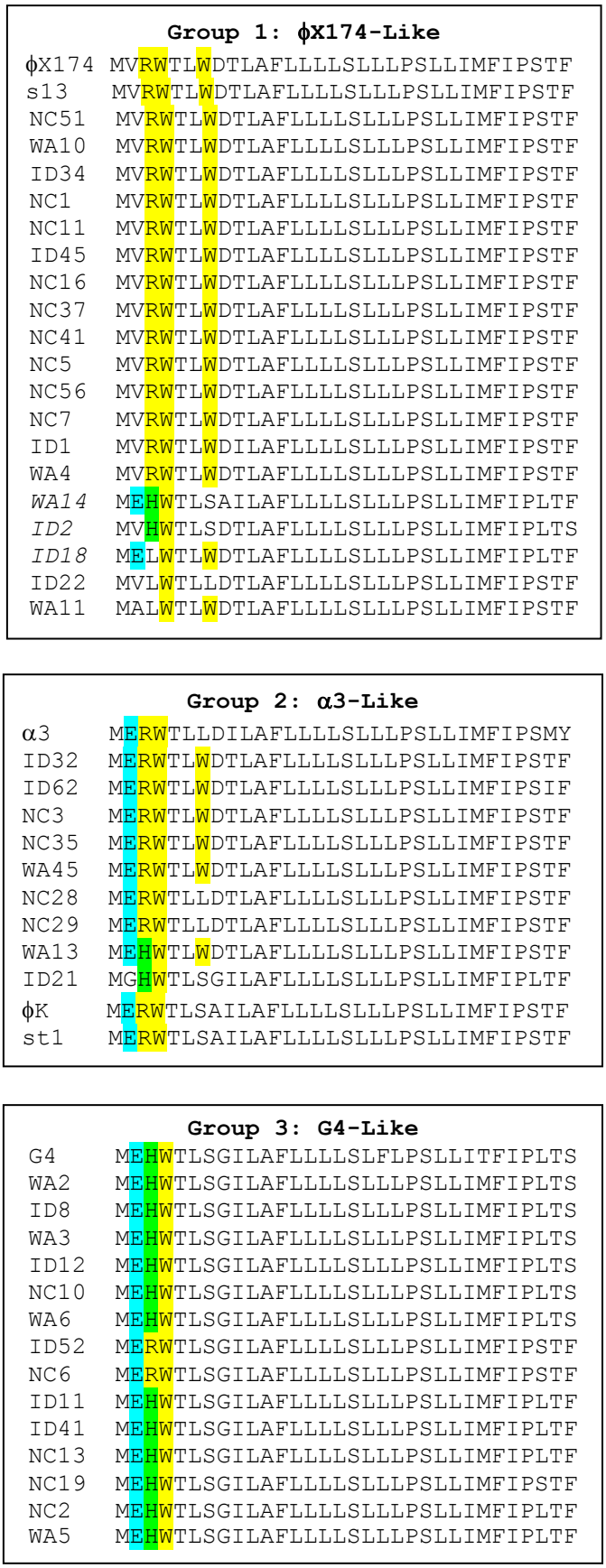


**Figure 1.36: Sequence of protein E homologues across various bacteriophages**

## 1.8 Aims of the Project

In this project, we hypothesise that the RWXXW motif of protein E inhibits MraY by interacting with Phe288. In order to investigate this hypothesis, synthetic peptide analogues of the RWXXW motif have been synthesised and tested against the activity of membrane bound MraY.

Initially, Arg-Trp dipeptide derivatives were prepared containing hydrophobic octyl substituents at either N- or C- terminus, designed to anchor the peptide in the membrane.

### *1.8.1 Compounds of Interest*

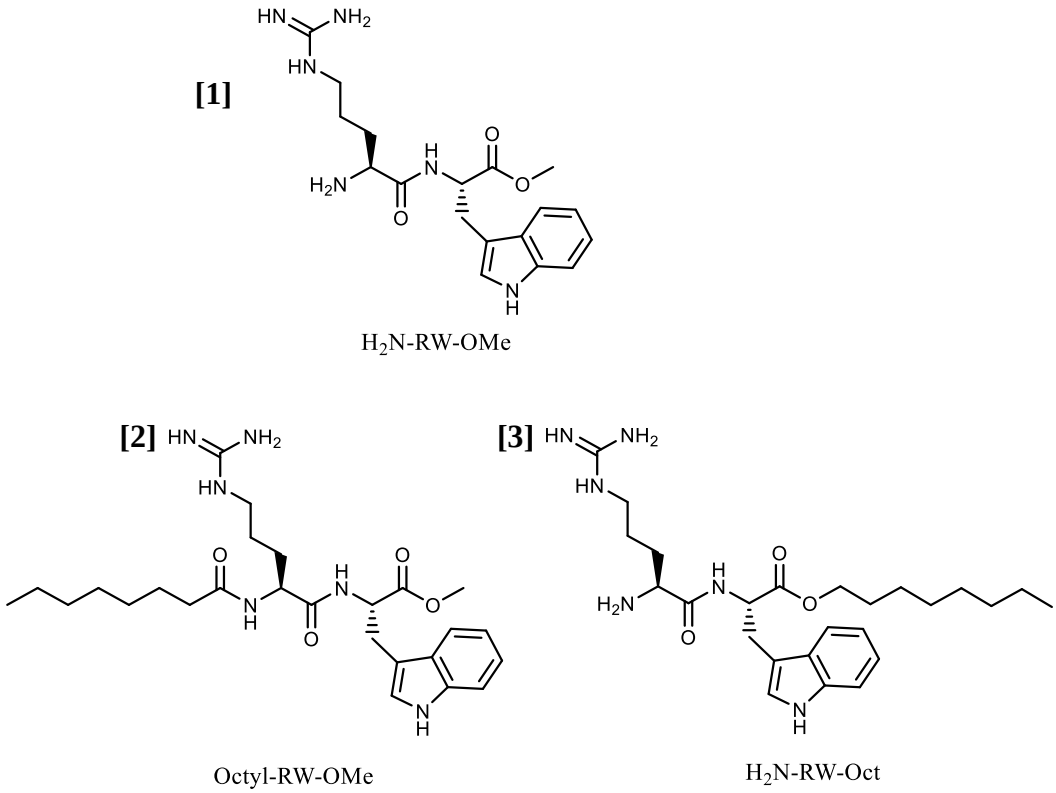


**Figure 1.37: Arg-Trp dipeptide derivatives**

To determine which interaction (electrostatic or π- π stacking) is most critical for the interaction between protein E and MraY, arginine and tryptophan were replaced with glycine (Figure 1.38).

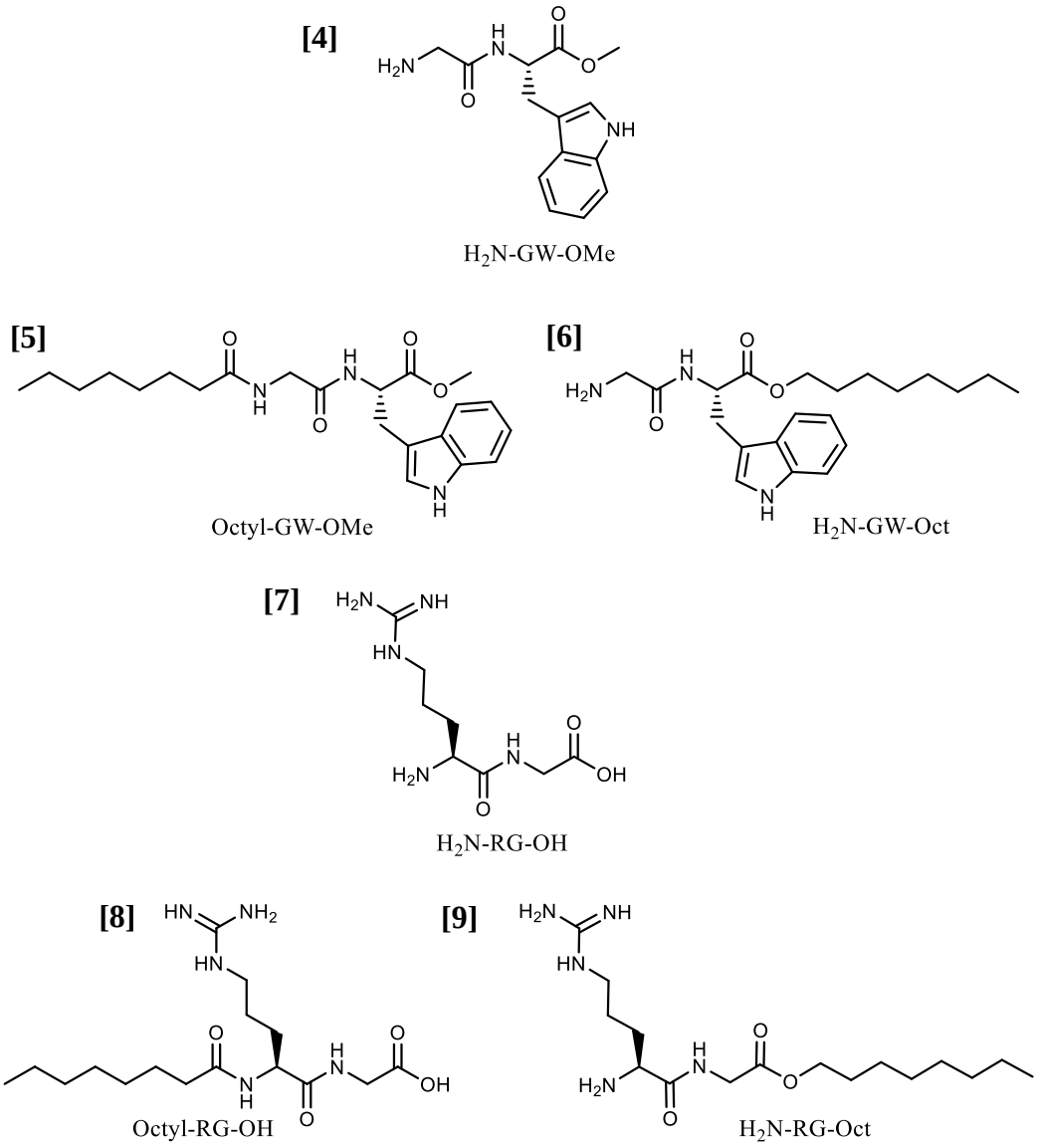


**Figure 1.38: Gly-Trp and Arg-Gly dipeptide derivatives**

Pentapeptide analogues of the RWXXW motif were also designed. For ease of synthesis, and since Thr-5 does not appear to interact with MraY according to our predicted structural model (Figure 1.33), Thr-5 was replaced with Leu. In ΦX174-like bacteriophages (Group 1), Thr-5 is also commonly replaced by Leu (Figure 1.36), so RWGLW was considered the native sequence. To determine the binding efficiency

of individual amino acids in the RWXXW motif, each amino acid was replaced with glycine (Figure 1.39).

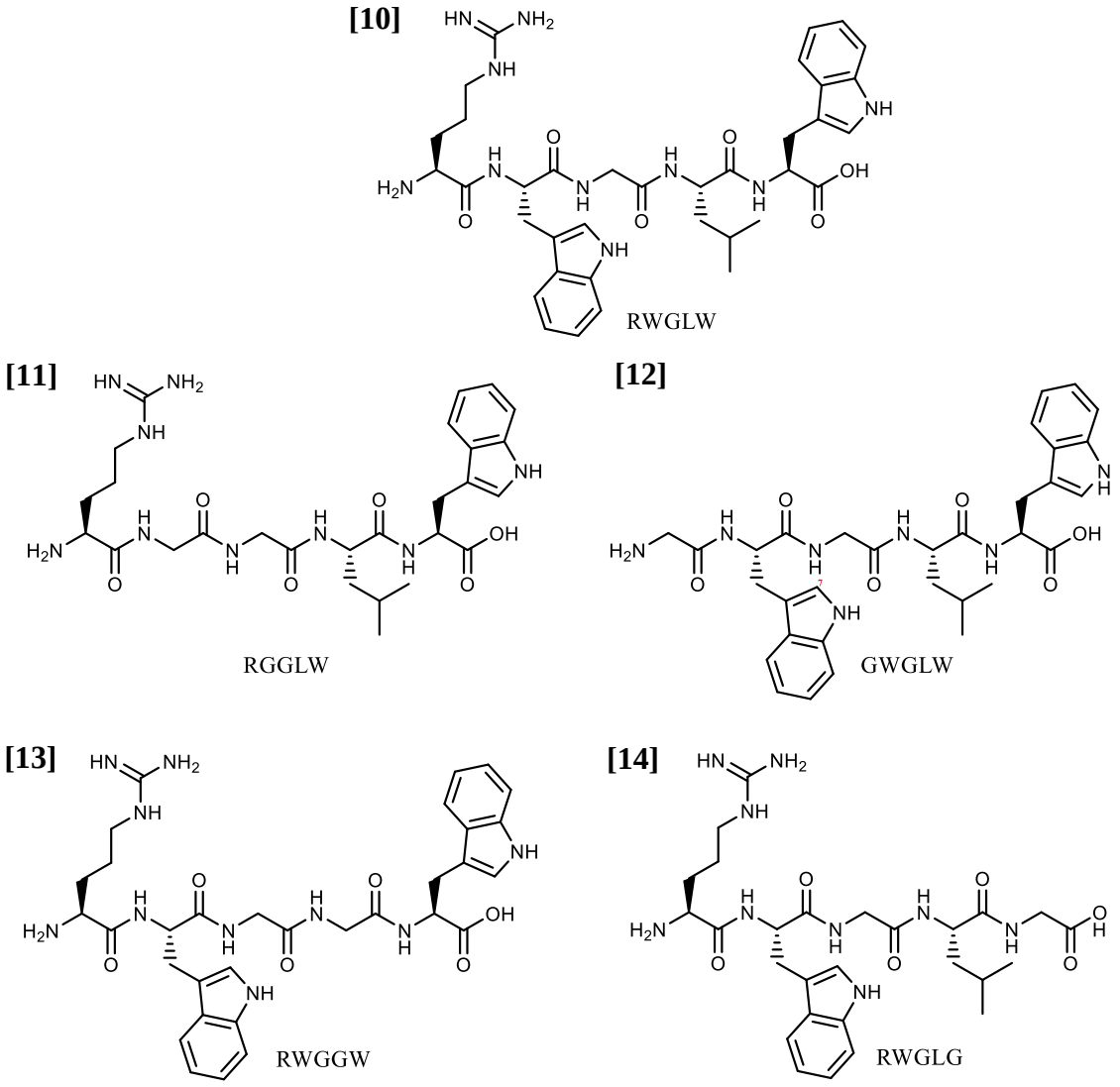


**Figure 1.39: RWXXW pentapeptide analogues**

Across various bacteriophages, the RWXXW motif is conserved (Figure 1.36). In group 2 and group 3 bacteriophages, a conserved Glu-2 residue precedes the RWXXW motif. Following our predicted structural model, this additional Glu-2 may interact with the Gln286 residue located on the MraY helix 8-helix 9 loop via hydrogen bonding. In group 3 bacteriophages, Arg-3 is often replaced by His which has similar chemical properties to Arg (Figure 1.36). Analogues of group 2 and group

3 protein E were therefore also synthesised and examined for activity against MraY (Figure 1.40).

**[15]**

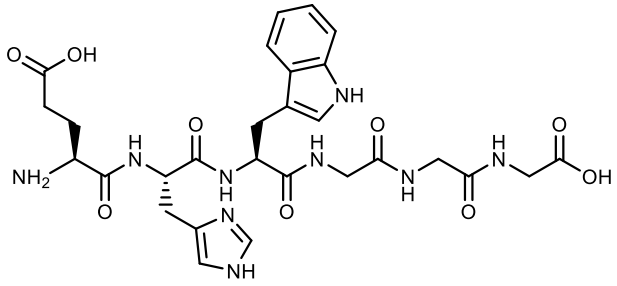

EHWGGG

**[16]**

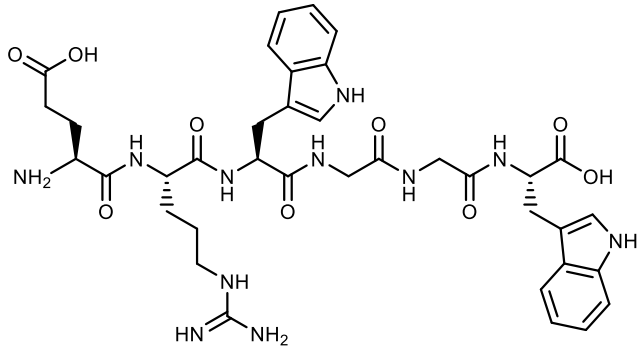

ERWGGW

**Figure 1.40: G4-like and α3-like protein E analogues**

**Table 1.2: RWXXW analogues synthesised within the scope of this research**

| | Compound | Formula | Mass (g/mol) |
|---|---|---|---|
| **[1]** | $H_2N$-RW-OMe | $C_{18}H_{26}N_6O_3$ | 374.207 |
| **[2]** | Octyl-RW-OMe | $C_{26}H_{40}N_6O_4$ | 500.311 |
| **[3]** | $H_2N$-RW-Oct | $C_{25}H_{40}N_6O_3$ | 472.316 |
| **[4]** | $H_2N$-GW-OMe | $C_{14}H_{17}N_3O_3$ | 275.127 |
| **[5]** | Octyl-GW-OMe | $C_{22}H_{31}N_3O_4$ | 401.231 |
| **[6]** | $H_2N$-GW-Oct | $C_{21}H_{31}N_3O_3$ | 373.237 |
| **[7]** | $H_2N$-RG-OH | $C_8H_{17}N_5O_3$ | 231.133 |
| **[8]** | Octyl-RG-OH | $C_{16}H_{31}N_5O_4$ | 357.238 |
| **[9]** | $H_2N$-RG-Oct | $C_{16}H_{33}N_5O_3$ | 343.258 |
| **[10]** | $H_2N$-RWGLW-OH | $C_{36}H_{48}N_{10}O_6$ | 716.376 |
| **[11]** | $H_2N$-RGGLW-OH | $C_{27}H_{41}N_9O_6$ | 587.318 |
| **[12]** | $H_2N$-GWGLW-OH | $C_{32}H_{39}N_7O_6$ | 617.296 |
| **[13]** | $H_2N$-RWGGW-OH | $C_{32}H_{40}N_{10}O_6$ | 660.313 |
| **[14]** | $H_2N$-RWGLG-OH | $C_{27}H_{41}N_9O_6$ | 587.318 |
| **[15]** | $H_2N$-EHWGGG-OH | $C_{28}H_{35}N_9O_9$ | 641.256 |
| **[16]** | $H_2N$-ERWGGW-OH | $C_{37}H_{47}N_{11}O_9$ | 789.356 |

# Chapter 2: Synthesis of Peptides

## 2.1 Steps in Peptide Synthesis

The aim of this research project was to develop novel inhibitors of MraY. Exploiting the predicted structure-activity relationship of lytic E and MraY, 16 short RWXXW analogues were synthesised via manual SPPS and solution peptide synthesis. Efficient peptide synthesis required careful utilization of the following four steps: protection, activation, coupling and deprotection[162,163,164].

### *2.1.1 Protection*

Strategic protection of the carboxyl (COOH) and amino ($NH_2$) functional groups was crucial; otherwise undesired products could form upon peptide coupling. A peptide bond or amide bond is a covalent chemical bond that is formed between the carboxyl group of one amino acid with the amino group of another amino acid[164].

If an amino acid is left unprotected at both termini, it can react with itself and form a variety of dipeptides, tripeptides and other polymers. If two different amino acids are left unprotected, there are four possible dipeptide products that can form. In the case of unprotected arginine and tryptophan, dipeptides $H_2N$-Arg-Arg-OH, $H_2N$-Arg-Trp-OH, $H_2N$-Trp-Arg-OH and $H_2N$-Trp-Trp-OH can be formed.

To maximize the yield and purity of the desired dipeptide, the N-terminus of one amino acid and the C-terminus of the other amino acid must be protected. Protecting groups vary according to protocol. In SPPS, the N-terminus is typically protected by Fluorenylmethyloxycarbonyl (Fmoc). The advantage of the Fmoc protecting group is that it is cleaved under very mild basic conditions (e.g. piperidine), but stable under acidic conditions[165].

In SPPS, the C-terminus is protected by a polymeric resin particle. The first polymeric support was the Merrifield resin which was developed by Robert Merrifield in 1963[166]. The Merrifield resin is composed of polystyrene cross-linked with chloromethylstyrene and divinylbenzene (<5%) (Figure 2.1)[167].

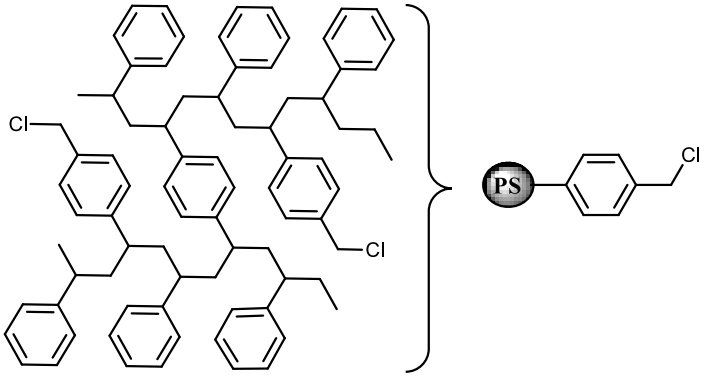


**Figure 2.1: Merrifield Resin**

Originally the Merrifield resin was considered a permanent protecting group to aid in peptide coupling and purification[168]. However, isolation of peptides from the Merrifield resin required vigorous treatment with anhydrous HF which consequently caused degradation[169]. Modern resins such as the Wang resin and 2-chlorotrityl chloride resin are modified Merrifield resins. The Wang resin has a *p*-hydroxybenzyl alcohol linker and 2-chlorotrityl chloride resin has a trityl chloride linker (

Figure 2.2)[168,170]. The addition of these linkers enhances reactivity and allows cleavage with milder reagents such as TFA and $H_2O$[171-172].

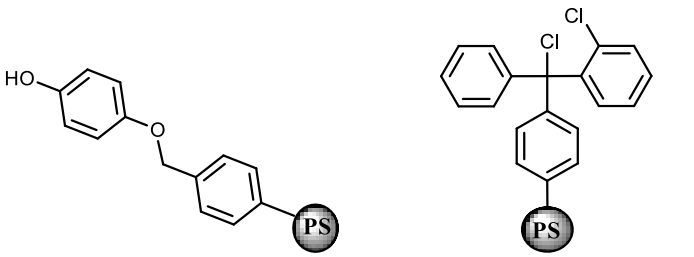


**Figure 2.2: Modified Merrifield resins**

In solution peptide synthesis, the C-terminus and the N-terminus can be protected by any soluble R group such as Boc or *t*Bu.

In addition to protecting the termini, many amino acids also have reactive side chain groups which need to be protected. Reactive side chain groups can interact with free termini or other side chain groups during synthesis[162]. If unprotected, side chain groups can negatively influence the yield and purity of a reaction; this is the case for histidine and lysine which have reactive amine groups. The guanidinium side chain group of arginine is not very reactive and therefore does not need a side chain protecting group. However, in the absence of a side chain protecting group, Fmoc-Arginine-OH exists as an unmanageable paste which complicates peptide coupling and yield determination. To overcome this issue, an acid labile side chain protecting group such as PMC or the HCl salt of Fmoc-Arg-OH is necessary. The structure of a fully protected arginine amino acid is given in

Figure 2.3.

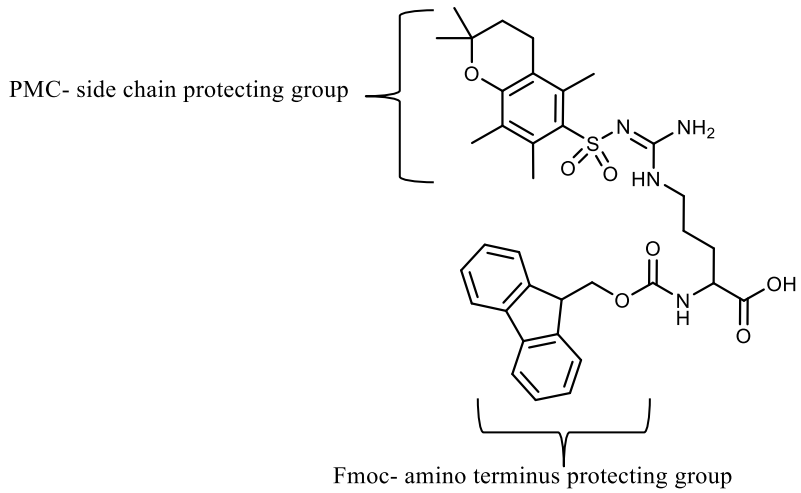


**Figure 2.3: Structure of a Fmoc-Arg(PMC)-OH (21).** The N-terminus is protected by base labile Fmoc. The side chain is protected by acid labile 2,2,5,7,8 - pentamethyl - chroman - 6 – sulfonyl (PMC).

### *2.1.2 Activation*

Activation of the C-terminus is energetically necessary to form a peptide bond. The activation energy involved in the formation of an amide bond from a carboxylic acid and an amine is too high to overcome under normal conditions (Figure 2.4)[173]. To overcome such high activation energy and to avoid the formation of ammonium carboxylate salts, chemical modification of the carboxylic acid is necessary.

In order for an amine to nucleophilically attack another compound, the target must be electrophilic and contain a good leaving group 'X'. The hydroxyl group of a carboxylic acid is a poor leaving group, as it is electron donating. If 'X' were a good leaving group and electron withdrawing, it would enhance the electrophilicity of the carbonyl by inducing a partial positive charge. Modification of amino acid leaving groups is accomplished by the use of coupling agents.

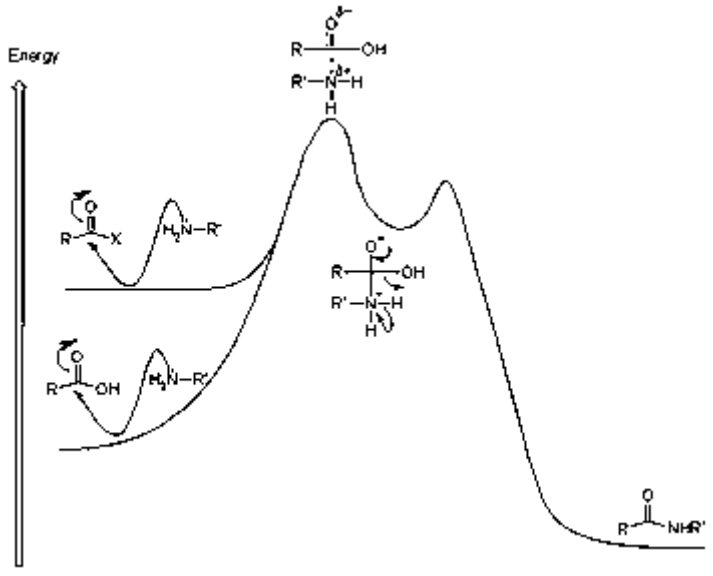


**Figure 2.4: Energy changes in the formation of a peptide bond.** The carboxylic acid (RCOOH) has a very low free energy. The carboxylic acid derivative (RCOX) has a higher energy, which allows it to overcome the high activation energy with greater ease than the carboxylic acid.

There are many commercially available coupling agents that are designed to activate amino acids. In this research project, N,N'-Dicyclohexylcarbodiimide (DCC), N,N′-Diisopropylcarbodiimide (DIC), 1-ethyl-3-(3-dimethylaminopropyl) carbodiimide (EDCI) and 2-(7-Aza-1H-benzotriazole-1-yl)-1,1,3,3-tetramethyluronium hexafluorophosphate (HATU) was used to synthesize Arg-Trp containing peptides (Figure 2.5). The order of reactivity/efficiency of these coupling agents is: DCC≈DIC≈EDCI<HATU[162].

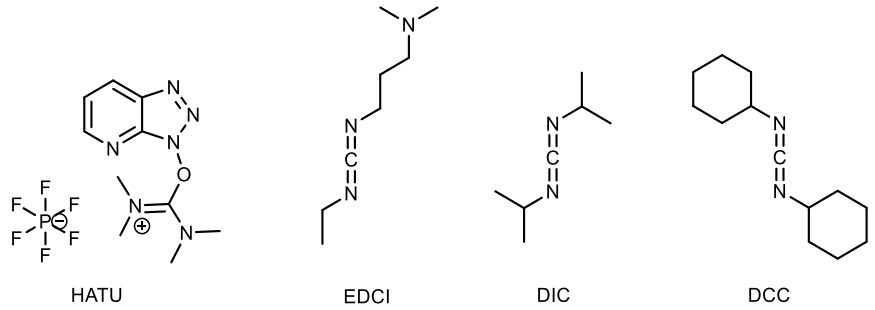


**Figure 2.5: Structures of coupling agents employed in RW peptide synthesis**
In order of reactivity: HATU> PyBOP>EDCI≈DIC≈ DCC

The carbodiimide class (DCC, DIC, EDCI) of coupling agents are the standard choice for most synthetic chemists due to their mild conditions and affordability.[174] The mechanism for carbodiimide mediated peptide coupling is given in Figure 2.6[175].

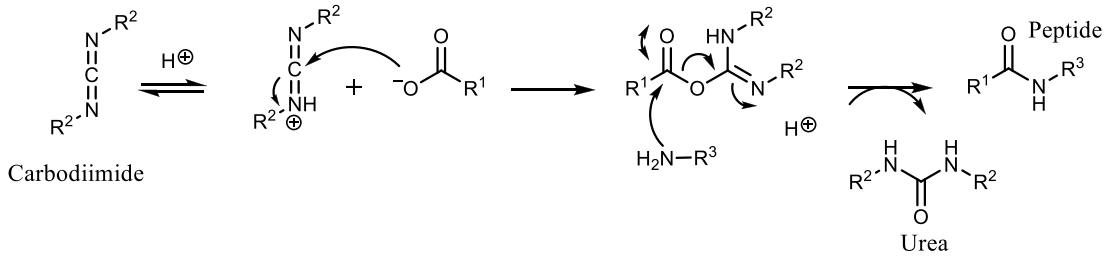


**Figure 2.6: Mechanism of peptide coupling using carbodiimides**

The difference between DCC, EDCI, and DIC lies in the solubility of its urea by-product. The by-product of DCC, N,N'-Dicyclohexylurea, is insoluble and precipitates from the reaction mixture as the reaction progresses[176]. DCC is not an

appropriate coupling agent for SPPS, as it would be very difficult to isolate the *N,N´*-dicyclohexylurea from the insoluble resin beads[177]. DCC is typically used in solution peptide synthesis, as the insoluble urea can be removed by filtration. However, in practice the insoluble urea seems to continuously precipitate out, complicating purification and yield determination. For these reasons, DIC and EDCI were the preferred choice of carbodiimides. The DIC urea byproduct, NN'-diisopropylurea, is soluble in many organic solvents[162]. The solubility of N,N'-diisopropylurea is 5.2g/L in $CH_2Cl_2$ compared 1.5g/L for N,N'-dicyclohexylurea[176]. The fishy smelling EDCI produces a water soluble urea by-product which can be easily removed by aqueous extraction in solution peptide synthesis or removed with successive washes in SPPS.

The biggest challenges of carbodiimide-mediated peptide coupling are the evolution of unreactive by-products and racemisation. The nucleophilic centre of the *O*-acyl-isourea intermediate competes with the incoming amino acid for its intramolecular acyl residue and forms an unreactive *N*-acylurea[164] (Figure 2.7). The formation of *N*-acylurea effectively deactivates the carboxylic acid and makes it unavailable to form a peptide bond with the incoming amino acid.

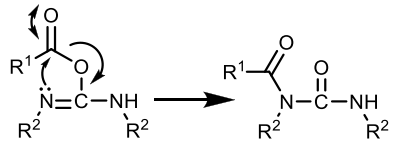

**Figure 2.7: Formation of unreactive *N*-acylureas**

Racemisation of activated amino acids can occur in carbodiimide-mediated peptide coupling via formation of a cyclic oxazolone intermediate[176]. The electron-withdrawing effect of the N-protecting group, Fmoc, extends to the α-carbon and promotes abstraction of the hydrogen atom by a base (Figure 2.8)[164]. Proton abstraction from the α-carbon yields a resonance stabilized ion. Since racemisation is

base catalysed, a sterically hindered base is often used during peptide coupling. The tertiary amine, N,N-Diisopropylethylamine (DIPEA) for example, cannot efficiently approach the chiral center of the reactive amino acid intermediate and therefore hinders racemisation.

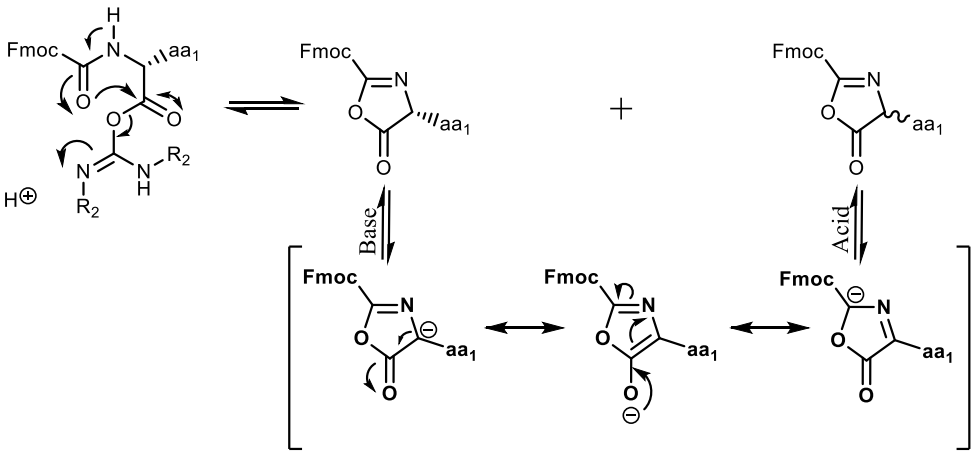


**Figure 2.8: Mechanism of racemisation**

Both racemization and *N*-acylurea formation can be minimized by the addition of auxiliary nucleophiles such as 1-hydroxybenzotriazole (HOBt). This auxiliary nucleophile binds to the electrophilic carbonyl group, reducing the concentration and shortening the lifetime of the over activated *O*-acyl-isourea[164] (Figure 2.9). The incoming amino acid can then easily pick up the acyl residue without experiencing racemisation.

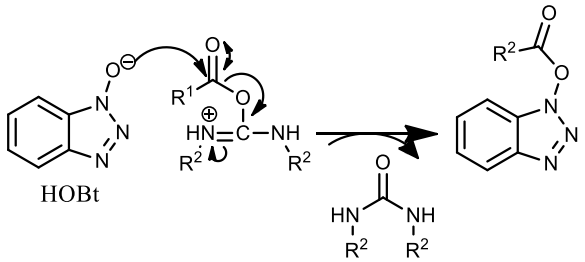


**Figure 2.9: Sequestration of O-acyl-isourea by HOBt**

In 2005, HOBt was reclassified by the United Nations as a desensitized explosive under the category UN3880[178]. This made it illegal to ship HOBt by air or sea and

made land shipment very expensive. Due to a very limited supply of HOBt available in the research group, only a few reactions were carried out with this racemisation agent. Fortunately, in 2009 a non-explosive alternative of HOBt was developed[179]. Merck chemicals Ltd. tested this new compound and found that Oxyma Pure was similar to HOBt in reactivity, effectiveness and even in its physical properties (Figure 2.10)[180].

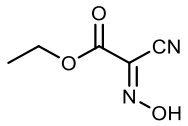


**Figure 2.10: Structure of Oxyma Pure**

In recent years, uronium based and phosphonium based coupling agents have become the preferred tool for carboxyl activation[162]. In the presence of a tertiary base, PyBOP and HATU smoothly convert protected amino acids into active species without compromising optical activity[174]. The phosphonium based agent, PyBOP, produces an amino acid OBt ester. The uronium based agent, HATU, produces a more reactive OAt ester (Figure 2.11). OAt esters are more reactive than OBt esters owing to the lower pKa of HOAt[174]. HATU is regarded as the most effective coupling agent. However due to its cost it is usually only employed for very difficult and unusual couplings involving bulky and charged amino acids such as tryptophan and arginine.

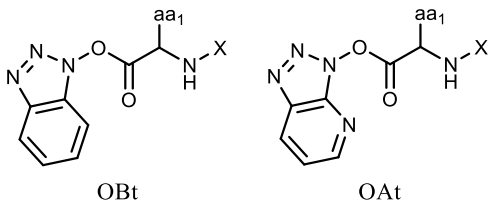


**Figure 2.11: Active esters of PyBOP and HATU, respectively**

Once the carboxyl group was activated using the mentioned coupling agents, the protected amino acids can be coupled.

### *2.1.3 Coupling*

Once the amino acids have been protected and activated, coupling can occur. 4-Dimethylaminopyridine (DMAP) was found to be useful in the enhancement of peptide coupling reactions mediated by carbodiimides[181]. For phosphonium and uronium based coupling agents, N,N-Diisopropylethylamine (DIPEA) and N-Methylmorpholine (NMM) have been recorded to catalysed difficult couplings[174]. Due to their non-nucleophilic properties, these tertiary bases are particularly efficient in peptide synthesis[176]. In both cases, only a catalytic amount of these bases was needed to facilitate peptide coupling.

### *2.1.4 Deprotection*

To isolate the desired peptide, bulky protecting groups such as Fmoc, PMC, Boc and the resin must be removed. To cleave the N-terminal protecting group, Fmoc, a mild base such as 20% piperidine in DMF is used[162].

The C-terminus and the side chain protecting groups are removed by treatment with TFA[182]. Certain amino acids have been shown to cause problems during TFA cleavage. The indole ring of tryptophan is susceptible to oxidation and alkylation by other reactive side chains[183]. Arginine's side chain protecting group, PMC, is extremely reactive leading to reattachment or modification of other unprotected side chains, such as the *O*-sulfation of tyrosine, serine or threonine[184]. To reduce undesirable side reactions, scavengers such as phenol, water, thioanisole, EDT, 1-dodecanethiol, TIPS, methanesulfonic acid, indole, DTT and TES are often introduced.

## 2.2 Synthesis of Amino Acid Precursors

### *2.2.1 Synthesis of esters*

In hopes of aiding membrane insertion, dipeptide esters such as $H_2N$-RW-Octyl ester **[3]** were synthesized. Unlike protein E, which is made inside the bacterial cell, these dipeptide analogues need to cross the membrane in order to reach MraY. The addition of long ester chains may assist in the localisation of these compounds in the membrane. Furthermore, esterification of amino acids provides protection of the C-terminus during peptide coupling.

The synthesis of tryptophan methyl ester **[17]** was accomplished by treatment of L-tryptophan with freshly distilled TMSCl in MeOH. This produced a pure white solid with 90% yield. MeOH's low boiling point allowed easy isolation of the ester without the assistance of distillation or flash chromatography.

TMSCl was not effective in esterifying carboxylic acids with larger alcohols such as 1-octanol. To esterify 1g of L-tryptophan with 10mL of 1-octanol (12.6 eq), excess $H_2SO_4$ was used. After 30 minutes, the reaction reached completion producing tryptophan octyl ester **[18]**. Due to the high boiling point of 194-195°C,[185] excess 1-octanol could not be removed *in vacuo*. As a result, vacuum distillation and flash chromatography was utilized.

The octyl ester was isolated by vacuum filtration at 116°C with 62% yield. However, trace amounts of the alcohol was still present in the ester sample. Under vacuum, 1-octanol was expected to be removed at 130°C which is only 14°C above the temperature the ester was found. This small difference in boiling point may have led to trace amounts of the alcohol being distilled with the ester (

Figure 2.12).

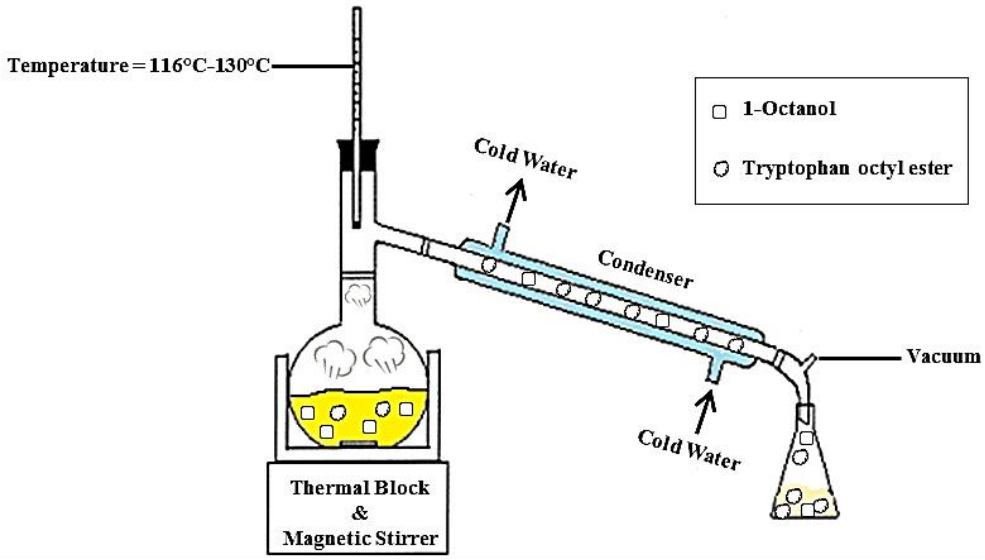


**Figure 2.12: Vacuum distillation of 1-octanol and tryptohan octyl ester.** Between 116°C-130°C trace amounts of 1-octanol was distilled with tryptophan octyl ester.

To isolate the ester by flash chromatography, the silica gel was first deactivated using 5% TEA in EtOAc. This ensured that the free amine of trypothan octyl ester **[18]** was not trapped in the column. 1-octanol was found to have an Rf of 0.7 in 100% EtOAc. **[18]** was sequestered from the deactivated silica baseline by adding MeOH. With an 86% yield, flash chromatography was the better method to isolate the ester from the alcohol. Flash chromatography was quicker and involved less equipment than vacuum distillation.

In the case of glycine octyl ester **[19]**, the Steglich and Hassner method of esterification was used [186,187]. This method involved the treatment of Fmoc-glycine with 1-Octanol, EDCI and DMAP/DCM (Figure 2.13).

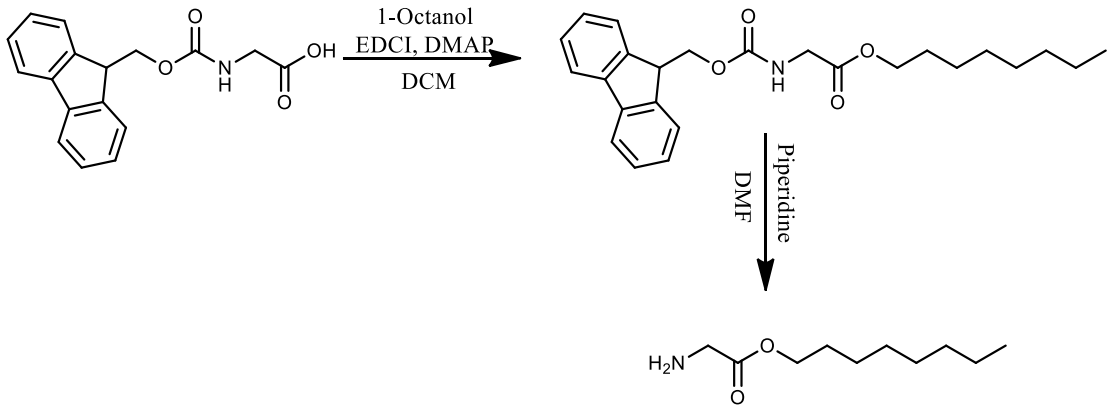


**Figure 2.13: Synthesis of glycine octyl ester**

In the reaction mechanism, the carboxylic acid reacts with EDCI to form Fmoc-glycyl-*O*-acyl-isourea. The nucleophilic catalyst DMAP (4-Dimethylaminopyridine) is then used to catalyse the Stelgich rearrangement via an acetylpyridium ion intermediate[188] (Figure 2.14).

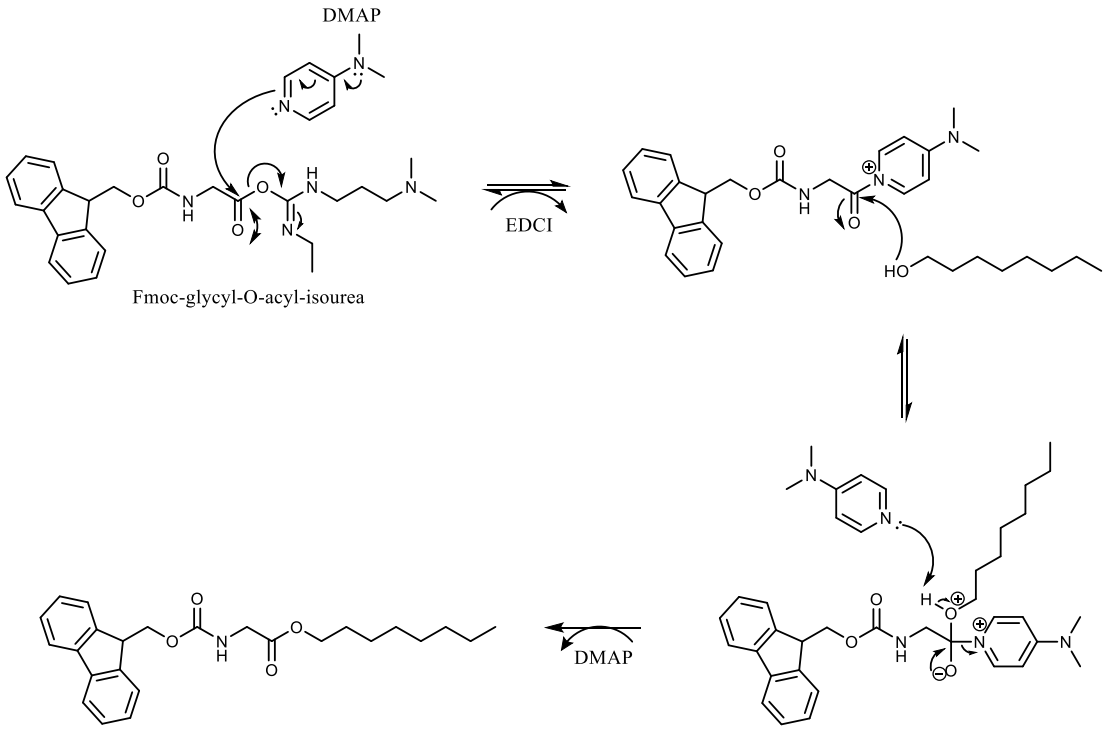


**Figure 2.14: Steglich and Hassner esterification.**

Using this method, Fmoc-glycine octyl ester was synthesized with 92% yield, in comparison to the reported maximum yield of 97% using this methodology[189]. 1-

Octanol did not cause any conflicts in isolation as only the exact equivalence needed was used. The overall yield however, dropped to 60% as a result of deprotection with piperidine to form the final product, **[19]**.

### *2.2.2 Synthesis of N-acyl amino acids*

Modification of the N-terminus, e.g. octanoyl-glycine **[20]** and octanoyl-Arg(PMC)-OH **[22]**, was also desired as an alternative way to localise compounds in the membrane. Acylated amino acid precursors were prepared via the Schotten-Baumann acylation method[190].

The Schotten-Baumann acylation method involved dissolving the amino acid, glycine or $H_2N$-Arg(PMC)-OH, in water with 1.6eq of $NaHCO_3$. To this solution, octanoyl chloride in THF was added dropwise. The salt, $NaHCO_3$, optimised the reaction by ensuring that the amine remained uncharged and deprotonated. This encouraged the addition-elimination reaction, pushing the equilibrium towards the formation of product (Figure 2.15). Extraction into water followed by acidification caused precipitation of the pure products **[20]** or **[22]**.

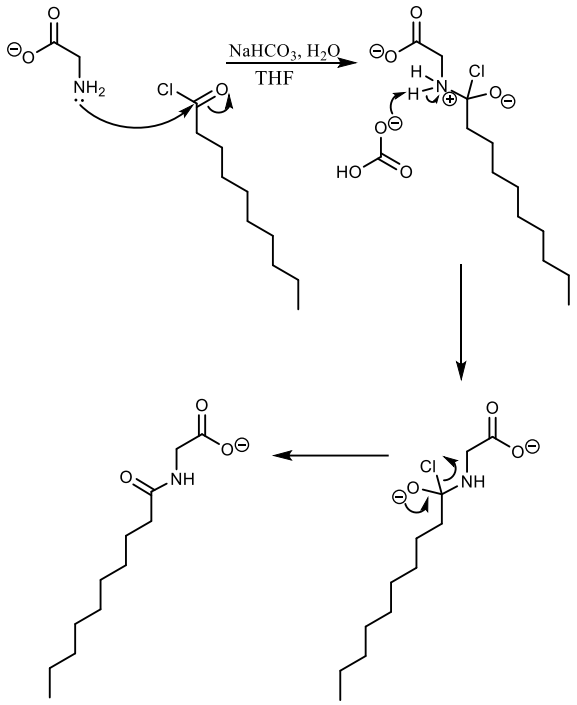


**Figure 2.15: Mechanism of Schotten-Baumann acylation of glycine**

**[20]** and **[22]** were synthesized with 81% and 67% yields, respectively. These yields were likely affected by the final separation step which involved separating a thick oil from an aqueous solution.

## 2.3 Peptide Coupling

Strategic protection of amino acids facilitated the success of peptide couplings. Peptides were synthesized in solution and via SPPS.

### *2.3.1 Solution Peptide Synthesis*

Solution peptide synthesis was first approached in a similar manner as SPPS. Base labile N-protected amino acids were activated using a coupling agent (Figure 2.5) and coupled to the free amine of a C-protected amino acid in the presence of a base ( Figure 2.16). To isolate the dipeptide ester, the fully protected dipeptide was treated with 20% piperidine in DCM.

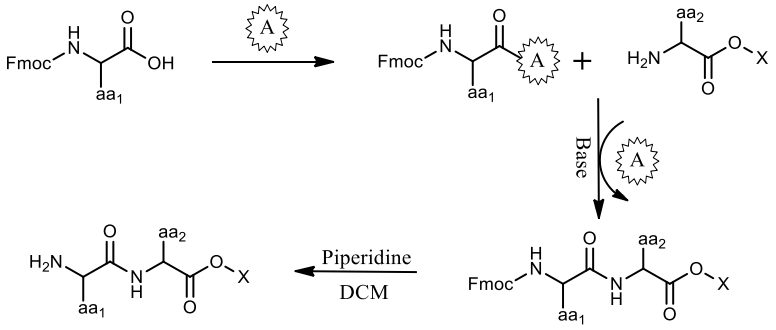


**Figure 2.16: Base labile N-protected peptide couplings.** Where A= activating agent such as HATU, EDCI, DIC, DCC, X=ester

This scheme was attempted on 4 different dipeptides, but was only successful in coupling $H_2N$-RW-Oct **[3]** with 46% overall yield. In every case, the fully protected dipeptide ester was observed by ESI-MS after two days of stirring. After treatment with piperidine, the dipeptide ester was not observed in either the aqueous or organic layer. Using a base labile N-protecting group isn't common in solution peptide synthesis and may have caused undesirable side reactions to consume the dipeptide. Upon treatment with piperidine, ESI-MS revealed a common mass across all four dipeptide reactions, *m/z* 264.2 $[M+H]^+$. This mass corresponded to the fmoc-piperidine adduct which is released upon Fmoc-deprotection (Figure 2.17)[162]. This suggests that fmoc-deprotection by piperidine was successful and further reaction of the dipeptide ester must have occurred.

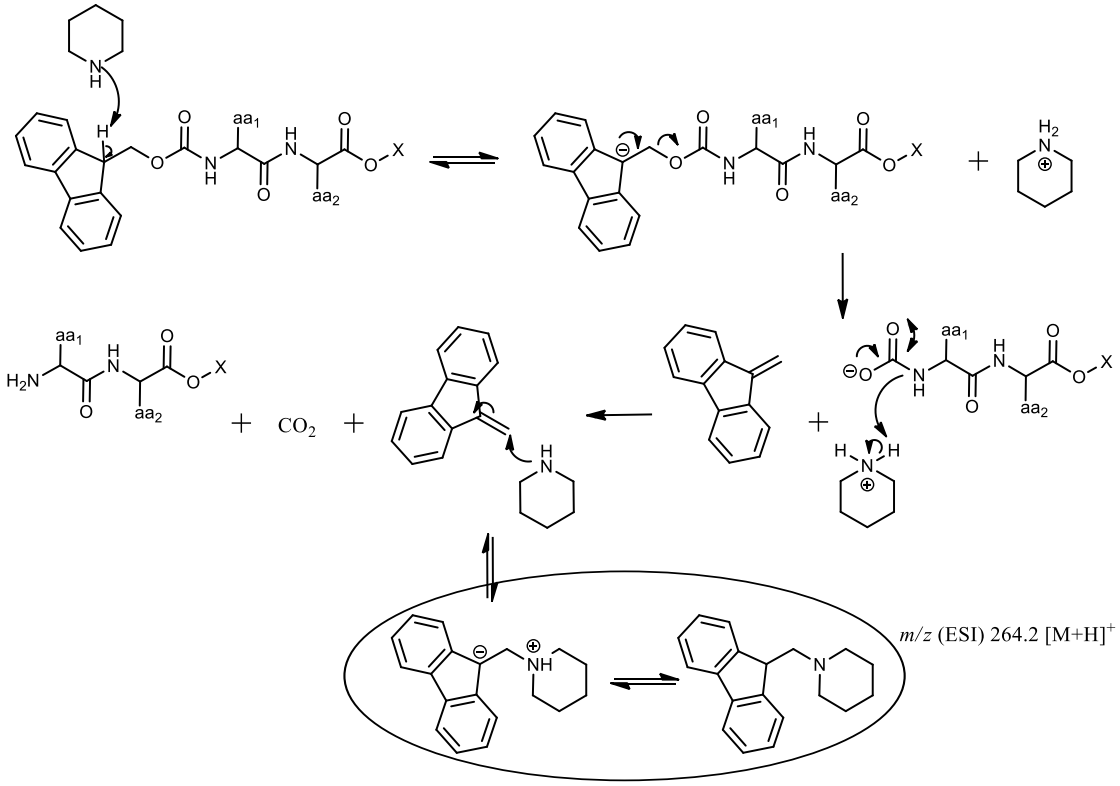


**Figure 2.17: Mechanism of Fmoc-deprotection**

It is possible that during work-up the dipeptide ester may have undergone spontaneous cyclisation under the presence of a base (Figure 2.18)[164]. $Na_2CO_3$(*sat)* may have been too strong of a base for work-up, preventing the dipeptide ester's amine from becoming positively charged. As a result, the amine may have been able to intramolecularly attack the ester carbonyl to form a stable 6-membered ring, 2,5-diketopiperazine.

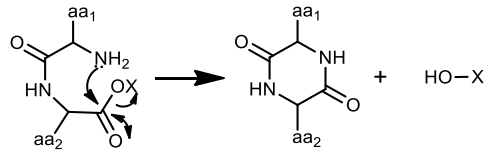

**Figure 2.18: Base-catalysed cyclisation of dipeptide esters to form 2,5-diketopiperazines**

In diketopiperazines, the amide hydrogen and the carbonyl oxygen are *cis* to each other. The conversion from the more stable *trans* confirmation to the less stable *cis* confirmation requires energy. The formation of the stable 6-membered ring 2,5-diketo

piperazine, provides the necessary driving force to induce this *trans/cis* isomerisation[176]. This conformational change is further facilitated by the absence of a bulky side chain. Therefore, ring closure is particularly pronounced in peptides containing glycine[164]. Due to the bulkiness of arginine and tryptophan, conversion from the *trans* to *cis* confirmation may have required more energy than the 2,5-diketopiperazine releases. As a result, $H_2N$-RW-Oct **[3]** was able to escape spontaneous cyclisation.

To avoid this side reaction, the remaining dipeptide esters were synthesized using an acid labile N-protecting group, such as Boc. N-acyl dipeptides did not require cleavage of the N-protecting group and were treated in a similar manner without TFA treatment.

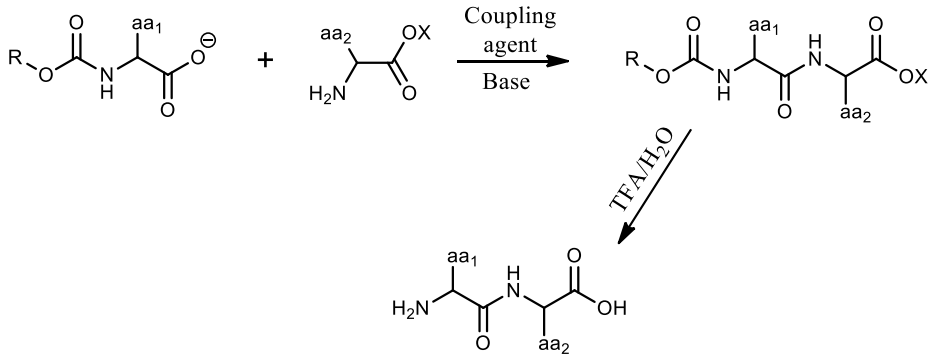


**Figure 2.19: Acid-labile N-protected peptide couplings.** Where R=Boc for dipeptides esters, or Acyl for N-acyl dipeptides, X=ester. When R=Acyl, TFA cleavage is not necessary.

Dipeptides coupled via this route were synthesized in rather low yields ranging from 20-44% (Table 2.1). These low yields are primarily due to the difficulty of coupling arginine and tryptophan which are both very bulky. In addition, side reactions and impurities, which are common in peptide couplings, furthered limited the success of these reactions.

**Table 2.1: Dipeptide couplings**

| Dipeptides | Amino acid precursors | Coupling Agent | % yield |
|---|---|---|---|
| **[1]** $H_2N$-RW-OMe | Boc-Arg-OH, $H_2N$-Trp-OMe | HATU | 30 |
| **[2]** Octanoyl-RW-OMe | Octyl-Arg(PMC)-OH, $H_2N$-Trp-OMe | HATU | 22 |
| **[3]** $H_2N$-RW-Oct | Fmoc-Arg(PMC)-OH, $H_2N$-Trp-Oct | HATU | 42 |
| **[4]** $H_2N$-GW-OMe | Boc-Gly-OH, $H_2N$-Trp-OMe | HATU | 33 |
| **[5]** Octanoyl-GW-OMe | Octyl-Gly-OH, $H_2N$-Trp-OMe | HATU | 20 |
| **[6]** $H_2N$-GW-Oct | Boc-Gly-OH, $H_2N$-Trp-Oct | EDCI | 44 |
| **[7]** $H_2N$-RG-OH | Fmoc-Arg(PMC)-OH, Fmoc-Gly-OH | DIC via SPPS | 35 |
| **[8]** Octanoyl-RG-OH | Octyl-Arg(PMC)-OH, $H_2N$-Gly-OtBu | DCC | 40 |
| **[9]** $H_2N$-RG-Oct | Boc-Arg-OH, $H_2N$-Trp-Oct | EDCI | 38 |

By-products were sometimes observed from side reactions. In the synthesis of octanoyl-glycine **[20]** (Chapter 2.2.2), a small excess of octanoyl chloride formed some octanoic anhydride **[21]** (Figure 2.20). Due to similarities in chemical shift, this side product went undetected by $^1$H-NMR.

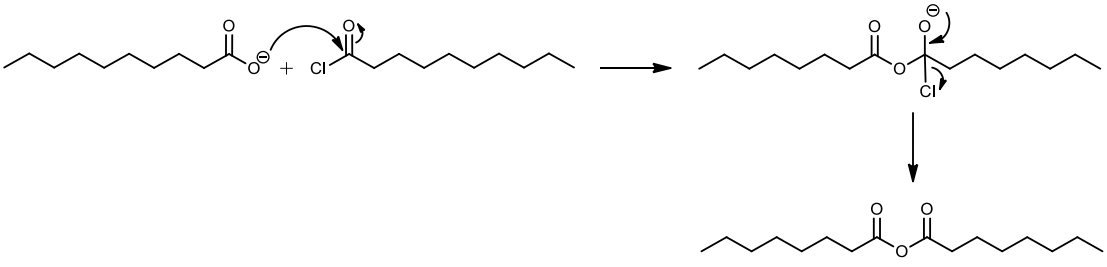


**Figure 2.20: Synthesis of octanoic ahydride.** Addition-elimination reaction of octanoyl chloride and octanoic acid. Octanoic acid originates from the reaction of octanoyl chloride with water.

Upon reaction of the octanoyl-glycine/octanoic anhydride mixture with $H_2N$-Trp-OMe **[17],** two different products formed. The two products were isolated and purified by flash chromatography. ESI-MS identified the major species to have an *m/z* of 343.2 $[M+H]^+$ and the minor species to have an *m/z* of 401.2$[M+H]^+$ - a difference

of 58 Da. $^{1}$H-NMR revealed that the major species was missing one of its α-protons. NMR and mass spectroscopy data revealed that Octanoyl-Trp-OMe **[23]** was the major product and Octanoyl-GW-OMe **[5]** was the minor product.

**[23]** resulted from the reaction of **[21]** with **[17]**. The free amine of $H_2N$-Trp-OMe **[17]** nucleophilically attacked the anhydride **[21]** to form the shorter peptide product and caprylic acid (common name for octanoic acid) (Figure 2.21). This product lacked $C_2H_3NO$ which has a molar mass of 57 Da. Octanoic anhydride **[21]** is expected to be more reactive than octanoyl-glycine **[20]**,[191] which is why this shorter peptide was the major species. It is clear from this example, that it is vital to properly characterize and purify all intermediates in multi-step reactions.

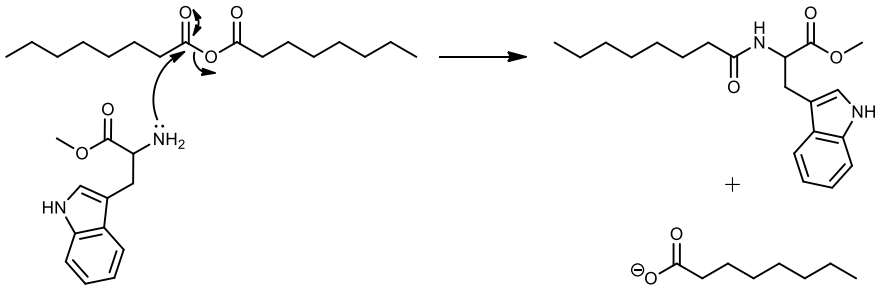

**Figure 2.21: Reaction of octanoic anhydride with $H_2N$-Trp-OMe**

Another peculiar reaction involved the synthesis of $H_2N$-RW-OMe **[1]** using an acid labile N-protecting group. Boc-Arg-OH was treated with HATU in minimum dried DCM. L-tryptophan methyl ester hydrochloride was added to the stirred solution and cooled to 0°C. TEA was added and the reaction was stirred for 3 days. After work-up, the organic layer was dried with $MgSO_4$ and concentrated *in vacuo*. In order to characterize the compound by ESI-MS, MeOH was added. The addition of MeOH caused a white precipitate to form. ESI-MS identified the liquid to be the desired intermediate, Boc-RW-OMe **[24]**. The precipitate was insoluble in most solvents with the exception of acetone, where it was partially soluble. With permission from the

NMR technicians at the University of Warwick, an NMR experiment was conducted on the partially soluble product. $^{1}$H-NMR produced a spectrum that was interpreted as Boc-RW-OH **[25]**. It is possible that ester linkage of **[24]** may have partially hydrolysed during acid extraction to form Boc-RW-OH•HCl. Boc-RW-OH•HCl may have then formed an insoluble quaternary ammonium salt with TEA via a process called quaternisation[192]. The formation of this insoluble product caused a dramatic loss in the yield of **[24]**. **[24]** was then treated with 7:3 TFA/DCM to isolate the desired product, **[1]**.

Carbodiimides such as DCC or DIC generally gave very low yields for Arg-Trp dipeptide couplings, indicating that they are sensitive to steric hindrance. In practice they were only able to tolerate one bulky amino acid per coupling, not two. As a result, Octanoyl-RG-OH **[8]**, $H_2$N-RG-Oct **[9]** and $H_2$N-GW-Oct **[6]** were the only compounds synthesised using carbodiimides (Table 2.1). The remaining bulky amino acids required treatment with more reactive coupling agents such as HATU.

Racemisation did not occur when 1-2eq of Oxyma pure or HOBt was used in carbodiimide couplings, as judged by $^{1}$H-NMR. As expected, HATU couplings did not experience racemisation.

In conclusion, due to the difficulties of coupling Arg- and Trp- amino acid derivatives, solution peptide synthesis was not the optimal method for the synthesis of most of the desired dipeptides. Side reactions and impurities significantly affected the yield of these dipeptide derivatives. These reactions were not optimised, as only a small amount of product was needed for biological testing.

The remaining peptides were synthesised via manual SPPS, which proved to be the more reliable and superior coupling procedure.

### *2.3.2 Solid Phase Peptide Synthesis*

Lytic E RWXXW peptide analogues were synthesized on a fritted-filtered reaction vessel using a standard Fmoc SPPS procedure[162] (Figure 2.22).

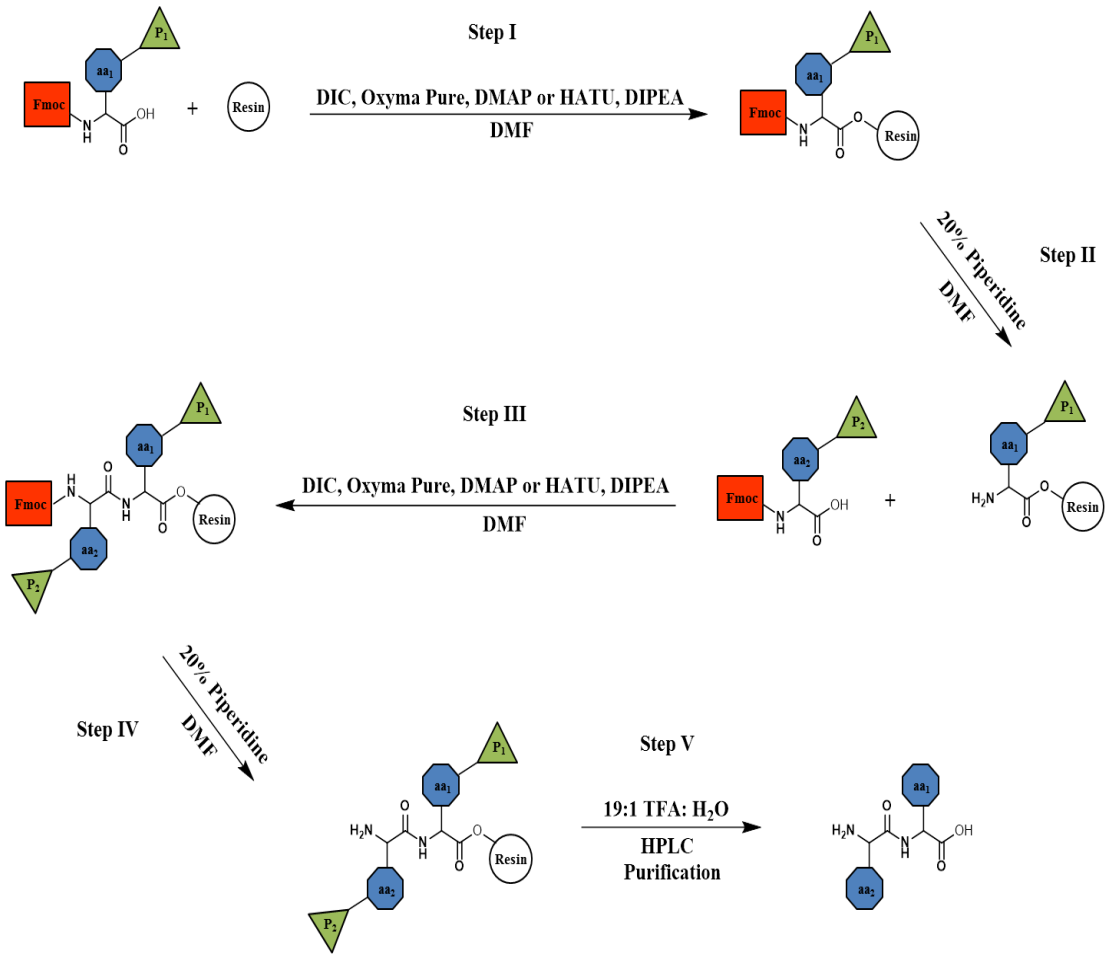


**Figure 2.22: Scheme for SPPS**

Similar to solution peptide synthesis, SPPS requires activation of the C-terminus to assist in peptide couplings. In a dried RBF Fmoc-protected amino acids (2-4eq) were dissolved in minimum dried DMF/DCM. Following the addition of a coupling agent (2-4eq) and a catalytic base such as DMAP or DIPEA (1-2.5eq), the mixture was immediately added to 1eq. of swollen resin and agitated gently with $N_2$ gas for 1-2 days. To cap any remaining unloaded resin beads, anhydrous MeOH was later added to the resin and agitated under $N_2$ gas for 1 hour.

Upon several washes with dried DMF and DCM, Fmoc-protecting groups were removed by treatment with 20-30% piperidine in DMF for 2 hours. Following another series of washes, activated amino acids were added to the loaded resin in a similar manner to the first step.

Total isolation of dipeptides involved Fmoc-deprotection followed by treatment with TFA/$H_2O$. Loaded resins were dried under vacuum for 30 minutes and transferred to a dried RBF in preparation for resin cleavage. The dried resin was treated with 19:1/TFA:$H_2O$ (1mL per 100mg of loaded resin), flushed with $N_2$ gas, and stirred gently overnight. The resin was removed by filtration under reduced pressure using a sintered glass funnel. The resin was washed twice with neat TFA to assist in the removal of any loosely bound peptide product. Filtrates were combined and TFA was evaporated using a $CO_2$/acetone rotary evaporator. Cold ether was used to precipitate the oligopeptides. The product was isolated and dried further with a high vacuum pump. The dried product was then dissolved in water and lyophilized overnight.

Due to its affordability and mild treatment conditions, Wang resin is the standard resin used in Fmoc chemistry for C-terminus acids.[193] $H_2N$-RG-OH **[7]** was synthesised on the Wang resin using 4 eq. DIC, 4 eq. Oxyma Pure and 1 eq. DMAP in minimum dried DMF. This product was purified via HPLC with 25% yield relative to resin loading (Table 2.1). A range of different coupling agents, solvents and reaction times were explored in the hopes of synthesising $H_2N$-GW-OMe **[5]** and $H_2N$-RW-OMe **[1]**, but none of these products could be synthesised using the Wang resin.

One common experimental error in manual SPPS is insufficient swelling time. The nucleophilic linkers of resins are located in small cavities inside the resin beads. Peptide coupling takes place inside these cavities and not on the surface of the resin[194]. If the resin is not properly swelled with DCM these cavities remain very tight

and narrow, preventing amino acids from entering.[195] With swelling times over 1.5 hours, triple the recommended time[162], it is unlikely that the resin was not properly swelled. Other factors such as steric hindrance, lack of fluidity and poor reactivity are the most probable reasons for experimental failure.

Attachment of the first amino acid is the most critical step in SPPS. This step involves a nucleophilic attack on the carbonyl of a protected and activated amino acid by the Wang resin's linker (Figure 2.23). The activating group and the side chain protecting group of Fmoc-Trp(Boc)-*O*-acyl-isourea sterically hinders the carbonyl. Typically, this can be compensated by solvent fluidity which increases the probability of contact between two chemical species. However, in manual SPPS the nucleophile is stationary and only minimal stirring can be achieved via $N_2$ gas. Steric hindrance as well as the weak reactivity of an $S_N2$ reaction severely limited the attachment of the first amino acid. As a result, only Fmoc-glycine-*O*-acyl-isourea was able to successfully attach to the Wang resin and produce $H_2N$-RG-OH **[7]**.

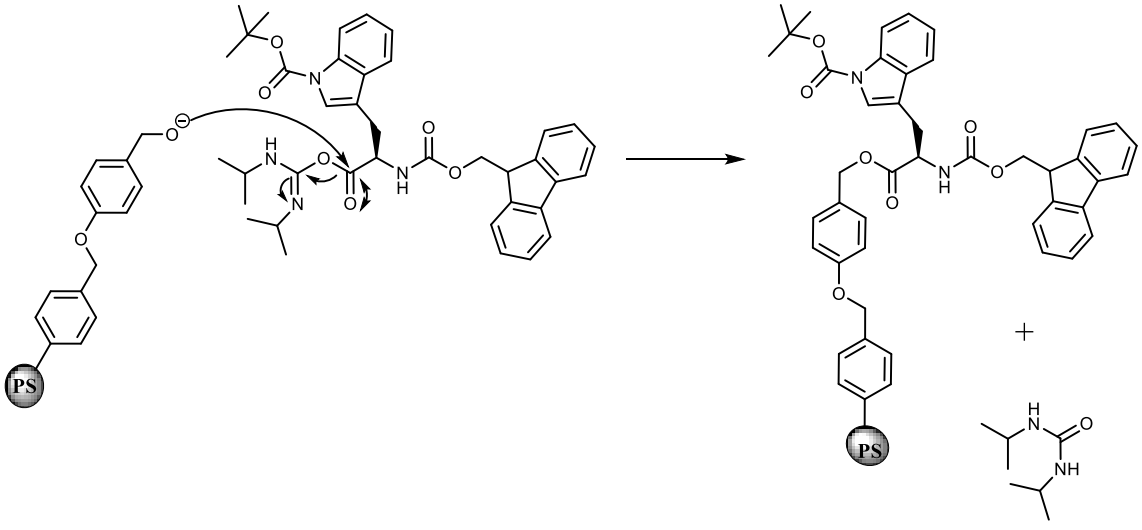


**Figure 2.23: Attachment of first amino acid to the Wang resin.** Nucleophilic attack on the carbonyl of Fmoc-Trp(Boc)-O-acyl-isourea.

To determine the level of attachment, a spectrophotometer was utilized. Using 20% piperidine/DMF as a blank, this experiment measured the loss of piperidine during deprotection to form the Fmoc-piperidine adduct (Figure 2.17). Amino acid loading was determined using Equation 2.1. This value was then compared to the actual resin loading determined by the manufacturer, Merck Novabiochem. The final yield for $H_2N$-RG-OH **[7]** was calculated relative to the resin loading determined from the spectrophotometer.

**Equation 2.1**

$$\text{Loading (mmol/g)} = (\text{Abs}_{290\text{nm}})/(\text{mg of sample} \times 1.75)^*$$

* = Based on a molar *absorptivity* ($\varepsilon$) = $5253 M^{-1}cm^{-1}$

Given the problems experienced with the Wang resin, alternative resins were investigated to synthesise the remaining peptides. 2-Chlorotrityl chloride resin was found to be an effective alternative to the Wang resin using the same SPPS procedure (Figure 2.22)[168]. Although more expensive than the Wang resin, this resin only required 2 eq. of Fmoc-amino acid compared to the 4 eq. needed by the Wang resin. The advantage of using 2-chlorotrityl resin over the standard Wang resin lies in its ability to attack a free carboxylic acid in an $S_N^1$ fashion (Figure 2.24). As a result, activation of the first incoming amino acid is not necessary allowing attachment of bulkier amino acids such as Fmoc-Trp(boc)-OH.

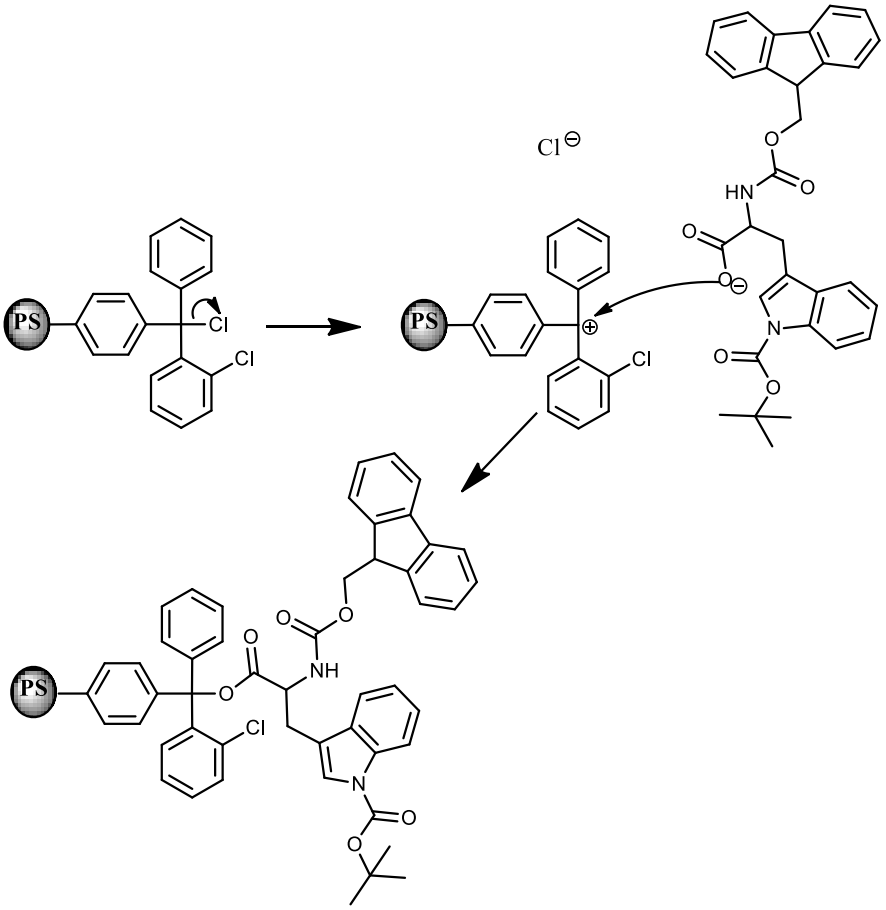


**Figure 2.24: Attachment of the first amino acid to 2-chlorotrityl chloride resin**

Using 2-chlorotrityl chloride resin RWGLW **[10]**, RGGLW **[11]**, GWGLW **[12]**, RWGGW **[13]**, RWGLG **[14]**, EHWGGG **[15]** and ERWGGW **[16]** were successfully prepared in yields ranging from 24%-87% on a $6.1 \times 10^{-4}$ mol scale (Table 2.2). Pentapeptides and hexapeptides were primarily synthesised using 2 eq. of HATU as the coupling agent. DIC (2 eq) and Oxyma pure (2 eq) was used when coupling consecutive glycines in compounds such as RGGLW **[11]**, EHWGGG **[15]**, ERWGGW **[16]** and RWGGW **[13]**. Using DIC at these specific steps lowered the overall cost of SPPS.

**Table 2.2: Pentapeptide and hexapeptide couplings using 2-Chlorotrityl chloride resin**

| Peptides | Coupling Agent(s) | Coupling time (days) | % yield | Cleavage (hrs) |
|---|---|---|---|---|
| **[10]** RWGLW | HATU | 8 | 87 | 24 |
| **[11]** RGGLW | DIC/HATU | 7 | 24 | 6 |
| **[12]** GWGLW | HATU | 7 | 50 | 12 |
| **[13]** RWGGW | DIC/HATU | 8 | 28 | 6 |
| **[14]** RWGLG | HATU | 7 | 36 | 6 |
| **[15]** EHWGGG | DIC/HATU | 9 | 75 | 18 |
| **[16]** ERWGGW | DIC/HATU | 10 | 69 | 18 |

Coupling times varied based on the number of adjacent bulky amino acids. Peptide couplings which involved two bulky amino acids such as Arg-Trp required two days of coupling. Peptide couplings which involved only one bulky amino acid such as Gly-Trp required only one day of coupling.

The use of a fritted-filtered reaction vessel also greatly affected the coupling time and success of peptide couplings. This reaction vessel hindered peptide couplings as it was unable to control reaction conditions and allowed moisture to collect. Unlike automated systems, which have short reaction times (<5min) and can regulate the temperature, partial pressure and other factors according to the type of coupling,[196] this reaction vessel only allowed couplings at room temperature and at atmospheric pressure, which resulted in multi-day experiments.

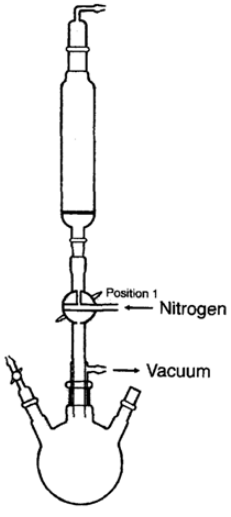


**Figure 2.25: Manual SPPS fritted-filtered reaction vessel.**

The yields of these compounds were heavily affected by TFA cleavage time. Compounds cleaved over 24 hours were isolated with yields between 87%-96% (Table 2.2). Compounds cleaved within 6 hours resulted in poor yields. To isolate any remaining bound peptides, resins were re-cleaved for an additional 18 hours. TFA/$H_2O$ was removed by a $CO_2$/acetone rotary evaporator followed by precipitation with cold ether. Unfortunately, the blue precipitate was insoluble and therefore could not be analysed by ESI-MS or NMR. It appeared that storage of loaded resins followed by re-cleavage may have caused degradation of the resin and/or peptide.

The use of scavengers such as phenol, water, thioanisole and EDT did not greatly affect the yield or purity of peptides upon TFA cleavage. These TFA cocktails had to be prepared anew before each use[162]. The lengthy preparation of these cocktails was found to be an unfavourable use of time, given that the yield or purity was not enhanced by its use. 19:1/TFA:water was found to be a simple and suitable TFA cocktail. This cocktail was effective at isolating the peptides whilst scavenging Boc, *i*Bu and PMC/Pbf.[197]

## 2.4 HPLC Purification

Purification of the RWXXW analogues via HPLC was accomplished in the three steps: (I) optimisation of the gradient, (II) collection of the desired peak and (III) analysis by HPLC and high resolution ESI-MS.

An Agilent Technologies series 6130 Quadrupole LC/MS instrument equipped with a C18 reverse phase column was initially used to determine the %B at which the desired peptide elutes. This employed a binary mixture of eluents A ($H_2O$ with 0.1%TFA) and B (MeOH with 0.1%TFA) and a standard linear gradient of 5% to 100%B in 60

minutes at a flow rate of 1 mL/min. By identifying the %B the peptide eluted at, the gradient was able to be optimised before purification on a preparative HPLC.

Purification was conducted on an Agilent Technologies series 1200 Preparative HPLC instrument equipped with an Agilent Xorbax XDB-C18 preparative column (P/No: 970150-902, size: 21.2x150mm 5micron). Depending on the tryptophan content, compounds were monitored at either 220nm or 280nm for compounds with multiple tryptophan residues. In the case of $H_2N$-GW-Oct **[6]** (Figure 2.26), the product was found to have a retention time of 12.2 minutes using a linear gradient of 50%-100%B over 20 minutes at 220nm.

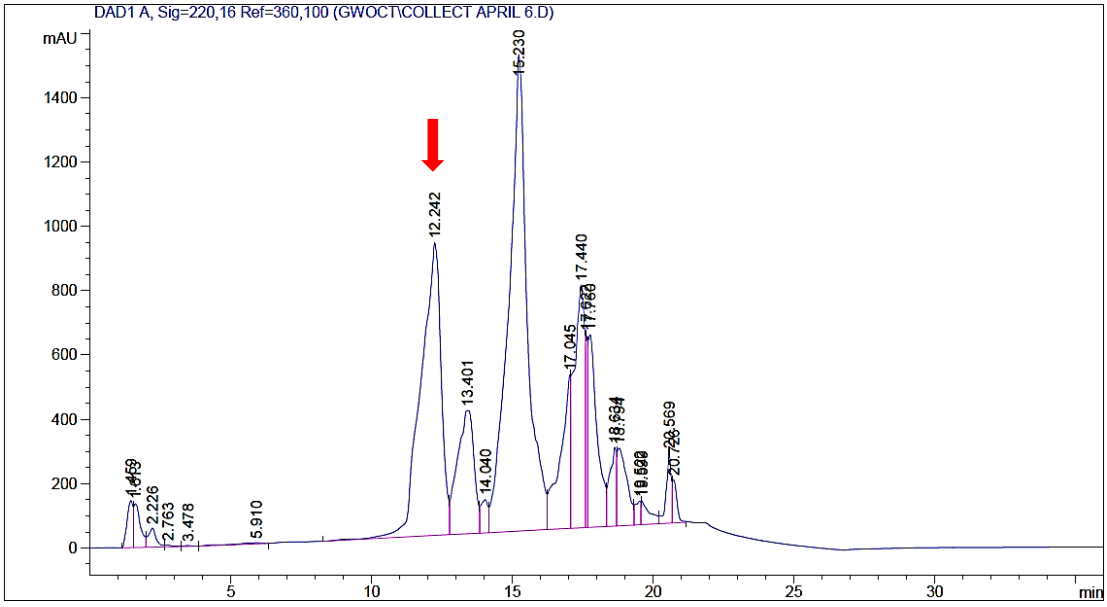


**Figure 2.26: Preparative HPLC chromatograph of $H_2N$-GW-Oct [6]**

To ensure purification was successful, the purified compound was re-injected to the preparative HPLC column using the same gradient but at a wavelength of 210nm. If the chromatograph contained multiple peaks, isolation of the desired peak was repeated. The chromatograph of the pure $H_2N$-GW-Oct **[6]** is given in Figure 2.27. The compound was found to be pure (>98%) with the exception of a small amount of simple salts which commonly elute instantly. A slight change in the retention time was also observed and may have resulted from the presence of an air bubble in the

column. $^{1}$H-NMR, $^{13}$C-NMR, and high resolution mass spectroscopy was also used to confirm purity.

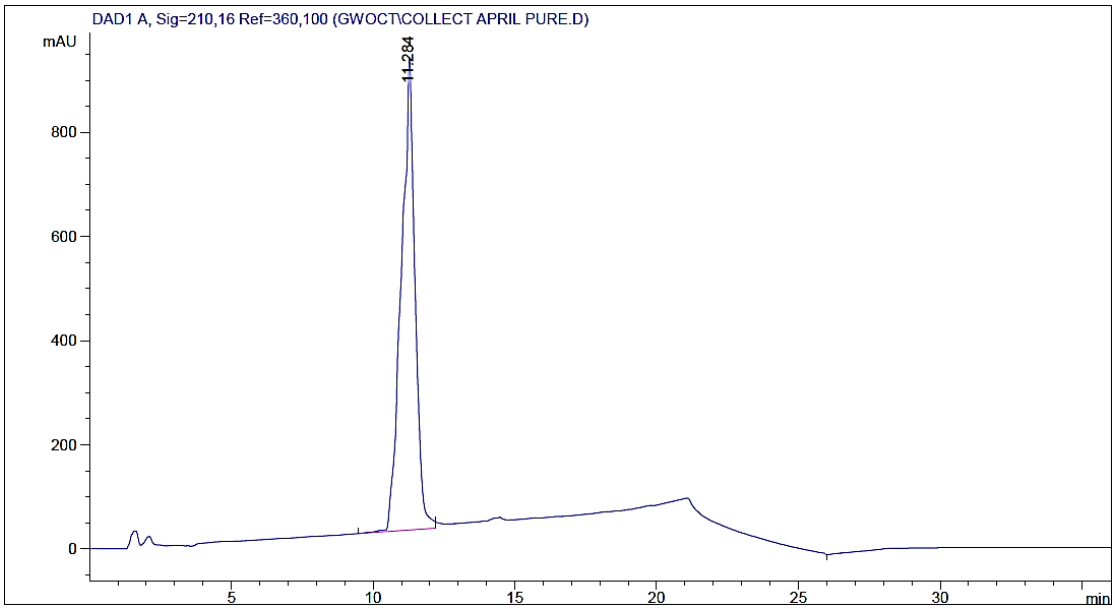


**Figure 2.27: Re-injection of pure $H_2$N-GW-Oct to a preparative HPLC column at 210nm.**

## 2.5 Conclusion

Synthesis of the desired Arg-Trp containing peptides was found to be more difficult than anticipated. Both Arg and Trp are relatively bulky amino acids, which meant there were relatively difficult peptides to synthesise[198].

In solution peptide synthesis, many side reactions occurred which limited the yield and purity of reactions. When using a base labile N-protecting group, spontaneous cyclisation of dipeptides esters often occurred upon work-up. The cyclised products, 2,5-diketopiperazines, were not readily observed by ESI-MS and could not be identified with confidence by $^{1}$H-NMR. However, identification of the Fmoc-piperidine adduct by ESI-MS suggested that Fmoc-deprotection was successful and that further reaction of the dipeptide ester must have occurred.

In the synthesis of amino acid precursors it was very important to use precise amounts of reagents. Excess acyl chloride led to the production of anhydrides which are more

reactive than *N*-acyl amino acids. As a result, a shorter peptide product evolved upon treatment with a C-protected amino acid. It is clear from this example, that it is vital to properly characterize and purify all intermediates in multi-step reactions.

The acid labile Boc N-protected group was the most reliable protecting group in solution peptide synthesis. This allowed all protecting groups to be removed simultaneously via acid treatment. However, poor yields were still reported using this route which led to adaptation of SPPS.

SPPS proved to be the superior method for the synthesis of bulky amino acids. The standard Wang resin was found to only accept small, unhindered amino acid for the initial attachment. 2-Chlorotrityl chloride resin was able to tolerate the attachment of bulky amino acids. This was facilitated by the more reactive $S_N1$ reaction involved in the attachment of the first amino acid.

# Chapter 3: *In vitro* Assays for MraY Activity

## 3.1 Fluorescence Enhancement Assay

A major goal of this project was to examine and characterise the inhibition of MraY by synthetic analogues of protein E which contain the RWXXW motif. In 1977, Weppner and Neuhaus reported that *S. aureus* MraY could accept substrate analogues with a fluorescent tag[199-200]. Certain fluorescent reporters such as dansyl chloride and fluorescein have been previously shown to exhibit polarity-dependent fluorescence which is especially pronounced upon entry into the membrane[201]. Utilising this polarity-dependent fluorescence, Weppner and Neuhaus were able to monitor the MraY reaction.

To generate the fluorescently tagged substrate, Weppner and Neuhaus treated 0.5µmol UDP-MurNAc-pentapeptide with 21µmol of 5-(dimethylamino)naphthalene-1-sulfonyl chloride (dansyl chloride) in 50% acetone and 0.25M $NaHCO_3$[199]. This led to the attachment of a dansyl functional group to the ε-amino of L-Lys or *m*-DAP of UDP-MurNAc-pentapeptide (Figure 3.1).

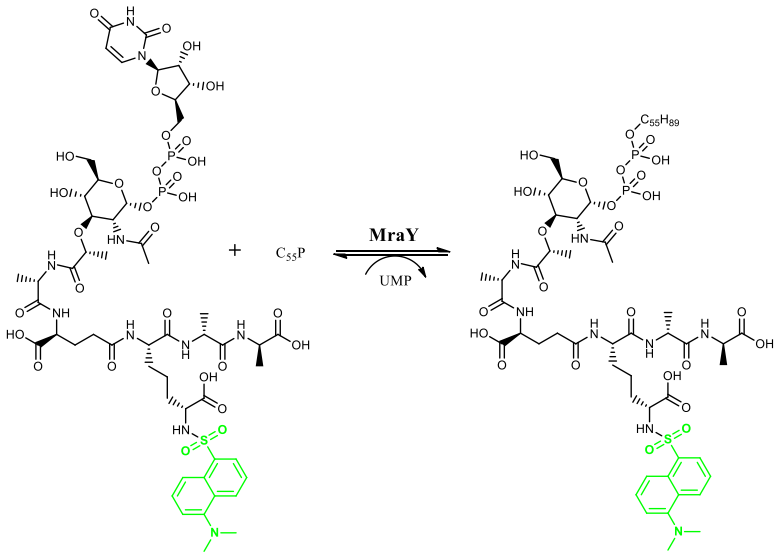


**Figure 3.1: MraY catalysed reaction of UDP-MurNAc-($N^{\varepsilon}$-Dns)pentapeptide with $C_{55}$-P to form dansyl-Lipid I**

In the presence of UDP-MurNAc-($N^{\varepsilon}$-Dns)pentapeptide Weppner and Neuhaus observed a 30nm blue shift in the fluorescence emission spectrum of the MraY reaction[199]. This shift corresponded to the incorporation of the dansyl moiety into the hydrophobic membrane to form dansyl-lipid I (Figure 3.1). Phospho-MurNAc-($N^{\varepsilon}$-Dns)pentapeptide, which is not a substrate for MraY, could not be incorporated in the membrane and therefore a shift in fluorescence was not observed[199].

Incorporation of the fluorescently tagged substrate into the membrane as dansyl-lipid I was confirmed by quenching studies which utilised nitroxyl stearate derivatives. Nitroxyl stearates are known to partition the fluid hydrocarbon region of the membrane[202]. Using various nitroxyl stearate derivatives which differ with respect to the depth of the nitroxide in the membrane, Weppner and Neuhaus demonstrated that dansyl-lipid I was embedded near the membrane surface[200].

Based on the work of Weppner and Neuhaus, Brandish (1995) developed a rapid continuous assay methodology[111-72] which has recently been used for inhibitor screening by PhD candidate Agnes Mihalyi (unpublished, 2013). This assay was used to test the inhibitory activity of synthetic RWXXW analogues against membrane bound MraY.

### *3.1.1 Isolation of membranes containing overexpressed MraY enzymes*

Previous studies on the inhibition of MraY by Epep were carried out using membranes containing overexpressed *E. coli* MraY. It was also of interest to assay against MraY enzymes from other bacterial strains in which residue Phe288 is not conserved. Protein E is known to not be active against *B. subtilis* MraY[64], which lacks Phe288, so this enzyme was of interest as a negative control. Antimicrobial peptides containing Arg-Trp are known to be active against *P. aeruginosa* and *S. aureus*,

which lack Phe288 but contain Phe residues nearby in transmembrane helix 9 (Bugg, unpublished).

In this research project, MraY was used to determine the inhibitory activity of RWXXW analogues. These various strains of MraY were of interest due to the presence and/or location of aromatic residue Phe288 (Table 3.1), which was previously shown to cause resistance to protein E in *E. coli* (Chapter 1.6).

**Table 3.1: Alignment of various strains of MraY relative to Phe288 of *E. coli* MraY**

| MraY strains | Sequence |
|---|---|
| *E. coli* | AVLLRQE**F**LLVIMGGVFVVE |
| *P. aeruginosa* | AVIVRQEIVL**F**IMGGVFVME |
| *S. aureus* | SIMLNQELSLI**F**IGLVFVIE |
| *B. subtilis* | AILTKLEILLVIIGGVFVIE |
| *M. flavus* | AIFTRTEILVAVLAGLMVAI |

In *P. aeruginosa* MraY, a Phe residue is present at position 291, 0.83 turns down the helix with respect to *E. coli* MraY (Figure 3.2). In *S. aureus* MraY, a Phe residue is present at position 292, 1.1 turns down the helix with respect to *E. coli* MraY. In B subtilis and *M. flavus* MraY, there are no aromatic residues in this region. Across these five strains of MraY, *E. coli* residue Glu287 is conserved. Using these various membranes, it will be possible to speculate on the importance and the flexibility in the interactions between protein E and *E. coli* MraY relative to residues Phe288 and Glu287.

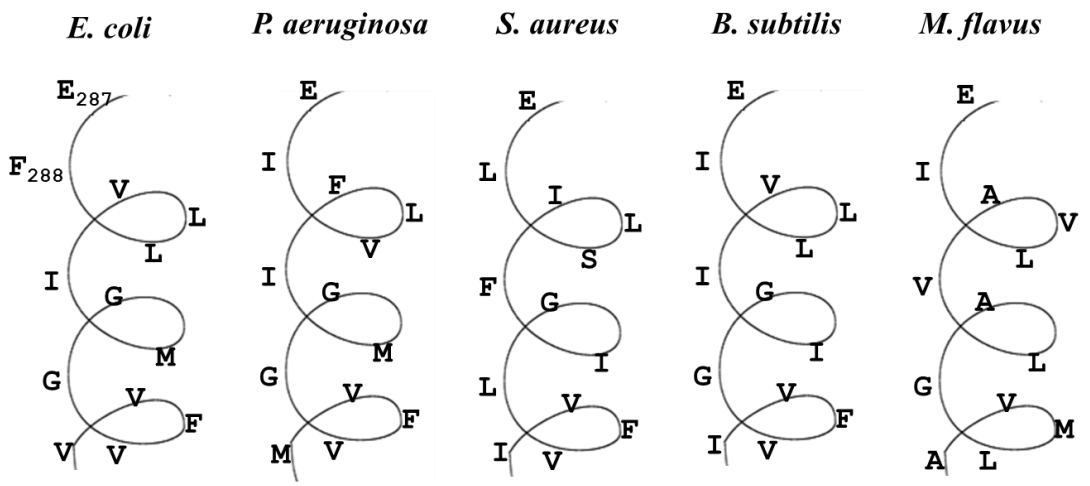


**Figure 3.2: Predicted secondary structure of MraY helix 9 relative to *E. coli* Phe288.**

Mihalyi overexpressed *E. coli* and *P. aeruginosa* membrane-bound MraY from a pJfy3c vector in *E. coli* DH5α cells. Strep-tagged *B. subtilis* and *S. aureus* MraY was cloned by MOAC project student Amy O'Reilly on to a pET52b plasmid and overexpressed in *E. coli* C43 cells. These overexpressed membrane bound MraY's were used in this project in the fluorescence assays. Although the membranes will contain some endogenous *E. coli* MraY, the abundance of the WT enzyme is very low and control assay using the corresponding empty vector showed >40 fold reduced activity in each case.

The total protein concentration of overexpressed membranes was determined using the Bradford assay. The total protein concentration of membranes is given in Table 3.2. These values correspond to the total protein concentration which includes overexpressed MraY and endogenous membrane proteins.

**Table 3.2: Total protein concentrations in MraY membranes**

| | mg/mL |
|---|---|
| *E. coli* MraY | 7.3 |
| *P. aeruginosa* MraY | 1.3 |
| *B. subtilis* MraY | 11 |
| *S. aureus* MraY | 3.3 |
| *M. flavus* MraY | 3.3 |

The fluorescent MraY substrate UDP-MurNAc-($N^{\varepsilon}$-Dns)pentapeptide was provided by Mihalyi who utilised methods from Lugtenberg *et al*, Fluoret *et al* and Weppner Neuhas[92,203,204].

Lipid carriers, $C_{55}$-P and $C_{35}$-P were purchased from Laroden AB. Heptaprenyl phosphate ($C_{35}$-P), a simple isoprenoid composed of 35 carbon units was reported to produce similar results *in vitro* as $C_{55}$-P (Mihalyi, unpublished 2013). As a result, $C_{35}$-P was frequently used in this research project.

### 3.2 Plate reader assay

A Tecan GENios plate reader was used to determine the inhibitory activity of synthetic RWXXW analogues. To a 96 well plate, 10µL of overexpressed MraY membranes was added to 85µL of master mix and 5µL of the inhibitor (final concentration 100µg/mL). The master mix contained 21.µM UDP-MurNAc-($N^{\varepsilon}$-Dns)pentapeptide and 47.2 µM of $C_{55}$-P or 70.6 µM of $C_{35}$-P in a buffer solution containing 100mM Tris base, pH 7.5 and 25mM $MgCl_2$. The final protein concentrations in *E. coli* and *P. aeruginosa* MraY membranes were 0.7 mg/mL and 0.13 mg/mL, respectively**.** The MraY catalysed reaction was monitored at an excitation wavelength of 340nm and an emission wavelength of 535nm.

The production of dansyl-lipid I corresponded to an increase in fluorescence which was measured at 5 minute intervals in quadruplicates (Figure 3.3). MeOH was used as the negative control. Tunicamycin and Epep, at a final concentration of 100µg/mL, were used as the positive controls. Over time, compounds that did not inhibit the production of dansyl-lipid I were expected to cause an increase in fluorescence and behave similar to the negative control. Compounds that did inhibit the production of

dansyl-lipid I were expected to behave similar to the positive controls and retain a relatively constant fluorescence emission spectrum.

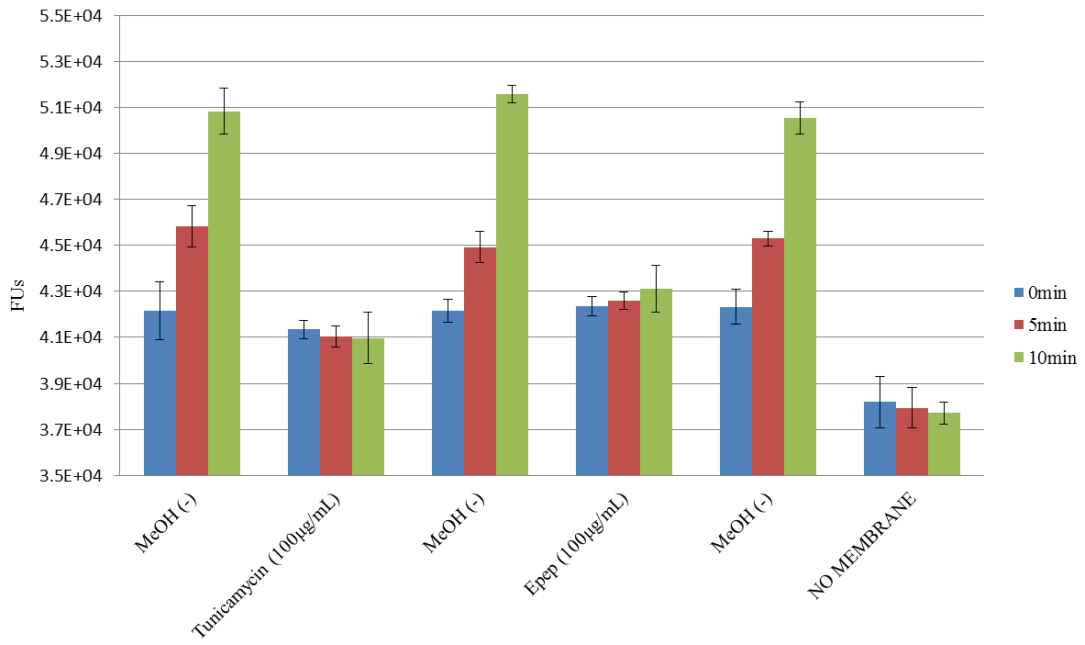


**Figure 3.3: Fluorescence emission of the *E. coli* MraY reaction in the presence of control inhibitors at 100µg/mL.** Fluorescence units (FUs) was recorded before the addition of membrane bound MraY (t=0) and within 5 minutes and 10 minutes of its addition.

Figure 3.4 shows the fluorescence emission spectrum of the *E. coli* MraY reaction in the presence of Arg-Trp dipeptide analogues at concentration 100µg/mL. The MraY reaction seemed to be inhibited by $H_2N$-GW-Oct **[6],** indicative by a lower fluorescence emission after 10 minutes in comparison to the negative control. A few other inhibitors reduced the fluorescence emission of the MraY reaction (RW-OMe **[1]**, GW-OMe **[4]**, $H_2N$-RG-OH **[7]**), but only 5-10% inhibition was observed at a concentration of 100µg/mL.

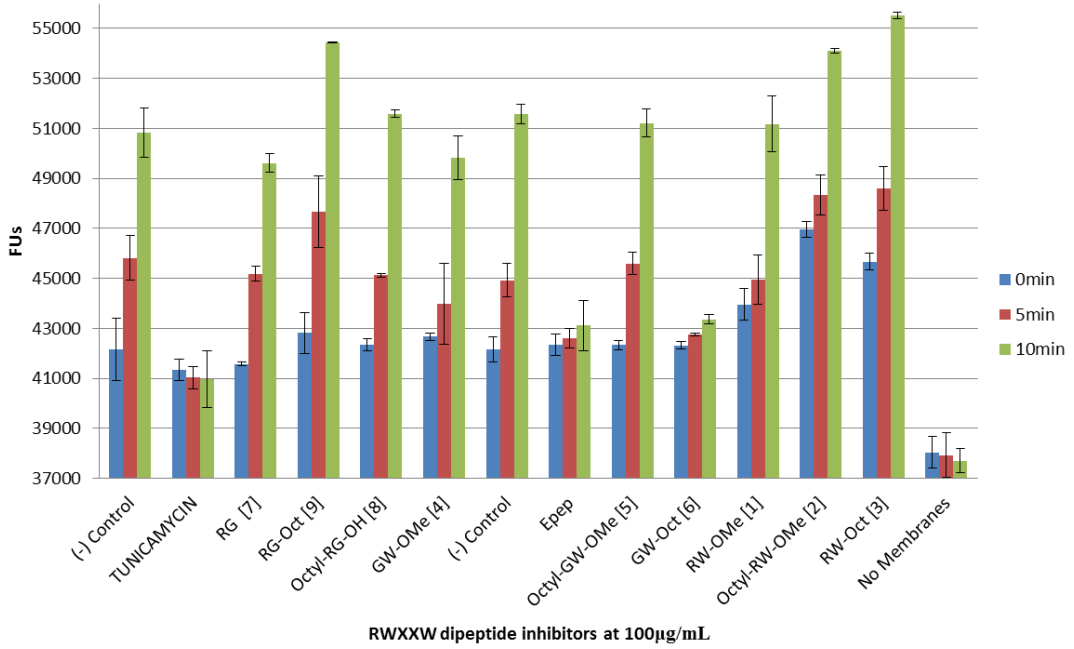


**Figure 3.4: Fluorescence emission of *E. coli* MraY upon treatment with RWXXW dipeptide analogues at 100µg/mL.** Fluorescence units (FUs) was recorded before the addition of membrane bound MraY (t=0) and within 5 minutes and 10 minutes of its addition.

The inhibitory activity of these Arg-Trp dipeptide analogues were tested against *P. aeruginosa* MraY (Figure 3.5). Epep did not inhibit the reaction of *P. aeruginosa* MraY, apparent by an increase in the fluorescence emission of the MraY reaction. In this assay, $H_2N$-GW-Oct **[6]**, $H_2N$-RG-OH **[7]** and Octyl-RG-OH **[8]** were found to limit the production of dansyl-lipid I by inhibiting *P. aeruginosa* MraY.

It's interesting that in both organisms, $H_2N$-GW-Oct **[6]** was able to affect the production of dansyl-lipid I. Dipeptide $H_2N$-RG-OH **[7]** was found to also inhibit *P. aeruginosa* MraY and *E. coli* MraY (though not extensively).

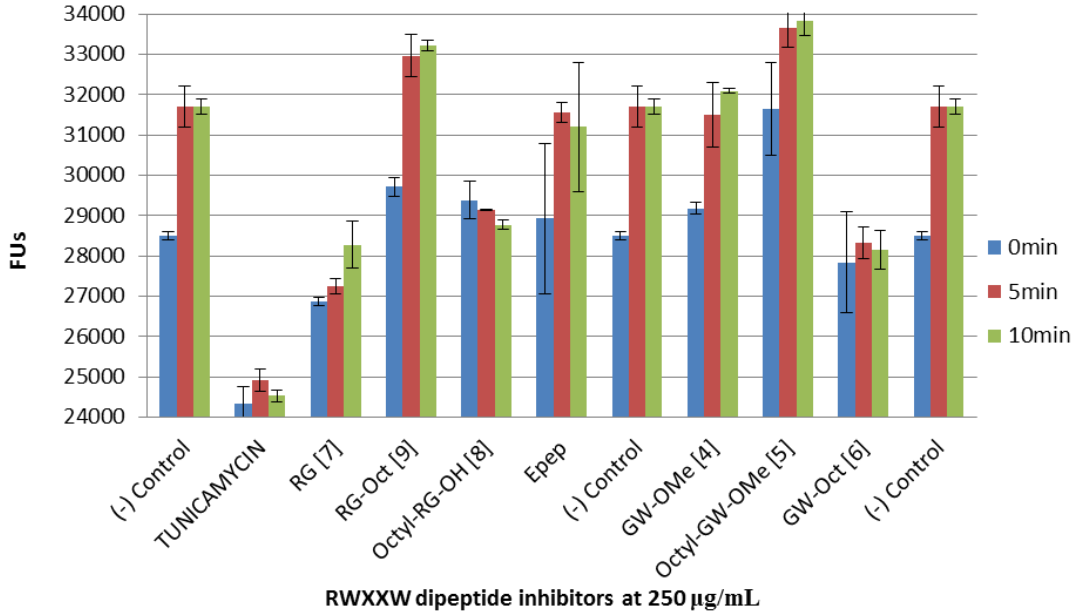


**Figure 3.5: Fluorescence emission of *P. aeruginosa* MraY upon treatment with RWXXW dipeptide analogues at 250µg/mL.** Fluorescence units (FUs) was recorded before the addition of membrane bound MraY (t=0) and within 5 minutes and 10 minutes of its addition.

A few problems arose from this plate reader assay. The Tecan GENios plate reader measured the fluorescence of each well with respect to the entire row or column. If any particular compound had some intrinsic fluorescence it overshadowed the changes in fluorescence of other compounds. As a result, the assay was not as sensitive as anticipated. This is evident from the fluorescence measurements of Octyl-RW-OMe **[2]** at time 0, before the addition of membrane bound MraY. At time 0, compound **[2]** had a higher fluorescence than the negative control (Figure 3.4; Figure 3.5). The addition of membrane bound MraY to **[2]**, led to a large increase in fluorescence over time. This large increase in fluorescence may have obscured the fluorescence effects from other compounds. As a result, it is difficult to conclude with confidence the inhibitory activities of these compounds via this method.

In addition, this assay was only able to take fluorescence measurements at specific time intervals. It is possible that major and important changes in fluorescence may have occurred in the first 30seconds-1minute. If so, it would be necessary to take

various measurements within this time frame to obtain conclusive data. To overcome these issues it would be beneficial to use a continuous assay that can accurately and with sensitivity monitor the MraY reaction. A continuous assay would provide more conclusive information on the inhibitory activity of individual compounds relative to the controls. In addition, kinetic information such as the $IC_{50}$ values can be determined.

### 3.3 Continuous Fluorescence Assay for MraY Activity

The continuous fluorescence assay developed by Brandish (1995) and later optimised by Mihalyi (2013) was the preferred method for the *in vitro* studies of protein E analogues against membrane-bound MraY. The MraY catalysed reaction was monitored by a Perkin Elmer fluorimeter at an excitation wavelength of 340nm and an emission wavelength of 530nm. To a Starna® sub-micro fluorimeter cell, 15µL of membrane bound MraY was added to 150µL of master mix and 15µL of inhibitor. The master mix contained 21.µM UDP-MurNAc-($N^{\varepsilon}$-Dns)pentapeptide and 47.2 µM of $C_{55}$-P or 70.6 µM of $C_{35}$-P in a buffer solution containing 100mM Tris base, pH 7.5 and 25mM $MgCl_2$. The final protein concentrations of membranes containing overexpressed *E. coli, P. aeruginosa, S. aureus, M. flavus* and *B. subtilis* MraY in this continuous assay were 0.6, 0.1, 0.28, 0.3, 0.3 and 0.9 mg/mL, respectively.

The continuous fluorescence assay revealed a rapid increase in fluorescence within the first two minutes of the MraY reaction, after which the assay was slightly non-linear, as found by Brandish (1995). This is presumably due to the reaction reaching equilibrium (Figure 3.6). MeOH was used as the negative control in *E. coli, B. subtilis, S. aureus* and *M. flavus* MraY. Water was used as the negative control in the reactions of *P. aeruginosa* MraY, as MeOH enhanced the fluorescence of the *P.*

*aeruginosa* MraY reaction and generated false readings. Tunicamycin, at a final concentration of 83µg/mL, was used as the positive control in all MraY strains. The addition of tunicamycin inhibited the production of dansyl-lipid I and as a result the fluorescence remained constant (Figure 3.6).

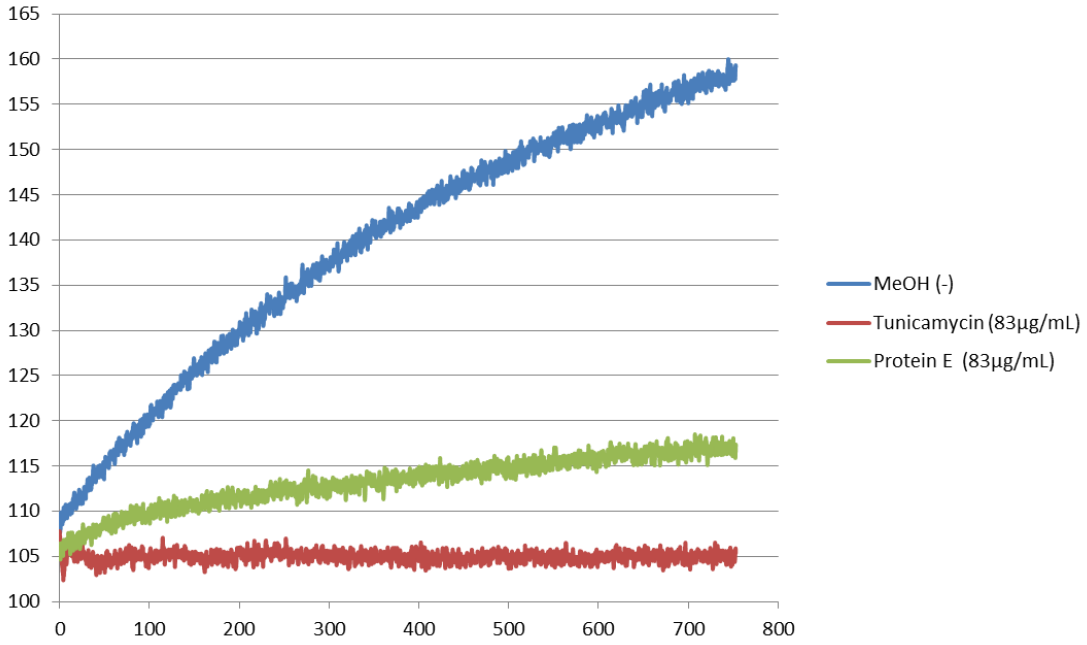


**Figure 3.6: The *E. coli* MraY reaction monitored via a continuous fluorescence assay**

### *3.3.1 Inhibition of E. coli MraY by Epep*

This continuous assay showed that Epep (83µg/mL) prohibited the production of dansyl-lipid I by inhibiting *E. coli* MraY. As expected, Epep did not inhibit *B. subtilis*, *S. aureus*, *M. flavus* or *P. aeruginosa* MraY. Three different concentrations of Epep were tested in order to determine the concentration necessary to inhibit the activity of *E. coli* MraY by half ($IC_{50}$). As expected, an increase in fluorescence was observed in more dilute samples of Epep (Figure 3.7).

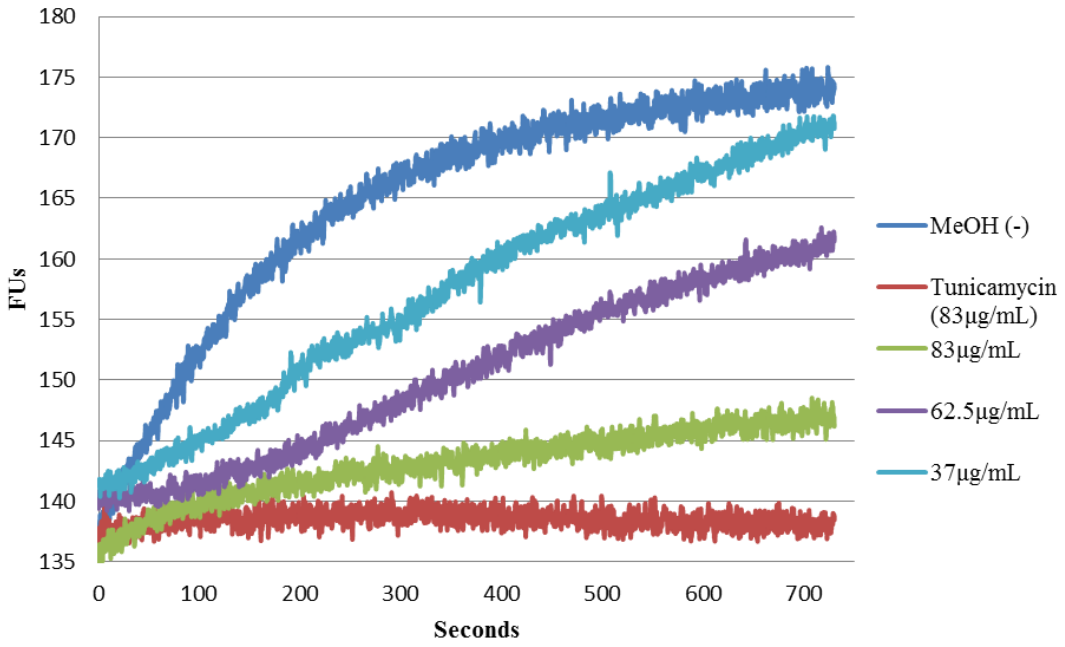


**Figure 3.7: Inhibition of *E. coli* MraY by Epep**

### *3.3.2 $IC_{50}$ determination*

Given that the greatest change in fluorescence occurred within the first 2 minutes, this region was further analysed to determine the $IC_{50}$ value of each inhibitor. The Perkin Elmer fluorimeter recorded the fluorescence of the MraY reaction every 0.1 seconds, allowing thorough analysis of the enzymatic reaction. In addition to qualitative duplicate measurements, these continuous measurements was treated as pseudo-repetition and provided a method to calculate error.

Utilising the software GenStat for Teaching and Learning, a linear regression was fitted to the first 500 data points. The slope of each line was then related to the percent activity of MraY in relation to the negative control; the negative control set to correspond to 100% enzyme activity. The percent activity of MraY was then plotted against the concentration of the inhibitor to produce an $IC_{50}$ graph (Figure 3.8). With assistance from the Quantitative Biology Centre (QuBic), GenStat was programmed

to fit a smoothing spline function through the data points. This spline identified the concentration of the inhibitor which reduced the enzyme activity by 50%, $IC_{50.}$

To calculate error, GenStat factors in the standard error associated with each data point (determined from the linear regression) as well as the distance between the data points and the smoothing spline. An $IC_{50}$ value of 30+/-3.5µg/mL was observed for Epep against *E. coli* MraY (Figure 3.8).

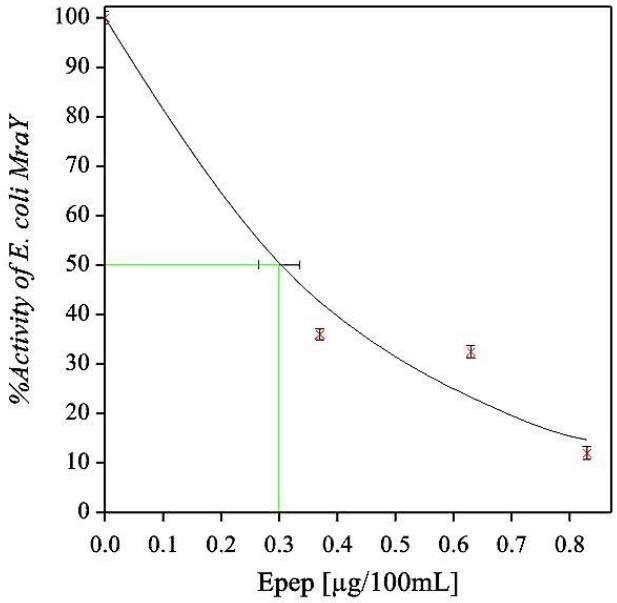


**Figure 3.8: $IC_{50}$ of Epep against *E. coli* MraY**

The $IC_{50}$ values of Arg-Trp dipeptide and peptapeptide analogues are given in Table 3.3. From these values the continuous assay was found to contain between 5%-20% error. These $IC_{50}$ values will be discussed in further detail in subsequent sections.

**Table 3.3: $IC_{50}$ values of RWXXW against MraY**

| µg/mL | *E. coli* | *P. aeruginosa* | *S. aureus* | *M. flavus* | *B. subtilis* |
|---|---|---|---|---|---|
| Epep | 30 +/- 3.5 | X | X | X | X |
| **[6]** GW-Oct | 294 +/-61 | 135 +/- 19 | 661 +/- 70 | 184 +/- 25 | 58 +/- 5.7 |
| **[4]** GW-OMe | X | X | X | X | 638 +/- 63 |
| **[10]** RWGLW | 425 +/- 85 | X | 226 +/- 53 | X | 679 +/- 84 |
| **[11]** RGGLW | 128 +/- 26 | X | X | X | 192 +/- 27 |
| **[15]**EHWGGG | 298 +/- 17 | 218 +/- 23 | 281 +/- 26 | 112 +/- 11 | X |

### *3.3.3 Inhibition of MraY by Arg-Trp dipeptide analogues*

According to the fluorescence emission spectrum of dansyl-UDP-MurNAc pentapeptide, $H_2N$-GW-Oct **[6]** inhibited the production of dansyl lipid I in *E. coli, B. subtilis, P. aeruginosa, S. aureus* and *M. flavus* (Appendix 1.1-1.5). The $IC_{50}$ value of this compound varied across MraY bacterial strains. Compound **[6]** was an especially strong inhibitor of *B. subtilis, P. aeruginosa* and *M. flavus* MraY with $IC_{50}$ values of 58.0, 135 and 184μg/mL, respectively (Table 3.3). A higher $IC_{50}$ value of 294 and 661μg/mL was observed against *E. coli* MraY and *S. aureus* MraY, respectively. Compound **[6]** may have participated in a π-π stacking interaction with a Phe residue in helix 9 of MraY. However, if this is the interaction responsible for inhibition, it is surprising that $H_2N$-GW-Oct **[6]** inhibited *M. flavus* MraY which lacks aromatic residues in helix 9 (Table 3.1; Figure 3.2).

Given the simplicity and similarity of compound **[6]** to the long hydrocarbon chains in household soaps, e.g. sodium octadecanoate ($C_{17}H_{35}COONa$), it could be possible that **[6]** is actually preventing the production of dansyl-lipid I by disturbing the membrane and forming micelles[205]. To rule out this possibility, analogues and intermediates of compound **[6]** were tested for *in vitro* activity against MraY via the continuous fluorescence assay. Intermediates $H_2N$-Trp-octyl ester **[18]**, $H_2N$-Gly-octyl ester **[19]** and dipeptide ester $H_2N$-RG-Oct **[9]** were all tested for *in vitro* activity against *E. coli, B. subtilis, P. aeruginosa* and *M. flavus* MraY, however none of these compounds were active inhibitors of these enzymes. Analogue $H_2N$-GW-OMe **[4]** which contains a methyl ester hydrocarbon instead of an octyl ester hydrocarbon chain was unable to inhibit *E. coli, P. aeruginosa, S. aureus* and *M. flavus* MraY. Compound **[4]** did inhibit *B. subtilis* MraY but at a substantially high concentration, $IC_{50}$ = 638μg/mL (Table 3.3, Appendix 1.6). Presumably, the octyl ester hydrocarbon

chain is important for localisation of the dipeptide in the membrane[206]. Interestingly, the location of the hydrocarbon chain appears to be important for the inhibition of MraY. None of the compounds which contain an N-octyl hydrocarbon chain was found to inhibit MraY.

From these examples it is clear that the exact sequence of $H_2$N-GW-Oct **[6]** is important for its inhibitory properties. In addition this compound was found to also have antibacterial activity against several strains of bacteria (Chapter 5).

### *3.3.4 Inhibition of MraY by RWXXW pentapeptides*

Of the five synthetic peptides, three (GWGLW **[12]**, RWGGW **[13]**, RWGLG **[14]**) were found to show intrinsic fluorescence which interfered with the continuous fluorescence assay.

RWGLW **[10]**, which has the most sequence similarity to protein E at the predicted site of interaction (RWGTW), was found to have an $IC_{50}$ value of 425μg/mL against *E. coli* MraY (Appendix 1.7), 226μg/mL against *S. aureus* MraY (Appendix 1.8) and 679μg/mL against *B. subtilis* MraY (Appendix 1.9).

Removal of the first tryptophan to form RGGLW **[11]** enhanced inhibition against *E. coli* and *B. subtilis* MraY ($IC_{50}$ = 128 and 192μg/mL, respectively; Appendix 1.10-1.11). Comparing the inhibitory activity of these two pentapeptides, it is possible that at certain orientations the first tryptophan residue hinders membrane insertion or association and therefore a higher concentration of RWGLW **[10]** is necessary to inhibit MraY. To circumvent this issue, Pro21 and Pro29 in native protein E may assist in kinking the helix to a position where the first tryptophan residue (Trp-4) does not interfere with cytoplasmic membrane insertion or association[146-147].

These results suggest that the C-terminal tryptophan (Trp-7) may be more important than the tryptophan near the N-terminus (Trp-4), which is in agreement with reports from Tanaka and Clemons[133]. To confirm the importance of Trp-7, Mihalyi tested the inhibition of MraY by GWGLW **[12]**, RWGGW **[13]** and RWGLG **[14]** using a radiochemical assay. The results of Mihalyi's radiochemical assay will be discussed in section 3.4.

### *3.3.5 Inhibition of MraY by α3-like and G4-like protein E homologues*

The fluorescence emission spectrum of the MraY reaction showed that changes in the RWXXW motif could be tolerated in the inhibition of *E. coli, P. aeruginosa and M. flavus* MraY (Table 3.3). Compounds ERWGGW **[16]** and EHWGGG **[15]** were designed to test whether MraY can be inhibited by homologues of protein E. ERWGGW **[16]**, an analogue of G4-like protein E, was found to have intrinsic fluorescence and therefore could not be tested via this continuous fluorescence assay. The results of Mihalyi's radiochemical assay on this compound will be discussed in section 3.4.

EHWGGG **[15]** was found to inhibit *E. coli, P. aeruginosa, S. aureus and M. flavus* MraY with $IC_{50}$ values 298, 218, 281 and 112μg/mL, respectively (Table 3.3: Appendix 1.12-1.15). Glu287 is conserved in MraY and could potentially interact with the histidine residue of compound **[15]**, in a similar manner as we predict Glu287 interacts with Arg-3 of native protein E (ΦX174). The lack of activity against *B. subtilis* MraY, which contains the conserved Glu287 residue but lacks a Phe residue in the region of interest (Figure 3.2), suggests that a π-π stacking interaction may be more crucial for inhibition of the enzyme.

In *E. coli*, *P. aeruginosa* and *S. aureus* MraY a glutamine residue is conserved at position 286, above Glu287 (Table 3.1). Gln286 may interact with the glutamic acid of **[15]** via hydrogen bonding (Figure 3.9). This additional site of interaction may assist in membrane insertion and could also promote a tighter and more stable interaction between the inhibitor and the enzyme. Glu286 is not conserved in *M. flavus* and *B. subtilis* MraY. The absence of Glu286 in *B. subtilis* MraY may have further hindered the interaction between the enzyme and **[15].** In *M. flavus* MraY, a threonine residue is present at position 286 and could participate in a hydrogen bonding interaction with the glutamic acid residue of **[15]** to enhance the interaction between the inhibitor and the enzyme**.**

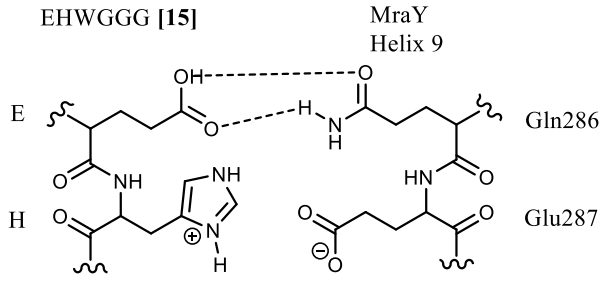


**Figure 3.9: Interaction between glutamic acid residue of EHWGGG [15] with Gln286 of MraY**

The inhibitory activity of EHWGGG **[15]** suggests that MraY can be inhibited by other homologues of protein E. In addition it suggests that the presence of Arg-3 in protein E (ΦX174) is not critical for activity. This is further supported by the inhibitory activity of $H_2N$-GW-Oct **[6]**.

## 3.4 Radiochemical Assay

Compounds which contained intrinsic fluorescence could not be tested via the continuous fluorescence assay. These fluorescent compounds include GWGLW **[12]**,

RWGGW **[13]**, RWGLG **[14]** and ERWGGW **[16]**. These compounds were tested on an alternative radiochemical assay by Mihalyi.

The radiochemical assay for MraY activity measures the transfer of [$^{14}$C]-phospho-MurNAc-pentapeptide to [$^{14}$C]-lipid I. The carbon-14 labelled lipid I product is extracted with *n*-butanol and analysed on a scintillation counter. This method was based on the work of Tanaka *et al*[207] and Brandish *et al*[111,71] which was optimised by Mihalyi (2013).

Mihalyi found that all four oligopeptides had similar inhibitory activity against *E. coli* MraY (Table 3.4; Appendix 2.1-2.4).

**Table 3.4: $IC_{50}$ values found by Mihalyi via the radiochemical assay**

| Pentapeptide | | $IC_{50}$ (μg/mL) |
|---|---|---|
| **[12]** | GWGLW | 129+/-14 |
| **[13]** | RWGGW | 154+/-17 |
| **[14]** | RWGLG | 161+/-20 |
| **[16]** | ERWGGW | 238+/-20 |

Tanaka and Clemons demonstrated the importance of the second tryptophan (Trp-7) in Epep for the inhibition of MraY[133], therefore we expected **[14]** to have a higher $IC_{50}$ value than RWGLW **[10]** (425μg/mL). The radiochemical assay revealed that **[14]** had a lower $IC_{50}$ value (161μg/mL) than **[10]**. Via the continuous fluorescence assay, we showed that the first tryptophan is not critical for inhibition, evident by the low $IC_{50}$ value of RGGLW **[11]** (128μg/mL). This could suggest that the location of tryptophan may not be as important as the number of tryptophans.

It's possible that these two methods of assays are not comparable. The continuous fluorescence assay measures the $IC_{50}$ value during the first 2 minutes of the MraY reaction. The radiochemical assay measures the $IC_{50}$ value after 30 minutes of reacting, by quantifying the radiolabelled lipid I product.

## 3.5 Inhibition Studies on Site-Directed mutants of *E. coli* MraY

Testing the inhibitory activity of protein E analogues provided compelling information on the importance of protein E residues for inhibition of WT MraY. Similarly we wished to determine the importance of MraY residues relative to our protein E analogues, in order to provide a more conclusive picture on the interaction of protein E and MraY. Although some information was provided by assaying other bacterial MraY's, these enzymes also contained many other point mutations, relative to *E. coli.*

Following our predicted structural model for the interaction of MraY and protein E (Figure 1.32), Glu287 and Phe288 appear to be key players in E-mediated lysis. In hopes of testing our hypothesis, these residues were mutated using site-directed mutagenesis. Active inhibitors of WT MraY (Chapter 3.3), were tested for inhibitory activity against MraY mutants.

MOAC project student Amy O'Reilly provided three *E. coli* MraY constructs with mutations F288A, F288L and E287A in a pET52b vector. These genes were cloned in with restriction enzymes SmaI and SacI. The pET52b vector has a T7 RNA Polymerase promoter and terminator which allowed transcription of the MraY gene upon IPTG induction. The pET52b vector confers ampicillin resistance which was especially useful in transformations. These MraY constructs were fused with an N-terminal Strep-tag II. Strep-tag II is composed of eight residues (Trp-Ser-His-Pro-Gln-Phe-Glu-Lys) which exhibit intrinsic affinity toward streptavidin[208]. A plasmid map for these mutants is given in Figure 3.10.

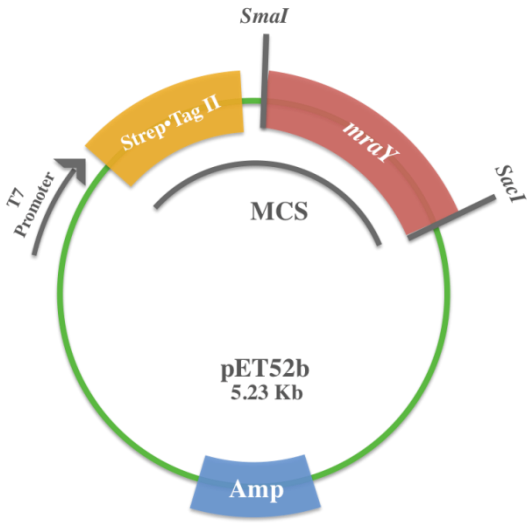


**Figure 3.10: Plasmid map of pET52b containing the *mraY* gene**

Mutants F288A, F288L and E287A were transformed into *E. coli* C43 competent cells in the presence of ampicillin (100µg/mL). Unlike DH5α, *E. coli* C43 cells carry the λDE3 lysogen which expresses T7 RNA polymerase from the l*ac*UV5 promoter[209]. T7 RNA polymerase can then bind to the T7 RNA polymerase promoter on the pET52b vector, facilitating overexpression of the *mraY* gene.

A single colony was isolated from a transformed plate and inoculated overnight in LB+Amp (100µg/mL). The start-up culture was then diluted 100-fold and allowed to grow to an $OD_{600}$ of 0.6. The cells were then induced with IPTG (1mM) for 4 hours, spun down and lysed using a cell disruptor. The lysed cells were spun down in a centrifuge and the supernatant was concentrated in an ultracentrifuge producing a brown gel which corresponded to the MraY containing membranes.

The presence and activity of MraY mutants was determined using the continuous fluorescence assay. Membrane-bound MraY mutants were diluted according to its fluorescence emission spectra in comparison to WT MraY. A Bradford assay was then utilised to determine the total protein concentration of these diluted membranes at 600nm. The standards for the Bradford assay contained 50µL of albumin (from egg

white) solution in 1.5mL of Bradford reagent at final concentrations of 0.25, 0.5, 1.0 and 1.4 mg/mL. The Bradford assay revealed that F288A and E287A had a total protein concentration of 23mg/mL and F288L had a total protein concentration of 13mg/mL. The total protein concentration of WT *E. coli* MraY membranes was found to be 7.3mg/mL (Table 3.2). Given that a higher concentration of mutant membranes is required to produce a similar fluorescence emission spectrum as WT MraY, it is plausible that MraY mutants have a lower specific activity than WT MraY. The addition of affinity tags like Strep II or $His_6$ to MraY have been previously shown to reduce the specific activity of MraY in comparison to the native enzyme[71]

### *3.5.1 Identification of MraY mutants*

To confirm the expression and identification of MraY mutants, two methods were explored. An empty pET52b vector was transformed in *E. coli* C43 cells. The corresponding membranes were isolated in a similar manner to the MraY mutants. These empty membranes contained only endogenous membrane proteins. Empty membranes were then diluted to 23mg/mL and 13mg/mL and compared to MraY mutants using the continuous fluorescence assay. In all three cases, the fluorescence emission spectrum showed that mutants F288A, F288L and E287A were overexpressed relative to the empty membranes (Figure 3.11). The reaction of F288L resulted in lower fluorescence relative to the other mutants; this is presumably due to the lower protein concentration.

The activity of F288A, E287A and F288L MraY mutants were further confirmed by the addition of UMP. Le Chateliers principle states that any change in a system at equilibrium will result in a shift of the equilibrium to counteract the change[210]. Given that UMP is another product of the reversible MraY reaction, the addition of UMP

was expected to shift the equilibrium towards the formation of substrate. To the negative control, 15µL of UMP (final concentration 83µg/mL) was added to the MraY reaction. The addition of UMP resulted in a decrease in fluorescence indicative that dansyl-Lipid I is being converted back to UDP-MurNAc-($N^{\varepsilon}$-Dns)pentapeptide and exported out of the membrane.

a)

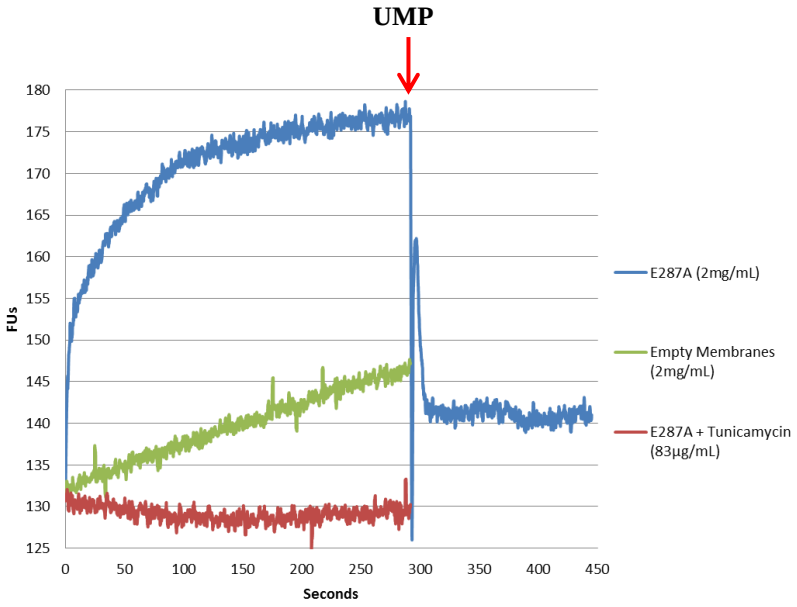


b)

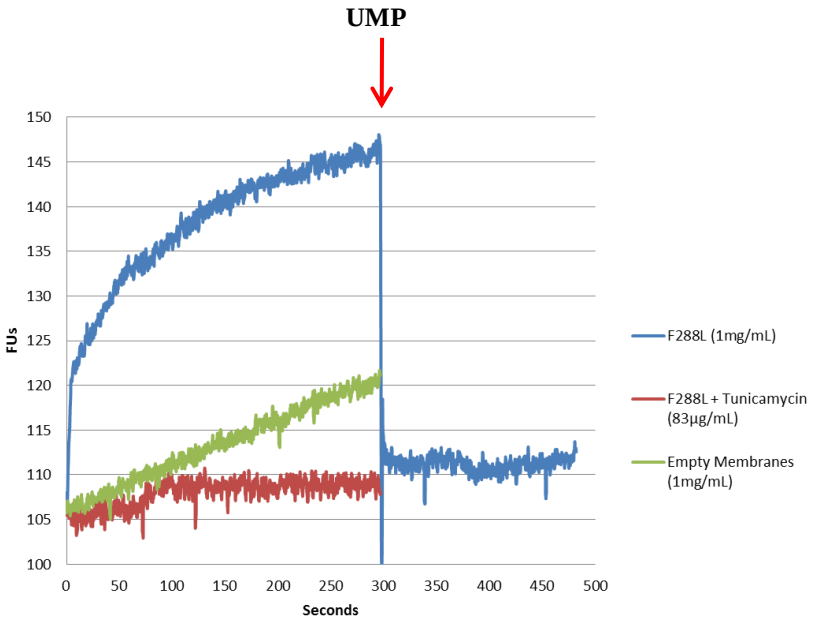

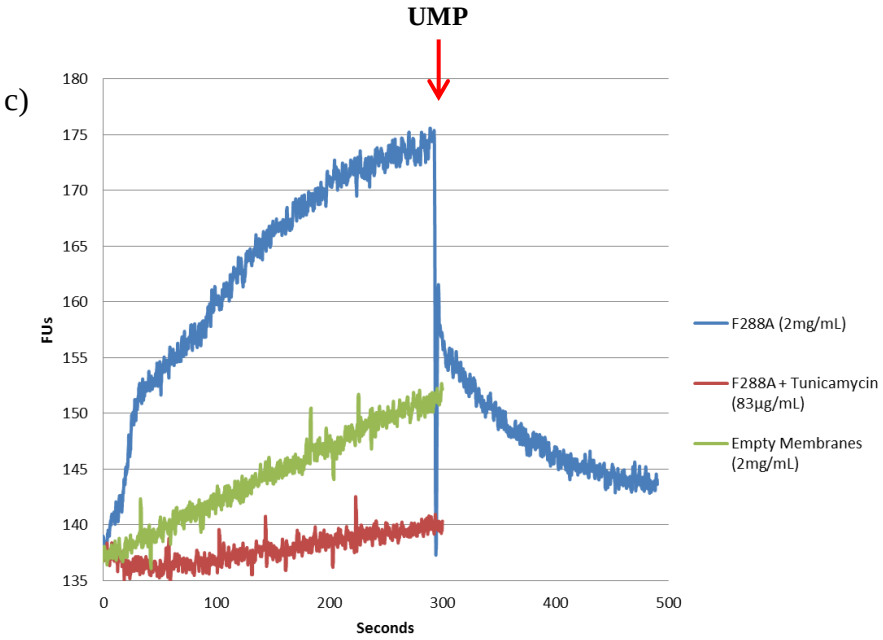


**Figure 3.11: Overexpression of MraY mutants relative to "empty" membranes.**
a) E287A MraY at a final concentration of 2mg/mL b) F288A MraY at a final concentration of 1mg/mL c) F288L MraY at a final concentration of 2mg/mL. Given that UMP is another product of the reversible MraY reaction, the addition of UMP caused a decrease in fluorescence indicative that the equilibrium has shifted towards the reformation and exportation of the substrate out of the membrane.

Another approach utilised to confirm the expression and identification of MraY mutants was Western blotting. There are very few examples of successful western blots in the characterisation of MraY. Lloyd *et al* characterised C-$His_6$-tagged MraY in 2004 upon extraction from the membrane[71]. Ma *et al* (2011) characterised C-$His_6$-tagged MraY produced from cell-free expression techniques in the presence of artificial lipids and detergents[211]. In both studies, the MraY band ran lower than expected at 32kDa.

A Western blot was performed on membrane-bound MraY mutants using Strep-Tactin Horse Radish Peroxidase (HRP) conjugate antibodies. Unfortunately, no bands were observed for MraY mutants. This could be due to the use of membrane bound MraY. The extensive lipid environment may have hindered recognition by the Strep-Tactin

HRP conjugated antibody. In addition, due the hydrophobic nature of membrane proteins like MraY, aggregation may have occurred upon denaturation[212].

Given the possibility that aggregation may have occurred preventing the protein from traveling down the SDS-gel and transferring correctly to a PVDF membrane, a Dot blot was performed. A dot blot is often used clinically in the detection of sexually transmitted diseases such as chlamydia and in the detection of antidiacyltrehalose antibodies in tuberculous patients[213]. A dot blot is a simple and quick technique for detecting and identifying proteins in the presence of antibodies. Unlike a Western blot, a dot blot cannot distinguish proteins by size; it is only able to confirm the presence of a tagged protein upon binding to an antibody[214].

To a nitrocellulose membrane paper, 5 and 20μL of membrane-bound MraY mutants (13 mg/mL) were spotted directly and allowed to air dry. To prevent nonspecific binding, the membrane was treated with 5% Bovine Serum Albumin (BSA) in PBS for 1 hour at 4°C. Following three consecutive washes with PBS-Tween buffer, the membrane was treated with 20μL of diluted Strep-Tactin HRP conjugate in 10mL of PBS-Tween buffer for 1 hour at 25°C with gentle shaking. The membrane was washed twice with PBS-Tween and PBS. The membrane was finally treated with Novex® Electrochemiluminescence (ECL) reagents which contained an electrochemiluminescence substrate used for immunodetection of HRP (Figure 3.12). The dot blot was subsequently exposed to film and developed using an AGFA Curix 60 processor.

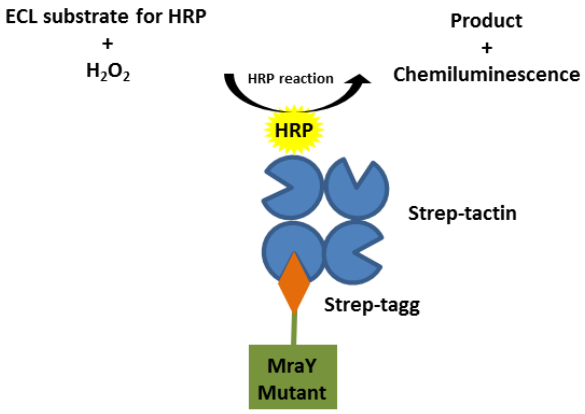


**Figure 3.12: Chemiluminescence reaction of Strep-Tactin HRP conjugate**

Incubation with ECL reagents for 30 seconds followed by 15 seconds exposure to film produced Figure 3.13a. ECL was able to detect the Strep-Tactin HRP conjugate antibody confirming the presence of Strep-tagged MraY in these samples. A small amount of nonspecific binding was observed in the negative control. Nonspecific binding commonly results from insufficiently blocking with BSA or an excessive concentration of the antibody[215].

Incubation with ECL reagents for 2 minutes followed by 60 seconds exposure to film produced Figure 3.13b. Prolonged incubation with ECL lead to the formation of halo like circles in the dot blot. These halos are often called ghost bands and are a result of high protein concentrations and long incubations times with ECL reagents[216]. A high concentration of protein results in a high concentration of the bound Strep-Tactin HRP conjugate. The addition of the ECL reagents resulted in a fast conversion of substrate to product. This led to a decrease in substrate concentration and therefore a decrease in the electrochemiluminescence reaction overtime. Because this reaction was not exposed to film quickly, the electrochemiluminescence reaction could not be accurately detected.

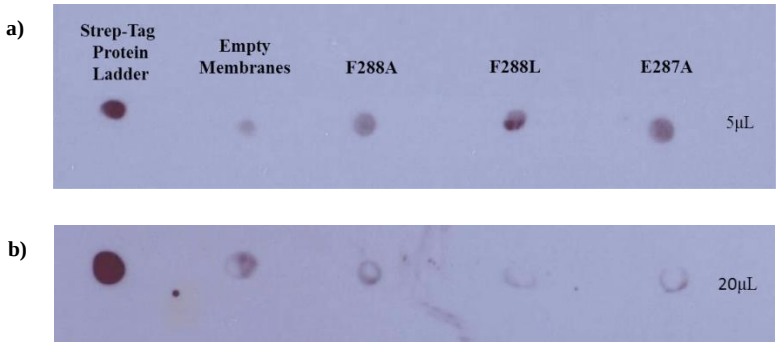


**Figure 3.13: Dot Blot for MraY mutants.**
a) 30 seconds incubation with ECL followed by 15 seconds exposure to film b) 2 minutes incubation with ECL followed by 1 minute film exposure. Excess ECL exposure time led to a lack of HRP substrate upon film exposure.

### *3.5.2 Continuous Fluorescence Assay using MraY mutants*

The activity of RWXXW analogues were tested against MraY mutants using the same procedure used for WT MraY (Chapter 3.2). The results from the continuous fluorescence assay using MraY mutants are given in Table 3.5.

**Table 3.5: Inhibitory activity of RWXXW analogues against MraY Mutants**

| μg/mL | *E. coli* | *E287A* | *F288L* | *F288A* |
|---|---|---|---|---|
| Epep | 30 +/- 3.5 | 211 +/- 51 | X | X |
| **[6]** $H_2N$-GW-Oct | 294 +/-60.5 | 769 +/- 127 | X | X |
| **[4]** $H_2N$-GW-OMe | X | X | X | X |
| **[10]** RWGLW | 425 +/- 85 | X | X | X |
| **[11]** RGGLW | 128 +/- 26 | X | X | X |
| **[15]**EHWGGG | 298 +/- 17 | X | X | X |

#### *3.5.2.1 Inhibition of F288L and F288A MraY*

Previous reports have shown that a mutation at Phe288 of *E. coli* MraY causes resistance to Epep. Our predicted structural model elucidates a potential π-π stacking interaction between Phe288 and Trp-4 and Trp-7 of Epep. As a result, a mutation to Phe288 should cause a decrease or complete loss of inhibitory activity for Epep and other analogues which contain a tryptophan residue. The continuous fluorescence

assay confirmed these reports and showed that Epep was not an active inhibitor of F288L or F288A (Appendix 1.16-1.17)

$H_2N$-GW-Oct **[6],** which was found to be an active inhibitor of *E. coli*, *P. aeruginosa*, *S. aureus*, *M. flavus* and *B. subtilis* MraY *in vitro* (Table 3.3), was unable to inhibit MraY mutants F288L and F288A. We anticipated that the tryptophan residue in compound **[6]** would interact with Phe88 in a similar manner as Epep. The loss in inhibitory activity for compound **[6]** as well as RWGLW **[10]**, RGGLW **[11]** and EHWGGG **[15]** against F288A and F288L MraY further strengthens our predicted structural model and the hypothesis that a π-π stacking interaction is involved in the inhibition of MraY by protein E.

### *3.5.2.2 Inhibition of E287A MraY*

Our predicted structural model, illustrates a potential interaction between Glu287 of *E. coli* MraY and Epep. Mutation E287A caused a large increase in the $IC_{50}$ of Epep (Appendix 1.18). Epep was found to have an $IC_{50}$ value of 211μg/mL compared to the $IC_{50}$ of 30μg/mL against WT *E. coli* MraY. Unlike native Epep which is produced by the host and transverses the membrane from the cytoplasm, *in vitro* studies require insertion of Epep from the periplasmic side of the membrane. In *in vitro* studies Glu287 could assist in membrane insertion via formation of a salt bridge with Arg-3 (Figure 1.32).

Mutation E287A completely abolished the inhibitory activity of pentapeptides RWGLW **[10]** and RGGLW **[11]**. In the absence of Glu287, the Arg residue in compounds **[10]** and **[11]** could not form an electrostatic interaction to assist in membrane insertion. This charged Arg residue therefore remained charged and exposed which may have complicated insertion into the hydrophobic membrane.

The α3-like protein E analogue EHWGGG **[15]** was also unable to inhibit MraY mutant E287A. Similar to compounds **[10]** and **[11],** the histidine residue of compound **[15]** could not form an electrostatic interaction with MraY in the absence of Glu287. The charged histidine residue may have subsequently hindered membrane insertion of EHWGGG **[15]** leading to a loss in inhibitory activity. These results further support our earlier findings, which suggested that MraY can be inhibited by protein E homologues of α3-like and G4-like bacteriophages (Chapter 3.3.5).

$H_2N$-GW-Oct **[6]** was found to have very minimal activity against E287A MraY, $IC_{50}$ = 769 +/- 127μg/mL (Appendix 1.19). The N-terminus of **[6]** could potentially form a similar electrostatic interaction as we predict Arg-3 of Epep forms with Glu287. As a result a mutation to residue Glu287 could lead to a decrease in the inhibitory activity of **[6]**. Phe288, which has been previously shown to be critical for the inhibition of MraY, is still present in mutant E287A and therefore could bind to **[6]** once it transverses the membrane.

## 3.6 Conclusion

To determine the *in vitro* activity of membrane-bound MraY in the presence of RWXXW containing peptides, a continuous fluorescence assay was utilised. The continuous fluorescence assay monitored the conversion of fluorescently tagged MraY substrate UDP-MurNAc-($N^{\varepsilon}$-Dns)pentapeptide to membrane-bound dansyl-lipid I.

Initially a Tecan GENios plate reader was used to monitor the fluorescence of the MraY reaction. Assays that can be performed on a microtitre plate are highly desirable for large scale screening. In practice, the application of this fluorescence assay to a microtitre plate resulted in a significant decrease in sensitivity. The Tecan

GENios plate reader measured the fluorescence of each reaction with respect to an entire row or column of the microtitre plate. If any particular compound had some intrinsic fluorescence it overshadowed the changes in fluorescence of other compounds. In addition, this assay was only able to take fluorescence measurements as specific time intervals. As a result, major fluorescence changes which occur within the first one minute of the reaction could not be observed.

To overcome these issues a continuous assay was explored. The fluorescence continuous assay was optimised by Mihalyi and utilised a Perkin Elmer fluorimeter. The fluorimeter was found to be much more sensitive than the plate readers and was able to measure the fluorescence of the MraY reaction every 0.1 seconds, allowing thorough examination of the enzymatic reaction.

The continuous fluorescence assay revealed that tryptophan may be important in the interaction between Epep and MraY. Compounds containing tryptophan residues were found to inhibit MraY while those that lack a tryptophan residue were not active inhibitors. We hypothesised that Trp-4 and Trp-7 of Epep interacts with MraY via a π-π stacking interaction with Phe288 of MraY. Mutation of Phe288 was found to cause resistance to Epep. This resistance may be due to the absence of the π-π stacking interaction. This pattern was also observed for RWXXW containing protein E analogues, which were unable to inhibit F288L and F288A MraY.

According to our predicted structural model, MraY residue Glu287 could form an electrostatic interaction with Arg-3 of Epep. Therefore we hypothesised that analogues which lack an arginine residue would be unable to inhibit MraY. However, we found that compounds which lacked arginine or contained a chemically similar amino acid, like histidine, were still able to inhibit MraY. $H_2N$-GW-Oct **[6]** and EHWGGG **[15]** were active inhibitors *of E. coli, P. aeruginosa, s. aureus and M.*

*flavus* MraY. Mutation to MraY residue Glu287 abolished inhibitory activity for most RWXXW peptides with the exception of compound **[6]** and Epep which were still able to inhibit MraY but at a much higher $IC_{50}$ value.

These results confirmed the importance of MraY residues Phe288 and Glu287. Phe288 appeared to be especially critical for the inhibition of MraY. Following our predicted structural model, these results suggest that a π-π stacking interaction between MraY and Epep is indeed plausible and critical for inhibition. The proposed electrostatic interaction between Glu287 of MraY and Arg-3 of Epep appeared to assist in inhibition but was not essential. This was surprising as electrostatic interactions are known to be stronger than noncovalent interactions between aromatic rings[217].

# Chapter 4: Antibacterial activity of synthetic Arg-Trp containing peptides

Having demonstrated that several synthetic Arg-Trp peptides were active inhibitors of the MraY reaction in the continuous fluorescence assay, we wished to test whether these peptides had antibacterial activity against *E. coli* and a range of Gram-negative and Gram-positive bacteria.

The minimal inhibitory concentration (MIC) is defined as the lowest concentration of an antimicrobial that can visibly inhibit the growth of a microorganism[218]. A compound that generates a low MIC and $IC_{50}$ value is especially desired in the development and quick approval of novel drugs.

## 4.1 Kirby-Bauer Antibiotic Susceptibility test

The antibacterial properties of RWXXW compounds were determined using qualitative and quantitative experiments. The Kirby-Bauer test for antibiotic susceptibility was initially used as a qualitative measure of antibacterial activity. The Kirby-Bauer test, first developed in 1966[219] and standardised by the World Health Organization in 1971[220], was established as a practical method of testing antibiotic susceptibility in clinical laboratories. In this method inhibition of the organism is visualised on an LB plate and is evident by the appearance of zones of inhibition in which no growth has occurred.

*E. coli* C43 and *B. subtilis* colonies were isolated from a standard agar plate and inoculated in 5mL of LB overnight at 37°C. 100μL of cultured bacteria was added to 2mL of melted low percent agar containing 0.5% agar. The mixture was vortexed and spread evenly across an agar plate. Once solidified, antibacterial discs saturated with

25µL of RWXXW compounds (125µg/mL) were placed on top of the seeded agar plate and incubated overnight at 37°C. In this experiment, ampicillin (125µg/mL) and MeOH were used as the positive and negative controls, respectively. Compounds which have antibacterial properties prevented the growth of bacteria around the disc. The Kirby-Bauer test revealed that $H_2N$-RW-Oct **[3]**, Octyl-RW-OMe **[2]** and $H_2N$-GW-Oct **[6]** had some antibacterial activity against *B subtilis*. This was evident by the appearance of small zones of inhibition surrounding the antibacterial discs (Figure 4.1). **[3]** appeared to be a better inhibitor of *B. subtilis* than **[2]** and **[6]**, given that it produced a larger zone of inhibition.

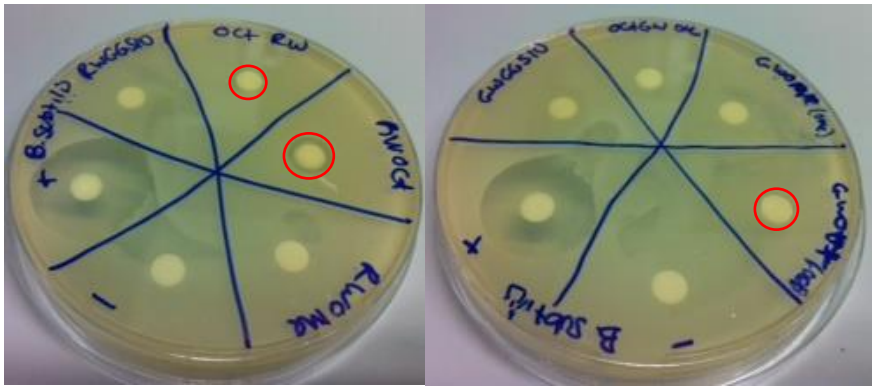

**Figure 4.1: Inhibition of B. subtilis by RWXXW analogues via the Kirby-Bauer antibacterial susceptibility test.** 25µL of ampicillin (100mg/mL) and 25µL MeOH was used as the positive and negative controls, respectively. Red circles highlight zones of growth inhibition.

The Kirby-Bauer test confirmed the presence of antimicrobial activity in a limited number of compounds but could not provide information related to the MIC value. Some articles suggested measuring the diameter of the zones of inhibition in order to determine the MIC values relative to the positive control[221]. The observed zones of inhibition were too small to measure with confidence and therefore could not be analysed accurately. RWXXW analogues did not appear to have antibacterial properties against *E. coli* C43. However, this may be due to very small zones of inhibition which could not be properly detected. As a result, this experiment was

found to be an inappropriate high throughput screening method for the determination of antibacterial properties[222].

## 4.2 Microtitre Broth Dilution Technique

To quantify the antibacterial properties of these compounds a microtitre broth dilution technique was utilised. The microtitre broth dilution technique has become an increasingly popular high throughput protocol that produces quantitative results (MIC)[223]. This method utilises liquid media containing a defined number of bacterial cells to test the antibacterial properties of an inhibitor across various concentrations in a deep well microtitre plate[224].

*E. coli*, *P. putida* and *B. subtilis* colonies were isolated from an agar plate and inoculated in 5mL of LB broth overnight at 37°C. A dilution series of the seeded LB was performed to get $10^{-1}$, $10^{-2}$, $10^{-3}$, $10^{-4}$, $10^{-5}$, $10^{-6}$, $10^{-7}$ and $10^{-8}$-fold dilutions. 0.5mL of each dilution was poured onto an agar plate and incubated overnight at 37°C. The colonies were then counted and the dilution that gave 1000 colony forming units per mL (CFU/mL) was chosen for MIC calculations (Table 4.1).

**Table 4.1: Broth dilution that produces $10^3$ CFU/mL**

| Bacterial Strain | LB dilution that produced $10^3$ CFU/mL |
|---|---|
| *E. coli* | $1.8x10^{-6}$ |
| *P. putida* | $3.9x10^{-7}$ |
| *B. subtilis* | $8.9x10^{-3}$ |

To a sterile deep well microtitre plate, 190µl of the seeded broth (CFU/mL = $10^3$) was added to each well. 10µL of RWXXW peptide analogues were added to the 96 deep well plate to give a final volume of 200µL and final inhibitor concentrations 125, 62.5, 31.25, 15.63, 7.82, 3.90, 1.95 and 0.97µg/mL, obtained by 2-fold serial

dilutions. Each inhibitor concentration was tested in duplicates. 10μL of water was added to one of the wells to serve as a growth control. Normal LB was also used as a negative control. The microtitre plate was covered with a sterile adhesive film and incubated overnight at 37°C with shaking. The solutions were then transferred to a standard 96 well plate for absorbance measurements ($OD_{595}$). The inhibitor concentration which reduced the growth by at least 50% was considered the MIC of the compound. The MIC of RWXXW peptide analogues is provided in Table 4.2.

**Table 4.2: MIC (μg/mL) of RWXXW peptide analogues**

| | (μg/mL) | *E. coli* | *P. putida* | *B. subtilis* |
|---|---|---|---|---|
| **[2]** | Octyl-RW-OMe | - | - | 125 |
| **[3]** | $H_2N$-RW-Oct | 31 | 31 | 8 |
| **[6]** | $H_2N$-GW-Oct | - | - | 16 |
| **[13]** | RWGGW | - | - | 125 |

The microtitre broth dilution technique revealed that four RWXXW analogues had antibacterial activity against *E. coli*, *P. putida*, and *B. subtilis* with MIC as low as 8μg/mL. Three of these compounds contained a hydrophobic chain which we anticipated could assist in membrane insertion. Dipeptide $H_2N$-GW-Oct **[6]** which was found to be an inhibitor of *E. coli, B. subtilis, S. aureus, P. aeruginosa* and *M. flavus* MraY (Chapter 3.3) showed antibacterial activity only against *B. subtilis.* Pentapeptide RWGGW **[13]** which was found to be an inhibitor of *E. coli* MraY also showed weak antibacterial activity against *B. subtilis*. Peptides RWGLW **[10]**, RGGLW **[11]** and EHWGGG **[15]** were not found to have antibacterial activity.

Unexpectedly, Arg-Trp derivatives **[2]** and **[3]** showed antibacterial activity despite not showing *in vitro* activity against MraY. This raised the questions of whether these compounds inhibited the growth of bacteria by acting at a site other than MraY or perhaps by permeabilising the membrane in a similar manner to detergents[205].

## 4.3 Antibacterial activity of $H_2N$-RW-Oct [3] against Gram-negative bacteria

We were especially intrigued by the antibacterial activity of $H_2N$-RW-Oct **[3]**. Initially, we suspected that this compound would have the most antibacterial and antimicrobial activity as a result of its structure. Compound **[3]** is cationic, contains the desired arginine and tryptophan residues and has a long hydrophobic chain which could potentially assist in membrane insertion. The absence of *in vitro* activity suggests that this compound might act at a site other than MraY, or that it permeabilises the membrane. To determine if compound **[3]** permeabilises the membrane, a fluorometric assay testing for the permeabilisation of Gram-negative bacteria was performed.

### *4.3.1 Use of the fluorescent probe 1-N-phenylnaphthylamine to investigate permeabilisation of Gram-negative bacteria by $H_2N$-RW-Oct [3]*

The use of fluorescent probes is a well-documented tactic in structural biology to determine the structure and function of membranes[225,226,227]. The nonpolar fluorescent probe 1-*N*-phenylnaphthylamine (NPN) is a particularly useful probe to study the properties of biological membranes as it strongly fluoresces in phospholipid environments but only weakly in aqueous environments[228,229]. The structure of the uncharged lipophilic dye NPN is given in Figure 4.2[230].

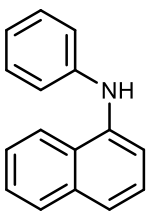


**Figure 4.2: Structure of fluorescent probe NPN**

NPN was used in this research project to investigate if $H_2N$-RW-Oct **[3]** permeabilises the outer membrane of Gram-negative bacteria**.** The outer membrane of Gram-negative bacteria is rich in lipopolysaccharides (LPS) which are used to exclude external hydrophobic molecules from entering the cell[231]. The integrity and stability of the outer membrane can be compromised by permeabilising substances which can intercalate and release vital components of the outer membrane[232]. Once the membrane has been permeabilised, the phospholipid bilayer becomes exposed, facilitating the entry of hydrophobic agents such as NPN. The uptake of NPN into the hydrophobic membrane causes an increase in the fluorescences of NPN which can be measured.

Using methods from Helander and Mattila-Sandholm (1999) an NPN uptake assay was adapted to a continuous fluorescence assay. A single colony of *P. putida* was isolated from a standard agar plate and inoculated in 5mL of LB overnight at 37°C with shaking. This start-up culture was diluted 100-fold with LB and allowed to grow to an $OD_{600}$ of 0.5. The culture was then centrifuged for 10 minutes at 1000g at 25°C. The pellet was resuspended in half the volume of 5mM HEPES buffer, pH 7.2.

Membrane permealisation of this bacterial suspension by **[3]** was determined on a Perkin Elmer fluorimeter at an excitation wavelength of 340nm and an emission wavelength of 435nm. To a Starna® sub-micro fluorimeter cell, 50µL of the bacterial suspension was added to 25µL of 40µM NPN and 25µL of the inhibitor. NPN and the inhibitors in question were dissolved in HEPES buffer, pH 7.2. The HEPES buffer solution was used as the negative control and EDTA (125µg/mL) was used as the positive control. EDTA is a known membrane permeabiliser that alters the outer membrane by releasing LPS[233].

The effect of $H_2N$-RW-Oct **[3]** on the membrane at various concentrations was monitored in duplicates. The results of this fluorometric assay are given in Figure 4.3.

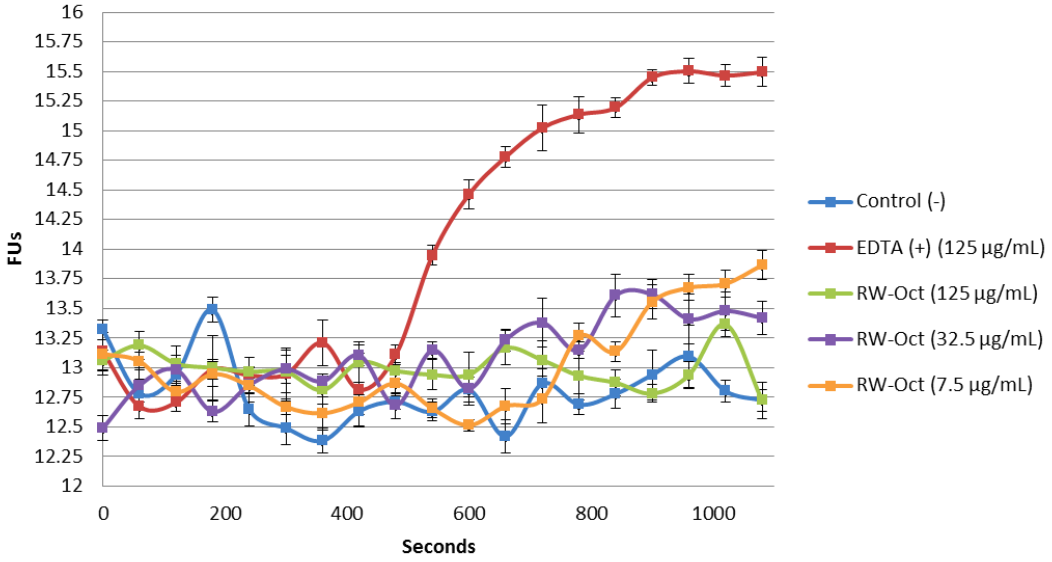


**Figure 4.3: NPN membrane permeabilisation assay of *P. putida* in the presence of $H_2N$-RW-Oct**

As expected, an increase in the fluorescence of NPN was observed after 500 seconds for cells treated with 125µg/mL EDTA. This indicated that EDTA successfully permeabilised the membrane and facilitated the entry of NPN molecules into the phospholipid bilayer. Cells treated with $H_2N$-RW-Oct **[3]** only gave small changes in fluorescence, which were not concentration dependent. This suggests that the membrane was not successfully permeated by **[3]** and therefore NPN could not enter the phospholipid bilayer.

The small increase in fluorescence observed for cells treated with compound **[3]** after 10 minutes might be as a result of inhibition of MraY, since MraY inhibition would lead to cell lysis upon cell division allowing NPN to enter the phospholipid bilayer.

### *4.3.2 Overexpression of mraY protects the cells from $H_2N$-RW-Oct mediated lysis*

To confirm that **[3]** does not permeabilise the membrane but instead inhibits MraY, a protection assay was performed. A protection assay was first performed by Zheng *et al* (2008) to confirm that MraY is the bacterial target of E-mediated lysis. Zheng *et al* reported that overexpression of *mraY* on a pBAD30 plasmid protects *E. coli* from lysis by the ΦX174 E gene, expressed on a λ prophage, due to the formation of a 1:1 protein complex. Since **[3]** shows antibacterial activity against *E. coli*, this method provided a method to test whether **[3]** interacted with MraY. If **[3]** forms a complex with MraY *in vivo*, then overexpression of *mraY* should protect *E. coli* from lysis by **[3]** and hence increase the MIC value.

In this study, a pET52b vector containing WT *mraY*, F288L *mraY* or E287A *mraY* was used. The pET52b vector contained a T7 RNA polymerase promoter and terminator which allowed transcription of the genes of interest upon IPTG induction.

The overexpression of integral membrane proteins has been recorded to be toxic to bacterial cells even at low levels of IPTG[234], which could complicate the protection assay. Given that only a modest 1.5-2 fold increase in activity has been reported for the overexpression of MraY[71], toxicity by MraY is not anticipated. Nevertheless, a growth experiment was conducted to determine the effect overexpression of integral membrane protein MraY has on bacterial growth.

*E. coli* C43 cells, containing an empty pET52b vector, was induced with 0.5mM IPTG and was monitored every 30 minutes for 8.6 hours. To determine if the overexpression of MraY is toxic to bacterial cells, a similar experiment was conducted on *E. coli* C43 cells containing an additional copy of the *mraY* gene on a pET52b plasmid. The results of these growth experiments are given in Figure 4.4.

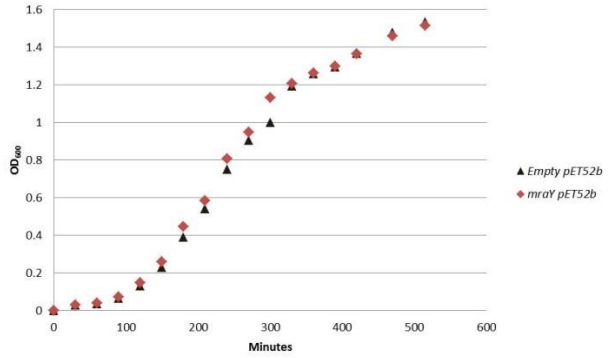


**Figure 4.4: Effects of 0.5mM IPTG induction on bacterial growth**

According to Figure 4.4, the growth of bacterial cells was not affected by the addition of 0.5mM IPTG or the overexpression of MraY. As a result, 0.5mM IPTG was used to induce the overexpression of *mraY* genes in the protection assay.

The protection assay utilised a microtitre plate to determine the MIC of **[3]** against cells overexpressing MraY. If **[3]** inhibits MraY, we would expect an increase in the MIC value at high concentrations of MraY. The excess MraY proteins will be able to overcompensate for the inhibition by **[3]** and continue producing peptidoglycan to avoid lysis. If **[3]** does not inhibit MraY, the MIC should not be affected by the overexpression of MraY.

WT *mraY* and *mraY* mutants F288L and E287A were transformed into *E. coli* C43 competent cells in the presence of ampicillin (100µg/mL). To serve as a negative control, an empty pET52b vector was transformed into *E. coli* C43 cells in the presence of ampicillin. A single colony was isolated from the transformed plate and inoculated in 5mL of LB+Amp (100µg/mL) overnight at 37°C with shaking. Due to the low transformation efficiency of *E. coli* C43 competent cells, broth dilution was not required to identify the dilution that produced 1,000 CFUs/mL. The start-up culture was then diluted 100-fold with LB and induced with 0.5mM IPTG. Ampicillin was not added at this change in order to assure that the only effect measured was that of the inhibitor, $H_2N$-RW-Oct **[3]**.

To a sterile deep well microtitre plate, 190µl of the IPTG-induced seeded broth was added to each well. 10µL of $H_2N$-RW-Oct **[3]** was added to the deep 96 well plate to give a final volume of 200µL and final inhibitor concentrations of 500, 450, 400, 350, 300, 250, 125, 62.5, 31.25, 15.63, 7.82, 3.90, 1.95 and 0.98µg/mL, obtained by 2-fold serial dilutions. Each inhibitor concentration was tested in duplicate. 10µL of water was added to one of the wells to serve as a growth control. Normal LB was also used as a negative control. The microtitre plate was covered with a sterile adhesive film and incubated at 37°C with shaking for 8 hours. The solutions were then transferred to a standard 96 well plate for absorbance measurements ($OD_{595}$). The inhibitor concentration which reduced the growth by 50% was considered the MIC of the compound. The MICs of compound **[3]** against *E. coli* cells overexpressed with MraY is provided in Table 4.3.

**Table 4.3: MIC of $H_2N$-RW-Oct against E. coli cells overexpressed with MraY**

| (µg/mL) | WT *E. coli* | (-) control Empty pET52b | MraY | F288L | E287A |
|---|---|---|---|---|---|
| **[3]** $H_2N$ RW-Oct | 31 | 31 | 250 | 500 | 300 |

The MIC of **[3]** against the negative control, which contained an empty pET52b vector, was found to be 31µg/mL. This is in agreement with the MIC value determined via the microtitre broth dilution technique. The MIC of **[3]** increased 8-fold in cells overexpressing MraY and nearly 10-fold in cells overexpressing E287A MraY. These increases in MIC suggest that **[3]** interacts with MraY and induces lysis of the cell.

The MIC of **[3]** increased 16-fold in cells overexpressing F288L MraY. This exceedingly high MIC may be due to a combination of two factors; (1) higher concentration of MraY and (2) weak binding interaction. We anticipated that $H_2N$-

RW-Oct **[3]** would interact with MraY via a π-π stacking interaction with Phe288. In the absence of Phe288 we would therefore expect a significant decrease in the inhibitory activity of **[3]**. In addition to there being an excess of F288L MraY proteins to overcompensate for the inhibition by **[3]**, it is plausible that **[3]** was unable to bind as tightly to MraY in the absence of Phe288. As a result, this led to an MIC much higher than *E. coli* cells overexpressing WT MraY or E287A MraY.

This protection assay further confirmed that $H_2N$-RW-Oct does not permeabilise the membrane, in agreement with the results found via the NPN membrane permeabilisation assay. The protection assay also showed that **[3]** inhibits MraY in a similar manner as the E gene does from the experiments of Zheng *et al*.

It is unclear why $H_2N$-RW-Oct **[3]** did not have *in vitro* activity against membrane bound MraY via the continuous fluorescence assay. The presence of multiple Arg or Lys residues in cationic antimicrobial peptides is needed to bind to the surface of bacterial membranes, so this may be why $H_2N$-RW-Oct **[3]** shows higher antimicrobial activity than $H_2N$-GW-Oct **[6]**.

#### *4.3.2.1 Protection assay of known antimicrobial peptides against E. coli*

Known antimicrobial peptides, containing the RWXXW motif (Table 4.4), were provided by Professor Robert E.W. Hancock (UBC, Canada) and tested for activity against MraY using the protection assay. If the antimicrobial action of these peptides is via inhibition of MraY, then we would expect to observe an increase in the MIC against cells overexpressing MraY. If these antimicrobial peptides do not inhibit MraY, the MIC should not be affected by the overexpression of MraY.

**Table 4.4: Sequence of known antimicrobial peptides**

| Antimicrobial peptide | Labeled Terminus[a] |
|---|---|
| MX226 | N-IL**RW**PWPWRRK-C<br>C-KR**RW**PWPWRLI-N |
| Indolicidin | C-R**RW**PW**W**PWKWPLI-N |
| Kai47 | C-K**RW**KW**W**RFKWKIF |
| Kai50 | C-R**RW**RW**W**RWKWRLI-N |
| Sub6 | C**-RW**WKIWVIRWWR-C |
| 1002 | N-VQ**RW**LIVWRIRK-C |
| 1020 | N-VRLRI**RW**WVLRK-C |

Using the same protocol as the protection assay (Chapter 4.3.2), the MIC of known antimicrobial peptides was determined (Table 4.5). The protection assay revealed that these antimicrobial peptides had antibacterial activity against *E. coli* with MIC values ranging from 8-150μg/mL. Surprisingly, the MIC of these compounds decreased in cells overexpressing MraY. From radiochemical assays carried by Agnes Mihalyi, we know that these peptides do inhibit *E. coli* MraY, showing 30-60% inhibition at a concentration of 100μg/mL (unpublished, 2013). These decreasing MIC value can be as a result of inhibition at another site. Some of these antimicrobial peptides such as indolicidin are believed to target intracellular processes including DNA synthesis upon forming pores in the cytoplasmic membrane[46,235]. Due to the sequence similarity between these antimicrobial peptides and protein E, it is plausible that the interaction of these peptides with MraY assists in membrane insertion. If so, an increase in the concentration of MraY would facilitate the entry of these compounds into the cell and would increase the probability of inhibition to their intracellular targets. As a result, an increase in the concentration of MraY would lead to a decrease in the MIC.

**Table 4.5: MIC of known antimicrobial peptides**

| (μg/mL) | (-) Control, pET52Bb | MraY | F288L | E287A |
|---|---|---|---|---|
| MX226 | 150 | 63 | 63 | 63 |
| Indolicidin | 63 | 16 | 31 | 63 |
| Kai47 | 31 | 16 | 16 | 16 |
| Kai50 | 31 | 16 | 16 | 16 |
| Sub6 | 16 | 8 | 8 | 16 |
| 1002 | 8 | 2 | 4 | 2 |
| 1020 | 16 | 4 | 16 | 4 |

## 4.4 Conclusion

The antibacterial activity of RWXXW analogues was determined using the Kirby-Bauer antibiotic susceptibility test and the microtitre broth dilution technique. The Kirby-Bauer test revealed that $H_2N$-RW-Oct **[3]**, Octyl-RW-OMe **[2]** and $H_2N$-GW-Oct **[6]** had some antibacterial activity against *B. subtilis*; this was evident by the appearance of small zones of inhibition surrounding the antibacterial discs. The observed zones of inhibition were too small to measure with confidence and therefore could not be analysed accurately to produce an MIC value. RWXXW analogues did not appear to have antibacterial properties against *E. coli* C43. However, this was due to very small zones of inhibition that could not be properly detected via this method. This experiment was able to qualitatively confirm antibacterial activity but could not provide meaningful information related to the MIC value. As a result this experiment was found to be an inappropriate high throughput method to screen the remaining compounds.

To quantify the antibacterial properties of these compounds a microtitre broth dilution technique was performed. This method utilised liquid media containing a defined

number of bacterial cells to test the antibacterial properties of RWXXW compounds in a microtitre plate. The microtitre broth dilution technique revealed that 4 compounds had antibacterial activity against *E. coli*, *P. putida*, and *B. subtilis* with MIC as low as 8μg/mL. Among these compounds, $H_2N$-GW-Oct **[6]** and RWGGW **[13]** which were found to inhibit the growth of *B. subtilis* (MIC = 16μg/mL and 125μg/mL, respectively) were also active inhibitors of MraY *in vitro*. The agreement between the antibacterial and antimicrobial activity of **[6]** and **[13]** suggests that they interact with MraY, inhibiting peptidoglycan biosynthesis and as a result cause cell lysis.

Unexpectedly, $H_2N$-RW-Oct **[3]** had antibacterial activity but did not have *in vitro* activity. This suggests that either this compound inhibited the growth of bacteria by acting at a site other than MraY or by permeabilising the membrane in a similar manner to detergents[205].

An NPN membrane permeabilisation assay was conducted to determine if **[3]** permeabilised the membrane. In the presence of EDTA, a known membrane permeabiliser, the fluorescence of NPN increased, indicative that NPN entered the hydrophobic membrane. This pattern was not observed in the presence of **[3]**, indicative that **[3]** does not permeabilse the membrane.

In addition, a protection assay was conducted to determine if $H_2N$-RW-Oct **[3]** inhibited the growth of bacteria via its interaction with MraY. This assay showed that the MIC of **[3]** increased in cells overexpressing MraY, F288L MraY and E287A MraY. Given that an increase in the concentration of MraY caused a decrease in the inhibitory activity of **[3]**, **[3]** is believe to inhibit the growth of bacteria by interacting with MraY. The MIC of **[3]** against F288L MraY was significantly higher (500μg/mL) and may be due to a weakened interaction with MraY. In the absence of

Phe288, $H_2N$-RW-Oct **[3]** may not be able to effectively interact with MraY via a π-π interaction. The combination of this weakened interaction and an excess of MraY protein significantly reduced the inhibitory activity of **[3]**.

# Chapter 5: Uridine-Containing Peptides

## 5.1 Introduction

Modification of existing classes of antimicrobials is an increasingly popular tactic to combat resistance of bacteria to standard antibiotic therapies[236-237]. Much effort has been put forward in particular to the modification of natural products, Uridyl Peptide Antibiotics (UPA). UPAs such as pacidamycin, tunicamycin, mureidomycin A, liposidomycin B and muraymycin are known to inhibit the cell-wall biosynthetic enzyme MraY[109,72,238]. It is believed that UPAs act as transition state analogues of MraY substrate UDP-MurNAc-pentapeptide[239]. This is likely as prior reports have shown that the uridine motif is crucial for activity *in vitro*[240]. As described in Chapter 1.4.1, UPA's have been reported to contain low levels or lack activity against human pathogens[241], presumably due to their high hydrophilicity which may hinder passive diffusion across the cytoplasmic membrane. The *in vitro* potencies of these peptidyl nucleoside antibiotics have sparked the scientific community with great interest in investigating the structure-activity relationships of nucleoside antibiotics as MraY inhibitors and antibacterials[72,103-17].

In the course of the project, we noticed that members of the UPA class contained some structural features that are also found in the RWXXW motif. Muraymycin contains a cyclic amino acid analogue of arginine while the pacidamycins contain a tryptophan residue and an electron rich meta-tyrosine (Figure 5.1).

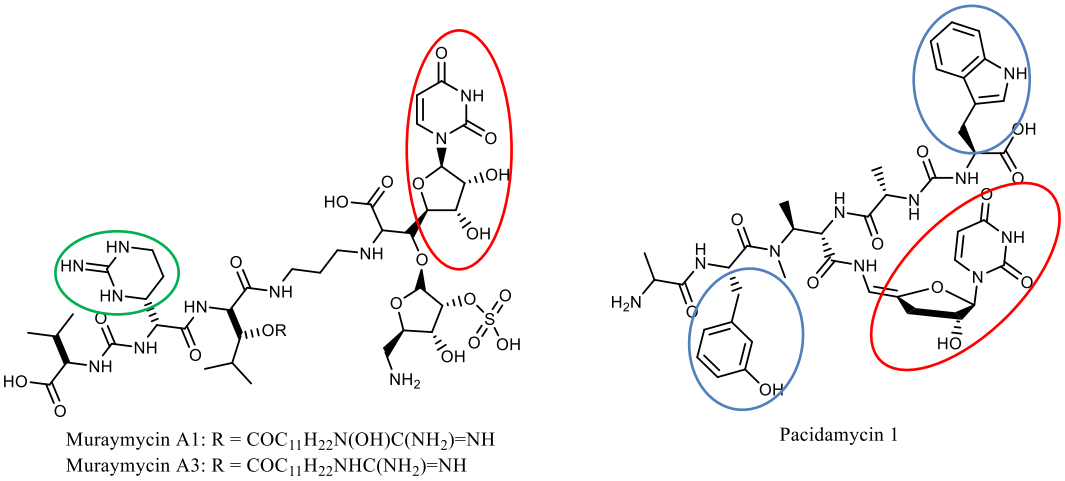


**Figure 5.1: Structures of Muraymycin and Pacidamycin 1.** In red is the crucial uridyl motif. Circled in blue are the common aromatic residues which are generally Trp, Phe or *m*-Tyr. In the case of muraymycin, $aa_2$ (green) a cyclic arginine is observed.

The presence of two aromatic residues and in some cases a cyclic arginine in UPAs bears a striking resemblance to the RWXXW motif we hypothesised is important for MraY inhibition. It therefore seemed possible that these UPAs form an initial interaction with MraY at the predicted protein E binding site in order to access the MraY active site from the exterior of the cell membrane. This is of particular interest as it is not known how these UPAs (≈800-1400kDa) cross the cell membrane. The two aromatic residues can form a π-π stacking interactions with Phe-288 of MraY in the same manner as protein E. *m*-Tyr in particular would be an excellent candidate for π-π stacking as it is more electron rich than a typical aromatic[242].

In 1996, previous members of our research group have shown that liposidomycin B and mureidomycin A are slow binding inhibitors of $MraY^{72-238}$. This mode of enzyme inhibition results from the reversible conversion of a loosely bound E•I complex into a more tightly bound E•I* complex (Figure 5.2). E•I* may represent either a conformational change or a reversible chemical reaction at the active site[243]. It is plausible that an initial interaction with MraY occurs at the protein E binding site to form E•I. This interaction may lead to a conformational change (E•I*) which may be

necessary to shuttle the large macromolecule to the MraY active site. The hypothesis is further supported by previous reports which have shown that liposidomycin B is a non-competitive inhibitor of MraY, which might indicate initial binding to an allosteric site in MraY[244].

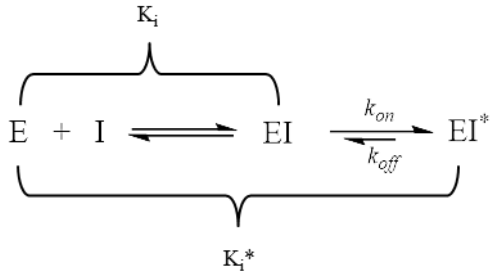


**Figure 5.2: Kinetic Scheme for slow binding inhibition.** $k_{on}$ and $k_{off}$ represent the unimolecular rate constants for the reversible conversion of EI to EI*[243]

To test this hypothesis, a small collection of compounds containing a uridine motif and segments of the RWXXW motif were designed and synthesised (Figure 5.3). In order to mimic the spacing found in UPAs, a succinyl-Gly-Gly linker was inserted between uridine and Arg-Trp. Also, analogue **[29]** was designed, containing two Trp residues. These compounds were then tested for activity against MraY and MraY mutants F288L and E287A to determine if this initial interaction is occurring.

**[26]**

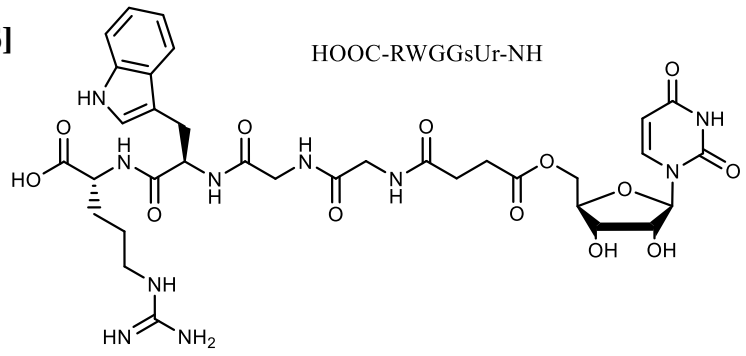

**[27]**

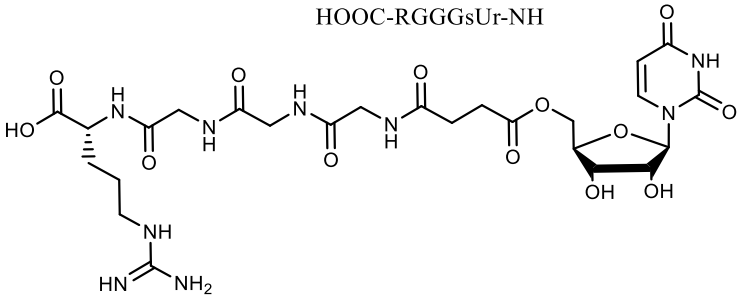


**[28]**

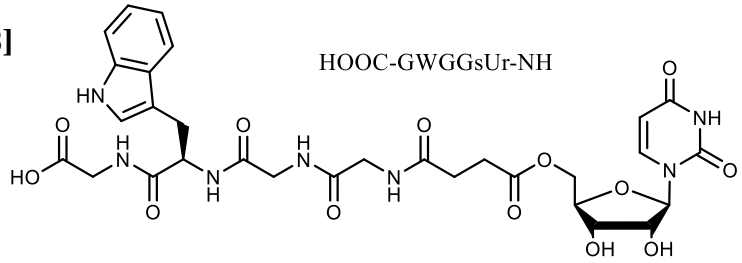


**[29]**

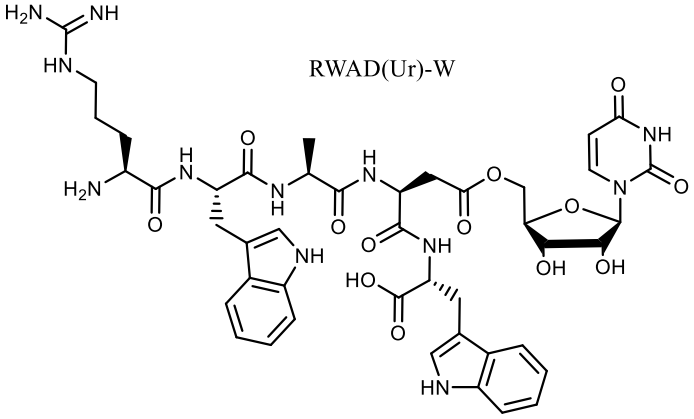


**Figure 5.3: UPA analogues containing Arg and/or Trp**

## 5.2 Synthesis of uridine derivatives

To provide flexibility to these uridyl containing compounds an extension to the 5´ OH of the ribose ring was desired. To specifically esterify the 5´ OH, protection of the vicinal diols (2´OH and 3´OH) was required. Uridine protected at this site is commercially available as 2',3'-*O*-isopropylidene uridine **[31]** for £129 (5g). Given

that a large quantity of **[31]** was needed to synthesise the desired uridyl containing oligopeptides, it was decided to synthesise **[31]**.

### *5.2.1 Formation of isopropylidene ketal*

Isopropylidene ketal or acetonide are the most common protecting groups of 1,2 and 1,3-diols as they are stable to most experimental conditions except treatment with acids[245]. In carbohydrate chemistry, where 1,2 and 1,3 diols are both present, the formation of the desired acetonide is dependent on whether the reaction is under kinetic or thermodynamic control. The difference between these two reaction conditions lies in the activation energy. Reactions under kinetic control have lower activation energy than thermodynamic controlled reactions.

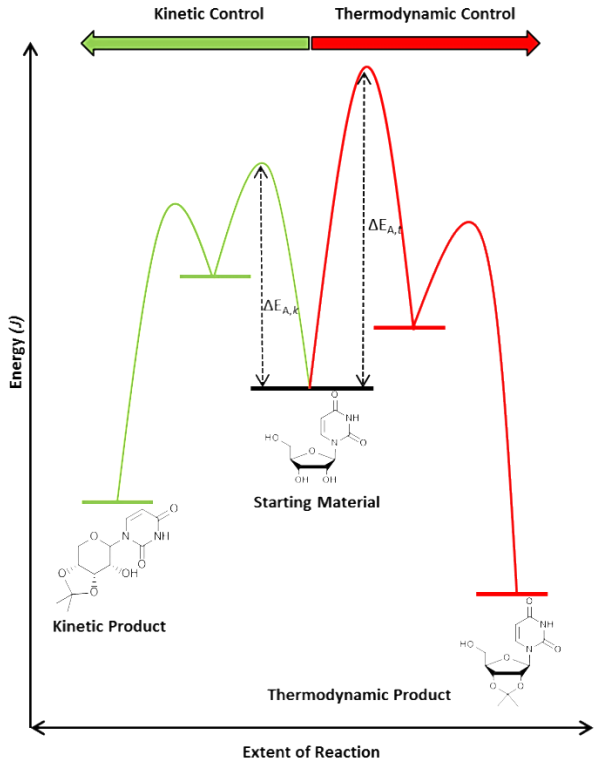


**Figure 5.4: Energy profile diagram comparing kinetic vs. thermodynamic controlled reaction for the protection of uridine diols**

Under kinetic control, 5-furan and 6-pyran ring systems exist in equilibrium (Figure 5.5). The 1° alcohol of the furanose ring is more nucleophilic and sterically accessible

than the 2° alcohol towards the attack of the 1´ carbon. As a result, the 6-pyranose form is the major isomer in solution (≈80%)[246].

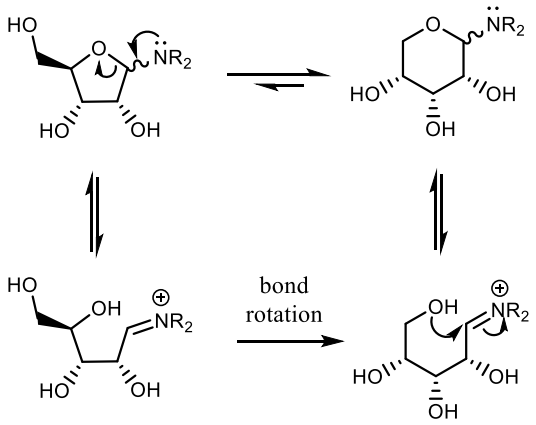


**Figure 5.5: Equilibrium conversion of furanose to pyranose**

Treatment of uridine with 2-methoxypropene under kinetic control, will therefore produce the undesired product, **[30]** (Figure 5.6). The activation energy of this reaction is much lower than 1,2-indol protection, and as result this reaction proceeds rather quickly[247] (Figure 5.4).

**[30]**

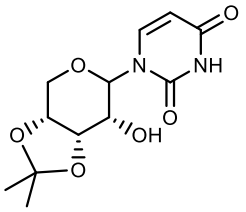


**Figure 5.6: Product of kinetic controlled indol protection of uridine**

Following the method of J Tomasz (1978), a solution of uridine (1eq) and *p*-toluenesulfonic acid (*cat.*) in $CHCl_3$ was stirred under reflux and treated with 2.4 eq of 2-methoxypropene overnight. Removal of the solvent and the MeOH by-product *in vacuo*, followed by a standard work up and purification produced **[31]** at 71% yield. The addition of heat provided the energy to initiate 1,2-indol protection of the less stable furanose ring[248] (Figure 5.7). However, a small amount of **[30]** did form which was removed by flash chromatography using 100% EtOAc.

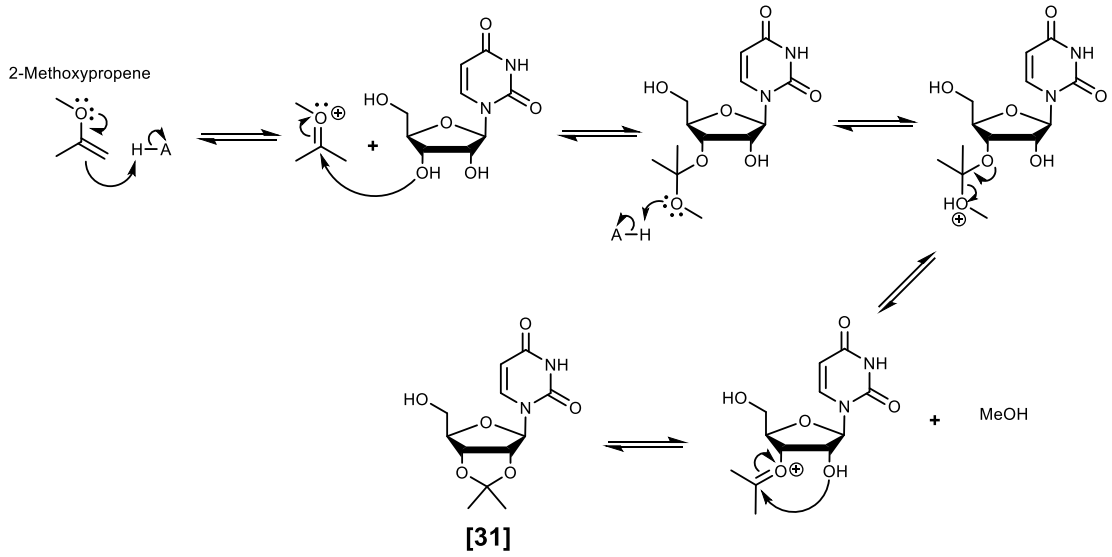


**Figure 5.7: Thermally controlled mechanism of 1,2-indol protection of uridine using 2-methoxypropene**

### *5.2.2 Elongation of 2',3'*-O-*isopropylidene uridine*

Previous work in the Bugg research group showed that **[31]** could be selectively acylated at C-5 with succinic anhydride[249]. This provided a convenient linker to couple to the amino terminus of a short peptide.

Esterification of succinic anhydride (0.94eq) with the 1° alcohol of **[31]** (1eq) was accomplished by treatment with TEA (0.9eq) at 0°C overnight in anhydrous DCM. The solvent was removed *in vacuo* and the resulting residue was cooled to 0°C and re-dissolved in $Na_2CO_{3(sat)}$. Washing with $Et_2O$ removed the organic base, TEA. Protonation of the corresponding carboxylic acid with 2M HCl, extraction into DCM and purification of the product by flash chromatography produced **[32]** at 57% yield.

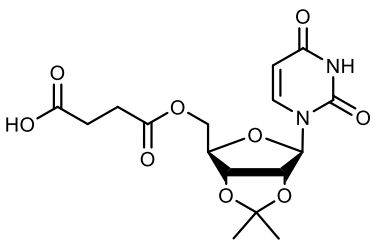

**Figure 5.8: 5'-succinyl-2', 3'-O-isopropylidene uridine [32]**

### *5.2.3 Esterification of Fmoc-Aspartic Anhydride*

The synthesis of **[29]** was desired as it has the most sequence similarity to the natural product muraymycin. Product **[29]** required esterification of the aspartic acid side chain with 2', 3'-O-isopropylidene uridine **[31]**. In hopes of approaching this in a similar manner as **[32]**, Fmoc-aspartic anhydride was first synthesised (Figure 5.9).

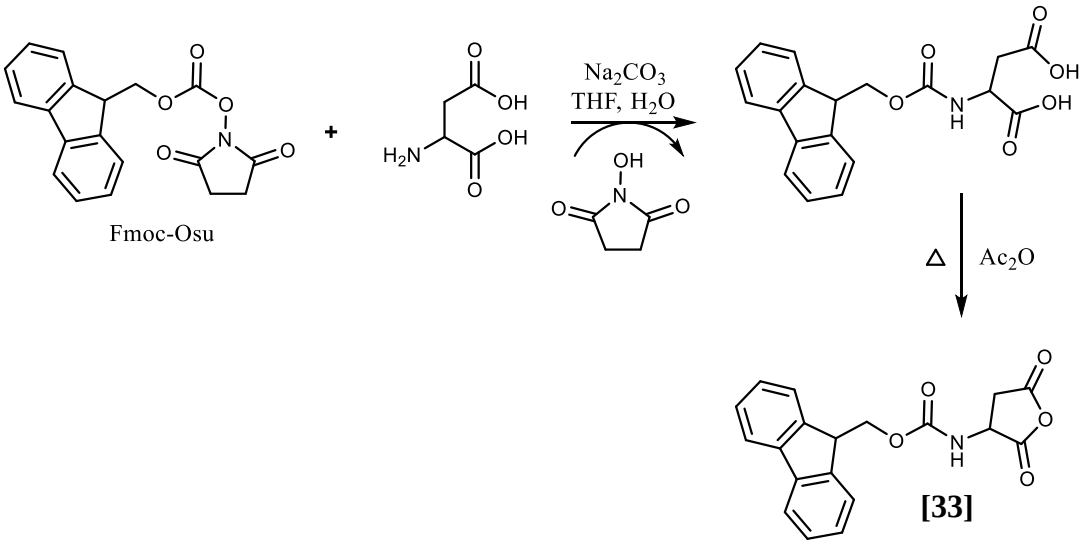


**Figure 5.9: Reaction scheme for the synthesis of Fmoc-aspartic anhydride[33]**

1 eq of Fmoc-OSu in THF was added to a solution of aspartic acid (1eq) and $Na_2CO_3$ (2.2 eq) in $H_2O$. After stirring at room temperature overnight, the mixture was washed with $Et_2O$. The aqueous layer was acidified to pH 2 and the desired intermediate Fmoc-aspartic acid was extracted into EtOAc. The organic phase was dried with $MgSO_4$ and concentrated *in vacuo*. The residue was then re-dissolved in $Ac_2O$ with rapid heating and stirring (10 minutes) and immediately cooled to room temperature causing **[33]** to precipitate out at 96% yield.

Esterification of **[33]** with the 1° alcohol of 2', 3'-O-isopropylidene uridine **[31]** (1eq) was accomplished by treatment with TEA (0.9eq) at 0°C overnight in dried DCM. Purification via flash chromatography using 100% EtOAc as the eluent isolated two products with Rf's 0.5 and 0.3. ESI-MS revealed that both species had an *m/z* of 620.2

[M-H]$^-$. In addition, the $^1$H-NMR spectra of these two species was nearly identical. It appeared that esterification of **[33]** with **[31]** was not regioselective and as a result a mixture of α and β esters were formed (Figure 5.10). Ibatullin and Stelivanov (2009) found that the regioselectivity of *N*-Fmoc-aspartic anhydride varied greatly depending on the polarity of the reaction media. In more polar solvents such as DMSO, acylation of the β carbonyl was the major product[250]. However, attempts to esterify **[33]** with **[31]** using DMSO as the solvent was unsuccessful.

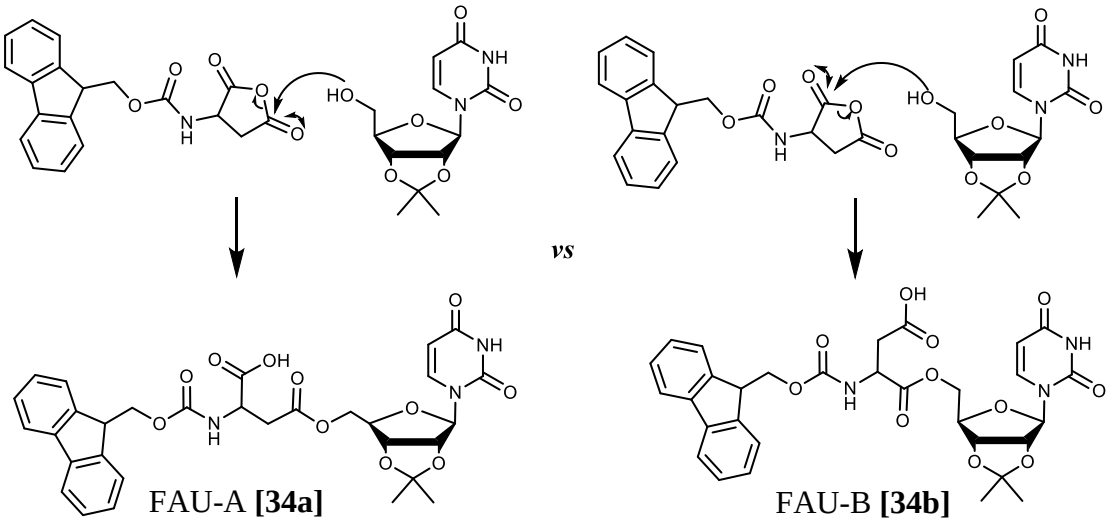


**Figure 5.10: Products of the non-regioselective esterification reaction of [33] with [31]**

Attempts to grow crystals and distinguish the two products via X-ray crystallography were also unsuccessful. Higher resolution NMR experiments were conducted with help from the experimental NMR officer Dr. Ivan Prokes. A two-dimensional Nuclear Overhauser Effect Spectroscopy (NOESY) experiment was conducted at 298 K using an AVIII-600 spectrometer and DMSO-$d_6$ as the solvent. The result of the high resolution NMR experiment for **[34b]** is given in Figure 5.11.

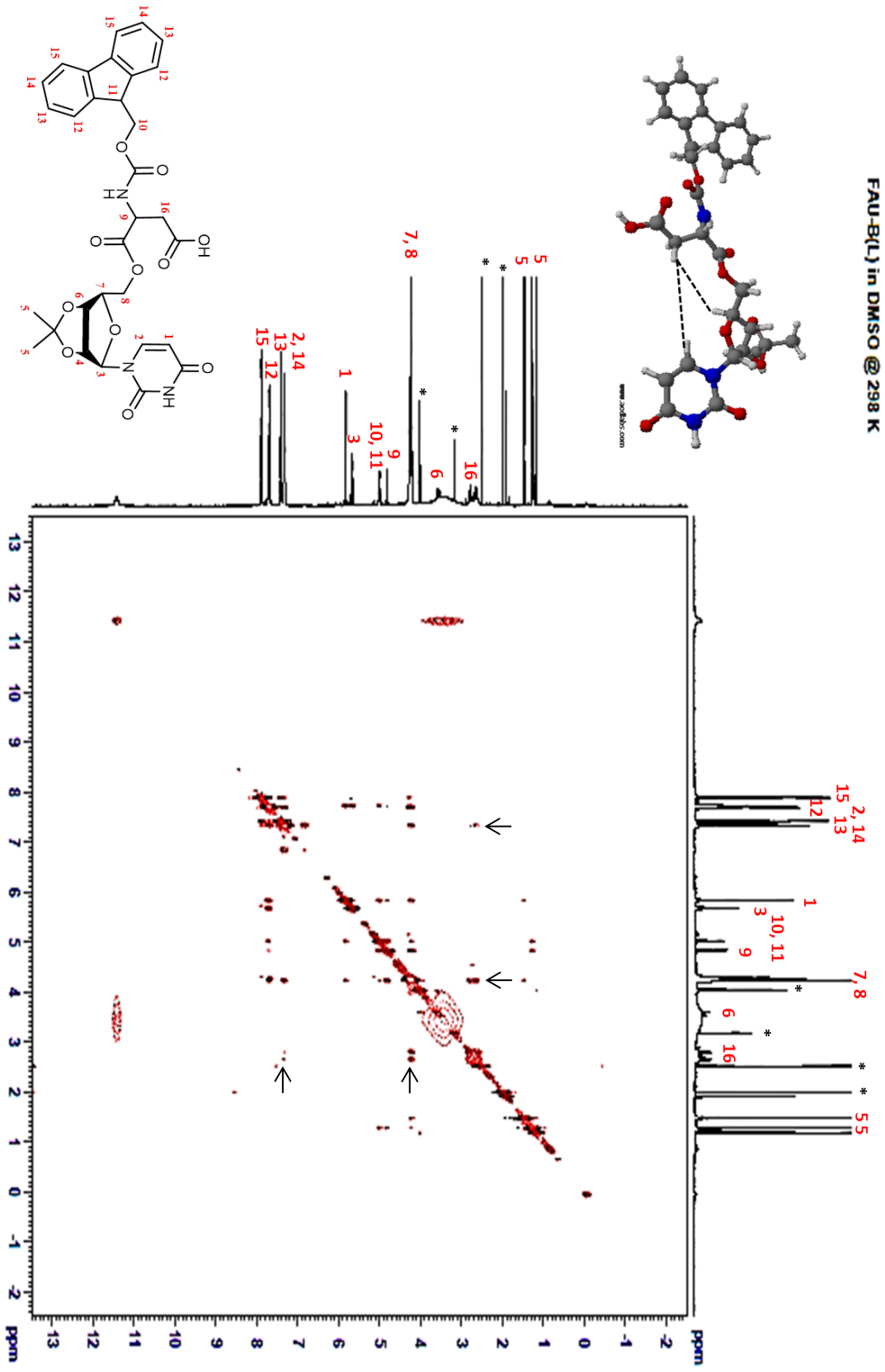


**Figure 5.11: NOESY spectra of [34b] in DMSO-$d_6$.** Long range coupling of H-16 with the H-2 of uracil and the H-7 and H-8 of the furanose ring suggests that [34b] has attached to the α-carboxyl of Fmoc-aspartic acid.

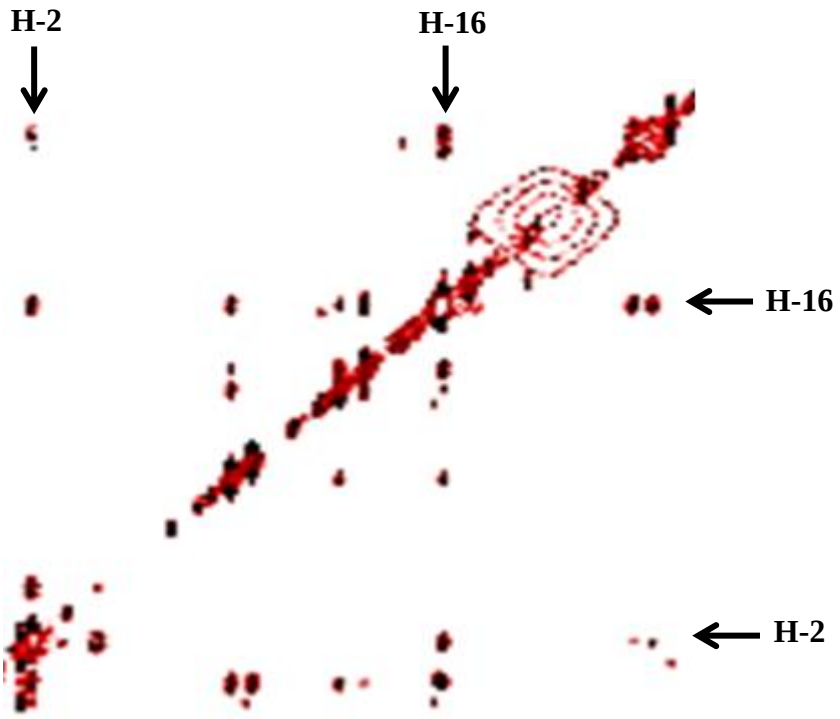


**Figure 5.12: Zoomed in view of the NOESY spectra for [34b] highlighting interactions of interest.**

The NOESY spectra of **[34b]** showed that H-16 interacted with the H-7 and H-8 of the uridyl moiety and the $sp^2$ hydrogen (H-2) of the uracil moiety. H-2 has a characteristically high chemical shift (≈7.2-7.8ppm) and in this spectrum appeared to have fused with an aromatic proton peak. The interaction of H-16 to H-2 is weak in comparison to the interaction with H-7 and H-8.

With respect to **[34a]**, an interaction was observed between H-9 and the H-7 and H-8 of the furanose ring. We did not observed an interaction between H-9 and H-2 of the uracil moiety (Figure 5.13), suggesting that H-2 and H-9 protons are too far away in space to interact.

From inspections of models, it appears that H-9 of **[34a]** has limited mobility in comparison to H-16 of **[34b]** which may hinder long range interactions with H-2. As a result, it seemed more likely that the NOESY spectra of Figure 5.11 corresponded to isomer **[34b]**. In both cases, the α-proton interacted with H-7 and H-8 but not H-2. No

other interaction was useful in distinguishing these two isomers. To distinguish with confidence X-ray crystallography would still be necessary.

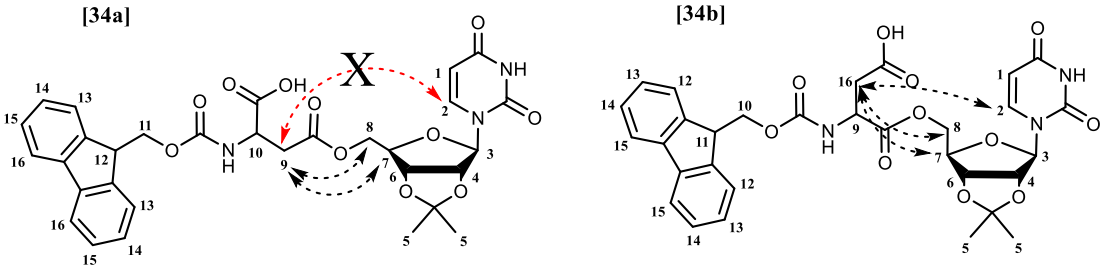


**Figure 5.13: NOESY interactions of [34a] and [34b].** H-9 of [34b] was found to couple to H-7 and H-8 but not to H-2, presumably due to a greater distance in space and limited mobility.

## 5.3 SPPS

UPA analogues were synthesized on a fritted-filtered reaction vessel using a standard Fmoc SPPS procedure[162] (Figure 5.14).

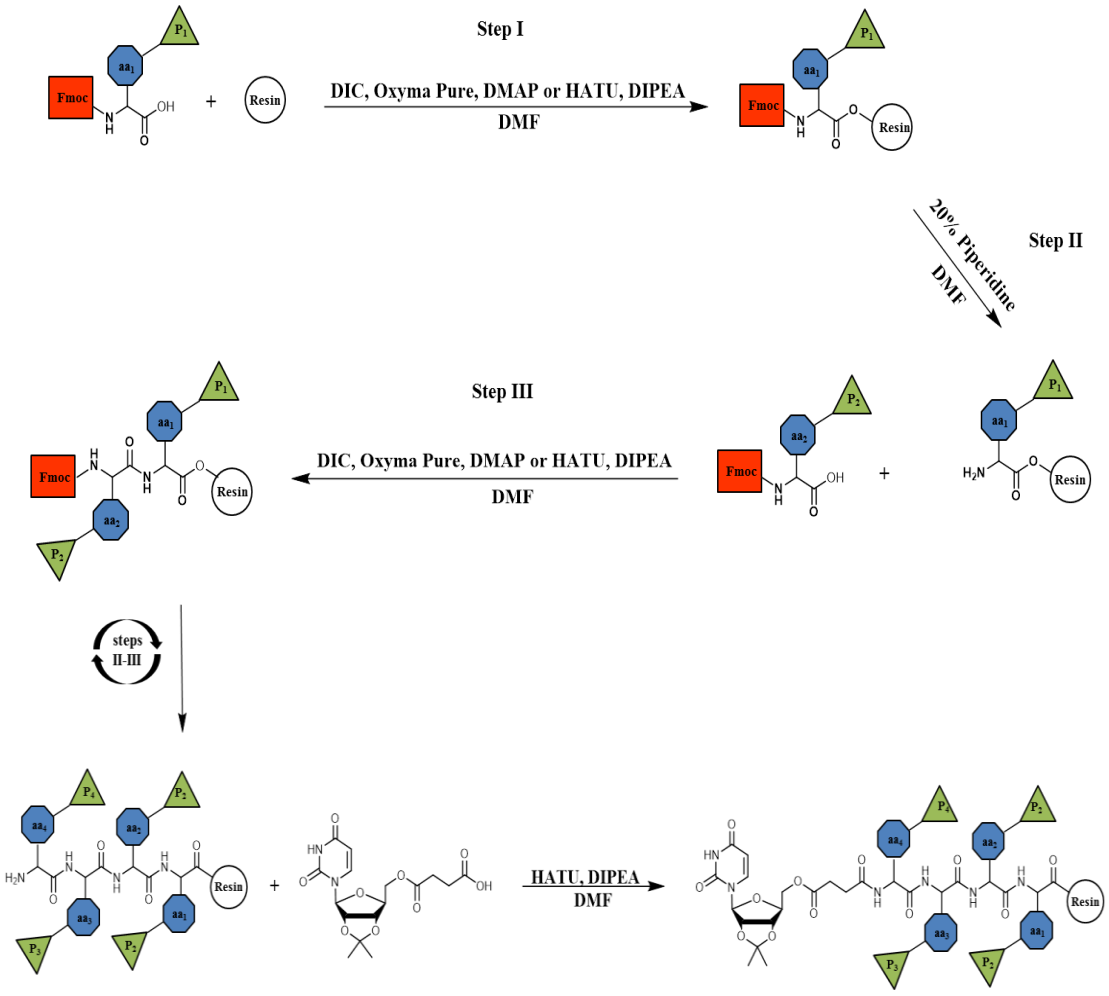


**Figure 5.14: Scheme for SPPS of UPA analogues**

In a dried RBF, Fmoc-protected amino acids (2-4eq) were dissolved in minimum dried DCM. Following the addition of a DIPEA (2.5eq), the mixture was immediately added to 1eq. of swollen 2-chlorotritylchloride resin and agitated gently with $N_2$ gas for 1-2 days. To cap any remaining unloaded resin beads, anhydrous MeOH was later added to the resin and agitated under $N_2$ gas for 1 hour.

Upon several washes with dried DMF and DCM, Fmoc-protecting groups were removed by treatment with 20-30% piperidine in DMF for 2 hours. Following another

series of washes, activated amino acids were added to the loaded resin in a similar manner to the first step. Upon several washes with dried DMF and DCM, Fmoc-protecting groups were removed as mentioned above.

The addition of uridine derivatives **[32]**, **[34a]** and **[34b]** to the peptide chain was achieved by activation with HATU (2eq) followed by treatment with DIPEA (2.5eq). The reaction mixture was immediately added to the loaded resin and agitated gently with $N_2$ gas for 2 days. Compounds **[34a]** and **[34b]**, which contained a free amino group (after fmoc-deprotection) was further coupled to other incoming amino acids to form **[29a]** and **[29b]**. The absence of an amino group in **[32]** prevented further peptide coupling and therefore was the terminal functional group in compounds **[26]**, **[27]** and **[28]**.

Cleavage and total deprotection of uridine containing peptides involved treatment with 19:1 TFA/$H_2O$ overnight. The resin was removed by filtration under reduced pressure and washed twice with neat TFA to assist in the removal of any loosely bound peptide product. Filtrates were combined and TFA was evaporated using a $CO_2$/acetone rotary evaporator. Cold ether was used to precipitate the oligopeptides. The product was isolated and dried further with a high vacuum pump and lyophilised.

TFA cleavage removed the side chain protecting groups, the diol protecting group and liberated the uridyl-oligopeptide from the resin. Products **[26]**, **[27]**, **[28], [29a]** and **[29b]** were purified by reverse phase HPLC at a flow rate of 20mL/min as described in Chapter 2.4. 64%, 96% and 91% of products **[26]**, **[27]** and **[28]** was isolated, respectively. Products **[29a]** and **[29b]** were isolated with very poor yields (<3%). Perhaps the acid treatment caused the product to degrade, cleaving the uridyl ester linkage.

## 5.4 Inhibition of MraY by uridyl oligopeptides determined by the continuous fluorescence assay

The MraY catalysed reaction was monitored using the continuous fluorescence assay described in Chapter 3.3 at an excitation wavelength of 340nm and an emission wavelength of 530nm. The final protein concentrations of membranes containing overexpressed *E. coli, P. aeruginosa, S. aureus, M. flavus* and *B. subtilis* MraY in this continuous assay were 0.6, 0.1, 0.28, 0.3, 0.3 and 0.9 mg/mL, respectively. The results of the enzymatic assay are provided in Table 5.1.

**Table 5.1: $IC_{50}$ (μg/mL) values of uridine peptide analogues against MraY**

| μg/mL | *E. coli* | E287A | F288L | *P. aeruginosa* | *S. aureus* | *M. flavus* | *B. subtilis* |
|---|---|---|---|---|---|---|---|
| [26] | X | X | X | X | X | X | X |
| [27] | 71 +/- 13 | X | X | 508 +/- 121 | 210 +/- 44 | 391 +/- 71 | 254 +/- 44 |
| [28] | X | X | X | X | X | X | X |
| [29a/b] | X | X | X | X | X | X | X |

HOOC-RGGGsUr **[27]** was found to be an inhibitor of *E. coli* MraY with an $IC_{50}$ of 71μg/mL (Appendix 3.1). **[27]** was also found to inhibit *P. aeruginosa, S. aureus, M. flavus* and *B. subtilis* MraY with $IC_{50}$ values of 508, 210, 391, and 254μg/mL, respectively (Appendix 3.2-3.5). In the case of **[27]**, it is possible that an electrostatic interaction was initially formed between Glu287 and the arginine residue of **[27]**. This interaction may have assisted in the translocation of the molecule across the membrane bilayer in a similar manner to antimicrobial peptides (Chapter 1.2.1). Once across the membrane bilayer, **[27]** may have interacted with MraY at the active site via its uridyl moiety.

None of the remaining uridyl oligopeptides were found to have activity against MraY. This was surprising since we hypothesised that the aromatic residues of these analogues may form an initial interaction with Phe288. In comparison to **[27]**, the

remaining uridyl oligopeptides are bulky and rigid. It is possible that the small size and flexibility of the tripeptide glycyl motif of **[27]** facilitated translocation across the membrane and ultimately inhibition of MraY.

### *5.4.1 Inhibition of E. coli MraY mutants by [27]*

To confirm if residues Glu287 and Phe288 are critical for the inhibition of MraY by **[27]**, the activity of **[27]** against MraY mutants F288L and E287A was determined (Table 5.1). This provided a more conclusive picture on the interaction of this natural product analogue with MraY.

Applying the same procedure used for WT MraY (Chapter 3.3), **[27]** was found to lose inhibitory activity against MraY mutants F288L and E287A. The lack of activity against E287A supports the hypothesis that **[27]** forms an initial electrostatic interaction with Glu287. The lack of activity against F288L was surprising given that **[27]** does not have an aromatic residue or any obvious motif that could interact with Phe288.

## 5.5 Antibacterial activity of uridyl oligopeptides

The antibacterial properties of these natural product analogues were determined via the microtitre broth dilution technique. Utilising the same procedure used for RWXXW analogues (Chapter 4.2), it was found that uridyl oligopeptides did not have antibacterial activity against *E. coli*, *P. putida* or *B. subtilis*. Though unfortunate, this was expected as most UPAs lack antibacterial activity against these organisms.

## 5.6 Inhibition of MraY by known UPAs determined by the continuous fluorescence assay

The $IC_{50}$ of known natural products against WT *E. coli* MraY and mutant MraY was determined using the continuous fluorescence assay. The structures of the UPAs tested, mureidomyin A, caprazamycin A, caprazamycin E, pacidamycin D and pacidamycin 1&2, are given in Figure 5.15.

(a)

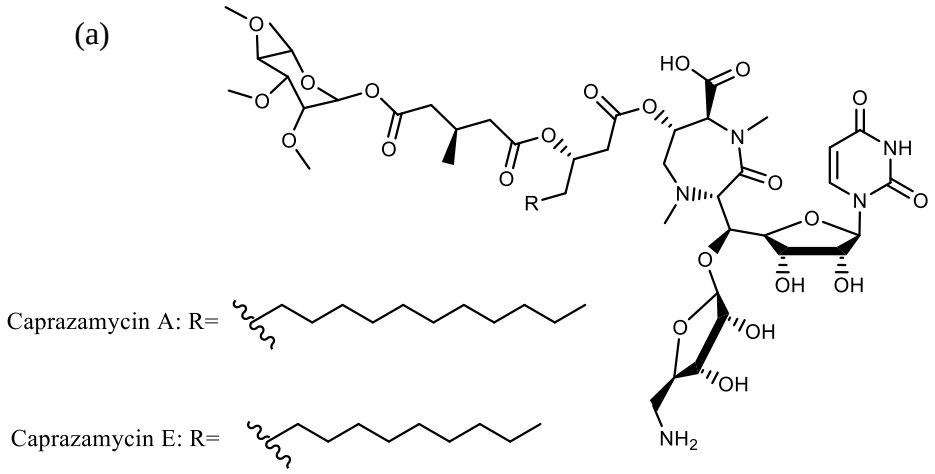


(b)

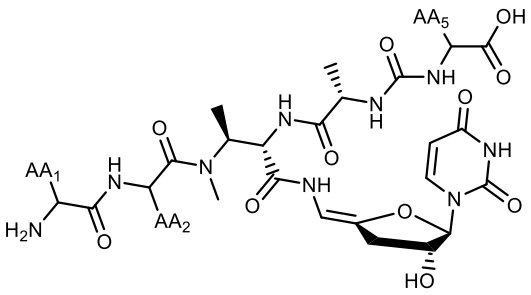

| Pacidamycin | $AA_1$ | $AA_2$ | $AA_5$ |
|---|---|---|---|
| 1 | Ala | *m*-Tyr | Trp |
| 2 | Ala | *m*-Tyr | Phe |
| D | - | Ala | Trp |

(c)

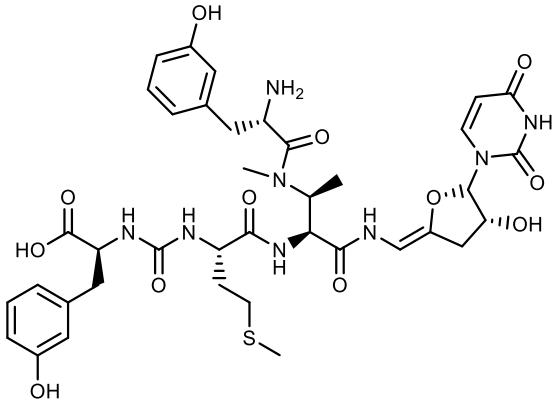

Mureidomycin A

**Figure 5.15: Structures of UPAs (a) Caprazamycin (b) Pacidamycin (c) Mureidomycin A**

The continuous fluorescence assay confirmed previous reports that UPAs caprazamycin A, caprazamycin E, pacidamycin 1&2, pacidamycin D and mureidomycin A are inhibitors of the MraY reaction (Appendix 3.6-3.10). Utilising the software GenStat for Teaching and Learning, the $IC_{50}$ value of each inhibitor was calculated (Table 5.2).

**Table 5.2: $IC_{50}$ values of UPA against E. coli MraY**

| UPAs | $IC_{50}$ (μg/ml) |
|---|---|
| Mureidomycin A | 0.60 +/- 0.10 |
| Caprazamycin A | 0.25 +/- 0.03 |
| Caprazamycin E | 0.16 +/- 0.03 |
| Pacidamycin D | 0.16 +/- 0.03 |
| Pacidamycin 1&2 | 0.071 +/- 0.011 |

These strikingly low $IC_{50}$ values highlight the high potency of the UPA antibiotics. To test if these natural products interact with MraY at the protein E binding site before inhibiting at the active or another allosteric site, the activity of these natural products against MraY mutants was determined.

### *5.6.1 Inhibition of F288L and E287A MraY by known natural products*

Due to the presence of aromatic residues, which we predict could form a π-π stacking interaction with Phe288 of MraY and the presence of a positively charged amino group, which could form an electrostatic interaction with Glu287, the inhibitory activity of known natural products against MraY mutants F288L and E287A was determined. The $IC_{50}$ value of these UPAs were determined using the continuous fluorescence assay and the software GenStat for Teaching and Learning (Table 5.3; Appendix 3.11-3.20).

Only a marginal 2-fold increase in the $IC_{50}$ of mureidomycin A was observed when Glu287 or Phe288 was mutated. This suggests that theses residues may not be important in the inhibitory mechanism of mureidomycin A. Similarly, no significant change was observed in the $IC_{50}$ values of caprazamycin A or E.

**Table 5.3: $IC_{50}$ values of known nattural products against F288L and E287A MraY.** Compounds whose increased in $IC_{50}$ value relative to WT MraY is noted.

| | $IC_{50}$ E287A (μg/mL) | Increase from WT | $IC_{50}$ F288L (μg/mL) | Increase from WT |
|---|---|---|---|---|
| Mureidomycin A | 1.17 +/- 0.13 | x2 | 1.05 +/- 0.3 | x2 |
| Caprazamycin A | 0.12 +/- 0.02 | - | 0.24 +/- 0.03 | - |
| Caprazamycin E | 0.12 +/- 0.03 | - | 0.39 +/- 0.08 | x2 |
| Pacidamycin D | 0.48 +/- 0.07 | x2 | 1.58 +/- 0.28 | x10 |
| Pacidamycin 1&2 | 107 +/- 27 (ng/mL) | - | 0.97 +/- 0.18 | x13 |

No significant change in the $IC_{50}$ values of Pacidamycin 1&2 or D was observed against MraY mutant E287A. A significant 10-13-fold increase was observed in the $IC_{50}$ values of pacidamycin 1&2 and D against MraY mutant F288L. This suggests that Phe288 is critical for the inhibition of MraY, presumably by assisting in the translocation of pacidamycin across the cell membrane. The aromatic residues of

pacidamycin could form a π-π stacking interaction with Phe-288 of MraY in the same manner as protein E (Figure 5.16).

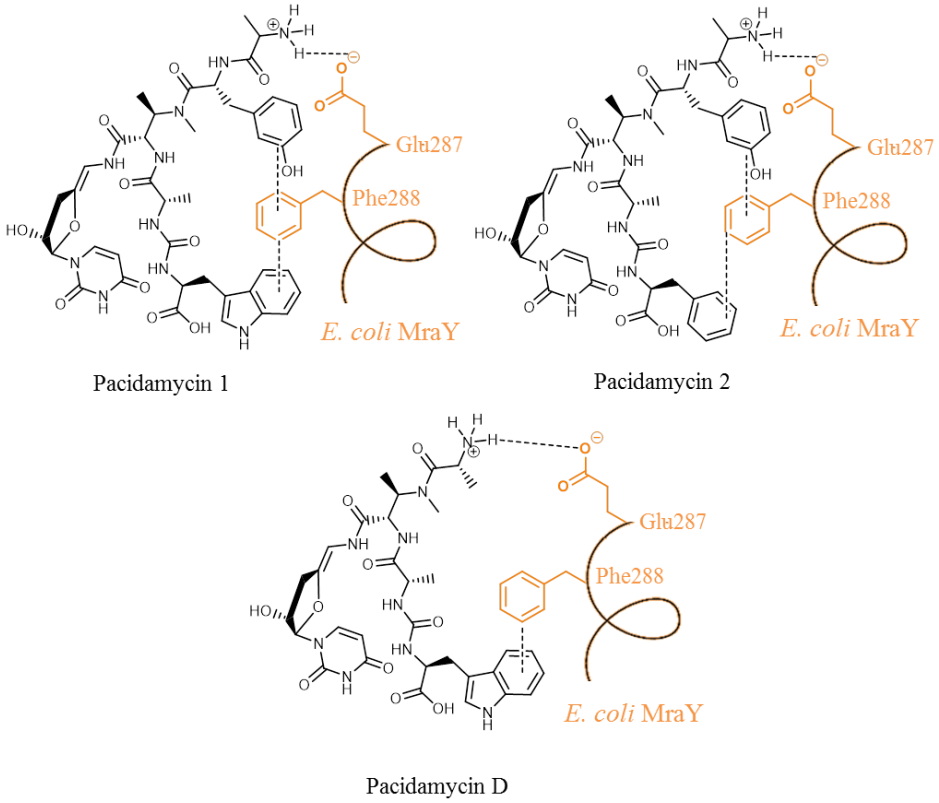


**Figure 5.16: Predicted interaction between Pacidamycins and *E. coli* MraY at the anticipated protein E binding site.** π-π stacking interactions can be formed between Phe-288 and the natural products aromatic residues. An electrostatic interaction can also be formed between Glu287 and the N-terminus.

## 5.7 Conclusion

The effective and complex design of antibiotics by bacteria has sparked great interest in the modification of their natural products in the development of novel drugs. Modification of UPA is an increasingly interesting topic due to their potency in inhibiting peptidoglycan biosynthesis. Using a general template for the structure of natural product inhibitors of MraY, an interesting relationship was discovered between protein E and UPA. Similar to protein E, we hypothesised that UPAs bind to MraY at the protein E site. This initial interaction may cause a conformational change to the protein allowing the translocation of UPAs to the active site. This hypothesis is

supported by kinetic reports, which showed the UPAs are slow binding inhibitors of MraY[72]. Some UPAs were also found to be non-competitive inhibitors of MraY, further strengthening out hypothesis[238].

Synthesis of uridyl oligopeptide analogues was achieved by a mixture of solution and solid phase chemistry. Uridyl oligopeptide analogues required protection of the uridine 1,2-indol with 2-methoxypropene (71%). This was thermodynamically controlled in order to prevent indol protection of the pyranose isomer of uridine.

In hopes of elongating and providing flexibility to these analogues, esterification at the 5'OH of 2',3'-*O*-isopropylidene uridine was performed. Esterification with fmoc-aspartic anhydride was not regioselective and as a result esterification occurred at the α or β carbonyl. Esterification at both the carbonyls did not occur presumably due to steric hindrance. Upon inspection of models and NOESY spectrums, we were able to hypothesise on the identity of these isomers. However, to confirm with confidence, an X-ray crystal structure would still be necessary. Unfortunately, attempts to grow crystals were unsuccessful. Esterification with succinic anhydride (57%) did not pose any problems as both carbonyls are equivalent.

Following a general method for solid phase peptide synthesis, uridyl derivatives were effectively added to peptide chains with yields ranging from 64-96%, when the uridyl derivative was the last component added to the loaded resin. The addition of the uridyl derivative at the second step of peptide synthesis (RWAD(Ur)-W and RWAD(W)-Ur) lead to poor yields (2-3%). These exceedingly low yields may also be as a result of degradation upon TFA cleavage.

The continuous fluorescence assay revealed that HOOC-RGGGsUr was an inhibitor of *E. coli, B. subtilis, P. aeruginosa, S. aureus* and *M. flavus* MraY. Mutation at Phe288 and Glu287 resulted in complete loss of inhibitory activity, suggesting that

these residues are important for binding. It's plausible that Glu287 is important in forming an electrostatic interaction with the arginine of HOOC-RGGGsUr. It's unclear the role or interaction of this inhibitor with Phe288.

To determine if Phe288 and Glu287 interact with UPAs, the $IC_{50}$ of mureidomyin A, caprazamycin A, caprazamycin E, pacidamycin D and pacidamycin 1&2 against WT MraY was compared to the $IC_{50}$ of these natural products against MraY mutants F288L and E287A. A 10-13-fold increase in the $IC_{50}$ of pacidamycin was observed against F288L. Pacidamycin may interact with Phe288 via a π-π stacking interaction. This interaction may facilitate the translocation of the 900kDa natural product across the cellular membrane and towards the active site of MraY.

# Chapter 6: Conclusion

This research project was motivated by the increasing number of multidrug resistant bacteria. Resistance to commercially available antibiotics has increased so drastically that it is now considered an epidemic. Much work has been invested in the development of new antimicrobials, yet in the past 40 years only three new classes of antibiotics have been developed. This is primarily due to the difficulty in identifying new lead compounds from high-throughput screening and the rapid evolution and spread of resistance.

Bacterial cell wall peptidoglycan biosynthesis is a well-established target for antibiotics. Many drugs have been developed to target various steps across the biosynthetic pathway of peptidoglycan with the exception of integral membrane protein MraY, which catalyses the first membrane bound step. In nature, MraY is a popular and effective target of the uridyl peptide antibiotics which include natural products tunicamycin, muraymycin and pacidamycin. MraY is also the target of lysis protein E from bacteriophage ΦX174. Previous research has shown that lysis protein E mediates cell lysis by an interaction with MraY at a site other than the active site. Genetic studies revealed that E-mediated lysis is dependent on the interaction between Phe288 of MraY and the transmembrane segment of protein E[120,133].

We have constructed an α-helical model for the predicted transmembrane interactions between protein E and MraY and shown that favourable interactions can be formed at the Phe288 site. Trp-4 and Trp-7 of protein E can participate in π-π stacking with Phe-288, while Arg-3 can interact with Glu287 of MraY via an electrostatic interaction. Together, these residues provide an RWXXW motif which could interact with MraY via Phe288 and Glu287. In order to investigate this hypothesis, synthetic peptide

analogues of the RWXXW motif was synthesised and tested against membrane bound MraY and mutants F288L and E287A.

Utilising a continuous fluorescence assay, developed by Brandish (1995) and optimised by Mihalyi (2013), the inhibitory activity of RWXXW analogues was determined. This assay revealed that RWXXW analogues were able to inhibit MraY with $IC_{50}$ values as low as 58μg/mL. Peptides which contained a tryptophan residue were especially good inhibitors of MraY presumably due to its interaction with Phe288. Mutation of Phe288 caused a dramatic decrease or complete loss to the inhibitory activity of peptides containing an aromatic residue. ***These findings support our hypothesis that a π-π stacking interaction may occur between Phe288 and the RWXXW motif of protein E.***

We hypothesised that MraY residue Glu287 could form an electrostatic interaction with Arg-3 of protein E. Therefore we expected compounds which lacked an arginine residue to be unable to inhibit MraY. However, we found that compounds which lacked arginine or contained a chemically similar amino acid, like histidine, were still able to inhibit MraY. It is possible that the N-terminus could interact with Glu287 via an electrostatic interaction. ***From these result it appeared that π-π stacking interaction is the crucial and dominant interaction in the inhibition of MraY.***

The presence of a hydrocarbon chain affected the inhibitory activity of peptides depending on which terminus it was acylated to. Compounds which contained an octyl group on the C-terminus were good inhibitors of MraY ($H_2$N-GW-Oct, $IC_{50}$=58μg/mL) while compounds which contained an octyl group on the N-terminus did not contain any inhibitory activity. Analogues which were *N*-acylated and lacked an N-terminal arginine (e.g. Octyl-GW-OMe) would be unable to form an electrostatic interaction with Glu287. As a result, this may hinder proper insertion in

the membrane and prevent the formation of a π-π stacking interaction between the perspective aromatics.

Given the potency and kinetics of uridyl peptide antibiotics, it was desired to design a compound which could interact with MraY at the protein E binding site in addition to the active site. Previous work in our research group has showed that natural products liposidomycin B and mureidomycin A are slow binding inhibitors of $MraY^{72-238}$. Kinetics studies revealed that a conformational change may be occurring prior to inhibition. We hypothesised that this conformational change may be a result of an initial binding at the predicted protein E binding site which allows the diffusion of the macromolecule across the membrane and to the active site. To test this hypothesis, we compared the inhibitory activity of some known natural products against WT MraY to that of MraY mutants F288L and E287A. In the case of pacidamycin 1&2, which contains a tryptophan and a *m*-tyrosine residue, a 10-13 fold increase in the $IC_{50}$ value was observed against MraY mutant F288L. ***This suggests that Phe288 plays some role in the inhibition of MraY by pacidamycin.*** It is possible that the aromatic residues of pacidamycin were able to engage in a π-π stacking interaction with Phe288. These observations support our hypothesis that uridyl peptide antibiotics interact with MraY at the protein E binding site before interacting at the active site. This is in agreement with the kinetics studies published by our research group in 2006.

To further test our hypothesis, a small collection of compounds containing a uridine motif and segments of the RWXXW motif were designed and synthesised. HOOC-RGGGs-Ur was found to be a good inhibitor of WT MraY ($IC_{50}$ = 71μg/mL) but not an inhibitor of F288L or E287A MraY. In the absence of Glu287, the arginine residue of HOOC-RGGGs-Ur would be unable to bind successfully to the protein which may

have hindered translocation across the membrane. The lack of activity against F288L was surprising given that HOOC-RGGGs-Ur does not have an aromatic residue or any obvious motif that could interact with Phe288.

The antibacterial activity of all compounds was determined using the microtitre broth dilution technique. Some of these analogues contained antibacterial activity across multiple strains of bacteria including *E. coli*, *B. subtilis* and *P. putida* with MIC as low as 8μg/mL. To determine if inhibition of MraY is the mechanism of action which prevented the growth of bacteria further experimentation was necessary.

A continuous fluorometric assay for the permeabilisation of Gram-negative bacteria was optimised and used to determine if a particular compound was a membrane permeabiliser instead of an enzyme inhibitor. With the use of 1-*N*-phenylnaphthylamine which strongly fluoresces in permeabilised membranes, it was found that $H_2N$-RW-Oct does not permeabilise the membrane in comparison to EDTA. To confirm if MraY was the target enzyme, *E. coli* cells overexpressing MraY were treated with an RWXXW analogue. The MIC of $H_2N$-RW-Oct was found to increase 10 fold in cells overexpressing MraY and MraY mutant E287A. If MraY and the inhibitor form a 1:1 complex, overexpression of MraY would cause an increase in the MIC given that a higher concentration of the inhibitor would be necessary to inhibit the excess proteins. ***This experiment showed that the antibacterial activity of $H_2N$-RW-Oct is strongly related to the inhibition of MraY.***

The MIC of $H_2N$-RW-Oct increased 16-fold in cells overexpressing F288L MraY. This exceedingly high MIC may be as a result of a weakened binding affinity between the inhibitor and the protein. In the absence of Phe288, $H_2N$-RW-Oct would be unable to participate in π-π stacking. As a result, this led to an MIC much higher than *E. coli* cells overexpressing WT MraY or E287A MraY.

This research project aimed to better understand the interaction between protein E and MraY. The results of this research project elucidated the importance of residues Phe288 and Glu287 of MraY and the RWXXW motif of protein E. The inhibitory activity of these RWXXW analogues appeared to be site specific and rely on the presence of Phe288. The antibacterial properties of these compounds were also found to be directly related to MraY. From this work, it appears that protein E binds to MraY at the site we hypothesised. Most importantly, this work identifies a promising target for the development of novel antimicrobial agents that is located on the outer face of the cytoplasmic membrane.

# Chapter 7: Experimental

All chemicals used during this research project were purchased from Sigma Aldrich and Merck Novabiochem. Biological reagents $C_{55}$-P and $C_{35}$-P were purchased from Larodan Fine Chemicals. UDP-MurNAc pentapeptide was purchased from UK Bacterial Cell Wall Assembly Network (BaCWAN) and fluorescently tagged by PhD candidate Agnes Mihalyi. Natural products pacidamycin D and pacidamycin 1&2 were provided by Dr. Rebecca Goss from the University of St. Andrews. Natural product mureidomycin A was provided from Dr. M. Inukai from Sankyo Ltd. Natural products caprazamycin A and caprazamycin E were provided by Dr. Bertolt Gust from Eberhard-Karls-Universität Tübingen.

Water used during these experimental procedures was deionized and autoclaved when necessary. Deuterated methanol, chloroform and DMSO used for recording NMR spectra were purchased from Cambridge Isotope Labelling Inc. HPLC grade solvents were purchased from Fischer Scientific. Anhydrous solvents were only used when stated and were used as supplied. Solvents were evaporated using a Buchi Rotavapor R-114 equipped with a Buchi Vacuum pump V-700 and a Buchi Heating bath B-480.

Flash column chromatography was conducted on Fluka Silica Gel (40-63μm, 60Å). Thin Layer Chromatograpy (TLC) was performed on aluminum backed plates pre-coated with Merck TLC Silica Gel 60 $F_{254}$ and were visualized under UV radiation. Semi-preparative HPLC purification was conducted on an Agilent Technologies series 1200 Preparative HPLC instrument equipped with an Agilent Xorbax XDB-C18 preparative column (P/No: 970150-902, size: 21.2x150mm 5micron).

Low resolution ESI mass spectra were recorded using a Bruker Esquire 2000 electrospray ionization spectrometer. High resolution mass spectra were recorded on a Bruker Micro TOF spectrometer equipped with an electrospray ionization source.

Infra-red spectra were recorded using a Perkin-Elmer Paragon 1000 Fourier Transform spectrometer. Only selected absorptions are reported in units of wavenumbers ($V_{max}/cm^{-1}$)

$^{1}$H-NMR spectra were recorded at 300, 400 or 600 MHz using Bruker DPX300, DPX400 or AV III-600 spectrometers, respectively. Chemical shifts ($\delta_H$) are quoted in ppm with reference to the residual solvent peak. The data in parenthesis follow the order (i) multiplicity: s, singlet; d, doublet, t, triplet; q, quartet; m, multiplet (ii) number of equivalent protons (iii) coupling constant (*J*) in Hz (iv) assignment. COSY and NOESY were used in selected cases to aid in assignments.

Specific rotation was determined using an Opitical Activity Ltd AA-10 Series Automatic Polarimeter.

Fluorescence data was recorded using a Tecan GENios plate reader and a Perkin Elmer LS55 fluorescence spectrometer equipped with a PTP-1 peltier temperature programmer.

Bacterial growth was monitored on a Thermo Electron UV-VIS spectrophotometer 335908P-000. Bacterial cells were lysed using a Constant Systems Ltd. TS Series Cabinet cell disruptor.

An AGFA Curix 60 processor were used to visualise proteins on a western blot and dot blot.

## 7.1 Synthesis of Amino Acid Precursors

### L-Tryptophan methyl ester Hydrochloride [17] [251]

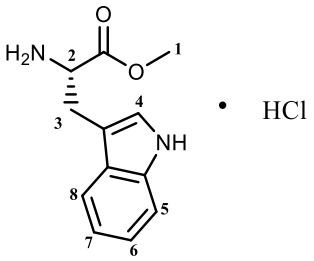

L-Tryptophan (1.02 g, 5.0 x $10^{-2}$ mol, 1 eq) was stirred in 25mL of MeOH. Freshly distilled TMSCl (1.27 mL, 1.0 x $10^{-2}$ mol, 2 eq) was added dropwise to the solution and allowed stir overnight at room temperature. The reaction mixture was concentrated *in vacuo*. The resulting white powder was dried under high vacuum (0.99 g, 3.9 x $10^{-3}$ mol, 78%).

**$R_f$** = 0.56 (8:2/EtOAc:MeOH) **m.p.** 218-222°C, lit m.p 218-220°C[252]; **Fourier Transform Infrared,** neat ($v_{max}/cm^{-1}$) 3297.9 (m, -NH-) 1742.6 (s, C=O) 1578.9 (s, -$NH_2$) 1362.0 & 1350.6 (d, -COO-CH2-); **$^1$H-NMR** (300MHz, MeOD) $\delta_H$: 3.40 (d, 2H, *J* = 7.0Hz, H-3), 3.82 (s, 3H, H-1) 4.34 (t, 1H, *J* = 6.0Hz, H-2 ), 7.14 (m, 3H, H-4 H-6 H-7), 7.41 (d, 1H, J = 8.0Hz, H-5), 7.56 (d, 1H, *J* = 8.0Hz, H-8) lit. $\delta_H$[251]; **HRMS:** m/z (ESI) calculated for $C_{12}H_{15}N_2O_2^+$: 219.1134 found: $[M+H]^+$: 219.1128

### L-Tryptophan octyl ester [18] [251]

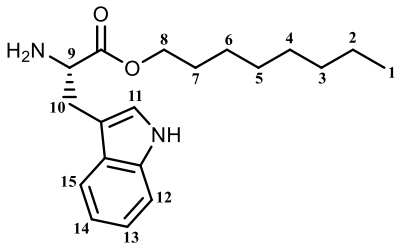

L-Tryptophan (1.02 g, 5.0 x $10^{-3}$ mol, 1 eq) was stirred in 1-octanol (10 mL, 6.3 x $10^{-2}$ mol, 12.6 eq) under reflux at 50°C. 5 mL of *conc.* $H_2SO_4$ was added to the reaction

mixture. Within 30 minutes of stirring, the maroon coloured reaction reached completion. The reaction mixture was taken up in EtOAc (25 mL) and washed with $Na_2CO_3$ (3 x 25 mL). The organic layer was isolated, dried with $MgSO_4$ and concentrated *in vacuo*. Excess 1-octanol was removed from the product by reduced pressure distillation or flash chromatography using deactivated silica and 100% EtOAc as the eluent. Procedure was modified from lit reference[253]; (6.8 g, 2.1 x $10^{-2}$ mol, 86 %).

**$R_f$** = 0.78 (8:2/EtOAc:MeOH) **Fourier Transform Infrared,** neat ($v_{max}/cm^{-1}$) 3320.6 (m, -NH-) 1742.2 (s, C=O); **$^1$H-NMR** (300MHz, MeOD) $\delta_H$: 0.80 (t, 3H, *J*=9.0Hz, H-1), 1.20 (m, 10H, H-2 H-3 H-4 H-5 H-6) 1.42 (m, 2H, H-7 ), 3.44 (t, 2H, *J*=6.5Hz, H-10), 3.66 (t, 1H, *J*=6.5Hz, H-9), 3.90 (t, 2H, *J*=6.0Hz, H-8), 6.93 (m, 3H, H-14 H-13 H-11), 7.23 (d, *J*=8.0Hz, H-12), 7.42 (d, *J*=7.5Hz, H-15), lit. $\delta_H$[254]; **HRMS:** m/z (ESI) calculated for $C_{19}H_{29}N_2O_2^+$: 317.2224 $[M+H]^+$. Found: $[M+H]^+$: 317.2224

**Glycine octyl ester [19]**[189]

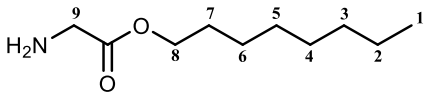


(i) A solution of Fmoc-Gly-OH (0.65 g, 2.2 x $10^{-3}$ mol, 1 eq), DMAP (0.13 g, 1.1 x $10^{-3}$ mol, 0.5 eq) and 1-octanol (0.40 mL, 2.5 x $10^{-3}$ mol, 1.14 eq) in 8 mL of DCM was cooled with stirring in an ice bath. *N*-(3-Dimethylaminopropyl)-N′-ethylcarbodiimide hydrochloride (0.46 g, 2.4 x $10^{-3}$ mol, 1.1 eq) was added and the reaction mixture was stirred at 0°C for 2 hours. The reaction was then stirred at room temperature overnight.

(ii) To the stirred solution, 20% piperidine in DMF was added and allowed to stir for 1 hour. The addition of the mild base caused the solution to become cloudy. The reaction mixture was concentrated to dryness *in vacuo* and was

taken up in EtOAc (25 mL). The organic layer was washed with $NaHCO_3$ (2 x 15 mL) and water (2 x 15 mL). The organic layer was dried with $MgSO_4$, concentrated *in vacuo* and dried further under high vacuum to produce a white thick oil (0.26 g, 1.37 x $10^{-3}$ mol, 62 %). Procedure was modified from lit reference[189].

**$R_f$** = 0.30 (8:2/EtOAc:MeOH) **Fourier Transform Infrared,** neat ($v_{max}/cm^{-1}$) 1738.6 (s, C=O) 1567.6 (s, -$NH_2$) 1433.7 & 1415.4 (d, -COO-CH2-); **$^1$H-NMR** (300MHz, MeOD) $\delta_H$: 0.90 (t, 3H, *J* = 7.0Hz, H-1), 1.31 (m, 8H, H-2 H-3 H-4 H-5) 1.52 (m, 2H, H-6 ), 1.70 (m, 2H, H-7), 3.84 (s, 2H, H-9), 4.24 (t, 2H, *J* = 6.5Hz, H-8) lit. $\delta_H$[255]; **HRMS:** m/z (ESI) calculated for $C_{10}H_{22}NO_2^+$: 188.1606 $[M+H]^+$, found: $[M+H]^+$: 188.1645

***N*-octanoyl glycine [20]**[190]

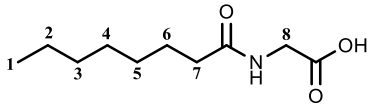


To a stirred solution of L-glycine (0.45 g, 6.04 x $10^{-3}$ mol, 1 eq) and $NaHCO_3$ (0.76 g, 9.06 x $10^{-3}$ mol, 1.5 eq) in water (20 mL), octanoyl chloride (1.03 mL, 6.04 x $10^{-3}$ mol, 1 eq) in THF (10ml) was added dropwise. The cloudy reaction mixture was stirred at room temperature overnight. Acidification of the reaction mixture to pH1, using 2M HCl, induced the precipitation of a clear oil. The resulting oil was separated from the aqueous layer and left to dry under high vacuum overnight (0.98 g, 4.90 x $10^{-3}$ mol, 81 %).

**$R_f$** = 0.45 (8:2/EtOAc:Hex) **Fourier Transform Infrared,** neat ($v_{max}/cm^{-1}$) 1738.1 (s, C=O) 1567.4 (s, -CONH-); **$^1$H-NMR** (300MHz, MeOD) $\delta_H$: 0.90 (t, 3H, *J* = 7.0Hz, H-1), 1.31 (m, 8H, H-2 H-3 H-4 H-5) 1.60 (m, 2H, H-6 ), 2.27 (t, 2H, *J* = 7.5Hz, H-

7), 3.90 (s, 2H, H-8) lit. $\delta_H$ [256]; **HRMS:** m/z (ESI) calculated for $C_{10}H_{20}NO_3^+$: 202.1398 $[M+H]^+$, found: $[M+H]^+$: 202.1434

***N*-Octanoyl-NG-2,2,5,7,8-pentamethylchroman-6-sulfonyl-L-arginine; Octanoyl-Arg(PMC)-OH [22]**

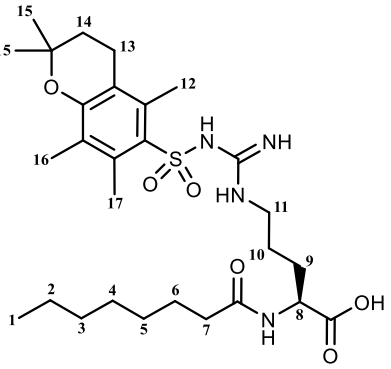


(i) Fmoc-Arg(PMC)-OH (9.94 g, 1.5 x $10^{-2}$ mol, 1 eq) was stirred in 40 mL of 20% Piperidine in DCM for 3 hours. The solution was concentrated to dryness *in vacuo* and dried further by high vacuum to produce a white paste corresponding to $H_2N$-Arg(PMC)-OH.

(ii) To a stirred solution of $H_2N$-Arg(PMC)-OH and $NaHCO_3$ (2.06 g, 2.45 x $10^{-2}$ mol, 1.6 eq) in $H_2O$ (50 mL), Octanoyl chloride (7.80 mL, 4.5 x $10^{-2}$ mol, 3 eq) in THF (25 mL) was added dropwise. The cloudy reaction mixture was stirred at room temperature overnight. Acidification of the reaction mixture to pH 0.5, using 2M hydrochloric acid, induced the precipitation of a thick yellow oil. The resulting oil was separated from the aqueous layer and left to dry under high vacuum overnight. Procedure was modified from lit reference to produce the novel product[190]**;** (5.65 g, 9.9 x $10^{-3}$ mol, 67 %)

**$R_f$** = 0.55 (8:2/EtOAc:MeOH) **Fourier Transform Infrared,** neat ($v_{max}$/$cm^{-1}$) 1611.8 (s, NH-C=O) 1723.5 (s, C=O) 2925.9 (m, Ar, C-H); **$^1$H-NMR** (300MHz, MeOD) $\delta_H$: 0.80 (t, 3H, *J*=7.0Hz, H-1), 1.26 (s, 6H, H-15) 1.4-1.9 (m, 16H, H-2 H-3 H-4 H-5 H6

H-9 H-10 H-14) 2.04 (s, 3H, H-17), 2.26 (m, 5H, H-7 H-12) 2.48 (s, 6H, H-13 H-16), 2.60 (t, 2H, *J*=6.5Hz, H-11), 4.57 (t, 1H, *J*=5.0Hz, H-8); **HRMS:** m/z (ESI) calculated for $C_{28}H_{47}N_4O_6S^+$: 567.3216 $[M+H]^+$. Found: $[M+H]^+$: 567.3222

## 7.2 Synthesis of Dipeptide Derivatives

### L-Arginyl-L-tryptophan methyl ester; $H_2N$-RW-OMe [1][257]

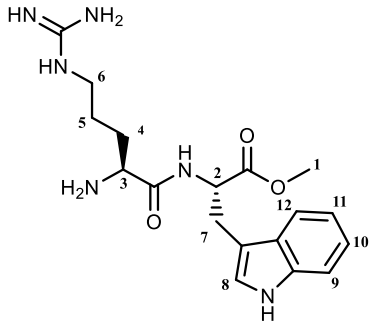


To a 3-necked RBF equipped with a magnetic stir bar, Boc-L-Arg-OH (0.70 g, 2.5 x $10^{-3}$ mol, 1 eq), HATU (0.95 g, 2.5 x $10^{-3}$ mol, 1 eq) and TEA (0.35 mL, 2.5 x $10^{-3}$ mol, 1 eq) was stirred in minimum dried DCM for 10 min. Upon the addition of **[17]** (0.64 g, 2.5 x $10^{-3}$mol, 1 eq) and TEA (0.35 mL, 2.5 x $10^{-3}$ mol, 1 eq), the reaction was cooled to 0°C. The reaction mixture was allowed to slowly return to room temperature with stirring for 3 days. The yellow reaction mixture was washed with 2M HCl (2 x 15 mL), water (15 mL) and 2M NaOH (2 x 15 mL). The organic layer was dried with $MgSO_4$ and the solvent was evaporated *in vacuo*. The addition of MeOH caused a precipitate to form. LRMS revealed that the yellow MeOH solution contained the desired Boc-protected product. The MeOH solution was then concentrated *in vacuo* and treated with 7:3 TFA/DCM for 4 hours. TFA and DCM were evaporated using a $CO_2$/acetone rotary evaporator. The remaining oil was re-dissolved in MeOH, concentrated *in vacuo* and dried under high vacuum pump to produce a pale yellow oil. Procedure was modified from lit reference[257]

The novel product was purified by reverse phase HPLC at a flow rate of 20 mL/min producing a white solid (0.28 g, 7.4 x $10^{-4}$ mol, 30 %). The method employed a binary mixture of eluents A ($H_2O$ with 0.1 % TFA) and B (MeOH with 0.1 % TFA). HPLC gradient B: 5%-100%; 0-30 mins, 100%; 30-35mins, 100%-5%; 35-40, 5%; 40-50mins. Retention time was found to be at 11.51mins.

**$R_f$** = 0.46 (8:2/MeOH:EtOAc); $[\alpha]_D^{22}$ = +14.0 (C=0.5, MeOH); **$^1$H-NMR** (400MHz, MeOD) $\delta_H$: 1.61 (m, 2H, H-5) 1.80 (dt, 2H, $J_1$=6.5Hz $J_2$=14.0Hz, H-4) 3.21 (m, 4H, H-6 H-7) 3.60 (s, 3H, H-1) 3.80 (t, 1H, $J$=6.5Hz, H-3) 4.70 (t, 1H, $J$=3.5Hz, H-2) 6.93 (t, 1H, $J$=7.0Hz, H-11) 7.03 (m, 2H, H-10 H-12) 7.23 (d, 1H, $J$=8.0Hz, H-8) 7.42 (d, 1H, $J$=8.0Hz, H-9); **$^{13}$C-NMR** (100MHz, MeOD) $\delta_C$: 19.2, 24.8, 29.8, 31.2, 46.1, 51.0, 53.8, 112.3, 114.8, 119.7, 122.6, 124.9, 125.2, 128.8, 132.3, 169.9, 179.8; **HRMS:** m/z (ESI) calculated for $C_{18}H_{27}N_6O_3^+$: 375.2145 $[M+H]^+$. Found: $[M+H]^+$: 375.2153

***N*-octanoyl-L-arginyl-L-tryptophan methyl ester; Octanoyl-RW-OMe [2]**

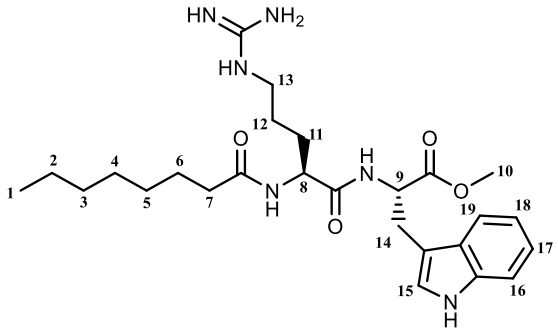


(i) To a 3-necked RBF equipped with a magnetic stir bar, **[22]** (1.42 g, 2.5 x $10^{-3}$ mol, 1eq), HATU (0.95 g, 2.5 x $10^{-3}$ mol, 1eq) and DIPEA (0.25 mL, 1.25 x $10^{-3}$ mol, 0.5 eq) were stirred in minimum dried DCM/DMF. The addition of **[17]** (0.64 g, 2.5 x $10^{-3}$ mol, 1eq) resulted in a yellow colour change. DIPEA (0.25 mL, 1.25 x $10^{-3}$ mol, 0.5eq) was added to the reaction mixture and

stirred for 2 days at room temperature. The yellow mixture was concentrated to dryness *in vacuo* and was taken up in EtOAc (100 mL). The yellow organic layer was washed with 10% citric acid (2 x 15 mL) and $H_2O$ (2 x 15 mL). The final organic layer was dried with $MgSO_4$. The solvent was evaporated *in vacuo* and the product was dried further under high vacuum.

(i) The dried product was treated with 9:1/TFA:DCM (10 mL), flushed with $N_2$ gas and stirred gently for 3 hours. TFA was evaporated using a $CO_2$/acetone rotary evaporator. Cold $Et_2O$ was used to precipitate the auburn dipeptide. The ether layer was decanted and the auburn product was dried under high vacuum. Procedure was modified from lit references[258,259,193,182,260,162,261]

The novel product was purified by reverse phase HPLC at a flow rate of 20 mL/min (0.28 g, 5.5 x $10^{-4}$ mol, 22 %). The method employed a binary mixture of eluents A ($H_2O$ with 0.1 % TFA) and B (MeOH with 0.1 % TFA). HPLC gradient B: 60%-65%; 0-5 mins, 65%-75%; 5-20mins, 75%-100%; 20-25mins, 100%-60%; 25-30mins, 60%; 30-35mins. Retention time was found to be at 6.49mins.

**$R_f$** = 0.37 (1:1/MeOH:EtOAc)**;** $[\alpha]_D^{22}$ = +40.0 (C=0.13, MeOH); **$^1$H-NMR** (300MHz, MeOD) $\delta_H$: 0.88 (t, 3H, *J*=5.0Hz, H-1) 1.29 (m, 8H's, H-2 H-3 H-4 H-5) 1.57 (m, 4H, H-6 H-12) 1.70 (m, 2H, H-11) 1.85 (m, 2H, H-7) 3.19 (m, 4H, H-13 H-14) 3.24 (s, 3H, H-10) 4.37 (m, 1H, H-8) 4.75 (m, 1H, H-9) 6.98 (m, 1H, H-18) 7.53 (m, 2H, H-16 H-17) 7.83 (dd, 1H, $J_1$=7.5Hz, $J_2$=14.0Hz, H-15) 8.09 (d, 1H, *J*=7.5Hz, H-19); **$^{13}$C-NMR** (100MHz, MeOD) $\delta_C$: 9.4, 19.3, 25.1, 26.0, 28.2, 30.1, 30.8, 34.9, 40.3, 53.2, 53.4, 55.2, 108.3, 111.2, 118.7, 119.1, 124.2, 127.0, 128.1, 139.9, 157.6, 166.5, 173.1; **HRMS:** m/z (ESI) calculated for $C_{26}H_{41}N_6O_4^+$: 501.3189 $[M+H]^+$. Found: $[M+H]^+$: 501.3184

**L-Arginyl-L-tryptophan octyl ester; $H_2N$-RW-Oct [3]**

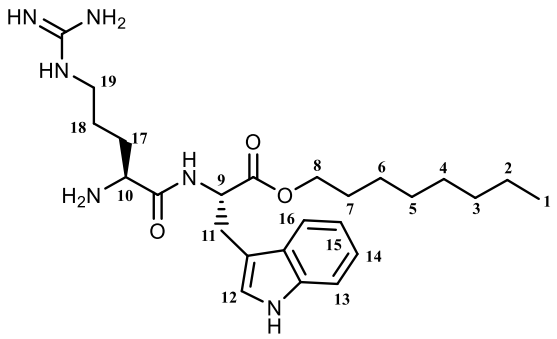

(i) In a dried RBF, Fmoc-Arg(PMC)-OH (1.66 g, 2.5 x $10^{-3}$ mol, 1 eq) was dissolve in neat TFA (6 mL), flushed with $N_2$ gas and stirred gently overnight. TFA was evaporated using a $CO_2$/acetone rotary evaporator. The side chain-unprotected amino acid (Fmoc-Arg-OH) was precipitated with $Et_2O$ to produce a thick white paste. The ether layer was decanted and the product was dried by high vacuum for 2 hours.

(ii) Fmoc-Arg-OH, HATU (0.95 g, 2.5 x $10^{-3}$ mol, 1 eq) and DIPEA (0.25 mL, 1.25 x $10^{-3}$ mol, 0.5 eq) were stirred in minimum dried DCM/DMF. A solution of **[18]** (0.79 g, 2.5 x $10^{-3}$ mol, 1 eq) and DIPEA (0.25 mL, 1.25 x $10^{-3}$ mol, 0.5 eq) in minimum dried DCM was added to the reaction mixture and stirred for 4 days at room temperature. LRMS was used to monitor the reaction.

(iii) 50% piperidine in DCM (10 mL) was added to the reaction mixture and stirred for 3 hours. The reaction mixture was concentrated to dryness *in vacuo* and was taken up in EtOAc (25 mL). The organic layer was washed with $Na_2CO_3$(*sat)* (2 x 15 mL) and $H_2O$ (2 x 15 mL) and dried with $MgSO_4$. The solvent was evaporated *in vacuo* and the product was dried under high vacuum to produce a thick orange liquid. Procedure was modified from lit references[258,259,193,182,260,162,261]

The novel product was purified by reverse phase HPLC at a flow rate of 20 mL/min (0.54 g, 1.1 x $10^{-3}$ mol, 46 %). The method employed a binary mixture of eluents A ($H_2O$ with 0.1 % TFA) and B (MeOH with 0.1 % TFA). HPLC gradient B: 60%-100%; 0-4mins, 100%-60%; 4-14mins, 60% 14-24mins. Retention time was found to be at 12.5mins.

**$R_f$** = 0.49 (1:1/EtOAc:MeOH); $[\alpha]_D^{22}$ = +150.0 (C=0.1, MeOH); **$^1$H-NMR** (300MHz, MeOD) $\delta_H$: 0.90 (t, 3H, *J*=7.0Hz, H-1) 1.25 (m, 8H, H-2 H-3 H-4 H-5) 1.47 (m, 2H, H-6) 1.57 (m, 2H, H-7) 1.77 (m, 2H, H-18) 1.91 (m, 2H, H-17) 3.22 (m, 2H, H-11) 3.31 (m, 2H, H-8) 3.80 (m, 2H, H-19) 4.01 (t, 2H, *J*=6.0Hz, H-10) 4.76 (t, 1H, *J*=6.5Hz, H-9) 7.07 (m, 2H, H-13 H-15) 7.43 (m, 2H, H-12 H-14) 7.80 (m, 1H, H-16); **$^{13}$C-NMR** (100MHz, MeOD) $\delta_C$: 14.5, 26.3, 28.4, 28.9, 29.1, 30.0, 30.2, 31.7, 32.0, 32.7, 42.2, 53.5, 55.1, 66.8, 112.8, 119.0, 120.0, 120.7, 121.8, 122.5, 124.3, 136.2, 157.1, 166.5, 173.4; **HRMS:** m/z (ESI) calculated for $C_{25}H_{41}N_6O_3^+$: 473.3235 $[M+H]^+$. Found: $[M+H]^+$: 473.3237

**Glycyl-L-tryptophan methyl ester; $H_2$N-GW-OMe [4]**

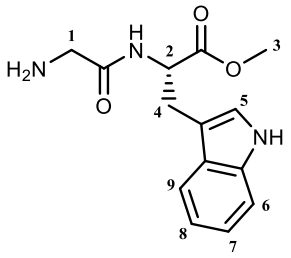


(i) In a dried RBF, Boc-Gly-OH (0.44 g, 2.5 x $10^{-3}$ mol, 1 eq), HATU (0.95 g, 2.5 x $10^{-3}$ mol, 1 eq) and DIPEA (0.25 mL, 1.25 x $10^{-3}$ mol, 0.5 eq) were stirred in minimum dried DCM. A solution of **[17]** (0.64 g, 2.5 x $10^{-3}$mol, 1 eq) and DIPEA (0.25 mL, 1.25 x $10^{-3}$ mol, 0.5 eq) in minimum dried DCM was added to the reaction mixture and stirred for 3 days. The yellow product was concentrated to dryness *in vacuo* and was taken up in EtOAc (100mL). The

organic layer was washed with 10% citric acid (2 x 15 mL) and water (2 x 15 mL). The final organic layer was dried with $MgSO_4$. The solvent was evaporated *in vacuo*.

(ii) The dried product was treated with 9:1/TFA:DCM (10 mL), flushed with $N_2$ gas and stirred gently for 3 hours. The TFA was evaporated using a $CO_2$/acetone rotary evaporator. The auburn product was further dried under high vacuum. Procedure was modified from lit references[258,259,193,182,260,162,261]

The novel product was purified by reverse phase HPLC at a flow rate of 20 mL/min (0.23 g, 8.3 x $10^{-4}$ mol, 33 %). The method employed a binary mixture of eluents A ($H_2O$ with 0.1 % TFA) and B (MeOH with 0.1 % TFA). HPLC gradient B: 0%-100%; 0-15 mins, 100%-0%; 15-20mins, 0%; 20-30mins. Retention time was found to be at 8.80mins.

**$R_f$** = 0.40 (8:2/EtOAc:$CHCl_3$); $[\alpha]_D^{22}$ = +120.0 (C=0.1, MeOH); **$^1$H-NMR** (300MHz, MeOD) $\delta_H$: 3.0-3.7 (m, 7H, H-1 H-3 H-4) 4.72 (dd, 1H, $J_1$=5.5Hz $J_2$=8.0Hz, H-2) 7.00 (m, 3H, H-7 H-8 H-9) 7.23 (d, 1H, $J$=8.0Hz, H-5) 7.41 (d, 1H, $J$=7.5Hz, H-6), lit. $\delta_H$[262]. **$^{13}$C-NMR** (100MHz, MeOD) $\delta_C$: 29.4, 41.9, 52.8, 54.7, 110.0, 112.2, 118.9, 119.9, 122.3, 124.4, 128.2, 136.8, 166.9, 173.1; **HRMS:** m/z (ESI) calculated for $C_{14}H_{18}N_3O_3^+$: 276.1348 $[M+H]^+$. Found: $[M+H]^+$: 276.1340

***N*-octanoyl-L-glycyl-L-tryptophan methyl ester; Octanoyl-GW-OMe [5]**

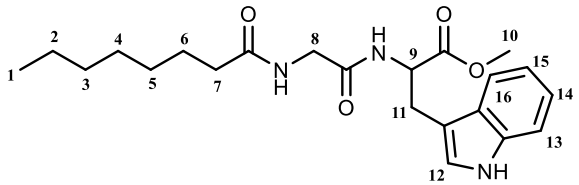


To a dried RBF, **[20]** (0.5 g, 2.5 x $10^{-3}$mol, 1 eq), HATU (0.95 g, 2.5 x $10^{-3}$ mol, 1 eq) and DIPEA (0.25 mL, 1.25 x $10^{-3}$ mol, 0.5 eq) were dissolved in minimum dried DCM. A solution of **[17]** (0.637 g, 2.5 x $10^{-3}$ mol, 1 eq) and DIPEA (0.25mL,

$1.25x10^{-3}$mol, 0.5eq) in minimum dried DCM was added to the reaction mixture and stirred for 3 days. The yellow mixture was concentrated to dryness *in vacuo* and was taken up in EtOAc (100 mL). The yellow organic layer was washed with 10% citric acid (2 x 15 mL) and water (2 x 15 mL). The final organic layer was dried with $MgSO_4$. The solvent was evaporated *in vacuo* and the product was dried further under high vacuum. The novel product was purified by flash chromatography using 5:3:2/$CHCl_3$:EtOAc:Pet ether as the eluent. Procedure was modified from lit references[258,259,193,182,260,162,261] (0.20 g, 5.0 x $10^{-4}$ mol, 20 %)

**$R_f$** = 0.43 (8:2/EtOAc:MeOH); $[\alpha]_D^{22}$ = +48.0 (C=0.5, MeOH); **$^1$H-NMR** (300MHz, MeOD) $\delta_H$: 0.78 (t, 3H, *J*=7.0Hz, H-1) 0.9-1.4 (m, 8H, H-2 H-3 H-4 H-5) 1.47 (m, 2H, H-6) 1.57 (m, 2H, H-7) 2.08 (m, 2H, H-11) 3.25 (s, 2H, H-8) 3.55 (s, 3H, H-10) 4.65 (t, 1H, *J*=6.0Hz, H-9) 6.98 (m, 3H, H-16 H-15 H-14) 7.23 (d, 1H, *J*=8.0Hz, H-12) 7.39 (d, 1H, *J*=8.0Hz, H-13); **$^{13}$C-NMR** (100MHz, MeOD) $\delta_C$: 26.1, 26.8, 28.5, 30.2, 30.4, 32.9, 34.8, 39.0, 43.4, 49.8, 54.8, 106.2, 110.3, 112.4, 119.2, 120.0, 122.6, 124.7, 154.2, 173.9, 176.8, 181.3; **HRMS:** m/z (ESI) calculated for $C_{22}H_{31}N_3NaO_4^+$: 424.2212 $[M+Na]^+$. Found: 424.2213

**Glycyl-L-tryptophan octyl ester; $H_2$N-GW-Oct [6]**[263]

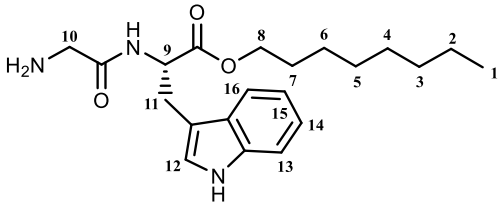


(i) To a 3-necked RBF equipped with a magnetic stir bar was added **[18]** (1.60 g, 5 x $10^{-3}$ mol, 1 eq), EtOH (20 mL), NMM (1.20 mL, 11 x $10^{-3}$ mol, 2.2 eq), Boc-Gly-OH (0.89 g, 5 x $10^{-3}$ mol, 1 eq) and HOBt (0.10 g, 7.5 x $10^{-4}$ mol, 0.15 eq, *cat.*). The mixture was cooled to 10°C and *N*-(3-

Dimethylaminopropyl)-N′-ethylcarbodiimide hydrochloride (1.15 g, 6.0 x $10^{-3}$ mol, 1.2 eq) was added. The reaction was stirred at 25°C for three days. Water (25 mL) was added to the reaction mixture and the noncrystalline product was extracted in DCM and dried with $MgSO_4$. The solvent was evaporated *in vacuo* and dried under high vacuum to produce a pale yellow oil.

(ii) The protected dipeptide product was treated with 7:3/TFA:DCM and stirred overnight under nitrogen. TFA was evaporated using a $CO_2$/acetone rotary evaporator. Cold $Et_2O$ was used to precipitate the brown dipeptide oil. The ether was decanted from the product. The wet product was dried further using a high vacuum pump to remove any residual ether. The dried product was then dissolved in water and lyophilised overnight to produce a deep maroon coloured oil.

The novel product was purified by reverse phase HPLC at a flow rate of 20 mL/min (0.82 g, 2.2 x $10^{-3}$ mol, 44%). The method employed a binary mixture of eluents A ($H_2O$ with 0.1 % TFA) and B (MeOH with 0.1 % TFA). HPLC gradient B: 50%-100%; 0-15 mins, 100%-50%; 15-20mins, 50%; 20-30mins. Retention time was found to be at 12.2mins.

$[\alpha]_D^{22}$ = +50.6 (C=0.5, MeOH); **$^1$H-NMR** (400MHz, MeOD) $\delta_H$: 0.81 (t, 3H, *J*=7.1Hz, H-1) 1.21 (m, 10H, H-2 H-3 H-4 H-5 H-6) 1.52 (m, 2H, H-7) 3.57 (s, 2H, H-10) 3.92 (d, 2H, *J*=5.0Hz, H-11) 4.00 (t, 2H, *J*=7.0Hz, H-8) 4.68 (m, 1H, H-9) 6.92 (t, 1H, *J*=6.5Hz, H-15) 7.00 (t, 1H, *J*=8.0Hz, H-14) 7.23 (d, 1H, *J*=8.0Hz, H-13) 7.43 (d, 1H, *J*=8.0Hz, H-12) 7.63 (d, 1H, *J*=8.0Hz, H-16); **$^{13}$C-NMR** (100MHz, MeOD) $\delta_C$: 14.4, 16.7, 19.7, 28.6, 30.4, 31.7, 35.3, 35.5, 63.4, 67.6, 111.2, 115.1, 122.0, 124.5, 129.6, 134.6, 135.1, 136.5, 137.7, 165.5, 168.7; **HRMS:** m/z (ESI) calculated for $C_{21}H_{32}N_3O_3^+$: 374.2444 $[M+H]^+$. Found: $[M+H]^+$: 374.2439

***N*-octanoyl-L-arginyl-glycine; Octanoyl-RG-OH [8]**

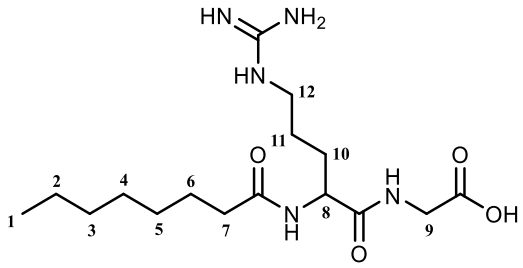


(ii) A stirred solution of **[22]** (1.23 g, 2.2 x $10^{-3}$ mol, 1 eq), Oxyma Pure (0.31 g, 2.2 x $10^{-3}$ mol, 1 eq), $H_2N$-Gly-OtBu•AcOH (0.42 g, 2.2 x $10^{-3}$ mol, 1 eq) and DMAP (0.07 g, 5.5 x $10^{-3}$ mol, 0.25 eq) in minimum dried DCM was cooled to 0°C. DCC (0.91 g, 4.4 x $10^{-3}$ mol, 2 eq) was added to the reaction mixture and stirred at room temperature for 3 days. The insoluble urea by-product was removed from the reaction mixture by filtration. The filtrate was concentrated to dryness *in vacuo* and was taken up in EtOAc (25 mL). The yellow organic layer was washed with 10% citric acid (2 x 15 mL) and water (2 x 15 mL) and was dried with $MgSO_4$. The solvent was evaporated *in vacuo* and the resulting yellow liquid was dried further under high vacuum.

(iii) The protected dipeptide, confirmed by LRMS, was treated with neat TFA (10 mL), flushed with $N_2$ gas, and stirred gently for 4 hours. The TFA was evaporated using a $CO_2$/acetone rotary evaporator. Cold ether was used to precipitate the greenish dipeptide. The ether layer was decanted and the green product was dried under high vacuum. Procedure was modified from lit references[258,259,193,182,260,162,261]

The novel product was purified by reverse phase HPLC at a flow rate of 20 mL/min (0.31 g, 8.7 x $10^{-4}$ mol, 40 %). The method employed a binary mixture of eluents A ($H_2O$ with 0.1% TFA) and B (MeOH with 0.1% TFA). HPLC gradient B: 40%-100%;

0-10 mins, 100%-40%; 10-15mins, 40%; 15-25mins. Retention time was found to be at 5.02 minutes.

**$R_f$** = 0.60 (1:1/MeOH:EtOAc)**;** $[\alpha]_D^{22}$ = +18.0 (C=0.25, MeOH); **$^1$H-NMR** (300MHz, MeOD) $\delta_H$: 0.80 (m, 3H, H-1) 1.20 (m, 8H's, H-2 H-3 H-4 H-5) 1.57 (m, 4H, H-6 H-11) 1.80 (m, 2H, H-10) 2.17 (t, 2H, *J*=7.5Hz, H-7) 3.11 (t, 2H, *J*=7.0Hz, H-12) 4.32 (m, 2H, H-8 H-9); **$^{13}$C-NMR** (100MHz, MeOD) $\delta_C$: 14.2, 23.8, 26.2, 26.4, 26.9, 30.2, 30.3, 32.9, 40.9, 41.8, 42.1, 54.2, 158.8, 172.9, 176.0, 174.4; **HRMS:** m/z (ESI) calculated for $C_{16}H_{32}N_5O_4^+$: 358.2454 $[M+H]^+$. Found: $[M+H]^+$: 358.2449

**L-Arginyl-glycine octyl ester; $H_2N$-RG-Oct [9]**[263]

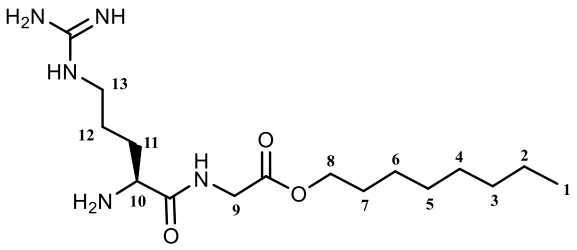


To a 3-necked RBF equipped with a magnetic stir bar was added **[19]** (0.50 g, 2.5 x $10^{-3}$ mol, 1 eq), EtOH (10 mL), NMM (0.60 mL, 5.5 x $10^{-3}$ mol, 2.2 eq), Boc-Arg-OH (0.69 g, 2.5 x $10^{-3}$ mol, 1 eq) and HOBt (0.06 g, 3.8 x $10^{-4}$ mol, 0.15 eq, *cat.*). The mixture was cooled to 10°C and *N*-(3-Dimethylaminopropyl)-N′-ethylcarbodiimide hydrochloride (0.466 g, 3.0 x $10^{-3}$ mol, 1.2 eq) was added. The reaction was stirred at 25°C overnight followed by the addition of water (25 mL). The noncrystalline product water was extracted in DCM and dried with $MgSO_4$. The solvent was evaporated *in vacuo* and dried under high vacuum to produce a pale yellow oil.

The novel product was purified by reverse phase HPLC at a flow rate of 20 mL/min (0.33 g, 9.5 x $10^{-4}$ mol, 38 %). The method employed a binary mixture of eluents A ($H_2O$ with 0.1% TFA) and B (MeOH with 0.1% TFA). HPLC gradient B: 5%-100%;

0-30 mins, 100%; 30-35 mins, 100%-5%; 35-40mins, 5%; 40-50mins. Retention time was found to be at 16.8 minutes.

**$R_f$** = 0.6 (1:1/MeOH:EtOAc)**;** $[\alpha]_D^{22}$ = +50.0 (C=0.25, MeOH); **$^1$H-NMR** (300MHz, MeOD) $\delta_H$: 0.80 (t, 3H, *J*=7.0Hz, H-1) 1.56 (m, 8H's, H-2 H-3 H-4 H-5 H-6) 1.86 (m, 6H, H-7 H-11 H-12) 3.17 (m, 3H, H-10 H-13) 3.25 (s, 2H, H-9) 4.05 (t, 2H, *J*=6.5Hz, H-8); **$^{13}$C-NMR** (100MHz, MeOD) $\delta_C$: 14.6, 23.7, 25.0, 25.5, 26.9, 28.6, 29.6, 30.3, 33.1, 36.2, 37.6, 53.9, 65.1, 158.9, 171.2, 175.8; **HRMS:** m/z (ESI) calculated for $C_{16}H_{34}N_5O_{3+}$: 344.2662 $[M+H]^+$. Found: $[M+H]^+$: 344.2656

**Solid Phase Peptide Synthesis of L-Arginyl-glycine; $H_2N$-RG-OH [7]**

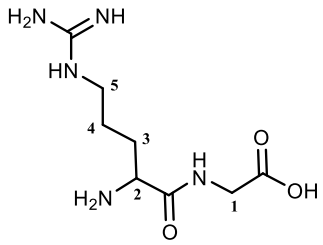


Resin preparation

In a fritted filtered funnel, dried Wang resin (0.5g, 0.55mmol loading, 1eq) was swollen with dried DCM (3x volume) for 30 minutes. Vacuum was applied to remove DCM. Dried DMF (3x volume) was added to the resin, agitated for 1 minute with $N_2$*(g)* and removed by vacuum. This washing process was repeated five times.

Coupling/Deprotection

*Cycle I-Attachment of the first amino acid to the resin*

In a dried 3-necked RBF, equipped with a calcium chloride drying tube, Fmoc-Gly-OH (0.65 g, 2.2 x $10^{-3}$ mol, 4 eq), Oxyma Pure (0.31 g, 2.2 x $10^{-3}$ mol, 4 eq) and DIC (0.35 mL, 3.4 x $10^{-3}$ mol, 6.2 eq) was dissolved in minimum dried DMF and stirred

for 10 minutes at 0°C. Following the addition of DMAP (0.07 g, 5.5 x $10^{-4}$ mol, 1 eq), the reaction mixture was immediately added to the swollen resin and agitated with $N_{2(g)}$ for 2 days.

*Estimation of first residue attachment*

A small sample of resin beads (Cycle I) was removed from the reaction vessel and dried by vacuum. The dried resin-bound amino acid was weighed and transferred to a 10mm matched silica UV cell filled with 3mL of freshly prepared 20% piperidine in DMF. The resin suspension was agitated with a Pasteur pipette for 5 minutes. The absorption spectrophotometer was zeroed at 290nm using 20% piperidine in DMF. The absorbance of the UV cells containing settled resin was read at 290nm and averaged together. Loading was calculated using Equation 1, based on a molar absorptivity ($\varepsilon$) = 5253$M^{-1}cm^{-1}$.

**Equation 2.1**

$$\text{Loading (mmol/g)} = (\text{Abs}_{\text{average}})/(\text{mg of sample x } 1.75)$$

Utilizing an absorption spectrophotometer, 68% of Fmoc-Gly-OH was estimated to have attached to the Wang resin after 2 days of reacting. Vacuum was applied to remove the reaction mixture from the resin. To cap unloaded resin beads, Benzoic anhydride (0.62 g, 2.75 x $10^{-3}$ mol, 5 eq) and pyridine (0.04 mL, 5.5 x $10^{-4}$ mol, 1 eq) in DMF was added to the loaded resin and agitated for 30 min with $N_{2(g)}$. Vacuum was applied to remove the solution from the resin. The resin was washed with DMF (5 x 10 mL) and DCM (5 x 10 mL).

*Fmoc-deprotection*

To remove the Fmoc protecting group, the resin was treated with 20% piperidine in DMF (10mL) for 2 hours. Vacuum filtration was applied to remove this solution from the resin. The resin was further washed with DMF (5 x 10 mL) and DCM (5 x 10 mL).

*Cycle II*

In a dried 3-necked RBF, equipped with a calcium chloride drying tube, Fmoc-Arg(PMC)-OH (1.46 g, 2.2 x $10^{-3}$ mol, 4 eq), Oxyma Pure (0.31 g, 2.2 x $10^{-3}$ mol, 4 eq) and DIC (0.34 mL, 3.4 x $10^{-3}$ mol, 6.2 eq) was dissolved in minimum dried DMF and stirred for 10 minutes at 0°C. Following the addition of DMAP (0.07g, 5.5x$10^{-4}$mol, 1eq), the reaction mixture was immediately added to the loaded resin and agitated with $N_{2(g)}$ overnight. A Kaiser test (Ninhydrin test) was used to monitor the disappearance of resin-bound free amines from cycle I. The resin was washed with DMF (5x10mL) and DCM (5x10mL). Fmoc-deprotection using the above procedure was used.

*Kaiser Test*

A small sample of resin beads (Cycle II) was removed from the reaction vessel and washed several times with ethanol. The beads were transferred to a glass vial, and were treated with two drops of 5% Ninhydrin in EtOH, 80% phenol in EtOH and 2% 0.001M KCN in pyridine. The resin solution was stirred manually and heated to 110°C. Solutions which turned blue indicated that the reaction was not complete and resin-bound free amines were still present. Solutions which turned yellow in colour indicated that the peptide coupling reaction was complete.

*Cleavage/Isolation*

The loaded resin was dried under vacuum for 30 minutes and transferred to a dried flask in preparation for resin cleavage. The dried resin was treated with 19:1/TFA:$H_2O$ (1 mL per 100 mg of loaded resin), flushed with $N_{2(g)}$, and stirred gently overnight. The resin was removed by reduced pressure filtration through a sintered glass funnel. The resin was washed twice with neat TFA. Filtrates were combined and TFA was evaporated using a $CO_2$/acetone rotary evaporator. Cold $Et_2O$ was used to precipitate the dipeptide. The ether layer was decanted and the remaining dipeptide was dissolved in water and lypholised overnight. Procedure was modified from lit references[258,259,193,182,260,162,261].

The known product was purified by reverse phase HPLC at a flow rate of 20mL/min (0.032 g, 1.38 x $10^{-4}$ mol, 25 %). The method employed a binary mixture of eluents A ($H_2O$ with 0.1%TFA) and B (ACN with 0.1%TFA). HPLC gradient A: 100% A; 0-5 mins, 100%-75%; 5-10mins, 75%-50%; 10-15mins, 50%-100%, 15-25mins. Retention factor was found to be at 6.90min.

**$R_f$** = 0.29 (1:1/MeOH:EtOAc); **$^1$H-NMR** (300MHz, MeOD) $\delta_H$: 1.76 (m, 3H, H-4) 1.93 (m, 2H, H-3) 3.23 (t, 2H, *J*=7.0Hz, H-5), 3.92 (m, 1H, H-2) 4.06 (s, 2H, H-1); **$^{13}$C-NMR** (100MHz, MeOD) $\delta_C$: 21.1, 29.7, 42.1, 42.1, 53.9, 158.3, 172.8, 179.9; **HRMS:** m/z (ESI) calculated for $C_8H_{18}N_5O_3^+$: 232.1410 $[M+H]^+$. Found: $[M+H]^+$: 232.1322

## 7.3 General Method for SPPS using 2-chlorotrityl chloride resin

Resin preparation

In a fritted filtered funnel, dried 2-chlorotrityl chloride resin (1.22 mmol/g loading) was swollen with DCM (3x volume) for 30 minutes. Vacuum was applied to remove DCM. Dried DMF (3x volume) was added to the resin, agitated for 1 minute with $N_2$*(g)* and removed by vacuum. This washing process was repeated five times

Coupling/Deprotection

*Cycle I-Attachment of the first amino acid to the resin*

In a dried RBF, 2eq* of Fmoc-protected amino acid was dissolved in minimum dried DCM. Following the addition of DIPEA (2.5eq)*, the reaction mixture was immediately added to the resin and agitated with $N_{2(g)}$ overnight (Fmoc-Trp(PMC)-OH and Fmoc-Arg(PMC)-OH was agitated over two nights). To cap the unloaded resin beads, anhydrous MeOH (3x volume) was added to the resin and agitated under $N_{2(g)}$ for 1 hour. Vacuum filtration was applied to remove the solution from the resin. The resin was then washed with DCM (5 x 10 mL) and DMF (5 x 10 mL).

*Fmoc-deprotection*

To remove the Fmoc protecting group, the resin was treated with 20% piperidine in DMF (10 mL) for 2 hours. Vacuum was applied to remove this solution from the resin. The resin was further washed with DMF (5 x 10 mL) and DCM (5 x 10 mL).

*Cycle II-IV*

In a dried RBF, 2eq* of Fmoc-protected amino acids (Fmoc-Arg(PMC)-OH, Fmoc-Trp(Boc)-OH, Fmoc-Gly-OH, Fmoc-Leu-OH, Fmoc-Ala-OH, Fmoc-His(Trt)-OH, Fmoc-Glu(OtBu)-OH) or 2eq* of urdiyl- derivatives and HATU (2eq)* were dissolved in minimum dried DMF. Following the addition of DIPEA (2.5eq)*, the reaction mixture was immediately added to the resin and agitated with $N_{2(g)}$ for 2 days. When Fmoc-Gly-OH was used, HATU was substituted with DIC and only 1 day of agitation with $N_{2(g)}$ was required. Vacuum was applied to remove the solution from the resin. The resin was then washed with DCM (5x10mL) and DMF (5x10mL). Fmoc-deprotection using the above procedure was used.

*Cleavage/Isolation*

The loaded resin was dried under vacuum for 30 minutes and transferred to a dried flask in preparation for resin cleavage. The dried resin was treated with 19:1/TFA:$H_2O$ (1mL per 100mg of loaded resin), flushed with $N_{(g)}$, and stirred gently overnight. The resin was removed by reduced pressure filtration through a sintered glass funnel. The resin was washed twice with neat TFA. Filtrates were combined and TFA was evaporated using a $CO_2$/acetone rotary evaporator. Cold $Et_2O$ was used to precipitate the oligopeptide. The ether layer was decanted. The wet product was dried further with a high vacuum pump to remove any residual ether. The dried product was then dissolved in water and lyophilized overnight. Procedure was modified from lit reference[168-264].

*relative to resin loading of 1.22mmol/g

**L-Arginyl-L-tryptophyl-glycyl-L-leucinyl-L-tryptophan; RWGLW [10]**

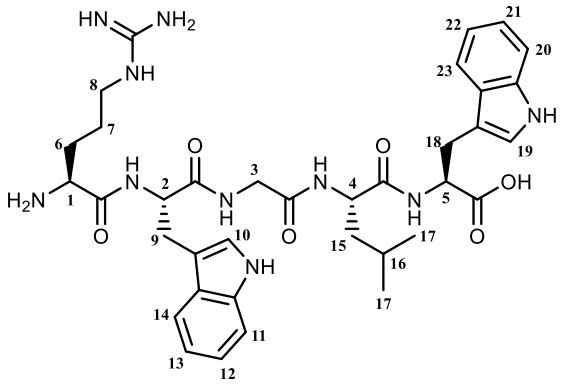

The novel product was purified by reverse phase HPLC at a flow rate of 20 mL/min. The method employed a binary mixture of eluents A ($H_2O$ with 0.1 % TFA) and B (MeOH with 0.1 % TFA). HPLC gradient B: 5%-100%; 0-30 mins, 100%; 30-35mins, 100%-5%; 35-40mins, 5% 40-50mins. Retention time was found to be at 17.4mins (0.38 g, 5.3 x $10^{-4}$ mol, 87 %). **$^1$H-NMR** (300MHz, MeOD) $\delta_H$: 0.77 (dd, 6H, $J_1$=6.0Hz $J_2$=12.0Hz, H-17) 1.4-1.7 (m, 7H, H-6 H-7 H-15 H-16) 2.44 (d, 4H, $J$=5.0Hz, H-9 H-18) 2.53 (t, 2H , $J$=6.5Hz, H-8) 3.21 (t, 1H, $J$=2.0Hz, H-1) 3.25 (s, 2H, H-3) 4.3-4.6 (m, 3H, H-2 H-4 H-5) 7.01 (m, 4H, H-12 H-13 H-21 H-22) 7.21 (m, 4H , H-10 H-11 H-19 H-20) 7.45 (m, 2H, H-14 H-23); **HRMS:** m/z (ESI) calculated for $C_{36}H_{48}N_{10}O_6^+$: 717.3837 $[M+H]^+$. Found: $[M+H]^+$: 717.3831

**L-Arginyl-glycyl-glycyl-L-leucinyl-L-tryptophan; RGGLW [11]**

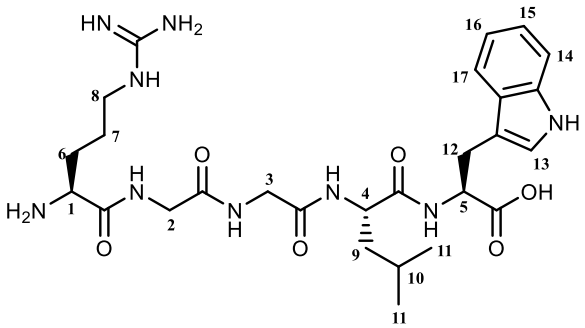

The product was purified by reverse phase HPLC at a flow rate of 20 mL/min. The method employed a binary mixture of eluents A ($H_2O$ with 0.1 % TFA) and B (MeOH

with 0.1 % TFA). HPLC gradient B: 5%-35%; 0-10 mins, 35%-60%; 10-25mins, 60%-100%; 25-30mins, 100% 30-35mins, 100%-5%; 35-40mins, 5% 40-50mins. Retention time was found to be at 17.6mins (0.09 g, 1.5 x $10^{-4}$ mol, 24 %). **$^{1}$H-NMR** (400MHz, MeOD) $\delta_H$: 0.79 (dd, 6H, $J_1$=6.5Hz $J_2$=13.0Hz, H-11) 1.14 (t, 2H, $J_1$=7.5Hz H-7) 1.20 (m, 1H, H-10) 1.44 (t, 2H, *J*=7.5Hz, H-9) 1.53 (m, 2H, H-6) 2.47 (d, 2H, *J*=8.0Hz, H-12) 3.07 (m, 2H, H-8) 3.90 (s, 4H, H-2 H-3) 4.01 (m, 1H, H-5) 4.37 (t, 1H, *J*=7.5Hz, H-4) 4.58 (m, 1H, H-1) 7.01 (m, 2H, H-15 H-16) 7.22 (d, 1H, *J*=8.0Hz, H-14) 7.45 (dd, 1H, $J_1$=8.0Hz $J_2$=18.0Hz, H-13) 7.90 (d, 1H, *J*=8.0Hz, H-17); **HRMS:** m/z (ESI) calculated for $C_{27}H_{41}N_9NaO_6^+$: 610.3077 $[M+Na]^+$. Found: $[M+H]^+$: 610.3072

**Glycyl-L-tryptophyl-glycyl-L-leucinyl-L-tryptophan; GWGLW [12]**

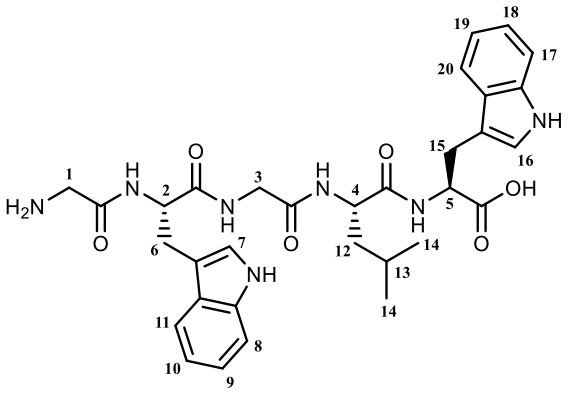

The product was purified by reverse phase HPLC at a flow rate of 20 mL/min. The method employed a binary mixture of eluents A ($H_2O$ with 0.1 % TFA) and B (MeOH with 0.1 % TFA). HPLC gradient B: 30%-100%; 0-30 mins, 100%; 30-35mins, 100%-30%; 35-40mins, 30% 40-50mins. Retention time was found to be at 12.3mins (0.19g, 3.1x$10^{-4}$mol, 50%). **$^{1}$H-NMR** (400MHz, MeOD) $\delta_H$: 0.61 (d, 3H, *J*=6.5Hz, H-14) 0.68 (d, 3H, *J*=6.5Hz, H-14) 1.2-1.8 (m, 3H, H-12 H-13) 3.00 (d, 2H, *J*=5.0Hz, H-15) 3.18 (d, 2H, *J*=3.5Hz, H-6) 3.42 (s, 2H, H-3) 3.90 (s, 2H, H-1) 4.16 (m, 1H, H-4) 4.30 (m, 1H, H-2) 4.60 (m, 1H, H-5) 6.75 (m, 2H, H-8 H-17) 6.9-7.6 (m, 4H, H-9 H-

10 H-18 H-19) 7.90 (m, 2H, H-7 H-16) 8.30 (m, 2H, H-11 H-20); **HRMS:** m/z (ESI) calculated for $C_{32}H_{40}N_7O_6^+$: 618.3040 $[M+H]^+$. Found: $[M+H]^+$: 618.3035

**L-Arginyl-L-tryptophyl-glycyl-glycyl-L-tryptophan; RWGGW [13]**

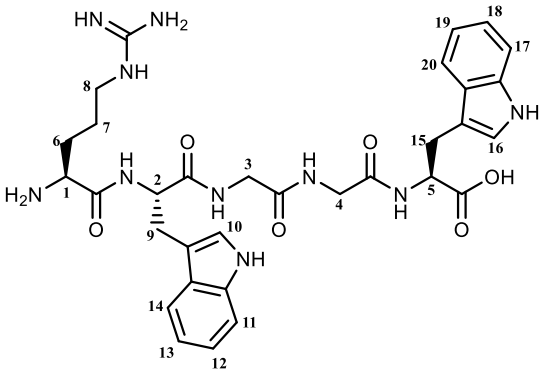

The product was purified by reverse phase HPLC at a flow rate of 20 mL/min. The method employed a binary mixture of eluents A ($H_2O$ with 0.1 % TFA) and B (MeOH with 0.1 % TFA). HPLC gradient B: 5%-100%; 0-30 mins, 100%; 30-35mins, 100%-5%; 35-40mins, 5% 40-50mins. Retention time was found to be at 15.2mins (0.11g, $1.7x10^{-4}$mol, 28%). **$^1$H-NMR** (400MHz, MeOD) $\delta_H$: 1.59 (m, 2H, H-7) 1.77 (m, 2H, H-6) 2.45 (d, 4H, *J*=8.0Hz, H-9 H-15) 2.52 (t, 2H , *J*=7.0Hz, H-8) 3.55 (d, 4H, *J*=2.0Hz, H-3 H-4) 4.07 (t, 2H, *J*=7.0Hz, H-1) 4.54 (m, 1H, H-5) 4.61 (m, 1H, H-2) 6.98 (m, 2H, H-11 H-17) 7.22 (m, 4H, H-12 H-13 H-18 H-19) 7.47 (m, 2H, H-10 H-16) 7.89 (m, br, 2H, H-14 H-20); **HRMS:** m/z (ESI) calculated for $C_{32}H_{41}N_{10}O_6^+$: 661.3211 $[M+H]^+$. Found: $[M+H]^+$: 661.3218

**L-Arginyl-L-tryptophyl-glycyl-L-leucinyl-glycine; RWGLG [14]**

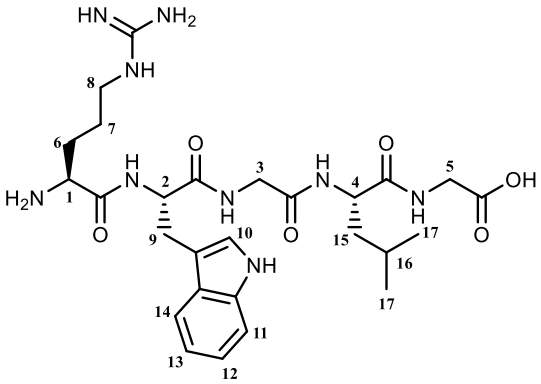

The product was purified by reverse phase HPLC at a flow rate of 20 mL/min. The method employed a binary mixture of eluents A ($H_2O$ with 0.1 % TFA) and B (MeOH with 0.1 % TFA). HPLC gradient B: 5%-35%; 0-10 mins, 35%-60%; 10-25mins, 60%-100%; 25-30mins, 100% 30-35mins, 100%-5%; 35-40mins, 5% 40-50mins. Retention time was found to be at 18.0mins (0.13 g, 2.2 x $10^{-4}$ mol, 36 %). **$^1$H-NMR** (300MHz, MeOD) $\delta_H$: 0.80 (m, 6H, H-17) 1.21 (t, 2H, *J*=7.5Hz, H-8) 1.6-2.1 (m, 5H, H-6 H-15 H-16) 3.1-3.3 (m, 4H, H-7 H-9) 3.6-3.8 (m, 2H, H-1 H-4) 3.88 (s, 4H, H-3 H-5) 4.40 (m, 1H, H-2) 7.00 (m, 2H, H-12 H-13) 7.23 (m, 1H, H-11) 7.48 (d, 1H, *J*=7.0Hz3, H-10) 7.64 (d, 1H, *J*=7.5Hz, H-14); **HRMS:** m/z (ESI) calculated for $C_{27}H_{42}N_9O_6^+$: 588.3258 $[M+H]^+$. Found: $[M+H]^+$: 588.3253

**L-Glutamyl-L-histidyl-L-tryptophyl-glycyl-glycyl-glycine; EHWGGG [15]**

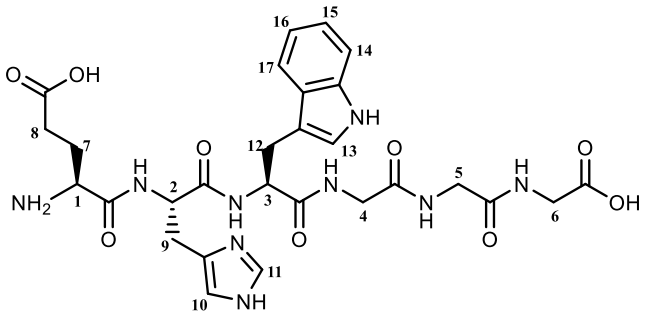

The product was purified by reverse phase HPLC at a flow rate of 20 mL/min. The method employed a binary mixture of eluents A ($H_2O$ with 0.1 % TFA) and B (MeOH

with 0.1 % TFA). HPLC gradient B: 5%-25%; 0-10 mins, 25%-60%; 10-25mins, 60%-100%; 25-30mins, 100%-5%; 30-35mins, 5%; 35-45mins. Retention time was found to be at 12.6 mins (0.29 g, 4.6 x $10^{-4}$ mol, 75 %). **$^{1}$H-NMR** (400MHz, MeOD) $\delta_H$: 1.95 (dt, 2H, *$J_1$=7.0*Hz, *$J_2$=13.5*Hz, H-7) 2.36 (t, 2H, *J=7.5*Hz, H-8) 3.10 (d, 2H, *J=6.5*Hz, H-12) 3.16 (d, 2H, *J=7.5*Hz, H-9) 3.80 (s, br, 6H, H-4 H-5 H-6) 3.88 (m, 1H, H-1) 4.50 (t, 1H, *J=7.0*Hz, H-3) 4.63 (t, 1H, *J=6.0*Hz, H-2) 6.9-7.1 (m, 2H, H-10 H-16) 7.24 (m, 2H, H-14 H-15) 7.50 (d, 1H, *J=8.0*Hz, H-13) 7.60 (d, 1H, *J=8.0*Hz, H-17) 8.59 (s, br, 1H, H-11); **HRMS:** m/z (ESI) calculated for $C_{28}H_{36}N_9O_9^+$: 642.2636 $[M+H]^+$. Found: $[M+H]^+$: 642.2631

**L-Glutamyl-L-arginyl-L-tryptophyl-glycyl-glycyl-L-tryptophan; ERWGGW [16]**

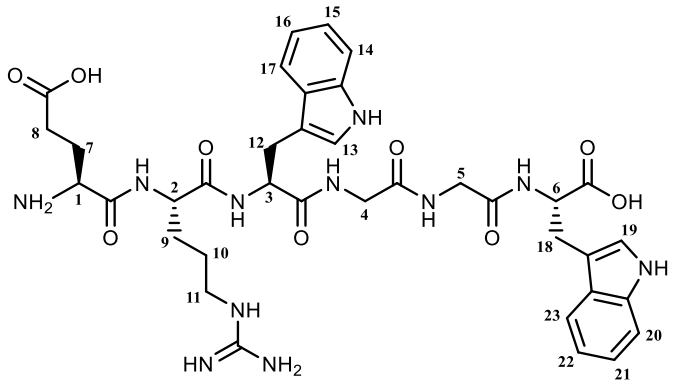

The product was purified by reverse phase HPLC at a flow rate of 20 mL/min. The method employed a binary mixture of eluents A ($H_2O$ with 0.1 % TFA) and B (MeOH with 0.1 % TFA). HPLC gradient B: 5%-35%; 0-10 mins, 35%-60%; 10-25mins, 60%-100%; 25-30mins, 100%-5%; 30-35mins, 5%; 35-45mins. Retention time was found to be at 17.7 mins (0.33 g, 4.2 x $10^{-4}$ mol, 69 %). **$^{1}$H-NMR** (400MHz, MeOD) $\delta_H$: 1.4-2.0 (m, 6H, H-7 H-9 H-10) 2.37 (t, 2H, *J*=7.5Hz, H-8) 3.0-3.3 (m, 6H, H-11 H-12 H-18) 3.52 (s, 2H, H-5) 3.56 (s, 2H, H-4) 3.90 (t, 1H, *J*=6.0Hz, H-1) 4.30 (t, 1H, *J*=6.0Hz, H-2) 4.50 (m, 1H, H-3) 4.62 (m, 1H, H-6) 6.8-7.1 (m, 2H, H-14 H-20) 7.2-7.6 (m, 4H, H-15 H-16 H-21 H-22) 8.25 (m, 2H, H-13 H-19) 8.37 (m, 1H, H-23) 8.47

(d, 1H, *J=7.5*Hz, H-17); **HRMS:** m/z (ESI) calculated for $C_{37}H_{48}N_{11}O_9^+$: 790.3636 $[M+H]^+$. Found: $[M+H]^+$: 790.3637

## 7.4 Synthesis of Uridyl-containing Peptides

**2',3'-O-Isopropylidene uridine [31]**[265]

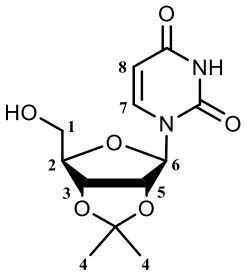


A suspension of uridine (3.50 g, 1.40 x $10^{-2}$ mol, 1 eq) and *p*-toluenesulfonic acid (0.14 g, *cat*) in $CHCl_3$(350 mL) was treated with 2-methoxypropene (3.30 mL, 3.50 x $10^{-2}$ mol, 2.4 eq). The mixture was heated to reflux and stirred overnight. The solvent was removed *in vacuo* to yield a purple foam. The product was purified by flash chromatography using EtOAc as the eluent (3.10 g, 1.1 x $10^{-2}$ mol, 71 %)

**$R_f$** = 0.42 (100% EtOAc); **m.p.** 163-166°C, lit m.p 163-166°C[266]; **$^1$H-NMR** (400MHz, DMSO-$d^6$) $\delta_H$: 1.29 (s, 3H, H-4) 1.49 (s, 3H, H-4) 3.5-3.6 (m, 2H, H-1) 4.09 (m, 1H, H-2) 4.76 (dd, 1H, $J_1$=3.5Hz $J_2$=6.5Hz, H-3) 4.88 (dd, 1H, $J_1$=3.0Hz $J_2$=6.5Hz, H-5) 5.65 (d, 1H, *J*=6.5Hz, H-6) 5.85 (d, 1H, *J*=3.0Hz, H-8) 7.80 (d, 1H, *J*=8.0Hz, H-7); **$^{13}$C-NMR** (100MHz, $CDCl_3$) $\delta_C$: 25.8, 63.3, 80.5, 82.7, 82.7, 86.9, 96.3, 103.0, 142.0, 175.4, 178.5; **HRMS:** m/z (ESI) calculated for $C_{12}H_{16}N_2NaO_6^+$: 307.0906 $[M+Na]^+$. Found: $[M+Na]^+$: 307.0901

**5'-succinyl-2', 3'-O-isopropylidene uridine [32]**[249]

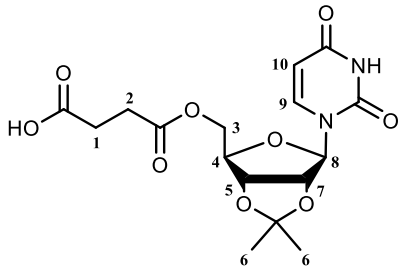

Succinic anhydride (1.03 g, 1.03 x $10^{-2}$ mol, 0.9 eq) was dissolved in dry DCM (100 mL) and a solution of **[31]** (3.101 g, 1.1 x $10^{-2}$ mol, 1 eq) in dry DCM (110 mL) was added. The mixture was treated with TEA (1.01 g, 1.4 mL, 1.0 x $10^{-2}$ mol, 0.90 eq) and was cooled to 0°C overnight. The reaction was allowed to warm to room temperature. The solvent was removed *in vacuo*, and the resulting residue was cooled to 0°C and dissolved in $Na_2CO_3$(*sat*). The aqueous layer was washed with $Et_2O$ (3 x 100 mL), cooled to 0°C and acidified with 2M HCl to pH 1.6. The product was then extracted with DCM (4 x 50 mL) and dried with $MgSO_4$. The solvent was removed *in vacuo*. The product was purified by flash chromatography using (8:2/EtOAc:$CHCl_3$) as the eluent (2.260 g, 5.88 x $10^{-3}$ mol, 57.0 %). **m.p.** 71-74°C $\mathbf{R_f}$ = 0.54 (8:2/EtOAc:$CHCl_3$); **$^1$H-NMR** (400MHz, DMSO-d$^6$) $\delta_H$: 1.34 (s, 3H, H-6) 1.54 (s, 3H, H-6) 2.57 (m, 4H, H-1 H-2) 4.05 (m, 1H, H-4) 4.24 (d, 2H, *J*=5.0Hz, H-3) 4.81 (dd, 1H, $J_1$=4.0Hz $J_2$=6.5Hz, H-5) 4.93 (dd, 1H, $J_1$=3.0Hz $J_2$=6.5Hz, H-7) 5.54 (d, 1H, *J*=6.5Hz, H-8) 5.83 (d, 1H, *J*=4.0Hz, H-10) 7.62 (d, 1H, *J*=8.0Hz, H-9); **$^{13}$C-NMR** (100MHz, $CDCl_3$) $\delta_C$: 25.5, 28.8, 28.9, 60.4, 64.0, 80.9, 84.6, 85.3, 94.9, 102.2, 142.5, 160.0, 164.4, 172.0, 176.4; **HRMS:** m/z (ESI) calculated for $C_{16}H_{20}N_2NaO_9^+$: 407.1066 $[M+Na]^+$. Found: $[M+Na]^+$: 407.1061

**5'-Succinyl-2',3'-O-isopropylideneuridyl-glycl-glycyl-L-tryptohyl-L-arginine [26]**

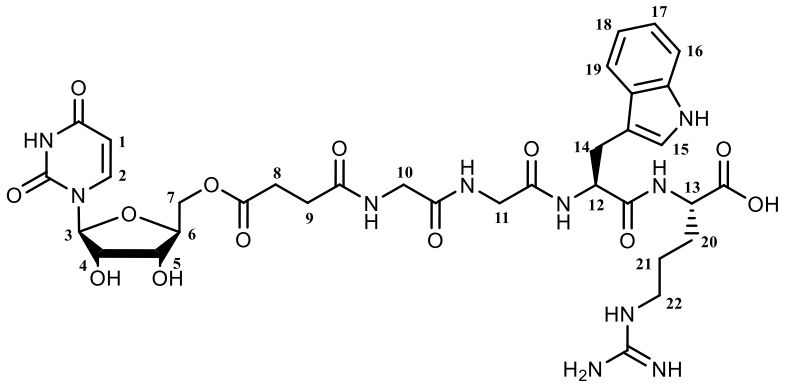

**[26]** was synthesised via SPPS following a general method using 2-chlorotrityl chloride resin (Chapter 7.3). The product was purified by reverse phase HPLC at a flow rate of 20 mL/min. The method employed a binary mixture of eluents A ($H_2O$ with 0.1 % TFA) and B (MeOH with 0.1 % TFA). HPLC gradient B: 50%-100%; 0-15 mins, 100%-50%; 15-20mins, 50%; 20-30mins. Retention time was found to be at 11.4mins (0.31 g, 3.9 x $10^{-4}$ mol, 64 %). **$^{1}$H-NMR** (400MHz, MeOD) $\delta_H$: 1.85 (m, 2H, H-21) 1.90 (m, 2H, H-20) 2.5-2.8 (m, 8H, H-8 H-9 H-14 H-22) 3.5-4.4 (m, 11H, H-4 H-5 H-6 H-7 H-10 H-11 H-12 H-13) 5.89 (d, 1H, *J*=3.5Hz, H-3) 5.91 (d, 1H, *J*=3.5Hz, H-1) 6.91 (t, 1H, *J*=6.0Hz, H-18) 6.98 (t, 1H, *J*=8.0Hz, H-17) 7.1-7.4 (m, 2H, H-15 H-16) 7.56 (d, 1H, *J*=8.0Hz, H-2) 7.93 (d, 1H, *J*=8.0Hz, H-19); **$^{13}$C-NMR** (100MHz, MeOD) $\delta_C$: 24.4, 30.3, 36.8, 41.6, 43.5, 44.4, 52.5, 53.4, 65.1, 65.7, 71.3, 72.2, 75.3, 76.1, 79.5, 80.3, 82.8, 83.4, 91.8, 103.6, 112.6, 119.6, 120.2, 122.7, 142.7, 169.6, 170.0, 171.9, 172.4, 190.1; **HRMS:** m/z (ESI) calculated for $C_{34}H_{46}N_{10}O_{13}^{+}$: 801.3162 $[M+H]^+$. Found: $[M+H]^+$: 801.3169

**5'-Succinyl-2',3'-O-isopropylideneuridyl-glycl-glycyl-glycyl-L-arginine [27]**

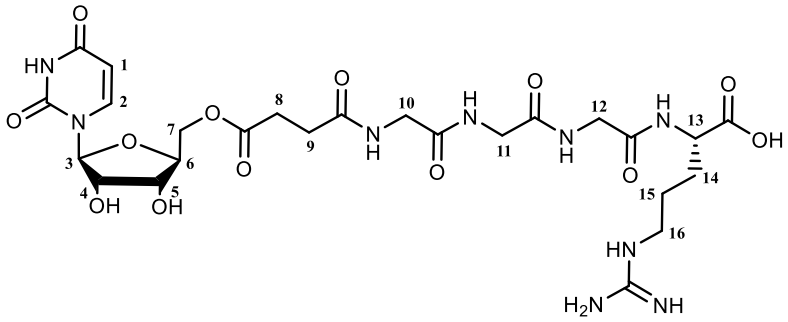

**[27]** was synthesised via SPPS following a general method using 2-chlorotrityl chloride resin (Chapter 7.3). The product was purified by reverse phase HPLC at a flow rate of 20 mL/min. The method employed a binary mixture of eluents A ($H_2O$ with 0.1 % TFA) and B (MeOH with 0.1 % TFA). HPLC gradient B: 5%-50%; 0-15 mins, 50%-100%; 15-20mins, 100%; 20-25mins, 100%-5%; 25-30mins, 5% 30-40mins. Retention time was found to be at 9.8mins. (0.392 g, 5.8 x $10^{-4}$ mol, 96%) **$^{1}$H-NMR** (400MHz, MeOD) $\delta_H$: 1.58 (m, 2H, H-15) 1.88 (m, 2H, H-14) 2.4-2.7 (m, 4H, H-8 H-9) 3.13 (m, 2H, H-16) 3.67 (dd, 1H, $J_1$=3.1Hz $J_2$=3.1Hz, H-4) 3.80 (m, 6H, H-7 H-11 H-12) 3.90 (s, 2H, H-10) 4.07 (m, 1H, H-13) 4.29 (dd, 1H, $J_1$=2.8Hz $J_2$=3.8Hz, H-5) 4.39 (q, 1H, $J$=4.6Hz, H-6) 5.63 (d, 1H, $J$=7.9Hz, H-3) 5.83 (d, 1H, $J$=4.5Hz, H-1) 7.91 (d, 1H, $J$=8.0Hz, H-2); **$^{13}$C-NMR** (100MHz, MeOD) $\delta_C$: 24.9, 28.4, 29.1, 32.0, 41.5, 41.8, 42.0, 44.0, 55.3, 62.9, 70.1, 71.8, 81.8, 98.5, 104.2, 150.1, 157.0, 164.0, 170.8, 171.0, 171.6, 174.3, 172.8; **HRMS:** m/z (ESI) calculated for $C_{25}H_{38}N_9O_{13}^+$: 672.2589 $[M+H]^+$. Found: $[M+H]^+$: 672.2584

**5'-Succinyl-2',3'-O-isopropylideneuridyl-glycl-glycyl-L-tryptophyl-glycine [28]**

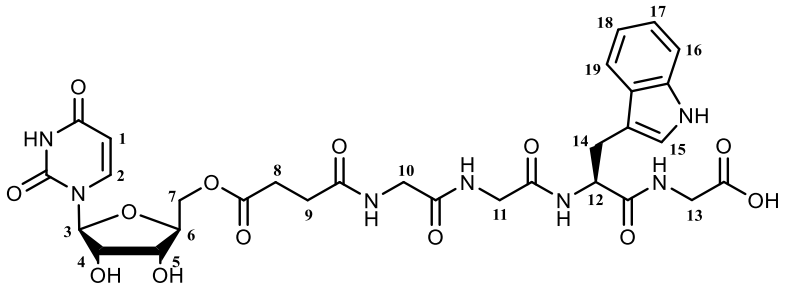

**[28]** was synthesised via SPPS following a general method using 2-chlorotrityl chloride resin (Chapter 7.3). The product was purified by reverse phase HPLC at a flow rate of 20 mL/min. The method employed a binary mixture of eluents A ($H_2O$ with 0.1 % TFA) and B (MeOH with 0.1 % TFA). HPLC gradient B: 5%-100%; 0-30 mins, 100%; 30-35mins, 100%-5%; 35-40mins, 5% 40-50mins. Retention time was found to be at 11.3 mins. (0.270 g, 3.8 x $10^{-4}$ mol, 91 %) **$^{1}$H-NMR** (400MHz, MeOD) $\delta_H$: 2.5 (m, 6H, H-8 H-9 H-14) 3.69 (s, 1H, H-10) 3.72 (s, 1H, H-13) 3.74 (s, 1H, H-11) 3.81 (m, 1H, H-6) 4.01 (m, 1H, H-4) 4.23 (m, 3H, H-5 H-7) 4.61 (dd, 1H, $J_1$=5.1Hz $J_2$=5.0Hz, H-12) 5.63 (d, 1H, $J$=8.0Hz, H-3) 5.71 (d, 1H, $J$=8.0Hz, H-1) 6.91 (t, 1H, $J$=7.5Hz, H-18) 7.00 (t, 1H, $J$=7.5Hz, H-17) 7.05 (d, 1H, $J$=5.5Hz, H-16) 7.21 (d, 1H, $J$=8.0Hz, H-2) 7.50 (d, 1H, $J$=8.0Hz, H-15) 7.60 (d, 1H, $J$=8.5Hz, H-19); **$^{13}$C-NMR** (400MHz, MeOD) $\delta_C$: 16.6, 289, 30.3, 31.5, 43.8, 44.4, 55.9, 65.1, 71.6, 75.5, 83.4, 91.8, 103.3, 111.5, 112.6, 118.5, 119.6, 120.5, 123.0, 125.2, 129.2, 142.7, 158.9, 161.7, 164.0, 167.9, 171.3, 173.3, 182.0; **HRMS:** m/z (ESI) calculated for $C_{30}H_{35}N_7NaO_{13}^+$: 724.2185 $[M+Na]^+$. Found: $[M+Na]^+$: 724.2190

**9*H*-fluoren-9-ylmethyl (2,5-dioxotetrahydrofuran-3-yl)carbamate; *N*-Fmoc-aspartic anhydride [33]**[250]

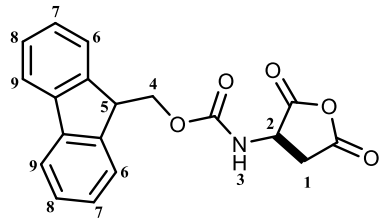

A solution of Fmoc-OSu (2.55 g, 7.5 x $10^{-3}$ mol, 1 eq) in THF (20 mL) was added with stirring to a solution of aspartic acid (1.00 g, 7.5 x $10^{-3}$ mol, 1 eq) in $H_2O$ (15 mL) containing $Na_2CO_3$ (1.75 g, 1.65 x $10^{-2}$ mol, 2.2 eq). After stirring at room temperature overnight, the mixture was washed with $Et_2O$ (2 x 20 mL). The aqueous layer was acidified with HCl to pH 2 and extracted with EtOAc (2 x 30 mL). The organic phase was dried with $MgSO_4$ and the concentrated *in vacuo*. The residue was then dissolved in $Ac_2O$ (8 mL) with rapid heating and stirring (10 minutes). The reaction mixture was then cooled to room temperature causing traces of precipitate to crash out. To encourage crystallization the mixture was left overnight under an ice bath. The precipitate was filtered off, washed with dry $Et_2O$ and dried under high vacuum (2.330 g, 7.2 x $10^{-3}$ mol, 96 %). **$^{1}$H-NMR** (400MHz, DMSO-$d_6$) $\delta_H$: 2.90 (dd, 2H, $J_1$=6.5Hz, $J_2$=12.5Hz, H-1) 3.33 (dd, 2H, $J_1$=8.5Hz, $J_2$=10Hz, H-1) 4.32 (t, 1H, $J$=6.5Hz, H-5) 4.54 (m, 2H, H-4) 4.71 (m, 1H, H-2) 7.41 (t, 2H, $J$=7.5Hz, H-7) 7.50 (t, 2H, $J$=7.5Hz, H-8) 7.73 (d, 2H, $J$=7.5Hz, H-6) 7.91 (d, 2H, $J$=7.5Hz, H-9) 8.20 (d, 1H, $J$=7.5Hz, H-3); **$^{13}$C-NMR** (100MHz, DMSO-$d_6$) $\delta_C$: 34.7, 46.6, 50.4, 66.0, 120.1, 120.2, 125.0, 125.1, 127.0, 127.1, 127.7, 140.8, 143.6, 155.9, 169.8, 172.1; **HRMS:** m/z (ESI) calculated for $C_{19}H_{15}NNaO_5^+$: 360.0848 $[M+Na]^+$. Found: $[M+Na]^+$: 360.0842

***N*-(9-Fluorenylmethoxycarbonyl)-L-aspartic acid-β-2',3'-O-isopropylidine uridyl ester; FAU-A [34a]**

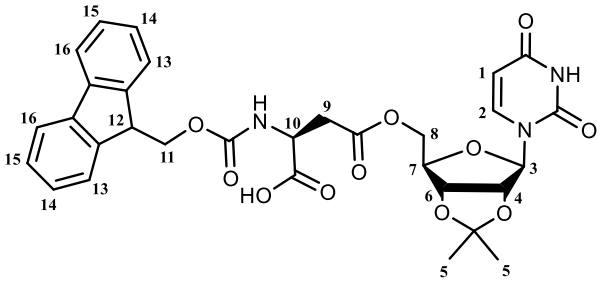

**[33]** (0.41 g, 1.25 x $10^{-3}$ mol, 1 eq) was dissolved in dry DCM (70 mL) and a solution of **[31]** (0.75 g, 1.25 x $10^{-3}$ mol, 1 eq) in dry DCM (110 mL) was added. The mixture was treated with TEA (0.4 mL, 2.5 x $10^{-3}$ mol, 2 eq) and was cooled to 0 °C. The reaction mixture was stirred at 0°C overnight and then allowed to warm to room temperature. The solvent was removed *in vacuo*, and the resulting residue was cooled to 0°C and dissolved in $Na_2CO_3$(*sat*). The aqueous layer was washed with diethyl ether (3 x 100 mL), cooled to 0°C and acidified with 2M HCl to pH 1.6. The product was then extracted with DCM (4 x 50 mL) and dried with $MgSO_4$. The solvent was removed *in vacuo*. The product was purified by flash chromatography using EtOAc as the eluent (0.231 g, 3.7 x $10^{-4}$ mol, 30 %).

**$R_f$** = 0.5 (100% EtOAc); **$^1$H-NMR** (400MHz, DMSO-$d_6$) $\delta_H$: 1.40 (s, 6H, H-5) 1.52 (s, 6H, H-5) 2.85 (m, 2H, H-9) 3.73 (dd, 1H, $J_1$=3.5Hz, $J_2$=12Hz, H-4) 3.97 (dd, 1H, $J_1$=2.5Hz, $J_2$=12Hz, H-6) 4.23 (m, 3H, H-7 H-8) 4.90 (m, 1H, H-10) 5.02 (m, 3H, H-11 H-12) 5.53 (d, 1H, *J*=3.5Hz, H-3) 5.78 (d, 1H, *J*=8.0Hz, H-1) 6.91 (d, 2H, *J*=7.5Hz, H-14) 7.30 (d, 1H, *J*=8.0Hz, H-2) 7.25 (d, 2H, *J*=7.5Hz, H-15) 7.56 (m, 2H, H-13) 7.72 (m, 2H, H-16); **$^{13}$C-NMR** (100MHz, DMSO-$d_6$) $\delta_C$: 25.6, 27.5, 31.2, 47.0, 51.0, 60.2, 66.3, 81.0, 84.5, 87.0, 21.6, 102.3, 113,5, 120.6, 125.7, 127.5, 128.1,

141.2, 142.4, 144.2, 150.8, 156.3, 163.6, 170.4, 171.5, 172.0, 172.8 **HRMS:** m/z (ESI) calculated for $C_{31}H_{30}N_3O_{11}^-$: 620.1880 $[M-H]^-$. Found: $[M-H]^-$: 620.1878

***N*-(9-Fluorenylmethoxycarbonyl)-L-aspartic acid- α -2',3'-O-isopropylidine uridyl ester; FAU-B [34b]**

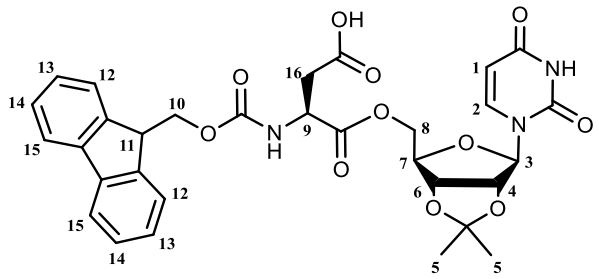


**[33]** (0.41 g, 1.25 x $10^{-3}$ mol, 1 eq) was dissolved in dry DCM (70 mL) and a solution of **[31]** (0.75 g, 1.25 x $10^{-3}$ mol, 1 eq) in dry DCM (110 mL) was added. The mixture was treated with TEA (0.4 mL, 2.5 x $10^{-3}$ mol, 2 eq) and was cooled to 0 °C. The reaction mixture was stirred at 0 °C overnight and then allowed to warm to room temperature. The solvent was removed *in vacuo*, and the resulting residue was cooled to 0 °C and dissolved in $Na_2CO_3$(*sat*). The aqueous layer was washed with diethyl ether (3 x 100 mL), cooled to 0 °C and acidified with 2M HCl to pH 1.6. The product was then extracted with DCM (4 x 50 mL) and dried with $MgSO_4$. The solvent was removed *in vacuo*. The product was purified by flash chromatography using EtOAc as the eluent (0.163 g, 2.6 x $10^{-4}$ mol, 21 %).

**$R_f$** = 0.3 (100% EtOAc); **$^1$H-NMR** (400MHz, DMSO-$d_6$) $\delta_H$: 1.39 (s, 6H, H-5) 1.51 (s, 6H, H-5) 2.73 (m, 2H, H-16) 3.60 (m, 2H, H-4 H-6) 4.24 (m, 1H, H-7) 4.44 (m, 2H, H-8) 4.87 (dd, 1H, $J_1$=3.0Hz, $J_2$=6.5Hz, H-9) 5.14 (dd, 1H, $J_1$=2.5Hz, $J_2$=6.5Hz, H-10 H-11) 5.72 (dd, 1H, $J_1$=3.0Hz, $J_2$=8.0Hz, H-3) 5.90 (d, 2H, $J$=2.5Hz, H-1) 7.46 (m, 3H, H-2 H-14) 7.52 (t, 2H, $J$=7.5Hz, H-13) 7.80 (m, 2H, H-12) 7.91 (m, 2H, H-

15); **$^{13}$C-NMR** (100MHz, DMSO-$d_6$) $\delta_C$: 25.6, 27.3, 47.0, 51.5, 64.3, 66.2, 80.9, 83.1, 84.2, 92.2, 102.4, 113.8, 120.6, 125.7, 127.7, 141.2, 142.9, 144.3, 150.9, 156.2, 163.5, 170.9, 172.9; **LRMS** m/z (ESI) 620.2 $[M-H]^-$; **HRMS:** m/z (ESI) calculated for $C_{31}H_{30}N_3O_{11}^-$ : 620.1880 $[M-H]^-$. Found: $[M-H]^-$: 620.1889

**L-Arginyl-L-tryptophyl-L-alanyl-L-aspartyl-α-tryptophyl-β-uridyl ester; RWAD(Ur)-W [29a]**

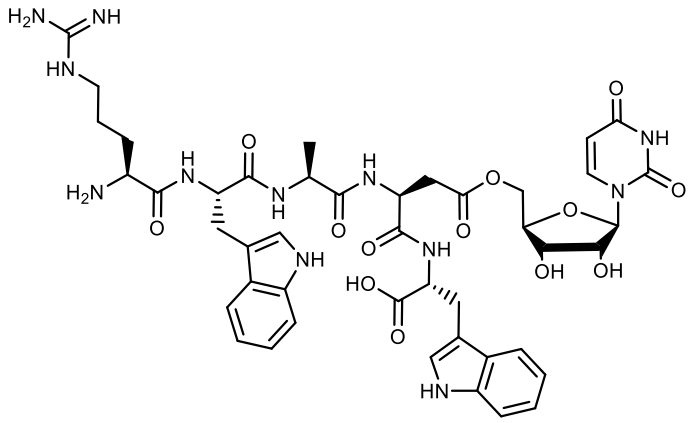

**[29a]** was synthesised via SPPS following the general SPPS method using 2-chlorotrityl chloride resin, Fmoc-protected amino acids and **[34a]** (Chapter 7.3). Due to poor yields (10mg, $1x10^{-5}$mol, 3%), the product was unable to be characterised by NMR. **HRMS:** m/z (ESI) calculated for $C_{31}H_{30}N_3O_{11}^-$ : 981.3826 $[M+Na]^+$. Found: $[M+Na]^+$: 981.3834

**L-Arginyl-L-tryptophyl-L-alanyl-L-aspartyl-β-tryptophyl-α-uridyl ester; RWAD(W)-Ur [29b]**

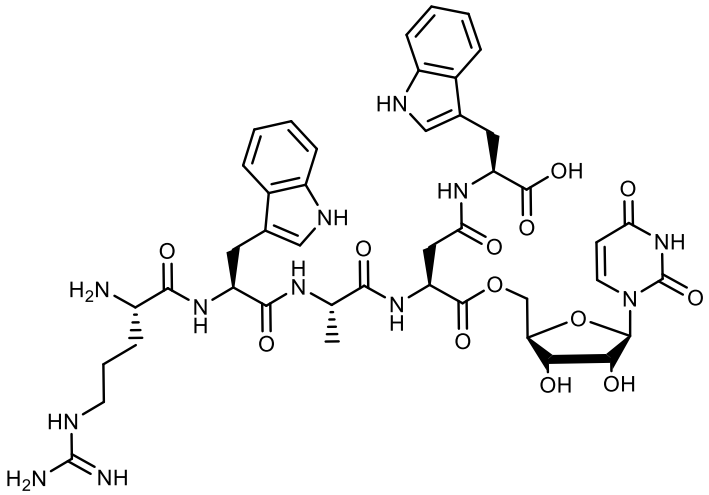

**[29b]** was synthesised via SPPS following the general SPPS method using 2-chlorotrityl chloride resin, fmoc-protected amino acids and **[34b]** (Chapter 7.3). Due to poor yields (8mg, $1x10^{-5}$mol, 2%), the product was unable to be characterised by NMR. **HRMS:** m/z (ESI) calculated for $C_{31}H_{30}N_3O_{11}^-$ : 981.3826 $[M+Na]^+$. Found: $[M+Na]^+$: 981.3832

## 7.5 Fluorescence Plate Reader Assay

A Tecan GENios plate reader was used to determine the inhibitory activity of synthetic RWXXW analogues at an excitation wavelength of 340nm and emission wavelength of 535nm. To monitor the formation of dansyl-Lipid I, membrane bound MraY was treated with a master mix containing dansyl-tagged UDP-MurNAc pentapeptide and lipid carrier $C_{55}$-P or $C_{35}$-P. Dansyl-tagged UDP-MurNAc pentapeptide was provided by Agnes Mihalyi.

$C_{55}$-P and $C_{35}$-P was purchased from Larodan Fine Chemicals in a chloroform/methanol (2:1) + 3 % (v/v) ammonia solution. 20 µl of the 10 mg/mL

stock solution (total 0.2 mg) was transferred to a small vial. The solvents were removed from this sample using a gentle stream of $N_{2(g)}$. Once the solution was completely dried it was redissolved in 2 mL of a buffer solution containing 50 mM Tris Base pH 7.5, 2 mM β-mercaptoethanol, 1mM $MgCl_2$, 20 % glycerol and 0.5 % TritonX100. The solution was vortexed and sonicated until the 100μg/mL solution became clear.

*Preparation of the Master Mix (MM)*

The master mix contained a mixture of buffer A, water, dansyl-UDP-MurNAc pentapeptide and lipid carrier $C_{55}$-P or $C_{35}$-P (Table 7.1). Buffer A contained a final concentration of 100 mM Tris base, pH 7.5 and 25 mM $MgCl_2$. The master mix contained 21.0 μM Dansyl-UDP-MurNAc pentapeptide and 47.2 μM $C_{55}$-P or 70.6 μM $C_{35}$-P.

*Preparation of Membrane-bound MraY*

Agnes Mihalyi overexpressed *E. coli* and *P. aeruginosa* MraY in *E. coli* DH5α cells. Membrane isolates were dissolved in a membrane buffer containing 50 mM Tris pH 7.5, 2 mM β-mercaptoethanol and 1 mM $MgCl_2$. The final protein concentrations of membranes containing overexpressed *E. coli* and *P. aeruginosa* MraY in this plate reader assay were 0.72 and 0.13 mg/mL, respectively.

**Table 7.1: Final concentrations in plate reader assay**

| | Stock | Volume | Concentration in MM | Concentration in each well |
|---|---|---|---|---|
| Dansyl-UDP-MurNAc pentapeptide (1427.20 g/mol) | 3.75 mg/mL | 40 µL | 21.0 µM | 17.9 µM |
| $C_{55}$-P (847.28 g/mol) or $C_{35}$-P (566.74 g/mol) | 0.1 mg/mL | 2 mL | $C_{55}$-P = 47.2 µM<br>$C_{35}$-P = 70.6 µM | $C_{55}$-P = 40.1 µM<br>or<br>$C_{35}$-P = 60.0 µM |
| Buffer A | 200 mM Tris base pH 7.5<br>50 mM $MgCl_2$ | 2.5 mL | 100 mM Tris base, pH 7.5<br>25 mM $MgCl_2$ | 85 mM Tris base, pH 7.5<br>21.25 mM $MgCl_2$ |
| Water | | 0.46mL | | |

*Plate reader assay protocol*

To a 96 well plate, 10 µL of overexpressed MraY membranes was added to 85 µL of master mix and 5 µL of the inhibitor (final concentration 100 µg/mL in MeOH). MeOH was used as the negative control. Tunicamycin and Epep, at a final concentration of 100 µg/mL in MeOH, were used as the positive controls. Fluorescence measurements were taken before the addition of membranes, $t$ =0, then at 5 minute intervals for 20 minutes.

## 7.6 Continuous Fluorescence Assay

The MraY catalysed reaction was monitored by a Perkin Elmer LS55 fluorimeter at an excitation wavelength of 340nm and an emission wavelength of 530nm. . To monitor the formation of dansyl-Lipid I, membrane-bound MraY was treated with a master mix containing dansyl-UDP-MurNAc pentapeptide and lipid carrier $C_{55}$-P or $C_{35}$-P. Dansyl-tagged UDP-MurNAc pentapeptide was provided by Agnes Mihalyi. $C_{55}$-P or $C_{35}$-P was prepared as mentioned in Chapter 7.5.

*Continuous assay protocol*

To a Starna® sub-micro fluorimeter cell, 15 µL of membrane bound MraY was added to 150 µL of master mix and 15 µL of inhibitor. The final protein concentrations of membranes containing overexpressed *E. coli, P. aeruginosa, S. aureus, M. flavus* and *B. subtilis* MraY in this continuous assay were 0.6, 0.1, 0.28, 0.3, 0.3 and 0.9 mg/mL, respectively. The final concentration of all reagents in the master mix and in the assay is given in Table 7.2.

**Table 7.2: Final concentrations in continuous fluorescence assay**

| | Stock | Volume | Concentration in MM | Concentration in cuvette |
|---|---|---|---|---|
| Dansyl-UDP-MurNAc pentapeptide (1427.20 g/mol) | 3.75 mg/mL | 40 µL | 21.0 µM | 17.5 µM |
| $C_{55}$-P (847.28 g/mol) or $C_{35}$-P (566.74 g/mol) | 0.1mg/mL | 2 mL | $C_{55}$-P = 47.2 µM $C_{35}$-P = 70.6 µM | $C_{55}$-P = 39.3 µM or $C_{35}$-P = 58.8 µM |
| Buffer A | 200 mM Tris base, pH 7.5 50 mM $MgCl_2$ | 2.5 mL | 100 mM Tris base, pH 7.5 25 mM $MgCl_2$ | 83.3 mM Tris base, pH 7.5 20.83 mM $MgCl_2$ |
| Water | | 0.46mL | | |

## 7.7 $IC_{50}$ determination

The $IC_{50}$ of novel MraY inhibitors were calculated using the statistical software GenStat for Teaching and Learning. A linear regression was fitted to the first 500 data points. The slope of each line was then related to the percent activity of MraY in relation to the negative control (Table 7.3). The negative control was assumed to correspond to 100 % MraY activity.

**Table 7.3: Slope dependent inhibition by Epep.**

| Epep [μg/mL] | Slope | Error in slope | % Activity of MraY | % Error |
|---|---|---|---|---|
| 0 | 0.112 | 0.002 | 100 | 1.35 |
| 37 | 0.041 | 0.001 | 36 | 1.20 |
| 62.5 | 0.037 | 0.001 | 32.5 | 1.17 |
| 83 | 0.014 | 0.001 | 12 | 1.26 |

The percent activity of MraY was plotted against the concentration of the inhibitor to produce an $IC_{50}$ graph. With assistance from the Quantitatvie Biology Centre (QuBic), GenStat was programmed to fit a smoothing spline function through the data points. A smoothing spline gently angulates between data points minimising the distance between the points and the line. The function of a spline is similar to an exponential function and has equation 3.1.

$$\boldsymbol{y = Ae^{-iB[C]}} \quad \textbf{[7.1]}$$

Where:

A: % activity of MraY
B: rate of decrease
C: concentration

Using this equation the concentration of the inhibitor that reduces the activity of the enzyme by 50 % can be determined.

$$\boldsymbol{-\frac{1}{B}\ ln(\frac{50}{100}) = C} \quad \textbf{[7.2]}$$

To calculate error, GenStat factors in the standard error associated with each data point (determined from the linear regression) as well as the distance between the data points and the smoothing spline. The error generated by this graph is relative to the concentration of the inhibitor.

## 7.8 Overexpression and Isolation of MraY mutants

*Transformation into E. coli C43*

MOAC summer project student Amy O'Reilly provided three *E. coli mraY* constructs with mutations F288A, F288L and E287A in a pET52b vector. 5 μL of these MraY containing vector DNA were added to 50 μL of *E. coli* C43 competent cells and incubated over ice for 30 minutes. The samples were incubated at 42 °C in a water bath for 45 seconds and immediately transferred to ice for 3 minutes. 300 μL of LB was added to each sample and incubated at 37°C with shaking (180 rpm) for 1 hour. 100 μL of the seeded LB was poured to a standard agar plate. An L-shaped cell spreader was used to assure the mixture was evenly distributed across the plate. The agar plate was incubated overnight at 37 °C.

*Isolation of E. coli membranes*

A single colony was isolated from the transformed plate and inoculated in 5 mL of LB+Amp (100 μg/mL) overnight at 37 °C with shaking. This start-up culture was diluted 100-fold with LB+Amp (100 μg/mL) and allowed to grow to an $OD_{600}$ of 0.6. The cells were then induced with IPTG (1 mM) and allowed to grow for 4 hours at 37 °C with shaking. The cells were spun down at 4,400 g for 15 minutes at 4 °C. The pellet was transferred to a pre-weighed falcon tube and resuspended in membrane buffer (3 mL/gram of pellet). Typically 1-2 grams of pellet was isolated. The membrane buffer contained 50 mM Tris pH 7.5, 2 mM β-mercaptoethanol and 1 mM $MgCl_2$. 2.5 mg of Lysozyme (from egg white) and 25 μg of DNAse I (from bovine pancreas) was added to each 1mL of membrane buffer. The cells were then lysed using a Constant Systems Ltd. TS Series Cabinet cell disruptor. The lysed cells were

spun down at 24,000 g for 20 minutes at 4 °C. The supernatant was then isolated and spun down at 40,000 rpm for 1 hour at 4 °C using an ultracentrifuge. The membrane pellet was homogenised in minimum membrane buffer (<2 mL) and flash frozen with liquid $N_2$ in 300 μL aliquots.

## 7.9 Protocol for Western Blot

*SDS-PAGE protocol*

Membrane-bound MraY mutant samples were determined by discontinuous-dodecyl-sulphate polyacrylamide gel electrophoresis (SDS-PAGE)[267]. The running gel was composed of 1.252 mL of 1.5 M Tris, pH 8.8, 2.025 mL of 29.1% (*w/v*) acrylamide, 1.678 mL of $dH_2O$, 51.2 μL of 10% SDS, 51.2 μL of 10 % APS and 4.45 μL of TEMED. The mixture was poured between two glass plates to solidify. The stacking gel was composed of 500 μL of 0.5M Tris, pH 6.5, 200 μL of 29.1% (*w/v*) acrylamide, 1.3mL of $dH_2O$, 20 μL of 10% SDS, 30 μL of 10% APS and 3 μL of TEMED. The stacking gel was poured over the solidified running gel, and a 10-well comb was inserted. While the gel solidified, protein samples were prepared. To 25 μg of membrane-bound MraY in a membrane buffer composed of 50 mM Tris pH 7.5, 2 mM β-mercaptoethanol and 1 mM $MgCl_2$, 5 μL of SDS dye was added and boiled at 60 °C for 10 minutes. Prestained molecular weight and strep tag markers were used in the gel. The gel was run for 55 minutes at room temperature at 180 volts and 400mA.

*Transfer process*

To analyse the molecular weight of the MraY proteins, the proteins were transferred from the SDS-PAGE gel to a PVDF membrane. The transfer buffer was composed of 2.9 g of glycine powder, 5.8 g of TRIS base powder, 200 mL of MeOH and $dH_2O$

(total volume of 1L). 2 sponges and 2 pieces of filter paper were soaked in the transfer buffer before being using in the transfer sandwich. The PVDF membranes were cut and activated in 20 mL of 100 % MeOH.

The transfer sandwich was prepared in the following order; sponge, filter paper, SDS-PAGE gel, activated PVDF membrane, filter paper and a sponge. Air bubbles were removed by evenly and firmly rolling a 50mL falcon tube over the sandwich. The transfer sandwich was clamped and placed in the transfer tank. The transfer process was run for up to 3 hours at 4 °C at 110v and 170mA in the transfer buffer.

*Blocking the membranes*

The PVDF membrane was blocked with 50 mL of blocking buffer at 4 °C for 1 hour. The blocking buffer was composed of 5 % albumin (from Marvel powdered milk) in 50 mL of PBS. The blocking buffer was decanted from the membrane and the membrane was washed 3 times with 20mL PBS-Tween buffer for 5 minutes with gentle shaking at room temperature.

*Antibody HRP-Conjugate binding*

10 mL of PBS-Tween buffer was added to the membrane. 10 μL of 0.1 % Strep-Tactin HRP-conjugate in PBS-Tween was added and incubated at room temperature for 1 hour with gentle shaking. The membrane was washed twice with PBS-Tween buffer and twice with PBS buffer for 1 minute at room temperature.

*Chemoluminescence*

The membrane was treated with 2 mL of Novex® Electrochemiluminescence (ECL) reagents A and B (1:1) for up to 2 minutes with gentle shaking. The membrane was

then transferred to a developing cassette and blotted onto film in a dark room. An AGFA Curix 60 processor was used to develop the film and visualise protein bands.

### 7.10 Protocol for Dot Blot

A dot blot was performed to confirm the presence of Strep-tagged proteins. Nitrocellulose membrane paper was cut into strips and spotted directly with 5 and 20 μL of membrane-bound MraY mutants (13 mg/mL in membrane buffer). The spots were air dried (≈ 1 hour).

*Blocking the membranes*

The loaded nitrocellulose membrane strips were blocked with 50 mL of blocking buffer at 4 °C for 1 hour. The blocking buffer was composed of 5 % albumin (from Marvel powdered milk) in 50 mL of PBS. The blocking buffer was decanted from the membrane strips. The membrane strips were then washed 3 times with 20 mL PBS-Tween buffer for 5 minutes with gentle shaking at room temperature.

*Antibody HRP-Conjugate binding*

10mL of PBS-Tween buffer was added to the membrane strips. 20 μL of 0.1 % Strep-Tactin HRP-conjugate in PBS-Tween was added and incubated at room temperature for 1 hour with gentle shaking. The membrane was washed twice with PBS-Tween buffer and twice with PBS buffer for 1 minute at room temperature.

*Chemoluminescence*

The membrane was treated with 2 mL of Novex® Electrochemiluminescence (ECL) reagents A and B (1:1) for up to 2 minutes with gentle shaking. The membrane strips

were then transferred to a developing cassette and blotted onto film in the dark room. An AGFA Curix 60 processor was used to develop the film and visualise protein spots.

### 7.11 Kirby-Bauer Antibiotic Susceptibility test

Luria Bertani broth (LB) was composed of 1 % tryptone, 0.5 % yeast extract and 1 % NaCl. *E. coli* C43 and *B. subtilis* colonies were isolated from a standard agar plate and inoculated in 5 mL of LB broth overnight at 37°C. 0.1 mL of cultured bacteria was then added to 2 mL of melted low percent agar. Low percent agar was composed of LB + 0.5 % (w/v) agar. The mixture was vortexed and immediately poured onto an agar plate. An L-shaped cell spreader was used to assure the mixture was evenly distributed across the plate. Once fully gelled, the plate was divided into eight sections and labelled. An antibacterial disc was added to each section. On the antibacterial disc 25 μL of a 5 mg/mL inhibitor was added. Ampicillin (125 μg/mL) and water were used as the positive and negative controls, respectively. The plates were then inverted an incubated overnight at 37°C.

### 7.12 Microtitre Broth Dilution Technique

Luria Bertani broth (LB) was composed of 1% tryptone, 0.5 % yeast extract and 1 % NaCl. *P. putida, E. coli* and *B. subtilis* colonies were isolated from an agar plate and inoculated in 5 mL of LB broth overnight at 37 °C. A dilution series of the seeded LB was performed to get a $10^{-1}$, $10^{-2}$, $10^{-3}$, $10^{-4}$, $10^{-5}$, $10^{-6}$, $10^{-7}$ and $10^{-8}$-fold dilutions. The dilution series was performed by taking 0.5 mL of the seeded LB and diluting it with 4.5 mL of LB. This was equivalent to a ten-fold dilution. 0.5 mL of this ten-fold dilution was then further diluted in 4.5mL of LB to get a 100-fold dilution. This was

repeated until a $10^{-8}$ -fold dilution was made. 0.5 mL of each dilution was then poured onto an agar plate. An L-shaped cell spreader was used to assure the solution was evenly distributed across the plate. The plates were then inverted and incubated overnight at 37 °C. The colonies were counted and the dilution that gave a CFU/mL of $10^3$ was chosen for MIC calculations

On a 96 deep welled plate, 190 µl of the seeded broth (CFU/mL = $10^3$) was added to each well. 2.5 mg/mL solutions of protein E analogues were serially diluted to obtain 7 different concentrations (1250, 625, 312.5, 186, 78.2, 39, and 19.5 µg/mL). 10 µL of these diluted inhibitors were added to the 96 deep well plate to give a final volume of 200 µL and final concentrations of 125, 62.5, 31.25, 15.63, 7.82, 3.90, 1.95 and 0.97 µg/mL. 10 µL of water was added to one of the wells to serve as a growth control. The deep 96 well plate was covered with a sterile adhesive film and incubated overnight at 37°C. The solutions were then transferred to a normal 96 well plate for optical density measurements ($OD_{595}$) using a Tecan GENios plate reader. The inhibitor concentration which reduced the growth by 50 % was considered the MIC of the compound.

### 7.13 Fluorometric assay of Gram-negative bacterial permeabilization[229]

A single colony of *P. putida* was isolated from a standard agar plate and inoculated in 5 mL of LB overnight at 37°C with shaking. This start-up culture was diluted 100-fold with LB and grown to $OD_{600}$ of 0.5 at 37 °C with shaking. The culture was then centrifuged for 10 minutes at 1000 g at 25 °C. The pellet was resuspended in half the volume of 5mM HEPES buffer, pH 7.2.

Membrane permealisation of this bacterial suspension by $H_2N$-RW-Oct **[3]** was determined on a Perkin Elmer fluorimeter at an excitation wavelength of 340nm and

an emission wavelength of 435nm. To a Starna® sub-micro fluorimeter cell, 50 μL of the bacterial suspension was added to 25 μL of 40 μM NPN and 25 μL of the inhibitor. NPN and **[3]** were dissolved in a HEPES buffer, pH 7.2. The HEPES buffer solution was used as the negative control and EDTA (125 μg/mL) was used as the positive control. The samples were monitored continuously for 20 minutes. Inhibitors were tested in duplicates.

### 7.14 Effects on the Growth of Bacteria by IPTG and MraY

*Transformation into E. coli C43 cells*

5 μL of empty pET52b vector DNA and 5μL of *mraY* containing pET52b vector DNA were added to 50 μL of *E. coli* C43 competent cells and incubated over ice for 30 minutes. The samples were incubated at 42°C in a water bath for 45 seconds and immediately transferred to ice for 3 minutes. 300 μL of LB was added to each sample and incubated at 37 °C with shaking (180 rpm) for 1 hour. 100 μL of the seeded LB was poured to a standard agar plate. An L-shaped cell spreader was used to assure the mixture was evenly distributed across the plate. The agar plate was incubated overnight at 37 °C.

*Monitorisation of growth*

A single colony was isolated from the transformed plate and inoculated in 5 mL of LB+Amp (100 μg/mL) overnight at 37 °C with shaking. This start-up culture was diluted 100-fold with LB and induced with 0.5 mM IPTG. The culture was allowed to grow with shaking at 37 °C. The optical density ($OD_{595}$) of the growing cells was measured every 30 minutes using a Thermo Electron UV-VIS spectrophotometer.

## 7.15 MIC of $H_2N$-RW-Oct [3] against E. coli cells overexpressing WT MraY and Mray mutants F288L and E287A

*Transformation into E. coli C43 cells*

MOAC summer project student Amy O'Reilly provided three *E. coli mraY* constructs in a pET52b vector. These constructs contained WT *mraY*, mutant F288L and mutant E287A *mraY* DNA. 5 µL of pET52b vector DNA were added to 50 µL of *E. coli* C43 competent cells and incubated over ice for 30 minutes. To serve as a negative control 5µL of an empty pET52b vector DNA was added to 50 µL of *E. coli* C43 competent cells and incubated over ice for 30 minutes. The samples were incubated at 42 °C in a water bath for 45 seconds and immediately transferred to ice for 3 minutes. 300 µL of LB was added to each sample and incubated at 37 °C with shaking (180 rpm) for 1 hour. 100 µL of the seeded LB was poured to a standard agar plate. An L-shaped cell spreader was used to assure the mixture was evenly distributed across the plate. The agar plate was incubated overnight at 37 °C.

*MIC determination*

A single colony was isolated from the transformed plate and inoculated in 5mL of LB+Amp (100 µg/mL) overnight at 37 °C with shaking. This start-up culture was diluted 100-fold with LB and induced with 0.5 mM IPTG. To a sterile deep well microtitre plate, 190 µl of the IPTG-induced seeded broth was added to each well. 10 µL of $H_2N$-RW-Oct **[3]** was added to the deep 96 well plate to give a final volume of 200 µL and final inhibitor concentrations of 500, 450, 400, 350, 300, 250, 125, 62.5, 31.25, 15.63, 7.82, 3.90, 1.95 and 0.98 µg/mL. Each inhibitor concentration was tested in duplicates. 10 µL of water was added to one of the wells to serve as a growth

control. Normal LB was also used as a negative control. The microtire plate was covered with a sterile adhesive film and incubated at 37 °C with shaking for 8 hours. The solutions were then transferred to a standard 96 well plate for absorbance measurements ($OD_{595}$). The inhibitor concentration which reduced the growth by 50% was considered the MIC of the compound.

# REFERENCES


1. S. L. Derderian, *River Acad. J.*, 2007, **3**, 1–5.

2. Centers for Disease Control and Prevention, *Natl. Vital Stat. Rep.*, 1998, **48**, 1–67.

3. A. Sonnega, *Res. High. Demogr. Econ. Aging*, 2006, **14**, 1–4.

4. R. E. Hancock, *Lancet Infect. Dis.*, 2001, **1**, 156–164.

5. R. P. Handfield-Jones, *J. Coll. Gen. Pr.*, 1965, **5**, 43–53.

6. S. Dzidic and V. Bedeković, *ACTA Pharm. Sin.*, 2003, **24**, 519–26.

7. S. B. Levy, *Sci. Am.*, 1998, **278**, 46–53.

8. W. Kirby, *Science (80-. ).*, 1944, **99**, 452–453.

9. H. F. Chambers, *Emerg. Infect. Dis.*, 2001, **7**, 178–181.

10. K. Bush, G. A. Jacoby, and A. A. Medeiros, *Antimicrob. Agents Chemother.*, 1995, **39**, 1211–1233.

11. W. Kirby, *J. Clin. Invest.*, 1944, **24**, 170–174.

12. R. G. Workman and W. E. Farrar, *J. Infect. Dis.*, 1970, **121**, 433–437.

13. P. W. A. M.-H. C. Mandell G.L., in *Goodman and Gilman's The Pharmacological Basis of Therapeutics*, eds. A. Gilman, L. Goodman, T. Rall, and F. Murad, McGraw-Hill Companies, New York, 9th edn., 1996, pp. 1073–1101.

14. A. P. Johnson, A. Pearson, and G. Duckworth, *J. Antimicrob. Chemother.*, 2005, **56**, 455–462.

15. M. P. Jevons, *Br Med J*, 1961, **1(5291)**, 124–125.

16. D. F. J. Brown and P. E. Reynolds, *FEBS lett.*, 1980, **122**, 275–278.

17. V. J. Lee and S. J. Hecker, *Med. Res. Rev.*, 1999, **19**, 521–542.

18. F. M. Barrett FF, McGehee RF Jr, *N. Engl. J. Med.*, 1968, **279**, 441–448.

19. M. Kuehnert, D. Kruszon-Moran, H. Hill, G. McQuillan, S. McAllister, G. Fosheim, L. McDougal, J. Chaitram, B. Jensen, S. Fridkin, G. Killgore, and F. Tenover, *J. Infect. Dis.*, 2006, **193**, 172–179.

20. G. Sakoulas and R. C. Moellering, *Clin. Infect. Dis.*, 2008, **46**, S360–S367.

21. B. Murray, *N. Engl. J. Med.*, 2000, **342**, 710–721.

22. T. D. Bugg, G. D. Wright, S. Dutka-Malen, M. Arthur, P. Courvalin, and C. T. Walsh, *Biochemistry*, 1991, **30**, 10408–10415.

23. C. T. Walsh, *J. Biol. Chem.*, 1989, **264**, 2393–6.

24. D. P. Levine, *Clin. Infect. Dis.*, 2006, **42**, S5–S12.

25. C. T. Walsh, S. L. Fisher, I. S. Park, M. Prahalad, and Z. Wu, *Chem. Biol.*, 1996, **3**, 21–28.

26. I. E. Robledo, E. E. Aquino, and G. J. Vázquez, *Antimicrob. Agents Chemother.*, 2011, **55**, 2968–2970.

27. A. M. Al-jasser, *Kuwait Med. J.*, 2006, **38**, 171–185.

28. J. D. D. Pitout and K. B. Laupland, *Lancet Infect. Dis.*, 2008, **8**, 159–166.

29. E. Hamouche and D. K. Sarkis, *Pathol. Biol. (Paris).*, 2012, **60**, 15–20.

30. A. K. Marr, W. J. Gooderham, and R. E. Hancock, *Curr. Opin. Pharmacol.*, 2006, **6**, 468–472.

31. J. N. Steenbergen, J. Alder, G. M. Thorne, and F. P. Tally, *J. Antimicrob. Chemother.*, 2005, **55**, 283–288.

32. D. L. Shinabarger, K. R. Marotti, R. W. Murray, a H. Lin, E. P. Melchior, S. M. Swaney, D. S. Dunyak, W. F. Demyan, and J. M. Buysse, *Antimicrob. Agents Chemother.*, 1997, **41**, 2132–2136.

33. M. Korczynska, T. A. Mukhtar, G. D. Wright, and A. M. Berghuis, *Proc. Natl. Acad. Sci. U. S. A.*, 2007, **104**, 10388–10393.

34. D. M. E. Bowdish, D. J. Davidson, Y. E. Lau, K. Lee, M. G. Scott, and R. E. W. Hancock, *J. Leukoc. Biol.*, 2005, **77**, 451–459.

35. R. E. W. Hancock and H.-G. Sahl, *Nat. Biotechnol.*, 2006, **24**, 1551–1557.

36. C. Loose, K. Jensen, I. Rigoutsos, and G. Stephanopoulos, *Nature*, 2006, **443**, 867–869.

37. M. R. Yeaman and N. Y. Yount, *Pharm. Rev.*, 2003, **55**, 27–55.

38. L. Yang, T. M. Weiss, R. I. Lehrer, and H. W. Huang, *Biophys. J.*, 2000, **79**, 2002–2009.

39. S. Qian, W. Wang, L. Yang, and H. W. Huang, *Proc. Natl. Acad. Sci. U. S. A.*, 2008, **105**, 17379–17383.

40. K. A. Brogden, *Nat. Rev. Microbiol.*, 2005, **3**, 238–50.

41. A. Spaar, C. Münster, and T. Salditt, *Biophys. J.*, 2004, **87**, 396–407.

42. D. Sengupta, H. Leontiadou, A. E. Mark, and S.-J. Marrink, *Biochim. Biophys. Acta*, 2008, **1778**, 2308–2317.

43. K. Bertelsen, J. Dorosz, S. K. Hansen, N. C. Nielsen, and T. Vosegaard, *PLoS One*, 2012, **7**, 1–12.

44. K. A. Brogden, *Nat. Rev. Microbiol.*, 2005, **3**, 238–250.

45. Z. Oren and S. Yechiel, *Pept. Synth.*, 1998, **47**, 451–463.

46. P. Nicolas, *FEBS J.*, 2009, **276**, 6483–6496.

47. A. Bouhss, A. E. Trunkfield, T. D. H. Bugg, and D. Mengin-Lecreulx, *FEMS Microbiol. Rev.*, 2008, **32**, 208–233.

48. J. van Heijenoort, *Glycobiology*, 2001, **11**, 25R–36R.

49. Y. Hu, L. Chen, S. Ha, B. Gross, B. Falcone, D. Walker, M. Mokhtarzadeh, and S. Walker, *Proc. Natl. Acad. Sci. U. S. A.*, 2003, **100**, 845–849.

50. S. Ha, B. Gross, and S. Walker, *Curr. Drug Targets Infect. Disord.*, 2001, **1**, 201–213.

51. S. Walker, *Harvard Univ. Chem. Biol.*, 2009, 1.

52. L. D. Tatar, C. L. Marolda, A. N. Polischuk, D. van Leeuwen, and M. a Valvano, *Microbiology*, 2007, **153**, 2518–2529.

53. D. S. Boyle and W. D. Donachie, *J. Bacteriol.*, 1998, **180**, 6429–6432.

54. T. D. H. Bugg, D. Braddick, C. G. Dowson, and D. I. Roper, *Trends Biotechnol.*, 2011, **29**, 167–173.

55. O. O. Coker and P. Palittapongarnpim, *Afr J Microbiol Res.*, 2011, **5**, 2555–2565.

56. C. M. Apfel, B. Takács, M. Fountoulakis, M. Stieger, and W. Keck, *J. Bacteriol.*, 1999, **181**, 483–492.

57. R.-T. Guo, T.-P. Ko, A. P.-C. Chen, C.-J. Kuo, A. H.-J. Wang, and P.-H. Liang, *J. Biol. Chem.*, 2005, **280**, 20762–20774.

58. M. El Ghachi, A. Bouhss, H. Barreteau, T. Touzé, G. Auger, D. Blanot, and D. Mengin-Lecreulx, *J. Biol. Chem.*, 2006, **281**, 22761–22772.

59. R. Bernard, A. Guiseppi, M. Chippaux, M. Foglino, and F. Denizot, *J. Bacteriol.*, 2007, **189**, 8636–8642.

60. K. J. Stone and J. L. Strominger, *Proc. Natl. Acad. Sci. U. S. A.*, 1972, **69**, 1287–1289.

61. M. Suzuki, K. Yamada, M. Nagao, E. Aoki, M. Matsumoto, T. Hirayama, H. Yamamoto, R. Hiramatsu, S. Ichiyama, Y. Iinuma, T. Study, F. Lakes, and S. Korea, *Emerg. Infect. Dis.*, 2011, **17**, 10–13.

62. D. Martin, *CNN*, 2011, 1.

63. A. El Zoeiby, F. Sanschagrin, and R. C. Levesque, *Mol. Microbiol.*, 2003, **47**, 1–12.

64. T. G. Bernhardt, D. K. Struck, and R. Young, *J. Biol. Chem.*, 2001, **276**, 6093–7.

65. P. Cassidy and F. Kahan, *Biochemistry*, 1973, **12**, 1364–1374.

66. D. H. Kim, W. J. Lees, K. E. Kempsell, W. S. Lane, K. Duncan, and C. T. Walsh, *Biochemistry*, 1996, **35**, 4923–4928.

67. J. Molina-López, F. Sanschagrin, and R. C. Levesque, *Peptides*, 2006, **27**, 3115–3121.

68. H. Barreteau, A. Kovac, A. Boniface, M. Sova, S. Gobec, and D. Blanot, *FEMS Microbiol. Rev.*, 2008, **32**, 168–207.

69. T. D. Bugg and C. T. Walsh, *Nat. Prod. Rep.*, 1992, **9**, 199–215.

70. J. B. W. Howard John Rogers, Harold Robert Perkins, *Microbial cell walls and membranes*, Chapman and Hall, 1980.

71. A. J. Lloyd, P. E. Brandish, A. M. Gilbey, and T. D. H. Bugg, *J. Bacteriol.*, 2004, **186**, 1747–1757.

72. P. E. Brandish, K. I. Kimura, M. Inukai, R. Southgate, J. T. Lonsdale, and T. D. Bugg, *Antimicrob. Agents Chemother.*, 1996, **40**, 1640–4.

73. T. Tanino, B. Al-Dabbagh, D. Mengin-Lecreulx, A. Bouhss, H. Oyama, S. Ichikawa, and A. Matsuda, *J. Med. Chem.*, 2011, **54**, 8421–8439.

74. M. Winn, R. J. M. Goss, K. Kimura, and T. D. H. Bugg, *Nat. Prod. Rep.*, 2010, **27**, 279–304.

75. T. Mohammadi, A. Karczmarek, M. Crouvoisier, A. Bouhss, D. Mengin-Lecreulx, and T. den Blaauwen, *Mol. Microbiol.*, 2007, **65**, 1106–1121.

76. J. V Höltje, *Microbiol. Mol. Biol. Rev.*, 1998, **62**, 181–203.

77. T. Mohammadi, V. van Dam, R. Sijbrandi, T. Vernet, A. Zapun, A. Bouhss, M. Diepeveen-de Bruin, M. Nguyen-Distèche, B. de Kruijff, and E. Breukink, *EMBO J.*, 2011, **30**, 1425–1432.

78. M. Matsuhashi, in *Bacterial Cell Wall*, eds. J.-M. Ghuysen and R. Hakenbeck, Elsevier Science BV, Amsterdam, 1994, pp. 55–71.

79. A. L. Lovering, L. H. De Castro, D. Lim, and N. C. J. Strynadka, *Science*, 2007, **315**, 1402–1405.

80. G. Huber, *J. Antibiot.*, 1979, **5**, 135–153.

81. B. Ostash and S. Walker, *Nat. Prod. Rep.*, 2010, **27**, 1594–1617.

82. L. Maliničová, M. Piknová, P. Pristaš, and P. Javorský, in *Current Research, Technology and Education Topics in Applied Microbiology and Microbial Biotechnology. The Formatex Microbiology Book Series*, ed. A. Mendez-Vilas, Formatex Research Center, Badajoz, Vol. 1., 2010, pp. 463–472.

83. K. H. Schleifer and O. Kandler, *Bacteriol Rev.*, 1972, **36**, 407–477.

84. B. Glauner, J. V Höltje, and U. Schwarz, *J. Biol. Chem.*, 1988, **263**, 10088–10095.

85. W. Lee, M. a McDonough, L. Kotra, Z. H. Li, N. R. Silvaggi, Y. Takeda, J. a Kelly, and S. Mobashery, *Proc. Natl. Acad. Sci. U. S. A.*, 2001, **98**, 1427–1431.

86. M. I. Page, in *Adv. Phys. Org. Chem.*, Academic Press Inc., London, 23rd edn., 1987, pp. 166–250.

87. B. J. Hartman and A. Tomasz, *J. Bacteriol.*, 1984, **158**, 513–516.

88. D. M. Livermore and N. Woodford, *Trends Microbiol.*, 2006, **14**, 413–420.

89. S. Homi, K. Takechi, K. Tanidokoro, H. Sato, S. Takio, and H. Takano, *Plant Cell Physiol.*, 2009, **50**, 2047–2056.

90. J. A. Thanassi, S. L. Hartman-neumann, T. J. Dougherty, B. A. Dougherty, and M. J. Pucci, *Nucleic Acids Res.*, 2002, **30**, 3152–3162.

91. M. Ikeda, M. Wachi, H. K. Jung, F. Ishino, and M. Matsuhashi, *J. Bacteriol.*, 1991, **173**, 1021–1026.

92. W. A. Weppner and F. C. Neuhaus, *Biochim. Biophys. Acta*, 1979, **552**, 418–427.

93. A. Bouhss, D. Mengin-lecreulx, and B. Structurale, *Mol. Microbiol.*, 1999, **34**, 576–585.

94. A. Bouhss, M. Crouvoisier, D. Blanot, and D. Mengin-Lecreulx, *J. Biol. Chem.*, 2004, **279**, 29974–29980.

95. B. C. Chung, J. Zhao, R. a Gillespie, D.-Y. Kwon, Z. Guan, J. Hong, P. Zhou, and S.-Y. Lee, *Science (80-. ).*, 2013, **341**, 1012–1016.

96. M. S. Anderson, S. S. Eveland, and N. P. Price, *FEMS Microbiol. Lett.*, 2000, **191**, 169–175.

97. B. Al-Dabbagh, X. Henry, M. El Ghachi, G. Auger, D. Blanot, C. Parquet, D. Mengin-Lecreulx, and A. Bouhss, *Biochemistry*, 2008, **47**, 8919–8928.

98. M. G. Heydanek, W. G. Struve, and F. C. Neuhauss, *Biochemistry*, 1969, **8**, 1214–1221.

99. D. Pless and F. Neuhaus, *J. Biol. Chem.*, 1972, **248**, 1568–1576.

100. D. Mengin-Lecreulx, J. Ayala, A. Bouhss, J. van Heijenoort, C. Parquet, and H. Hara, *J. Bacteriol.*, 1998, **180**, 4406–4412.

101. M. Ikeda, M. Wachi, H. K. Jung, F. Ishino, and M. Matsuhashi, *Nucleic Acids Res.*, 1990, **18**, 4014.

102. W. G. Struve, R. K. Sinha, and F. C. Neuhaus, *Biochemistry*, 1966, **5**, 82–93.

103. C. A. Gentle, S. A. Harrison, and T. D. H. Bugg, *J. Chem. Soc., Perkin Trans. 1*, 1999, 1287–1294.

104. F. Isono and M. Inukai, *Antimicrob. Agents Chemother.*, 1991, **35**, 234–236.

105. M. Inukai, F. Isono, and A. Takatsuki, *Antimicrob. Agents Chemother.*, 1993, **37**, 980–983.

106. A. Heifetz, R. W. Keenan, and A. D. Elbein, *Biochemistry*, 1979, **18**, 2186–2192.

107. J. . Ward, *FEBS lett.*, 1977, **78**, 151–154.

108. A. G. Myers, D. Y. Gin, and D. H. Rogers, *J. Am. Chem. Soc.*, 1994, **116**, 4697–4718.

109. K. Isono, M. Uramoto, H. Kusakabe, K. Kimura, K. Izaki, C. Nelson, and J. McCloskey, *J. Antibiot.*, 1985, **38**, 1617–1621.

110. K. Kimura, N. Miyata, G. Kawanishi, Y. Kamio, K. Izaki, and K. Isono, *Agric. Biol. Chem*, 1989, **53**, 1811–1815.

111. P. E. Brandish, PhD Thesis, University of Southampton, 1995.

112. L. Cheng, W. Chen, L. Zhai, D. Xu, T. Huang, S. Lin, X. Zhou, and Z. Deng, *Mol. Biosyst.*, 2011, **7**, 920–7.

113. L. A. McDonald, L. R. Barbieri, G. T. Carter, E. Lenoy, J. Lotvin, P. J. Petersen, M. M. Siegel, G. Singh, and R. T. Williamson, *J. Chem. Soc. Chem. Commun.*, 2002, **124**, 10260–10261.

114. Y. Zheng, D. K. Struck, T. G. Bernhardt, and R. Young, *Gen. Soc. Am.*, 2008, **180**, 1459–1466.

115. C. A. Hutchison, S. Phillips, M. H. Edgell, S. Gillam, P. Jahnke, and M. Smith, *J. Biol. Chem.*, 1978, **253**, 6551–6560.

116. F. Sanger, A. R. Coulson, T. Friedman, B. G. Barrell, J. C. Fiddes, C. A. Hutchinson III, P. M. Slocombe, and M. Smith, *J. Mol. Biol.*, 1978, **276**, 236–247.

117. K. D. Young, R. J. Anderson, and R. J. Hafner, *J. Bacteriol.*, 1989, **171**, 4334–4341.

118. U. Bläsi, R. Young, and W. Lubitz, *J. Virol.*, 1988, **62**, 4362–4364.

119. A. Witte, G. Schrot, and P. Scho, *Mol. Biol.*, 1997, **26**, 337–346.

120. T. G. Bernhardt, W. D. Roof, and R. Young, *Proc. Natl. Acad. Sci. U. S. A.*, 2000, **97**, 4297–4302.

121. D. E. Bradley, C. A. Dewar, and D. Roberston, *J. Gen. Virol.*, 1969, **74**, 113–121.

122. W. D. Roof and R. Young, *J. Bacteriol.*, 1993, **175**, 3909–3912.

123. G. Halfmann and W. Lubitz, *J. Bacteriol.*, 1986, **166**, 683–685.

124. I.-N. Wang, D. L. Smith, and R. Young, *Annu. Rev. Microbiol.*, 2000, **54**, 799–825.

125. S. Mendel, J. M. Holbourn, J. a Schouten, and T. D. H. Bugg, *Microbiology*, 2006, **152**, 2959–2967.

126. D. Maratea, K. Young, and R. Young, *Gene*, 1985, **40**, 39–46.

127. S. Hottenrott, T. Schumann, A. Pluckthun, G. Fischer, and J. Rahfeld, *J. Biol. Chem.*, 1997, **272**, 15697–15701.

128. B. Bukau, E. Deuerling, C. Pfund, E. A. Craig, H. H. Str, and D.- Freiburg, *Cell Press*, 2000, **101**, 119–122.

129. S. Wagner, L. Baars, a J. Ytterberg, A. Klussmeier, C. S. Wagner, O. Nord, P.-A. Nygren, K. J. van Wijk, and J.-W. de Gier, *Mol. Cell. Proteomics*, 2007, **6**, 1527–1550.

130. K.-Y. Han, J.-A. Song, K.-Y. Ahn, J.-S. Park, H.-S. Seo, and J. Lee, *Protein Eng. Des. Sel.*, 2007, **20**, 543–549.

131. K. D. Young, R. J. Anderson, and R. J. Hafner, *J. Bacteriol.*, 1989, **171**, 4334–4341.

132. K. Buckley and M. Hayashi, *Mol. Gen. Genet.*, 1986, **204**, 120–125.

133. S. Tanaka and W. M. Clemons, *Mol. Microbiol.*, 2012, **85**, 975–85.

134. M. P. Waller, A. Robertazzi, J. A. Platts, D. E. Hibbs, and P. A. Williams, *J. Comput. Chem.*, 2006, **27**, 491–504.

135. B. W. Gung, X. Xue, and H. J. Reich, *J. Org. Chem.*, 2005, **70**, 3641–4.

136. G. B. Mcgaughey, M. Gagne, and A. K. Rappe, *J. Biol. Chem.*, 1998, **273**, 15458–15463.

137. C. Bissantz, B. Kuhn, and M. Stahl, *J. Med. Chem.*, 2010, **53**, 5061–5084.

138. E. V. Anslyn and D. Dougherty, in *Modern Physical Organic Chemistry*, University Science Books, 2006, pp. 145–207.

139. S. E. Thompson and D. B. Smithrud, *J. Am. Chem. Soc.*, 2002, **124**, 442–449.

140. J. Ma and D. A. Dougherty, *Chem. Rev.*, 1997, **97**, 1303–1324.

141. D. Dougherty, *Science (80-. ).*, 1996, **271**, 163–168.

142. W. Jing, A. R. Demcoe, and H. J. Vogel, *J. Bacteriol.*, 2003, **185**, 4938–4947.

143. S. K. Burley and G. A. Petsko, *FEBS lett.*, 1986, **1986**, 139–143.

144. Y. Zheng, D. K. Struck, C. a Dankenbring, and R. Young, *Microbiology*, 2008, **154**, 1710–1718.

145. S. Yu, W. Peng, W. Si, L. Yin, S. Liu, H. Liu, H. Zhao, C. Wang, Y. Chang, and Y. Lin, *Virol. J.*, 2011, **8**, 206–211.

146. S. Yohannan, S. Faham, D. Yang, J. P. Whitelegge, and J. U. Bowie, *Proc. Natl. Acad. Sci. U. S. A.*, 2004, **101**, 959–963.

147. F. S. Cordes, J. N. Bright, and M. S. P. Sansom, *J. Mol. Biol.*, 2002, **323**, 951–960.

148. A. Cherkasov, K. Hilpert, C. D. Fjell, M. Waldbrook, S. C. Mullaly, R. Volkmer, and R. E. W. Hancock, *ACS Chem. Biol.*, 2008, **4**, 65–74.

149. D. I. Chan, E. J. Prenner, and H. J. Vogel, *Biochim. Biophys. Acta*, 2006, **1758**, 1184–1202.

150. R. E. W. Hancock, K. Hilpert, A. Cherkasov, and C. Fjell, 2013, 1–22.

151. T. J. Falla and R. E. W. Hancock, *Antimicrob. Agents Chemother.*, 1997, **41**, 771–775.

152. M. E. Selsted, M. J. Novotnytll, W. L. Morris, Y. Tang, W. Smith, and J. S. Cullor, 1991, 4292–4295.

153. D. Oh, S. Y. Shin, S. Lee, J. H. Kang, S. D. Kim, P. D. Ryu, K. S. Hahm, and Y. Kim, *Biochemistry*, 2000, **39**, 11855–11864.

154. C. Lawyer, S. Pai, M. Watabe, P. Borgia, T. Mashimo, L. Eagleton, and K. Watabe, *FEBS lett.*, 1996, **390**, 95–98.

155. M. B. Strøm, O. Rekdal, W. Stensen, and J. S. Svendsen, *J. Pept. Res.*, 2001, **57**, 127–139.

156. A. Rozek, J.-P. S. Powers, C. L. Friedrich, and R. E. W. Hancock, *Biochemistry*, 2003, **42**, 14130–14138.

157. P. M. Hwang, N. Zhou, X. Shan, C. H. Arrowsmith, and H. J. Vogel, *Biochemistry*, 1998, **37**, 4288–4298.

158. P. van Hofsten, I. Faye, K. Kockum, J. Y. Lee, K. G. Xanthopoulos, I. a Boman, H. G. Boman, A. Engström, D. Andreu, and R. B. Merrifield, *Proc. Natl. Acad. Sci. U. S. A.*, 1985, **82**, 2240–2243.

159. W. E. Borrias, M. Hagenaar, R. Van Den Brekel, C. Kühlemeijer, and P. J. Weisbeek, *J. Virol.*, 1979, **31**, 288–298.

160. R. A. Bernal, S. Hafenstein, N. H. Olson, V. D. Bowman, P. R. Chipman, T. S. Baker, B. a. Fane, and M. G. Rossmann, *J. Mol. Biol.*, 2003, **325**, 11–24.

161. M. J. Betts and R. B. Russell, in *Bioinformatics for Geneticists*, eds. M. R. Barnes and I. C. Gray, John Wiley & Sons, Ltd., Essex, 2nd edn., 2003, vol. 4, pp. 289–316.

162. W. Chan and P. White, *Fmoc Solid Phase Peptide Synthesis; A Practical Approach*, Oxford University Press, 2000.

163. J. Jones, *Amino Acid and Peptide Synthesis*, Oxford University Press, Oxford, 2nd edn., 2002.

164. M. Bodanszky, *Peptide Chemistry; A Practical Approach*, Springer-Verlag, Princeton, NJ, 1993.

165. R. C. Sheppared and B. J. Williams, *J. Chem. Soc. Chem. Commun.*, 1982, **587**, 587.

166. R. B. Merrifield, *J. Am. Chem. Soc.*, 1963, **85**, 2149–2154.

167. F. Albericio and F. G. Martin, *Chem. Today*, 2008, **26**, 29–34.

168. F. García-Martín, N. Bayó-Puxan, L. J. Cruz, J. C. Bohling, and F. Albericio, *QSAR Comb. Sci.*, 2007, **26**, 1027–1035.

169. N. K. Terrett, in *Comb. Chem.*, Oxford University Press, Oxford, 1998, pp. 9–11.

170. S. Wang, *J. Org. Chem.*, 1975, **40**, 1235–1239.

171. D. S. King, C. G. Fields, and G. B. Fields, *Int. J. Pept. Protein Res.*, 1990, **36**, 255–266.

172. A. Biosystems, 1998, 1–12.

173. P. Teesdale-Spittle, *Victoria Univ. Wellingt.*, 2001.

174. Novabiochem, in *Peptide Synthesis*, Merck Chemicals Ltd, Nottingham, 2010, pp. 3.1–3.46.

175. M. Goodman, A. Felix, L. Moroder, and C. Toniolo, *J. Pept. Sci.*, 2003, **9**, 607–611.

176. S.-Y. Han and Y.-A. Kim, *Tetrahedron*, 2004, **60**, 2447–2467.

177. AAPPTec-LLC, *AAPPTec*, 2009. http://www.wangresin.com/#1

178. Novabiochem, *The role of HOBt in coupling reactions*, 2006.

179. R. Subirós-Funosas, R. Prohens, R. Barbas, A. El-Faham, and F. Albericio, *Chem. Eur. J.*, 2009, **15**, 9394–9403.

180. Novabiochem, *Non-explosive replacement for HOBt*, 2009.

181. S. Wang, J. Tam, B. Wang, and R. Merripield, *Int. J. Pept. Protein Res.*, 1981, **18**, 459–467.

182. A. Isidro-Llobet, M. Alvarez, and F. Albericio, *Chem. Rev.*, 2009, **109**, 2455–2504.

183. K. Wahlström and A. Undén, *Tetrahedron Lett.*, 2009, **50**, 2976–2978.

184. R. E. Reid and Patrick L Frachini, *Peptide and Protein Drug Analysis*, Marcel Dekker, Inc., New York, Vol. 101., 2000.

185. S. Budavari, Ed., in *The Merck Index*, Merck Research Laboratries, New Jersey, 12th edn.

186. B. Neises and W. Steglich, *Angew. Chem. Int.*, 1978, **553**, 12–14.

187. A. Hassner and V. Alexanian, *Tetrahedron Lett.*, 1978, **46**, 4475–4478.

188. S. Xu, I. Held, B. Kempf, H. Mayr, W. Steglich, and H. Zipse, *Chem. Eur. J.*, 2005, **11**, 4751–4757.

189. M. K. Dhaon, R. K. Olsen, and K. Ramasamy, *J. Org. Chem.*, 1982, **47**, 1962–1965.

190. A. I. Vogel, B. S. Furniss, A. J. Hannaford, V. Rogers, P. W. G. Smith, and A. R. Tatchell, *Vogel's Textbook of Practical Organic Chemistry, including qualitative organic analysis*, English Language Book Society/Longman, Longman, London, 4th edn., 1978.

191. A. Burrows, J. Holman, A. Parsons, G. Pilling, and G. Price, in *Chemistry*$^3$ *Introducing inorganic, organic and physical chemistry*, Oxford University Press, Oxford, 2009, pp. 1095–1131.

192. J. March and M. B. Smith, *Advanced Organic Chemistry: Reactions, Mechanisms, and Structure*, John Wiley & Sons Ltd., New York, 5th edn., 2001.

193. AAPPTec-LLC, 2009, 1–2. http://www.aapptec.com/broch/Coupling%20Reagents.pdf

194. K. ó Proinsias, PhD Thesis, 2010, unpublished

195. R. Santini, M. C. Griffith, and M. Qi, *Tetrahedron Lett.*, 1998, **39**, 8951–8954.

196. C. Hood, G. Fuentes, H. Patel, K. Page, M. Menakuru, and J. H. Park, *Am. Biotechnol Lab.*, 2008, **26**, 22–25.

197. M. Stawikowski and G. B. Fields, in *Curr. Protoc Protein Sci.*, ed. J. E. Coliga, John Wiley & Sons, Inc., Port St. Lucie, Florida, 2012, pp. 18.1.1–18.1.13.

198. R. Valerio, A. Bray, and N. Maeji, *Int. J. Pept. Protein Res.*, 1994, **44**, 158–165.

199. W. A. Weppner and F. C. Neuhaus, *J. Biol. Chem.*, 1977, **252**, 2296–2303.

200. W. A. Weppner and F. C. Neuhaus, *J. Biol. Chem.*, 1978, **253**, 472–478.

201. J. P. Reeves, E. Shechter, R. Weil, and H. R. Kaback, *PNAS*, 1973, **70**, 2722–2726.

202. W. D. Bieri VG, *Biochim. Biophys. Acta*, 1976, **443**, 198–205.

203. B. Flouret, D. Mengin-Lecreulx, and J. van Heijenoort, *Anal. Biochem.*, 1981, **114**, 59–63.

204. W. Wijsman and H. J. W. Wijsman, *J. Bacteriol.*, 1973, **113**, 96–104.

205. J. Toedt, D. Koza, and K. Van Cleef-Toedt, in *Chemical Composition Of Everyday Products*, Greenwood Publishing Group, Wesport, 2005, pp. 1–24.

206. D. Douroumis and A. Fahr, in *Drug Delivery Strategies for Poorly Water-Soluble Drugs*, eds. D. Douroumis and A. Fahr, John Wiley & Sons Ltd., New Delhi, 2013, pp. 49–52.

207. H. Tanaka, R. Oiwa, S. Matsukura, and S. Omura, *Biochem. Biophys. Res. Commun.*, 1979, **86**, 902–908.

208. T. G. Schmidt and A. Skerra, *Nat. Protoc.*, 2007, **2**, 1528 – 1535.

209. L. Dumon-Seignovert, G. Cariot, and L. Vuillard, *Protein Expr. Purif.*, 2004, **37**, 203–6.

210. *R. Soc. Chem.*, 2008, 1. http://www.rsc.org/chemsoc/timeline/pages/1884.html

211. Y. Ma, D. Münch, T. Schneider, H.-G. Sahl, A. Bouhss, U. Ghoshdastider, J. Wang, V. Dötsch, X. Wang, and F. Bernhard, *J. Biol. Chem.*, 2011, **286**, 38844–38453.

212. J. Kaur and A. K. Bachhawat, *Anal. Biochem.*, 2009, **384**, 348–349.

213. L. Vera-Cabrera, A. Rendon, M. Diaz-Rodriguez, V. Handzel, and A. Laszlo, *Clin. Diagn. Lab Immunol.*, 1999, **6**, 686–9.

214. M. Uritani and A. Hamada, *Biochem. Educ.*, 1999, **27**, 169–170.

215. C. Moore, *Introduction to Western Blotting Western Blotting*, AbD serotec, 2009.

216. T. Tip, *Chemiluminescent Western blotting technical guide and protocols*, 2013, vol. 0747.

217. J. M. Berg, J. L. Tymoczko, and L. Stryer., in *Biochemistry*, W.H Freeman, New York, 5th edn., 2002.

218. W. Winn, S. Allen, W. Janda, E. Koneman, G. Procop, P. Schreckenberg, and G. Woods, in *Koneman's Color Atlas and Textbook of Diagnostic*

*Microbiology*, ed. E. W. Koneman, Lippincott Williams & Wilkins, Baltimore, 5th edn., 2006, p. 945.

219. A. Bauer, W. Kirby, J. Sherris, and M. Turck, *Am J Clin Pathol.*, 1966, **45**.

220. H. Ericsson and J. C. Sherris, *ACTA Pathol. Microb.*, 1971, **217**, 1–90.

221. P. F. Wheat, *J. Antimicrob. Chemother.*, 2001, **48**, 1–4.

222. J. M. Andrews, *J. Antimicrob. Chemother.*, 2001, **48**, 5–16.

223. E. J. Goldstein, C. E. Cherubin, and M. Shulman, *Antimicrob. Agents Chemother.*, 1983, **23**, 42–45.

224. I. Wiegand, K. Hilpert, and R. E. W. Hancock, *Nat. Protoc.*, 2008, **3**, 163–175.

225. B. Loh, C. Grant, and R. E. Hancock, *Antimicrob. Agents Chemother.*, 1984, **26**, 546–551.

226. S. L. Helgerson and W. A. Cramer, *Biochemistry*, 1977, **16**, 4109–4117.

227. A. Bellemare, N. Vernoux, S. Morin, S. M. Gagné, and Y. Bourbonnais, *BMC Microbiol.*, 2010, **10**, 253.

228. H. Trauble and P. Overath, *Biochim. Biophys. Acta*, 1973, **307**, 491–512.

229. I. M. Helander and T. Mattila-Sandholm, *J. Appl. Microbiol.*, 2000, **88**, 213–219.

230. T. Tsuchido, I. Aoki, and M. Takano, *J. Gen. Microbiol.*, 1989, **135**, 1941–1947.

231. H. Nikaido, in *Escherichia coli and Salmonella typhimurium*, ed. F. C. Neidhardt, ASM Press, Washington, DC, 1st edn., 1996, pp. 29–47.

232. M. Vaara and T. Vaara, *Antimicrob. Agents Chemother.*, 1983, **24**, 114–122.

233. L. Leive, *Ann. N. Y. Acad. Sci.*, 1974, 109–129.

234. C. Löw, C. Jegerschöld, M. Kovermann, P. Moberg, and P. Nordlund, *PLoS One*, 2012, **7**, e38244.

235. H. Jenssen, P. Hamill, and R. E. W. Hancock, *Clin. Microbiol Rev.*, 2006, **19**, 491–511.

236. J. J. Bronson and J. F. Barrett, *Curr. Med. Chem.*, 2001, **8**, 1775–1793.

237. A. Malabarba and R. Ciabatti, *Curr. Med. Chem.*, 2001, **8**, 1759–1773.

238. P. E. Brandish, M. K. Burnham, J. T. Lonsdale, R. Southgate, M. Inukai, and T. D. H. Bugg, *J. Biol. Chem.*, 1996, **271**, 7609–7614.

239. C. Dini, P. Collette, N. Drochon, J. C. Guillot, G. Lemoine, P. Mauvais, and J. Aszodi, *Bioorg. Med. Chem. Lett.*, 2000, **10**, 1839–1843.

240. C. Dini, S. Didier-Laurent, N. Drochon, S. Feteanu, J. C. Guillot, F. Monti, E. Uridat, J. Zhang, and J. Aszodi, *Bioorg. Med. Chem. Lett.*, 2002, **12**, 1209–1213.

241. C. Lemoine, J. Blais, N. G. Vernier, C. G. Boojamra, K. A. Stein, A. Magon, S. Chamberland, S. J. Hecker, and V. J. Lee, *Bioorg. Med. Chem. Lett.*, 2003, **13**, 3305–3309.

242. S. RP and K. GD, *Biochemistry*, 1994, **33**, 8505–8514.

243. J. Morrison and C. T. Walsh, *Adv. Enzym. Relat. Area Mol. Biol.*, 1988, **61**, 201–301.

244. G. Tripathi, in *Cellular And Biochemical Science*, ed. G. Tripathi, International Publishing House Pvt. Ltd, New Delhi, 2010, pp. 125–149.

245. P. J. Kocieński, in *Protecting Groups*, Thieme, Stuttgart, 3rd edn., 2005, pp. 120–132.

246. J. Gelas and D. Horton, *Carbohydr. Res.*, 1975, **45**, 181–195.

247. J. Gelas, *Adv. Carbohydr. Chem. Biochem.*, 1981, **39**, 71–156.

248. N. J. Leonard and K. L. Carraway, *J. Heterocycl. Chem.*, 1966, **3**, 485–489.

249. A. E. Trunkfield, PhD Thesis,University of Warwick, 2008.

250. F. M. Ibatullin and S. I. Selivanov, *Tetrahedron Lett.*, 2009, **50**, 6351–6354.

251. J. Li and Y. Sha, *Molecules*, 2008, **13**, 1111–1119.

252. M. Garrido, M. L. López, and A. M. Sanz, *J. Heterocycl. Chem.*, 1980, **17**, 1943–5193.

253. Junzo Otera and J. Nishikido, *Esterification: Methods, Reactions, and Applications*, John Wiley & Sons Ltd., Darmstadt, Germany, 2nd edn., 2010.

254. F. Olang, PhD Thesis, Ball State University, 1995.

255. A. M. Grubb, S. Hasan, A. a. Kiryanov, P. Sampson, and A. J. Seed, *Liq. Cryst.*, 2009, **36**, 443–453.

256. N. R. McIntyre, E. W. Lowe, J. L. Belof, M. Ivkovic, J. Shafer, B. Space, and D. J. Merkler, *J. Am. Chem. Soc.*, 2010, **132**, 16393–16402.

257. A. El-Faham and F. Albericio, *ACS Chem. Rev.*, 2011, A–.

258. M. Masman, A. Rodriguez, L. Svetaz, S. Zacchino, C. Somiai, I. Csizmadia, B. Penke, and R. Enriz, *Bioorg. Med. Chem. Lett.*, 2006, **14**, 7604–7614.

259. R. B. Merrifield, *J. Am. Chem. Soc.*, 1963, **85**, 2149–2154.

260. J. Perez de Vega, T. Garcia-Lopes, L. Zaccaro, M. Royo, F. Albericio, A. Fernandez-Carvajal, A. Ferrer-Montiel, and R. Gonzalez-Muniz, *Molecules*, 2010, **15**, 4924–4933.

261. S. De Luca, S. Ulhaq, M. J. Dixon, J. Essex, and M. Bradley, *Tetrahedron Lett.*, 2003, **44**, 3195–3197.

262. *Chem. Books*, 2011.

263. Y. J. Pu, R. K. Vaid, S. K. Boini, R. W. Towsley, C. W. Doecke, and D. Mitchell, *Org. Process Res. Dev.*, 2009, **13**, 310–314.

264. J. M. Walker, *Antimicrobial Peptides: Methods and Protocols*, Humana Press, Italy, 618th edn., 2010.

265. J. Tomasz, *Nucleic Acid Chemistry*, John Wiley and Sons, New York, Vol. 2., 1978.

266. ChemicalBook, *Chem. Books*, 2007, 1.

267. Bio-rad, *Bio-Rad Bull. 6040A*, 2013, 1–47.

# Appendix 1: Fluorescence Emission Spectrum of MraY and MraY mutants in the presence of RWXXW analogues

## A1.1 Activity of $H_2N$-GW-Oct [6] against *E. coli* MraY

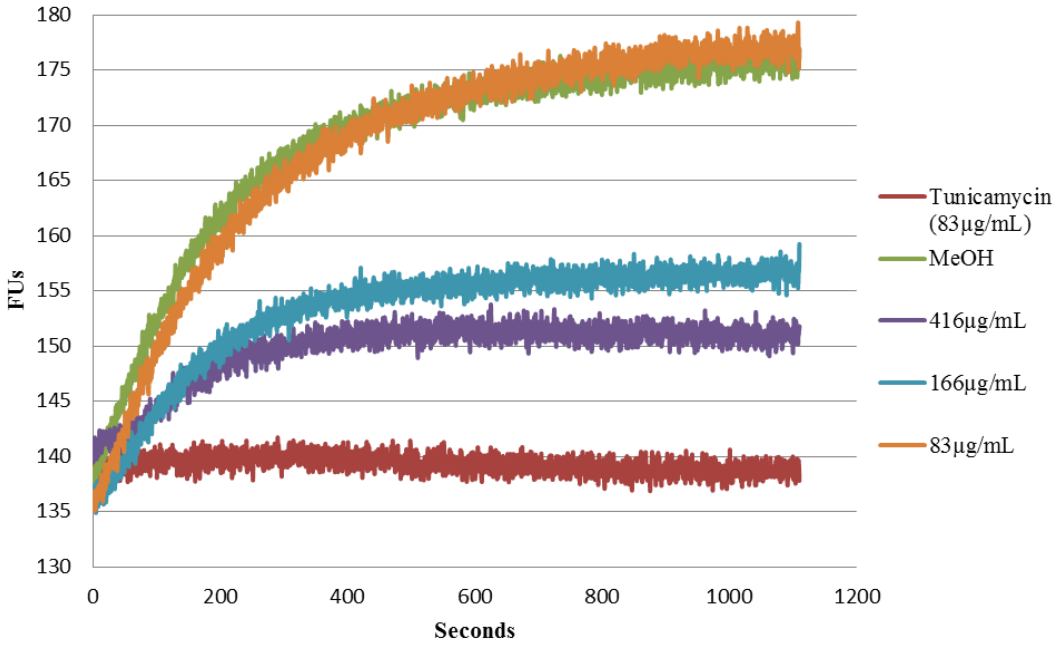


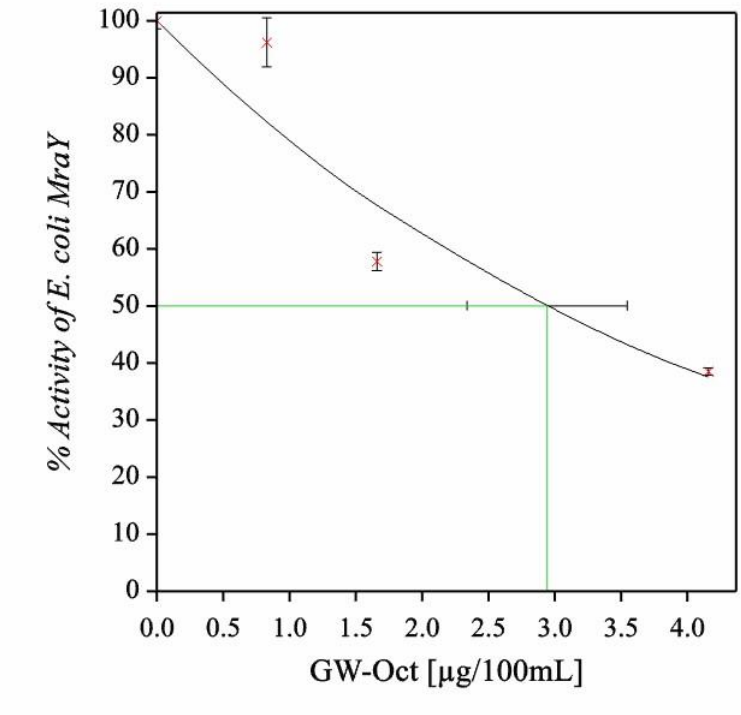

## A1.2 Activity of $H_2N$-GW-Oct [6] against *B. subtilis* MraY

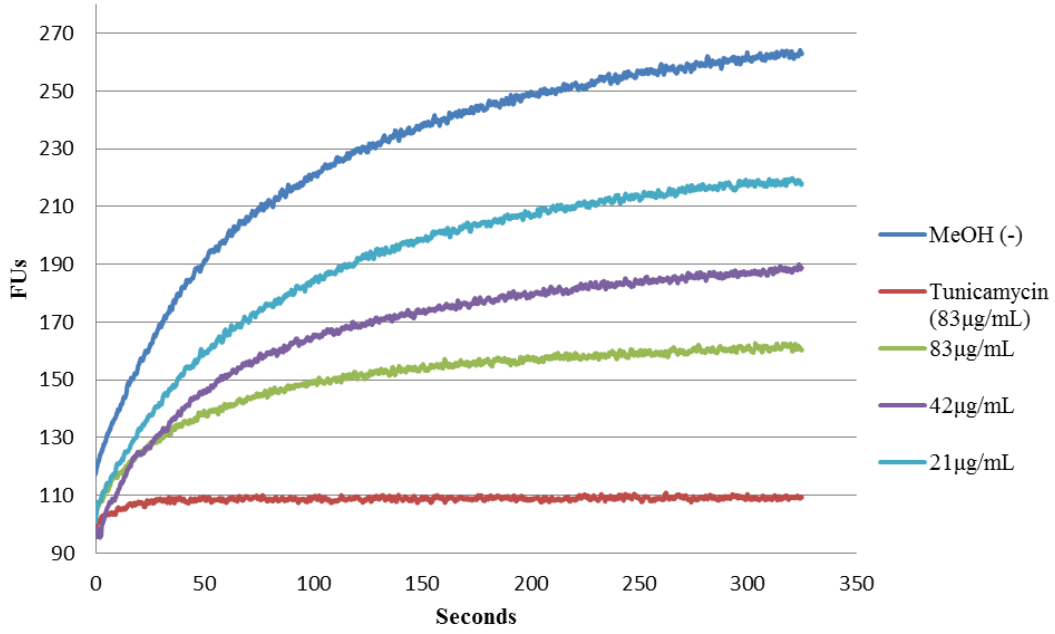


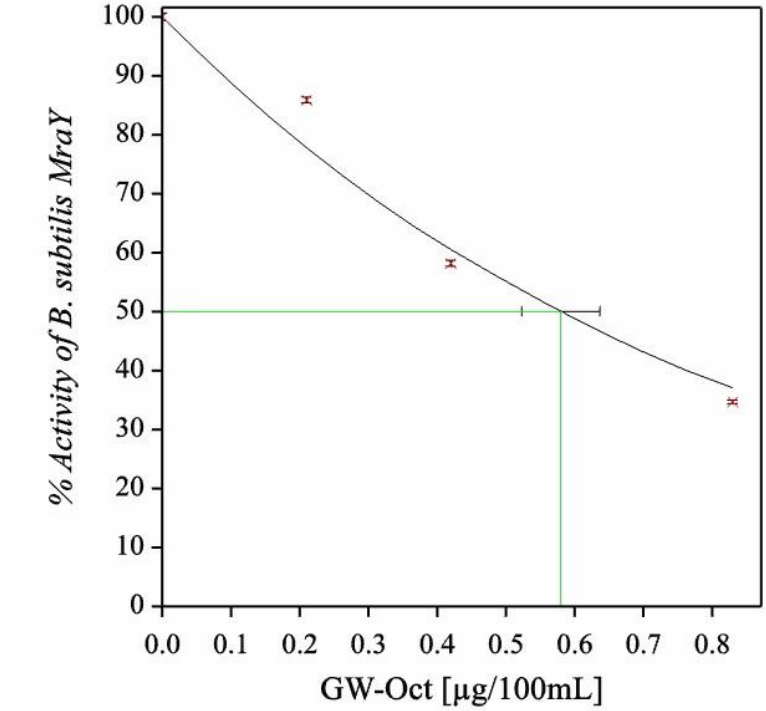

## A1.3 Activity of $H_2N$-GW-Oct [6] against *P. aeruginosa* MraY

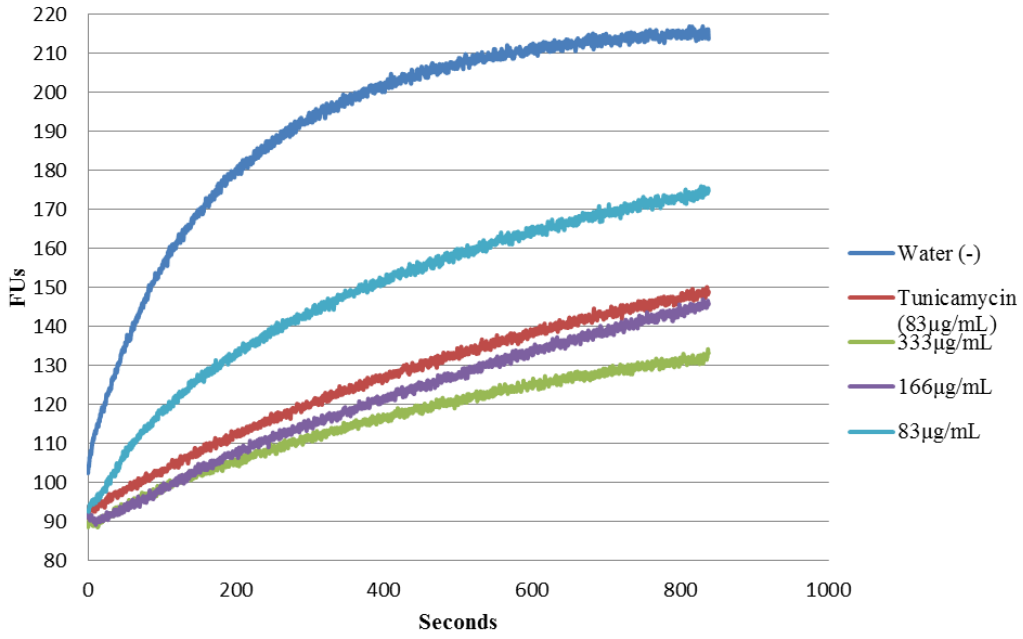


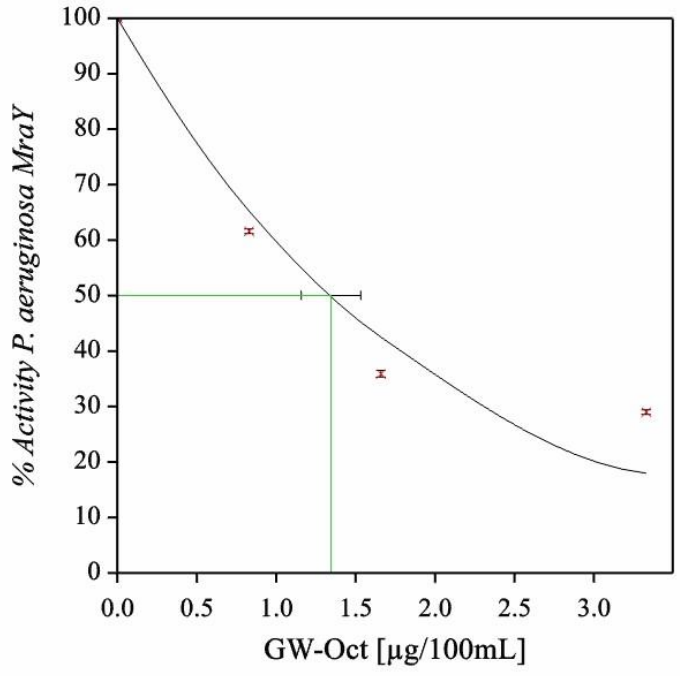

## A1.4 Activity of $H_2N$-GW-Oct [6] against *S. aureus* MraY

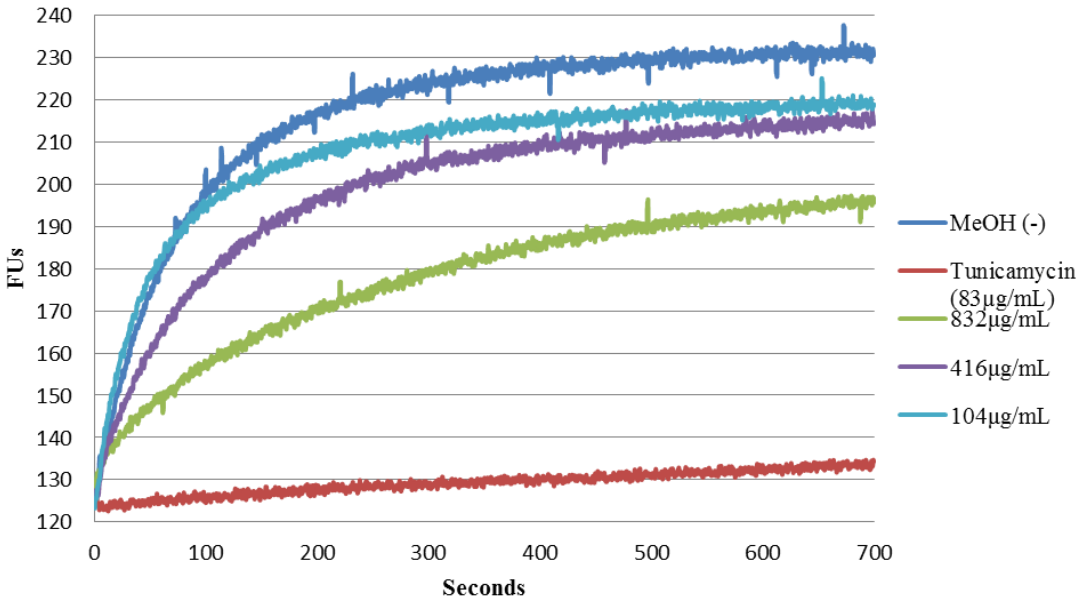


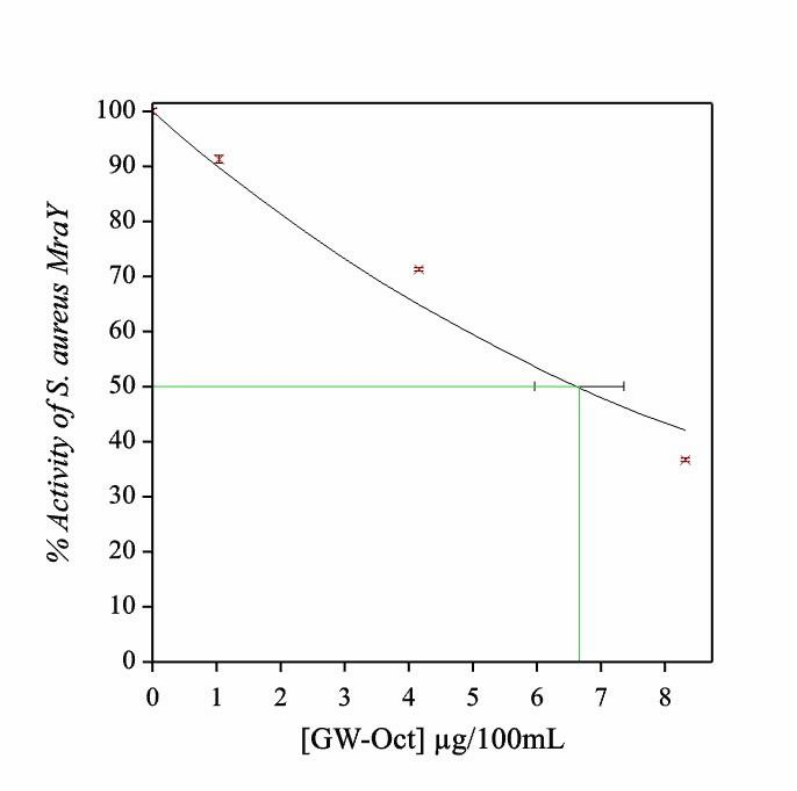

## A1.5 Activity of $H_2N$-GW-Oct [6] against *M. flavus* MraY

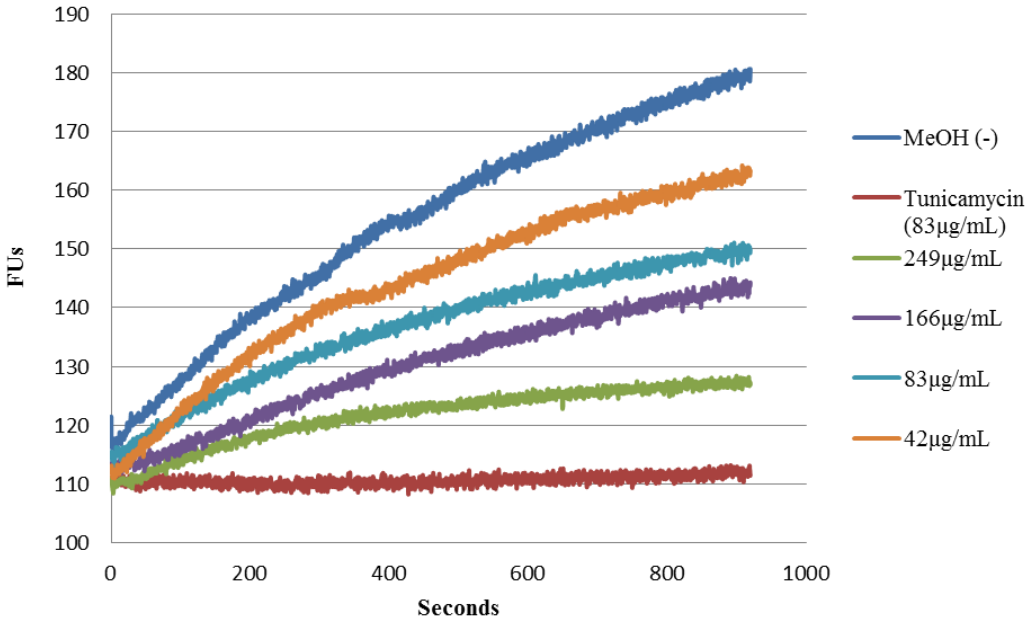


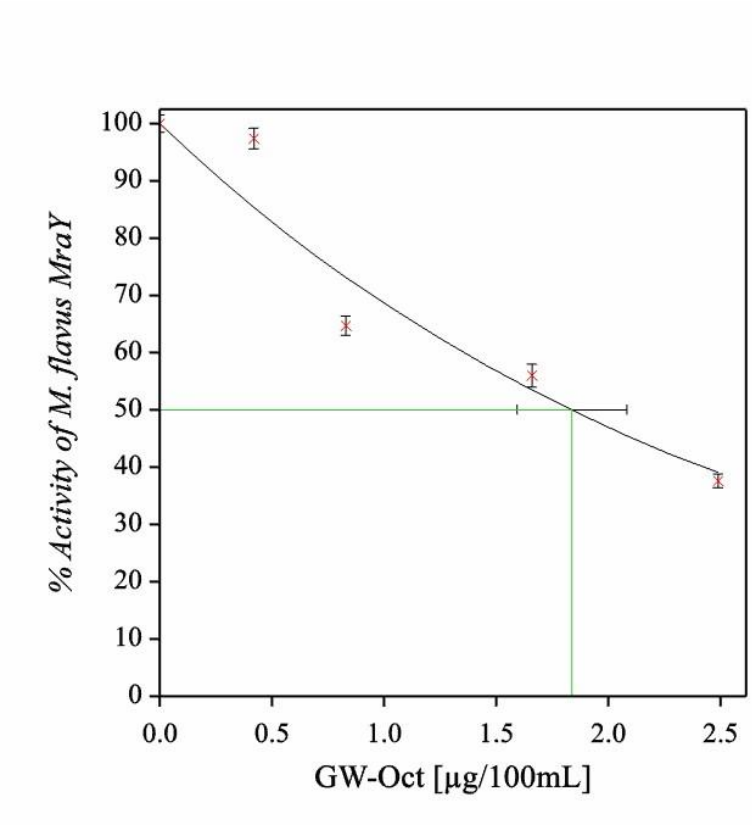

## A1.6 Activity of $H_2N$-GW-OMe [4] against *B. subtilis* MraY

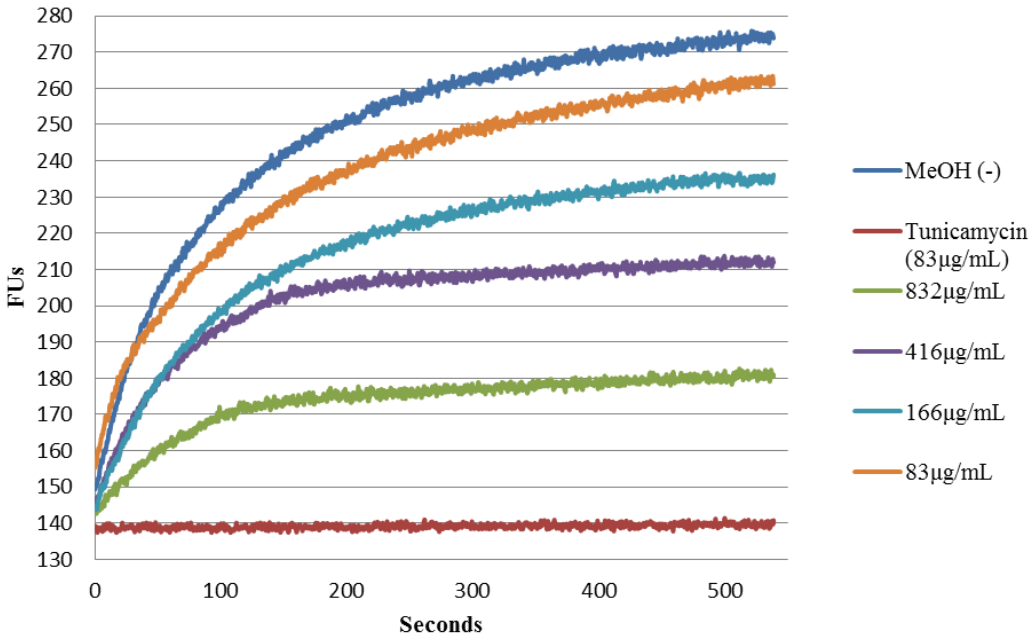


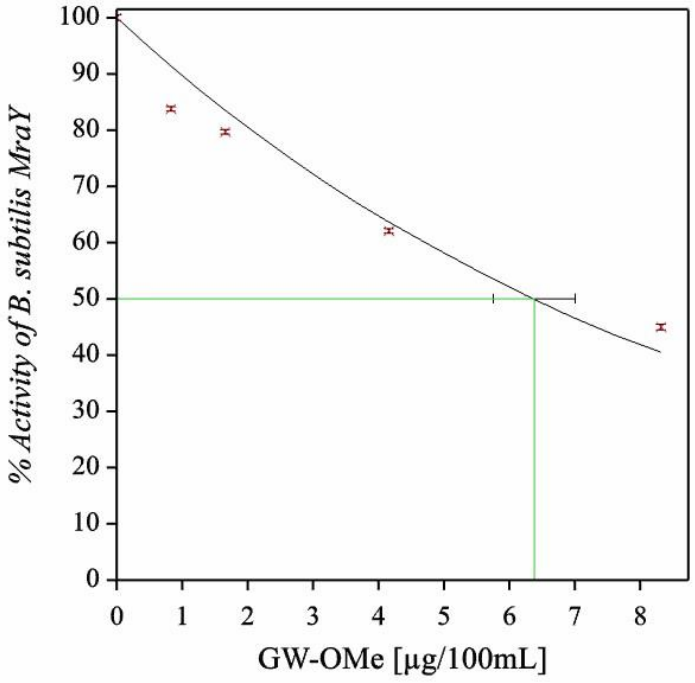

## A1.7 Activity of RWGLW [10] against *E. coli* MraY

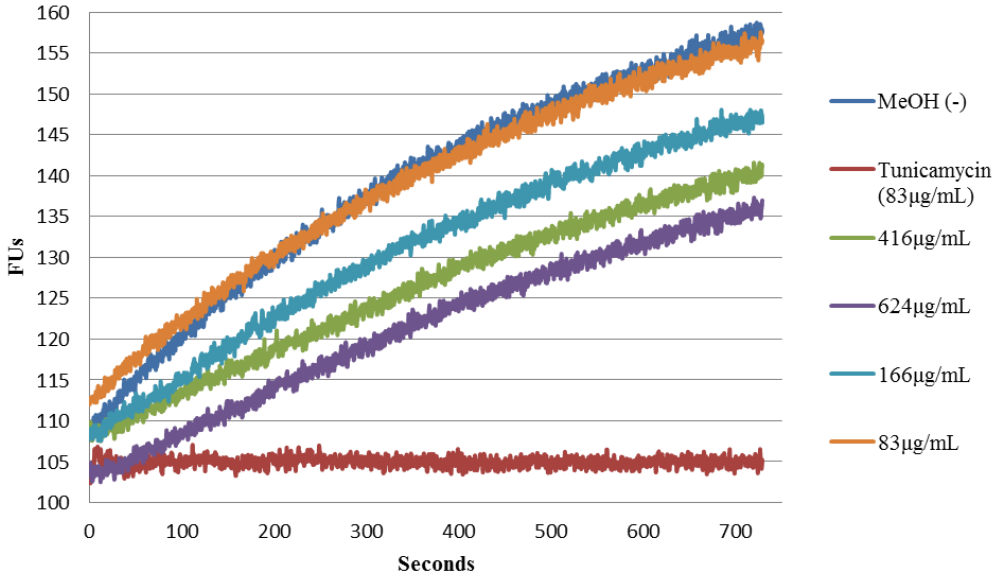


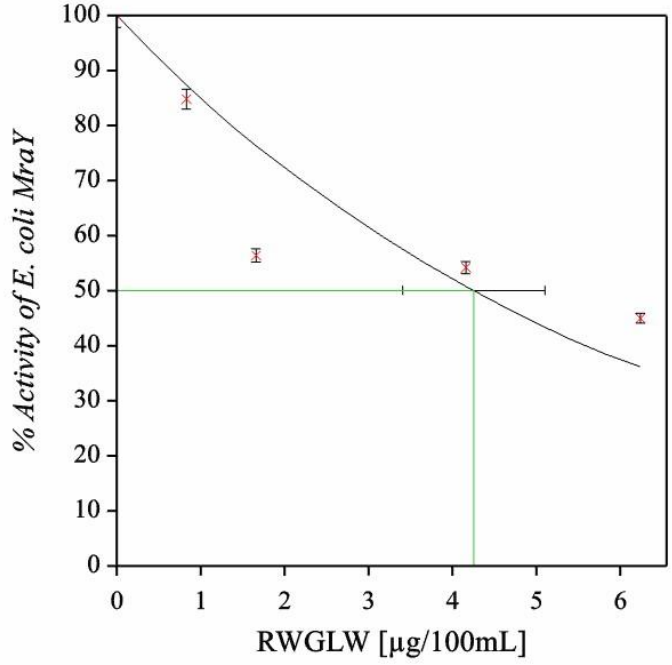

## A1.8 Activity of RWGLW [10] against *S. aureus* MraY

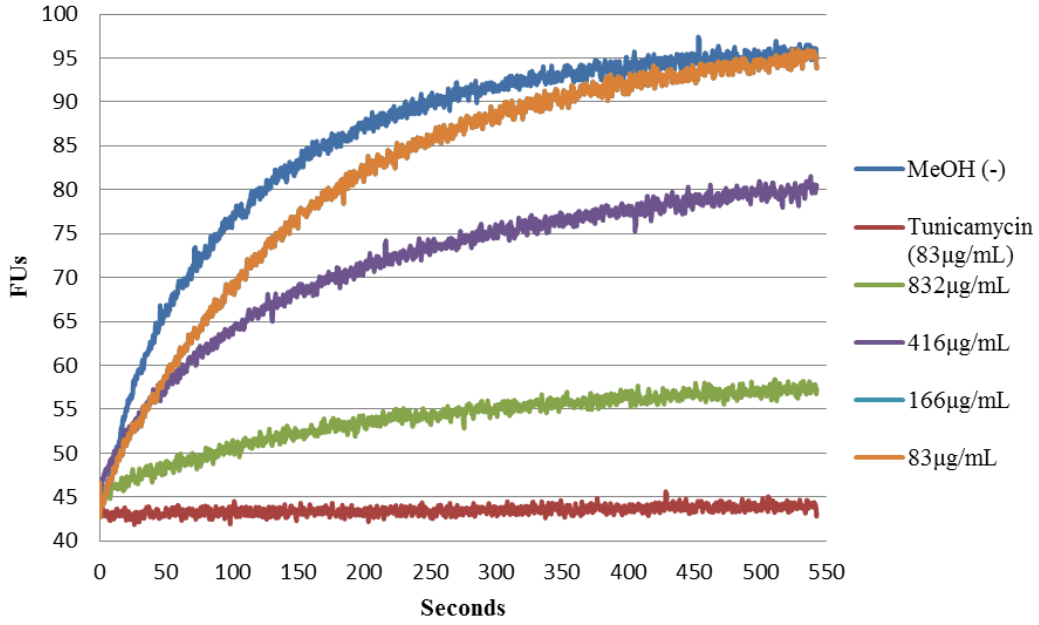


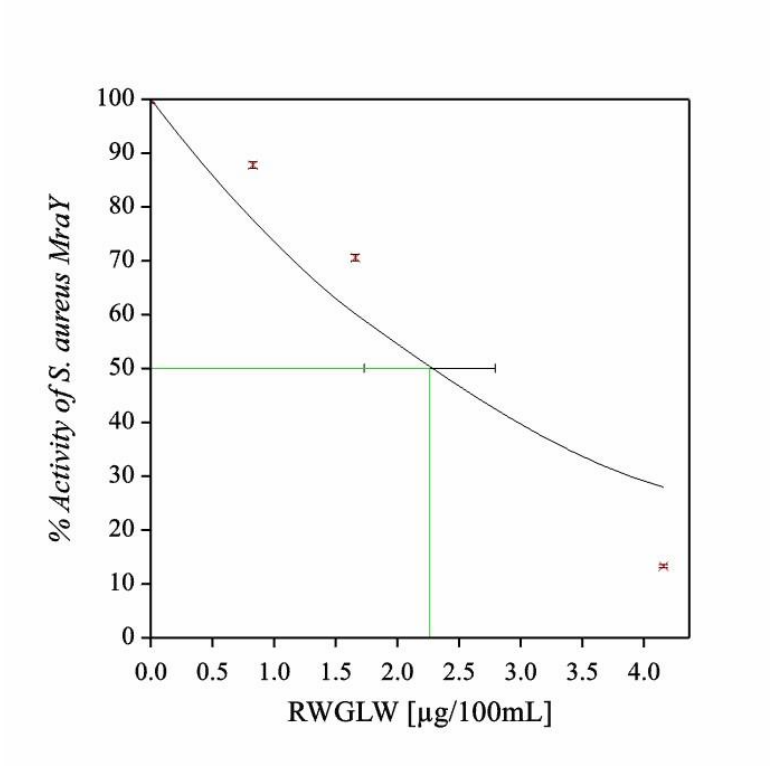

## A1.9 Activity of RWGLW [10] against *B. subtilis* MraY

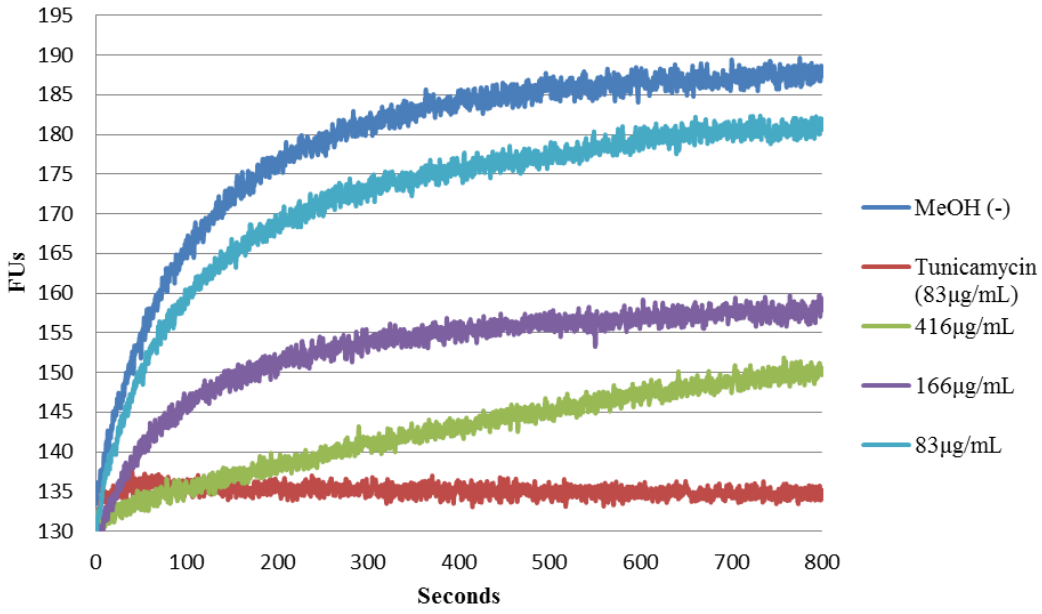


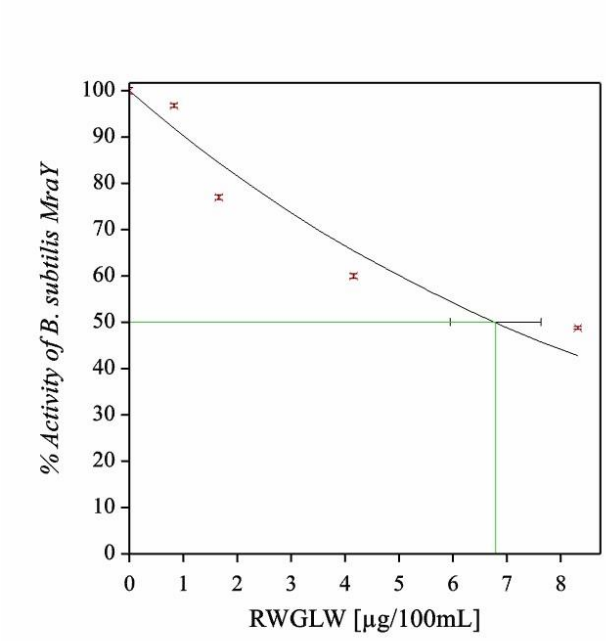

## A1.10 Activity of RGGLW [11] against *E. coli* MraY

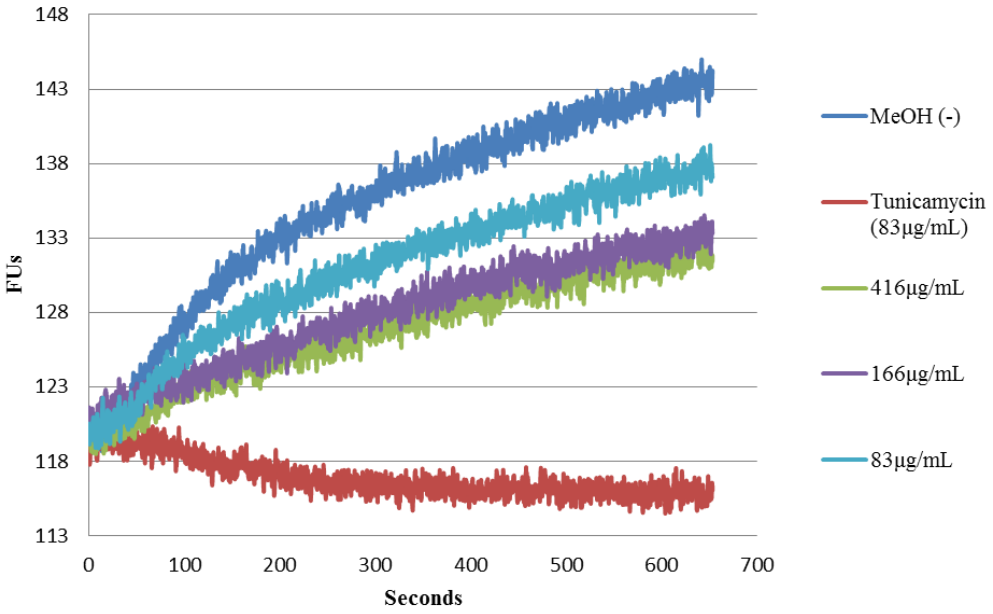


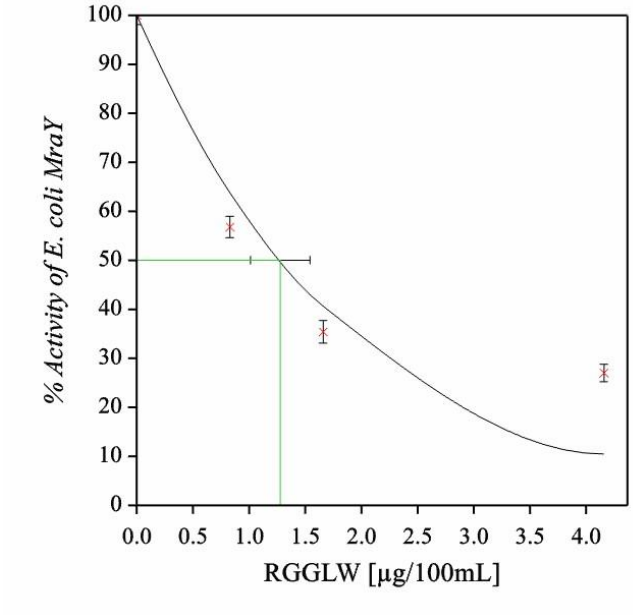

## A1.11 Activity of RGGLW [11] against *B. subtilis* MraY

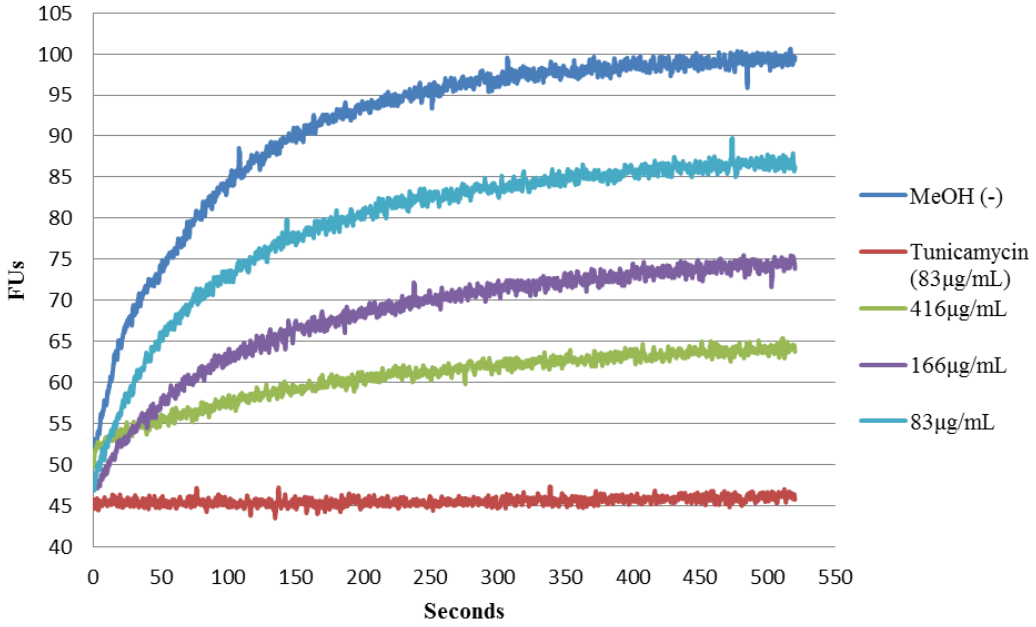


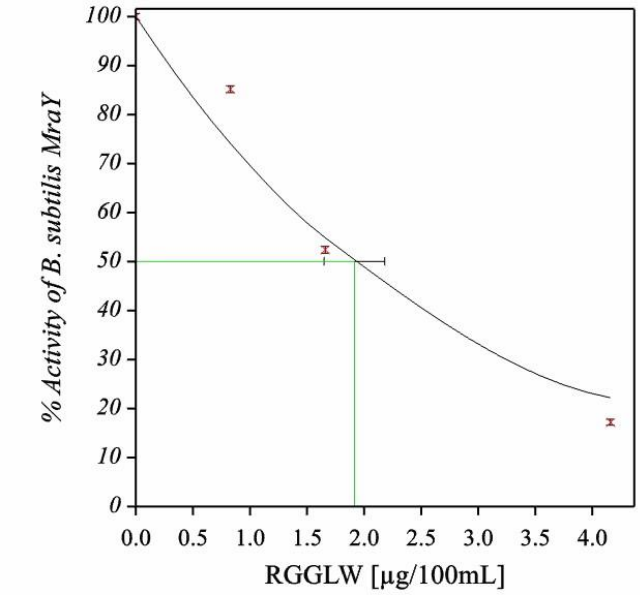

## A1.12 Activity of EHWGGG [15] against *E. coli* MraY

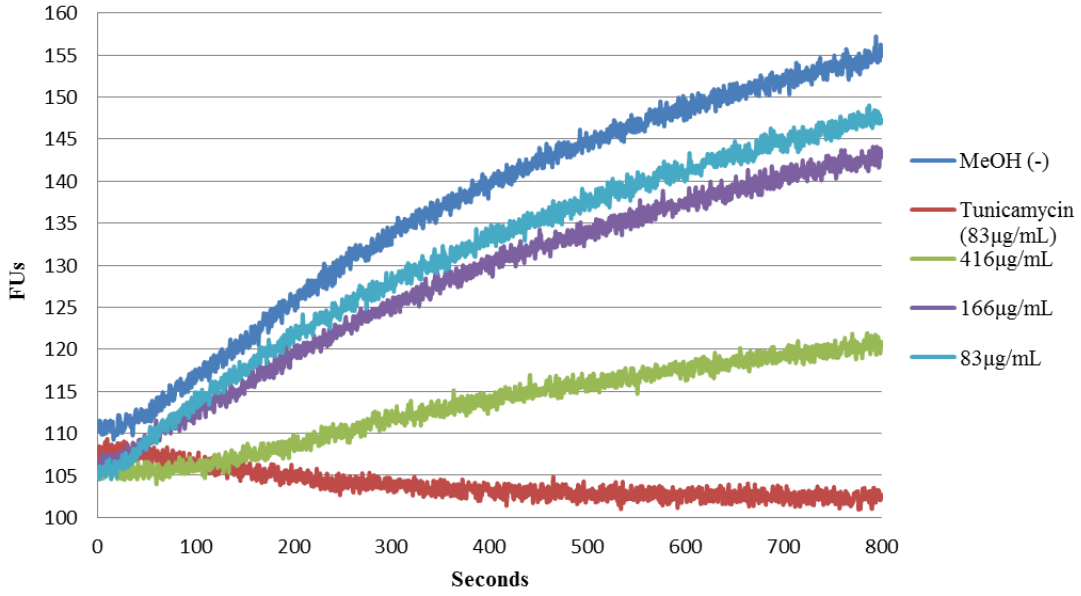


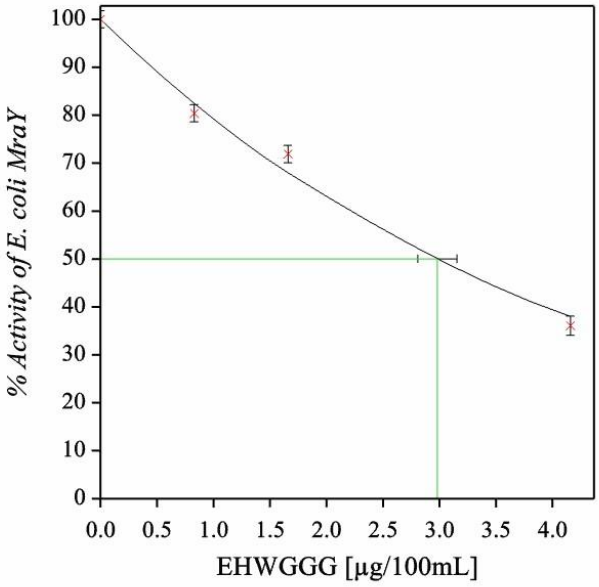

## A1.13 Activity of EHWGGG [15] against *P. aeruginosa* MraY

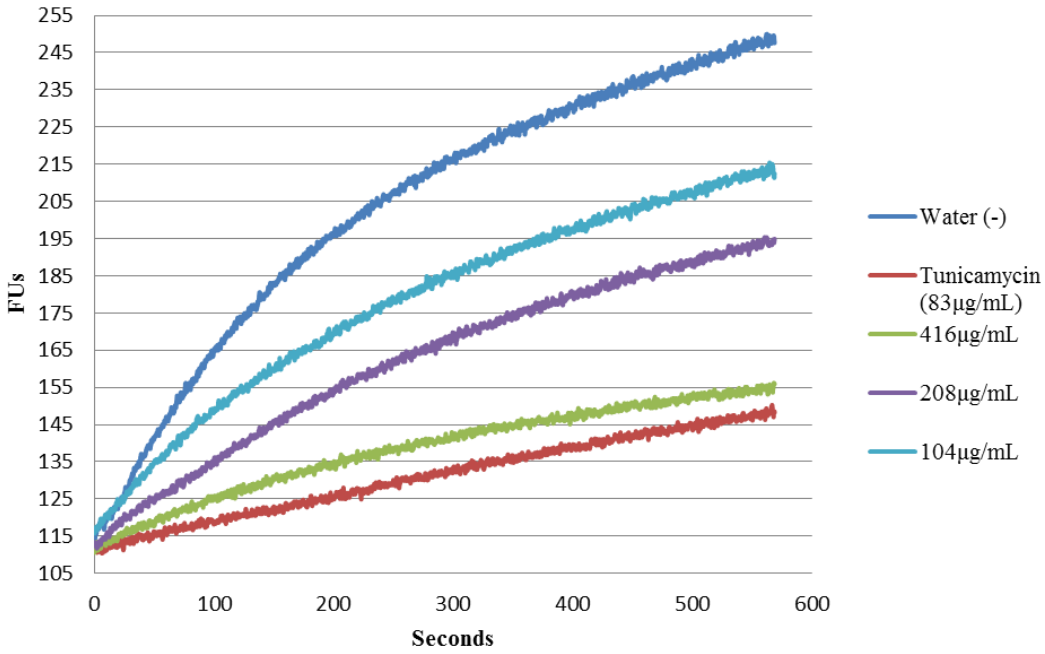


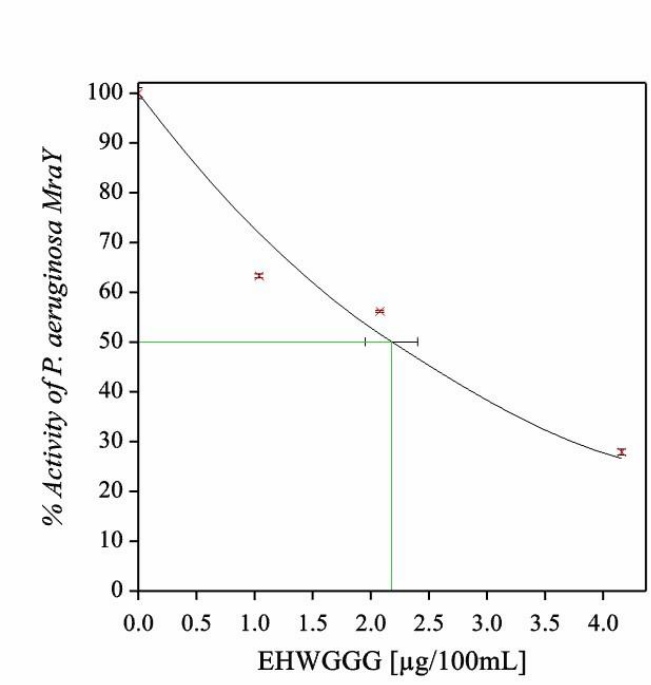

## A1.14 Activity of EHWGGG [15] against *S. aureus* MraY

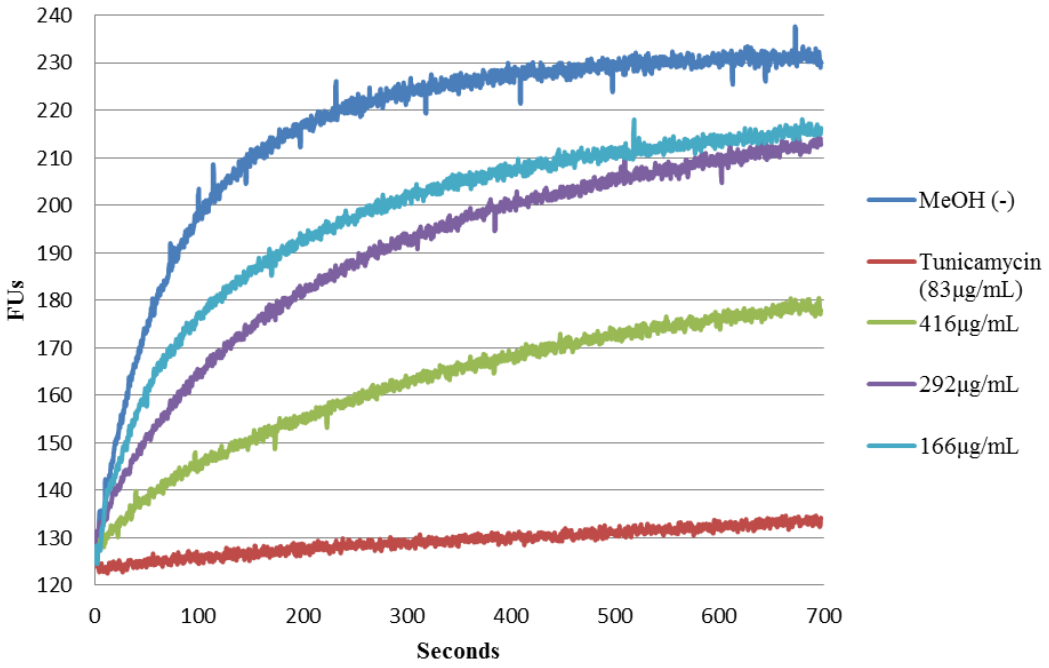


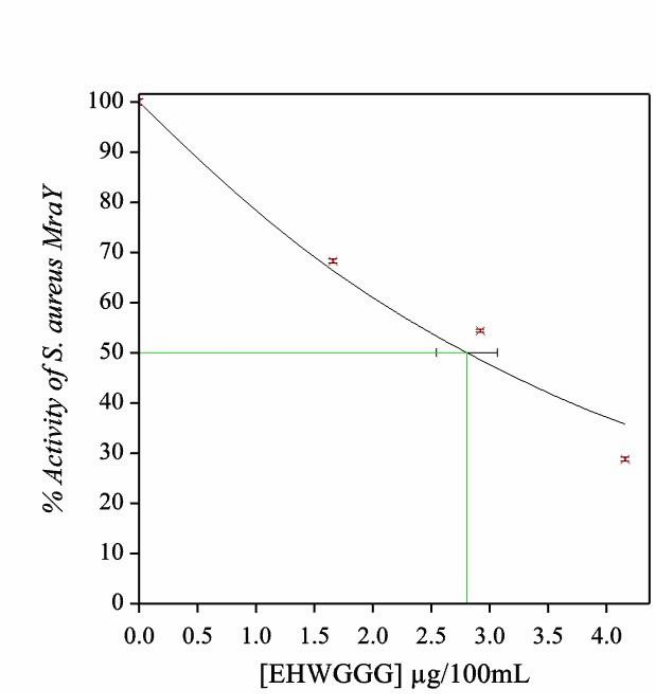

## A1.15 Activity of EHWGGG [15] against *M. flavus* MraY

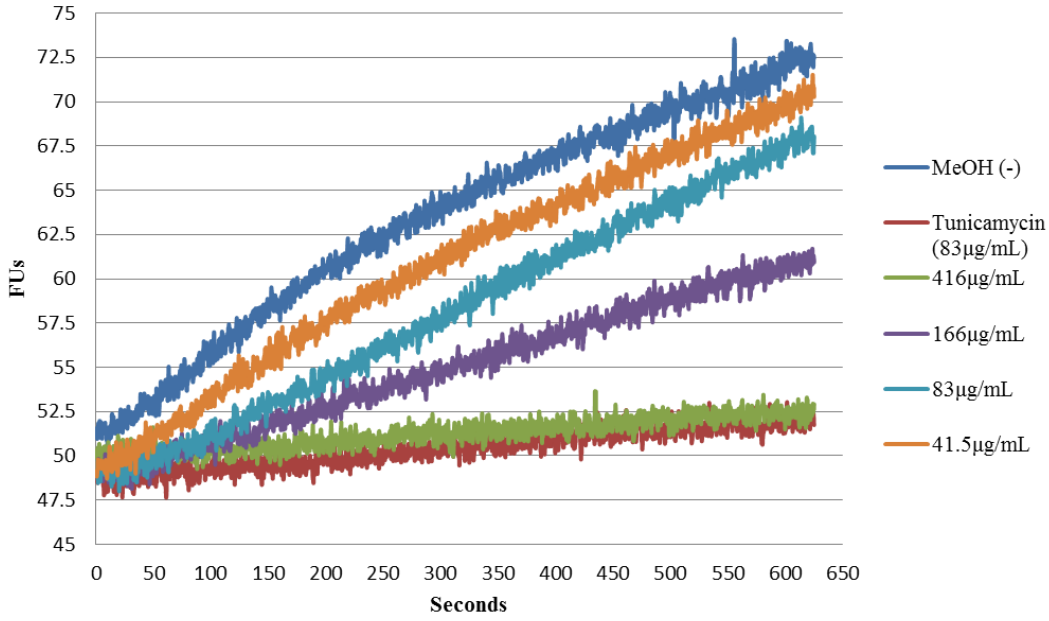


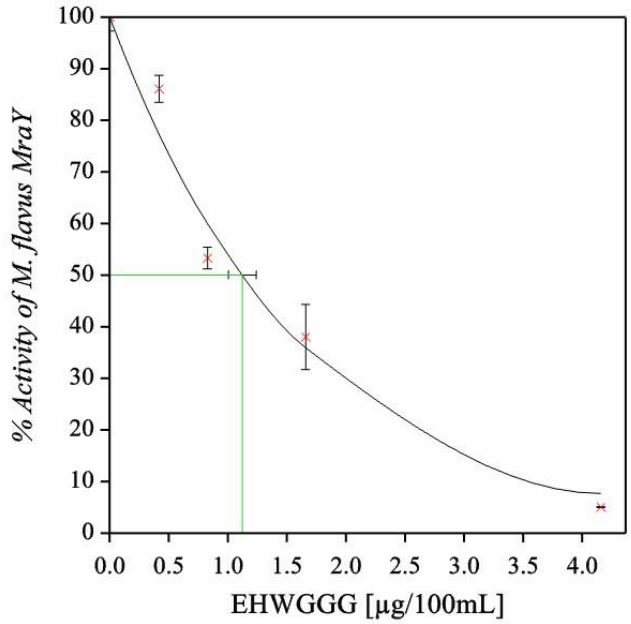

## A1.16 Activity of Epep against F288A MraY

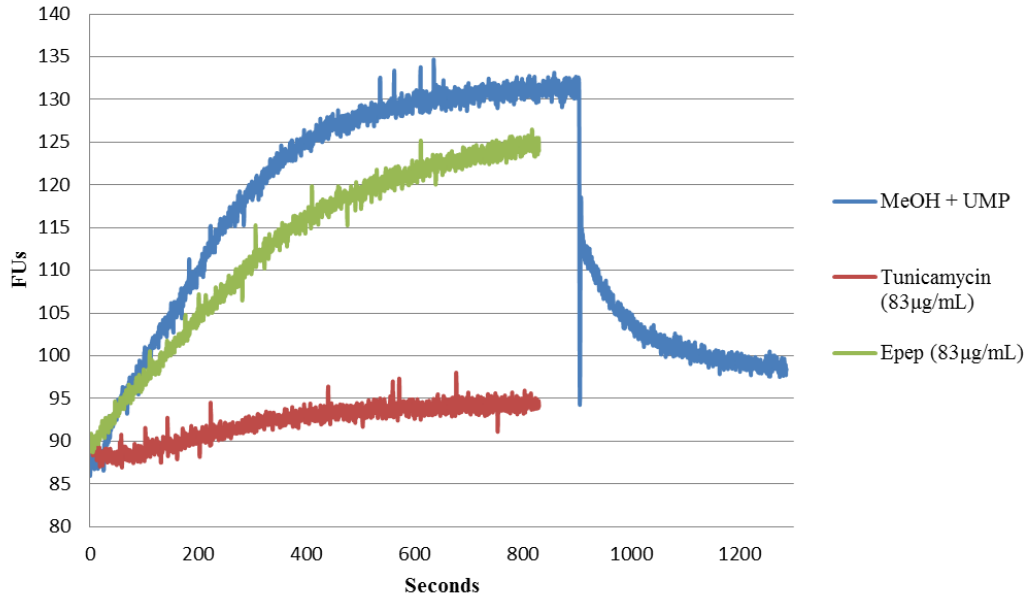


## A1.16 Activity of Epep against F288L MraY

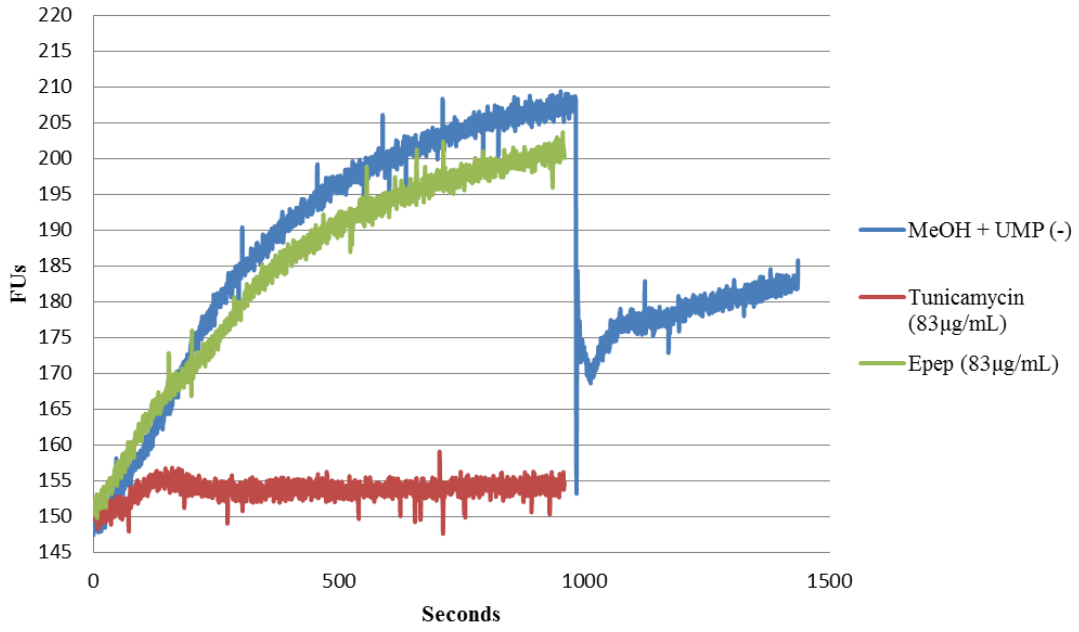

## A1.17 Activity of Epep against E287A MraY

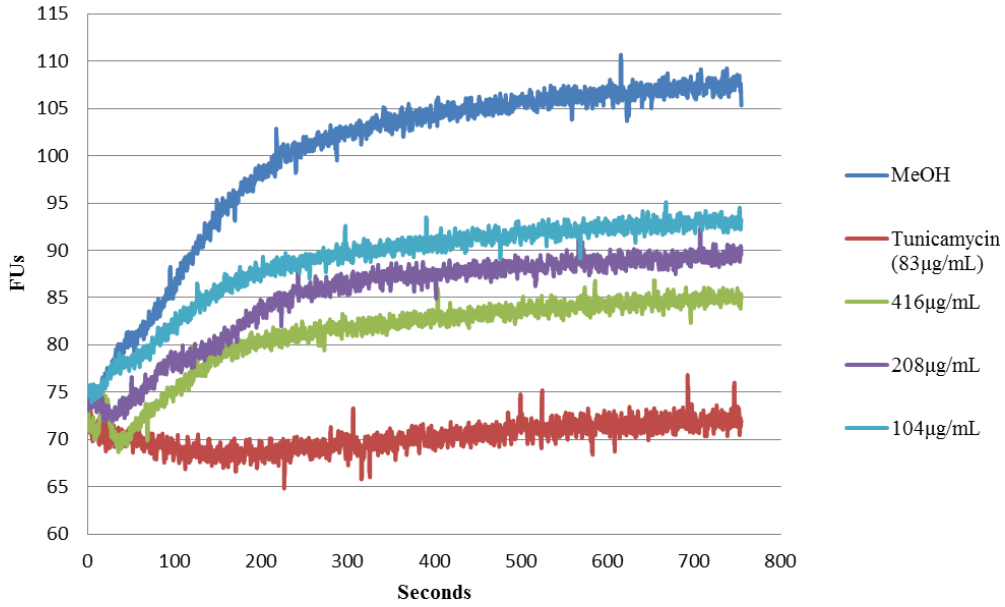


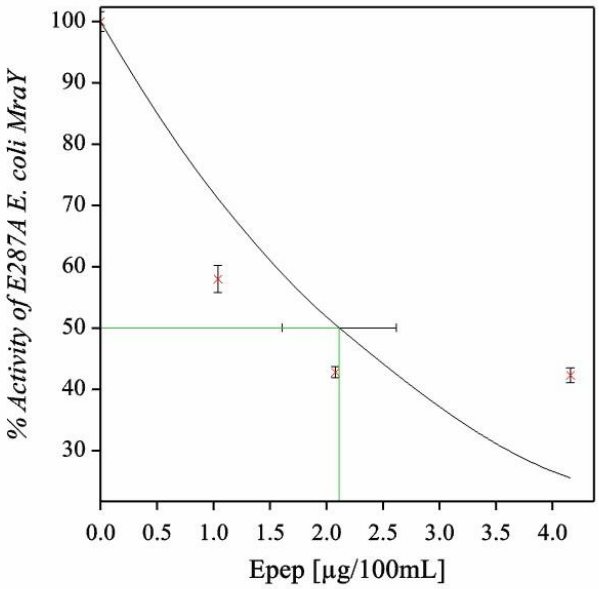

## A1.18 Activity of $H_2N$-GW-Oct [6] against E287A MraY

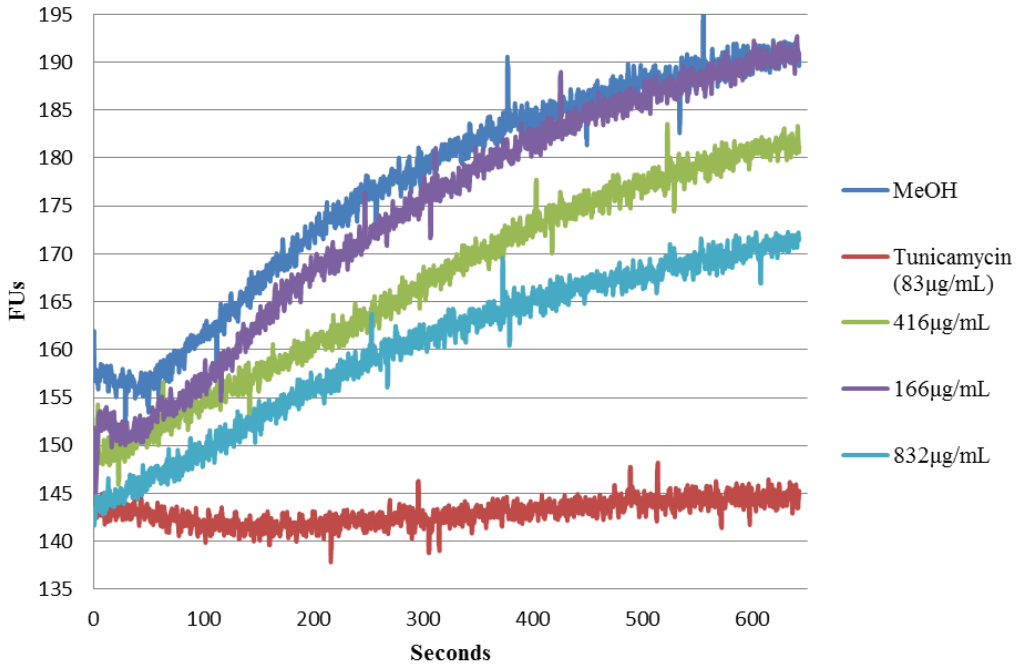


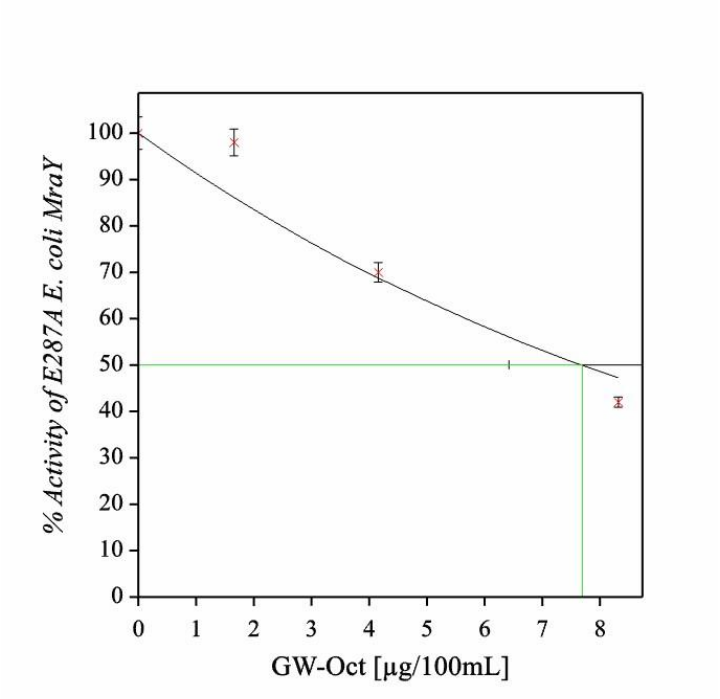

# Appendix 2: $IC_{50}$ values of compounds with intrinsic fluorescence against *E. coli* MraY

*Determined via radiochemical assay by Agnes Mihalyi*

## A2.1 $IC_{50}$ graph of GWGLW [12]

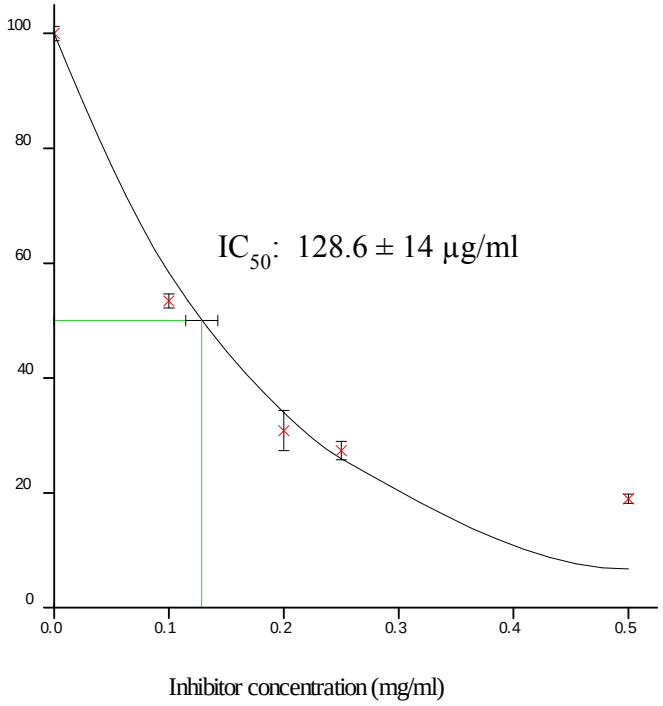

## A2.2 $IC_{50}$ graph of RWGGW [13]

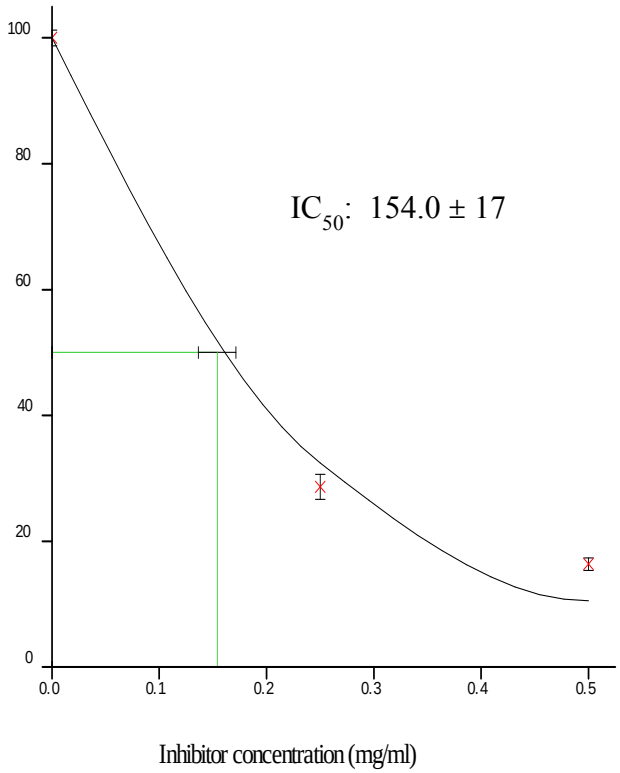


## A2.3 $IC_{50}$ graph of RWGLG [13]

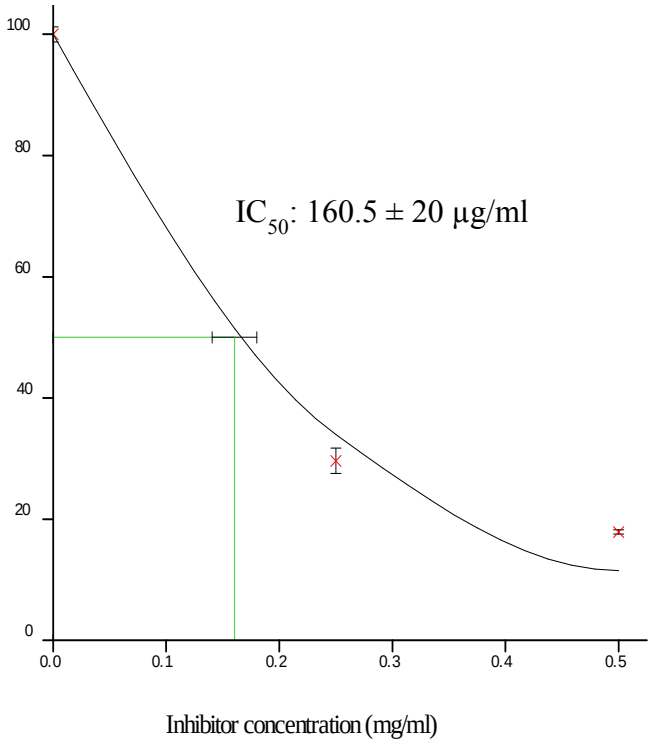

## A2.4 $IC_{50}$ graph of ERWGGW [16]

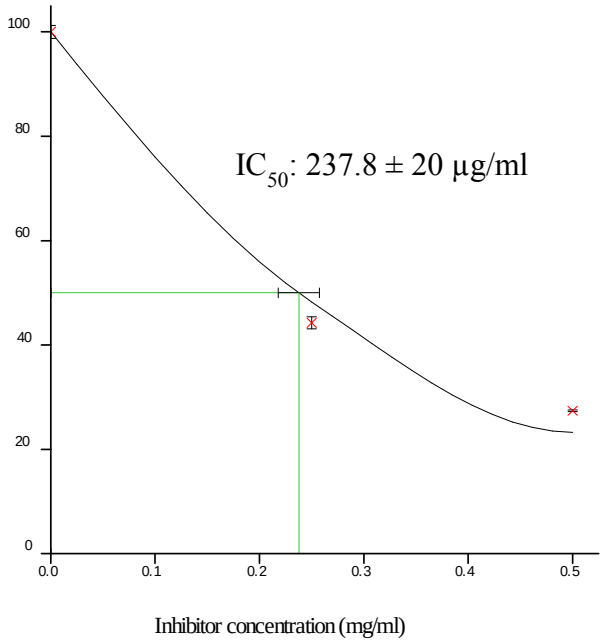

# Appendix 3: Emission Spectrum of MraY and MraY mutants in the presence of UPA's and UPA analogues

## A3.1 Activity of HOOC-RGGGsUr [27] against *E. coli* MraY

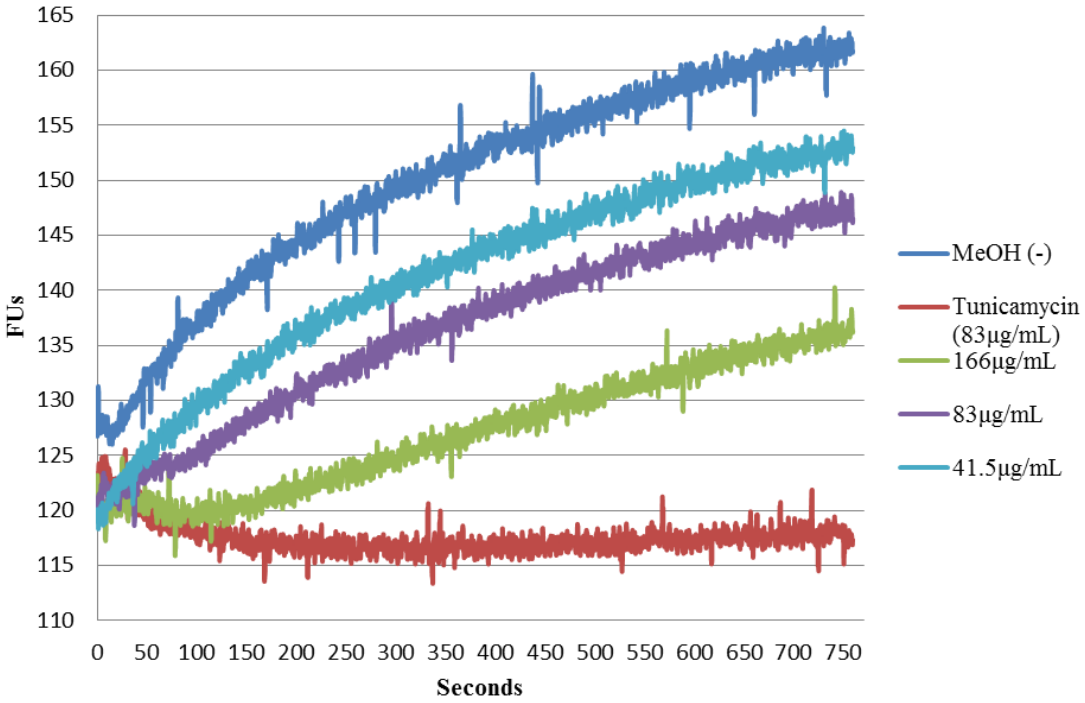


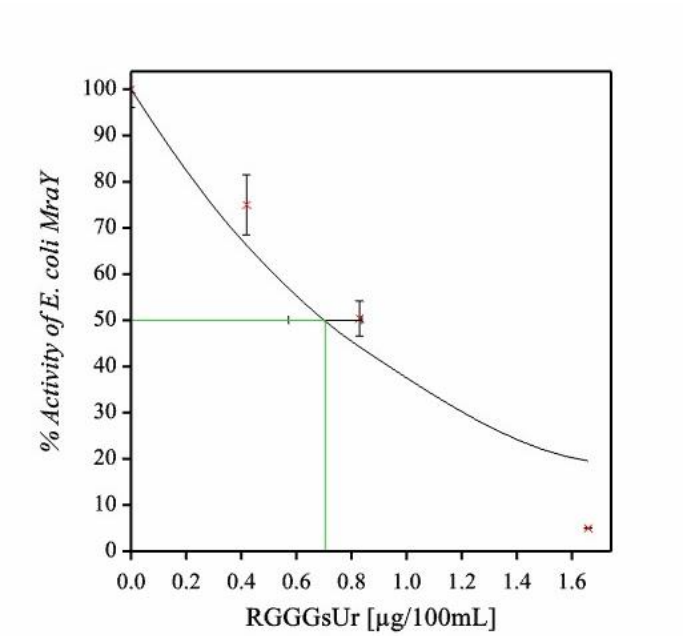

## A3.2 Activity of HOOC-RGGGsUr [27] against *P. aeruginosa* MraY

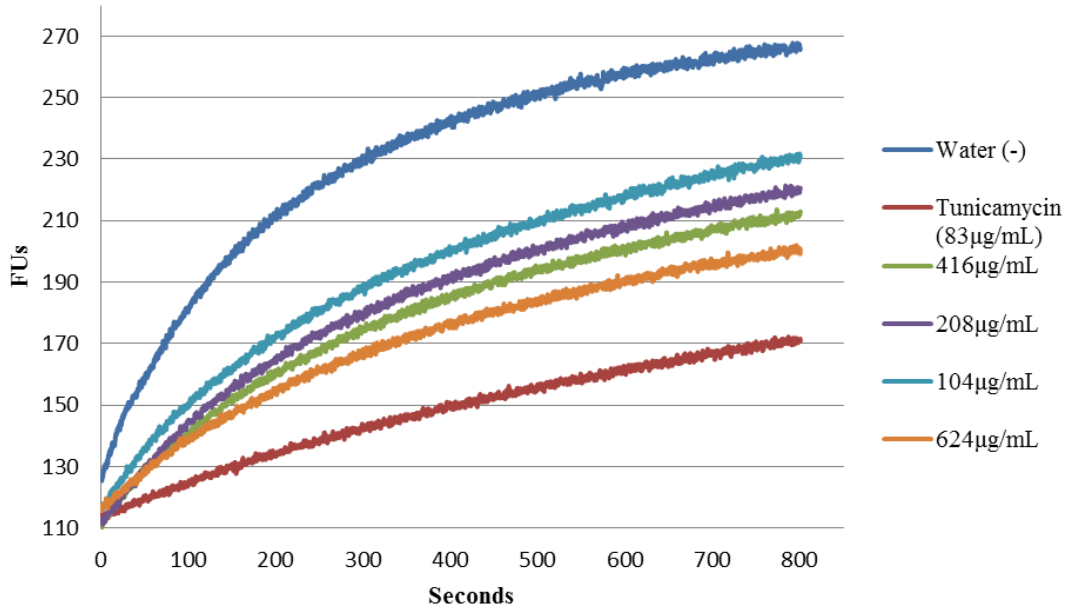


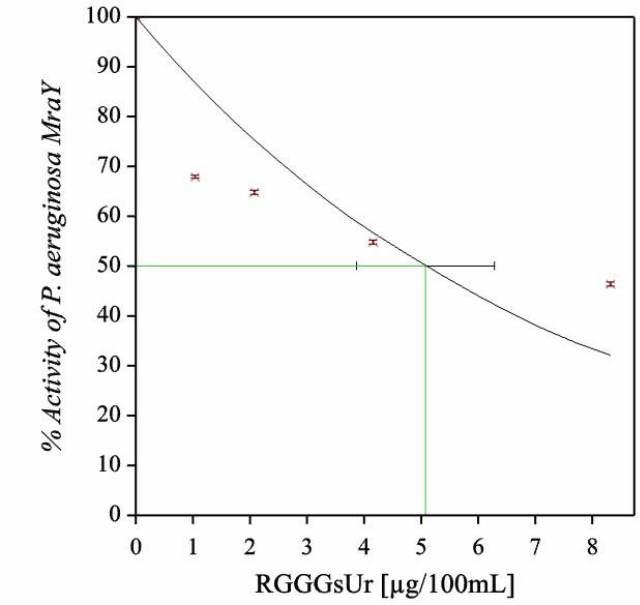

## A3.3 Activity of HOOC-RGGGsUr [27] against *S. aureus* MraY

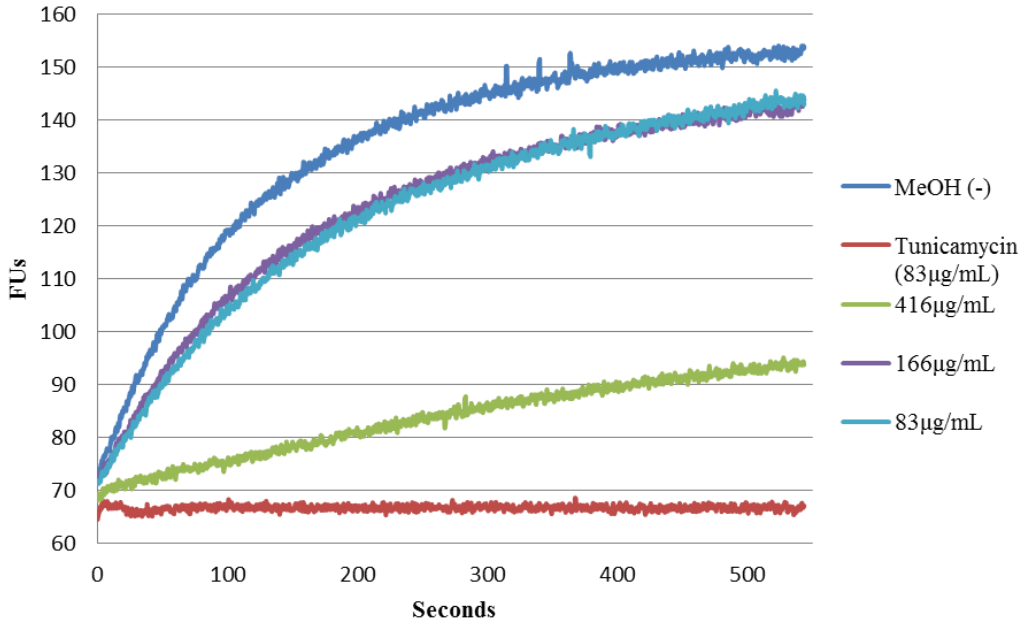


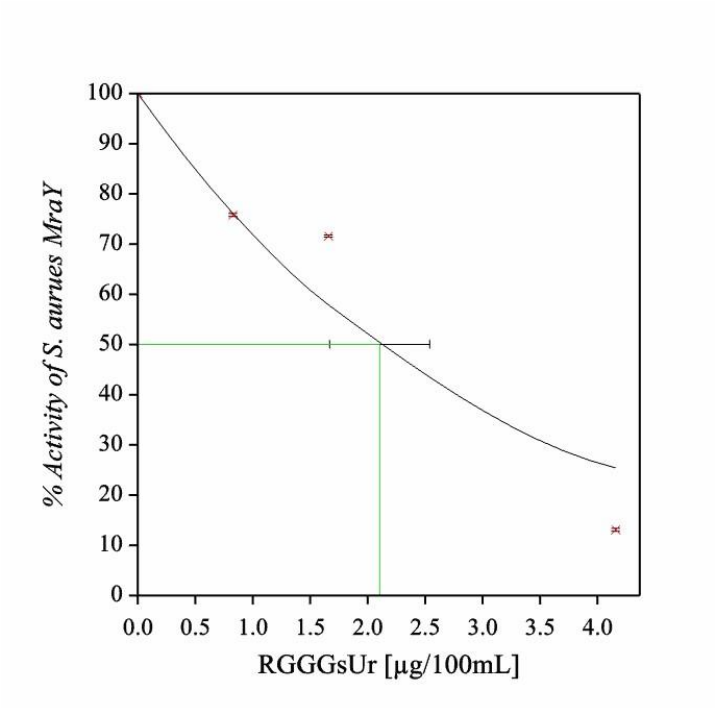

## A3.4 Activity of HOOC-RGGGsUr [27] against *M. flavus* MraY

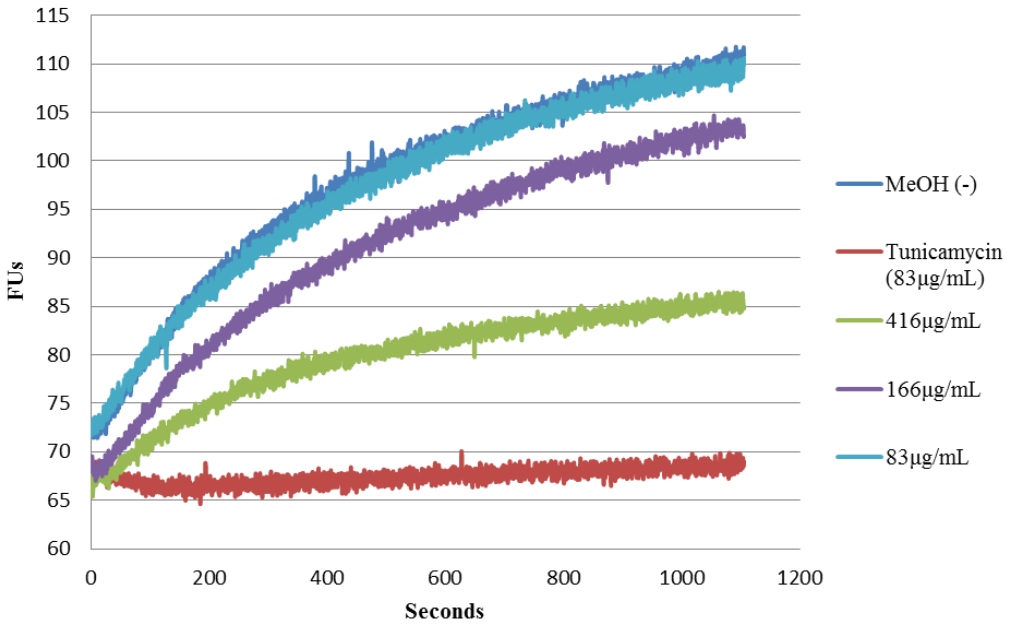


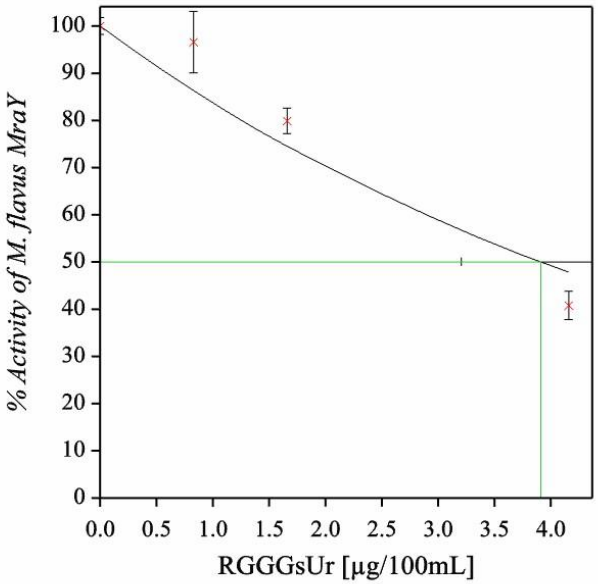

## A3.5 Activity of HOOC-RGGGsUr [27] against *B. subtilis* MraY

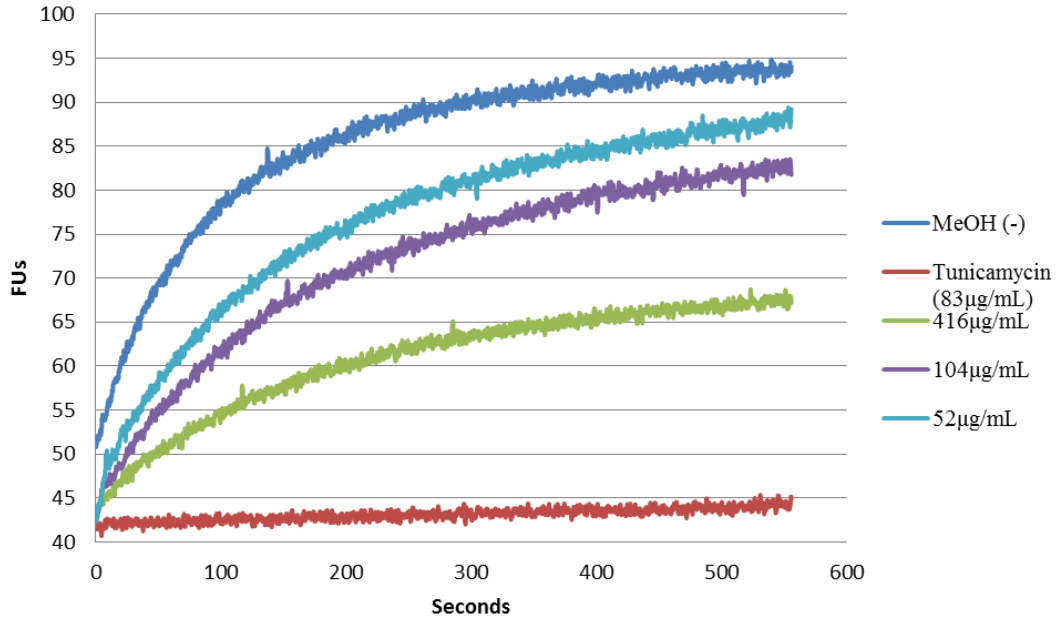


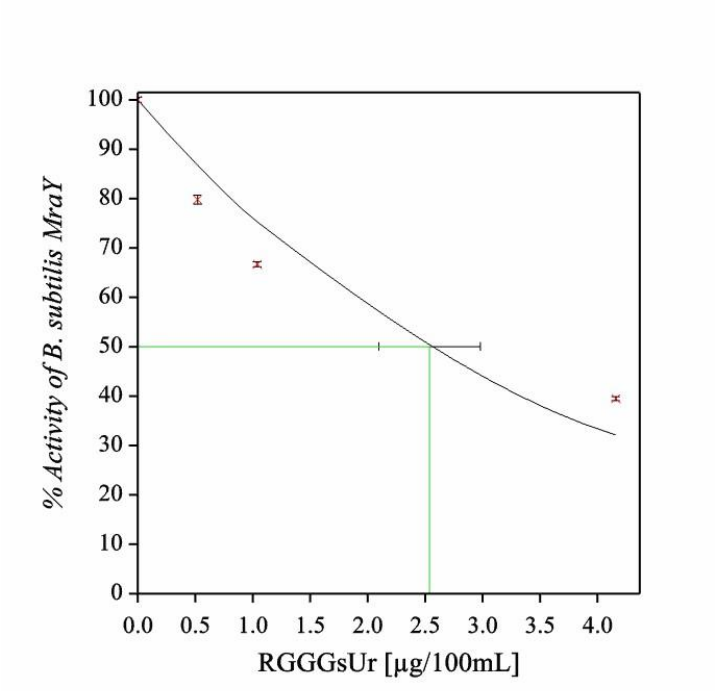

## A3.6 Activity of caparazamycin A against *E. coli* MraY

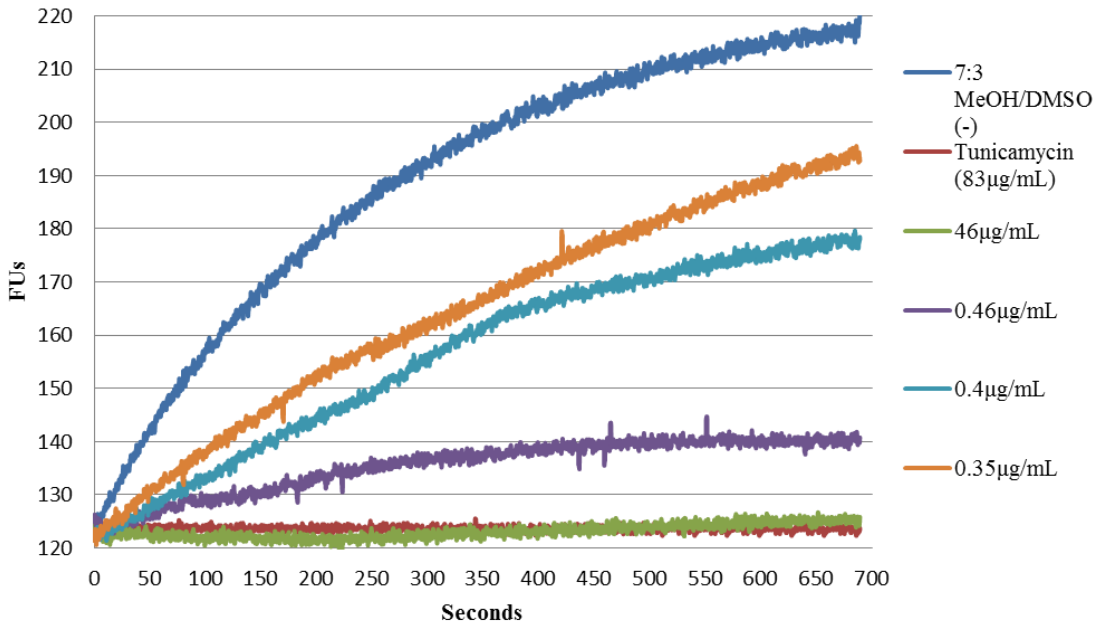


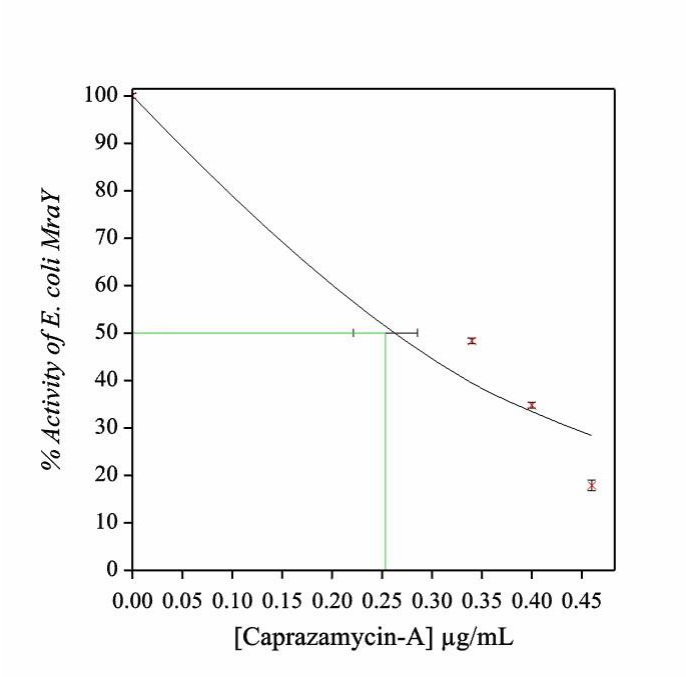

## A3.7 Activity of caparazamycin E against *E. coli* MraY

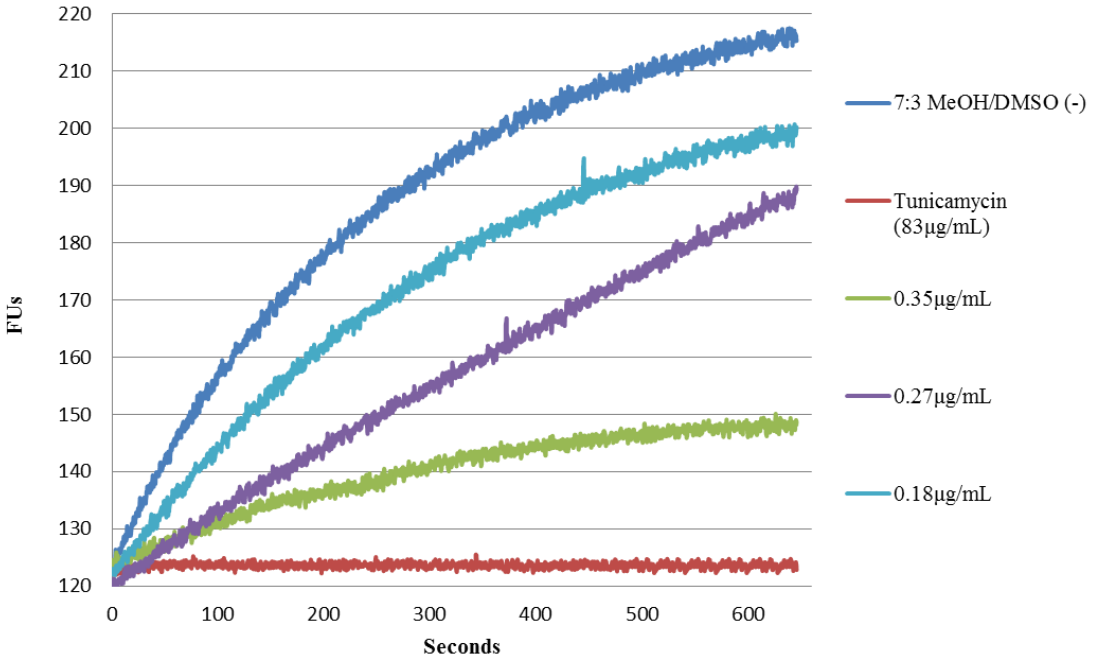


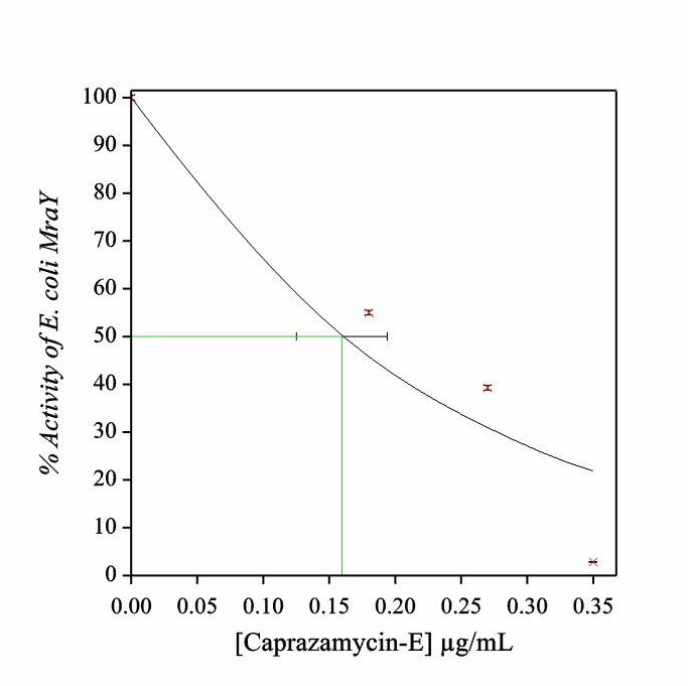

## A3.8 Activity of pacidamycin 1&2 against *E. coli* MraY

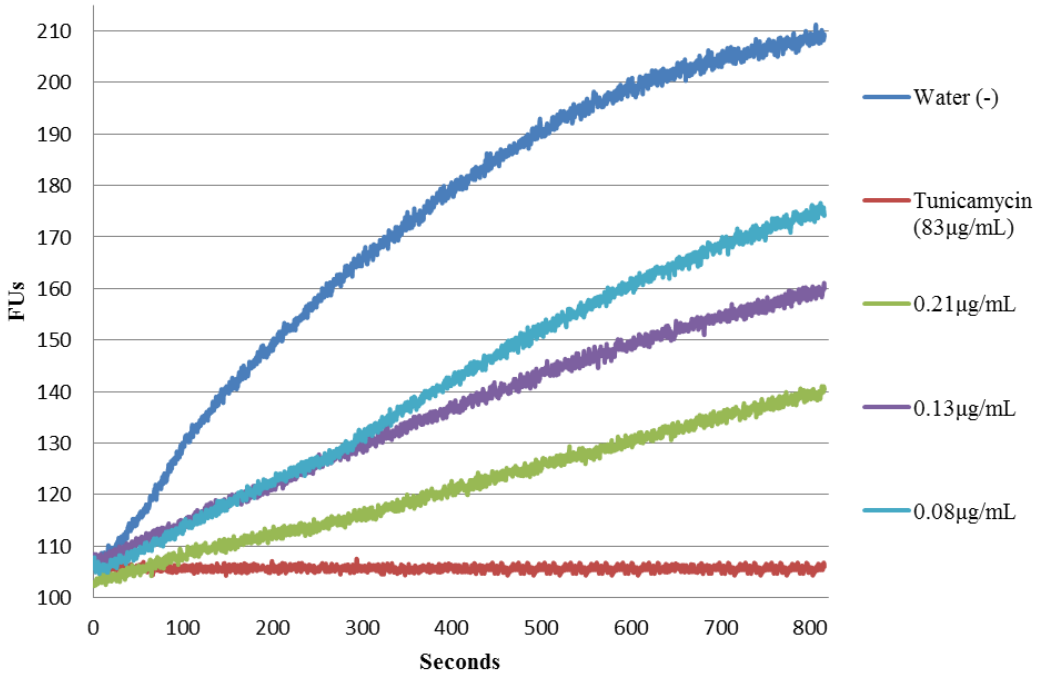


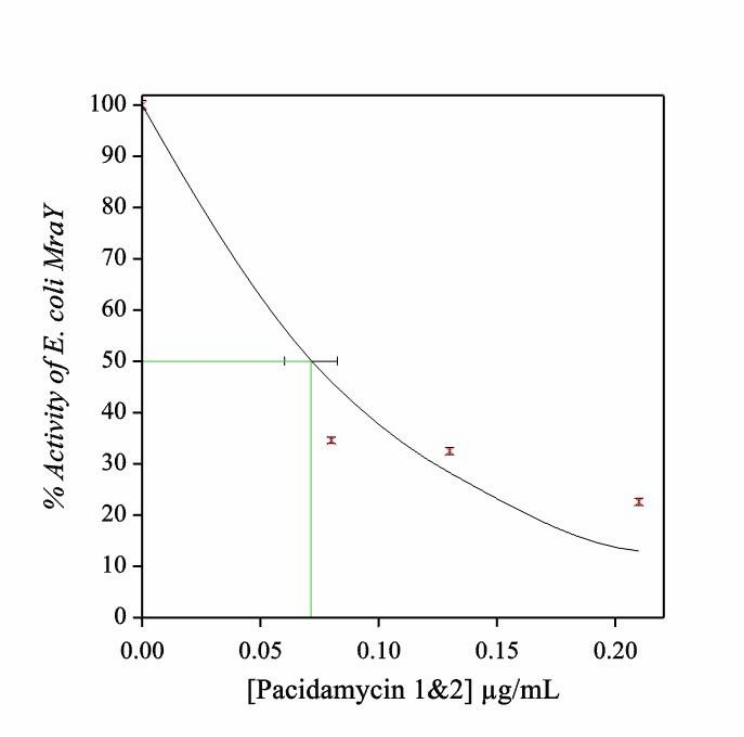

## A3.9 Activity of pacidamycin D against *E. coli* MraY

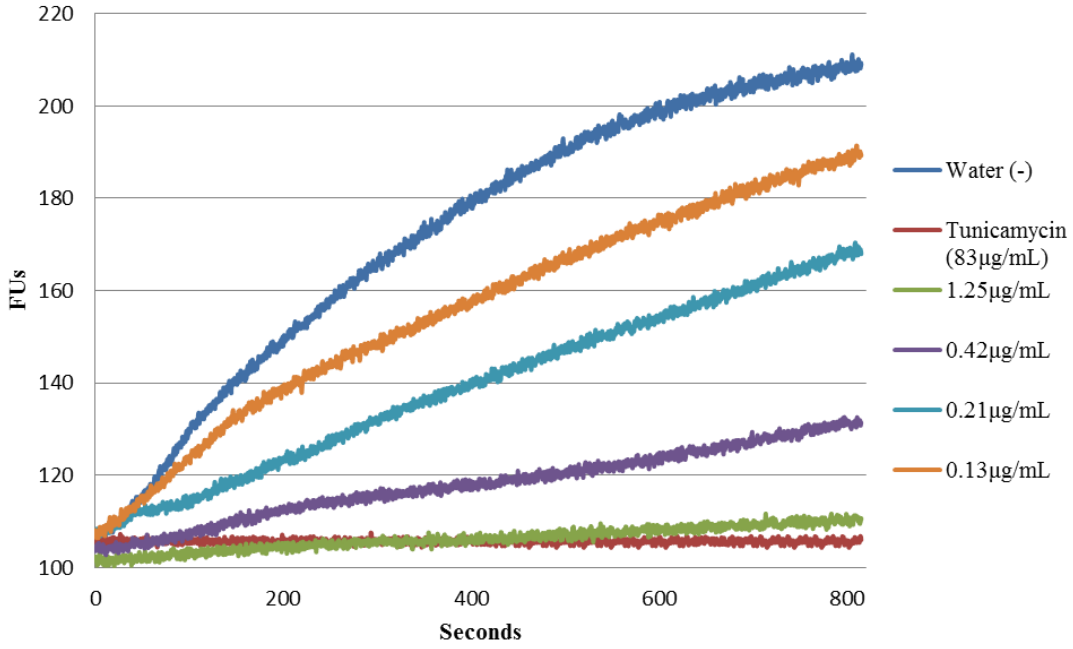


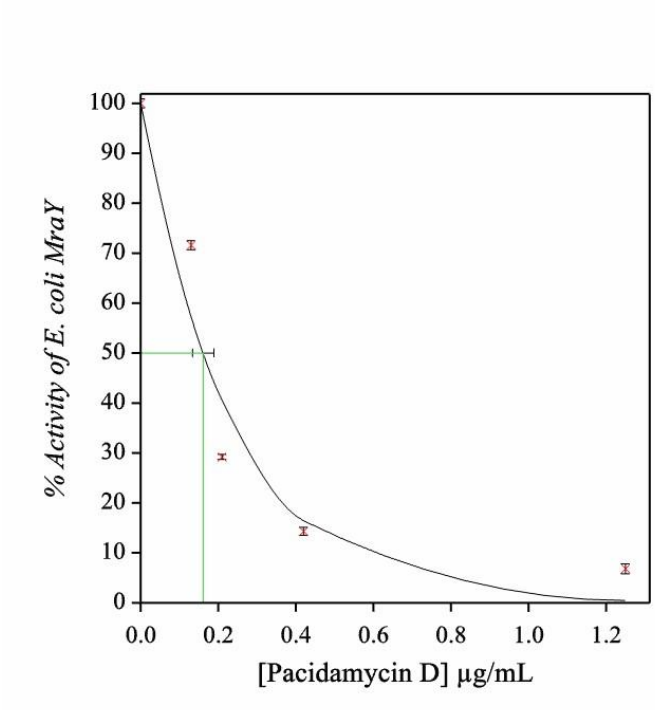

## A3.10 Activity of mureidomycin A against *E. coli* MraY

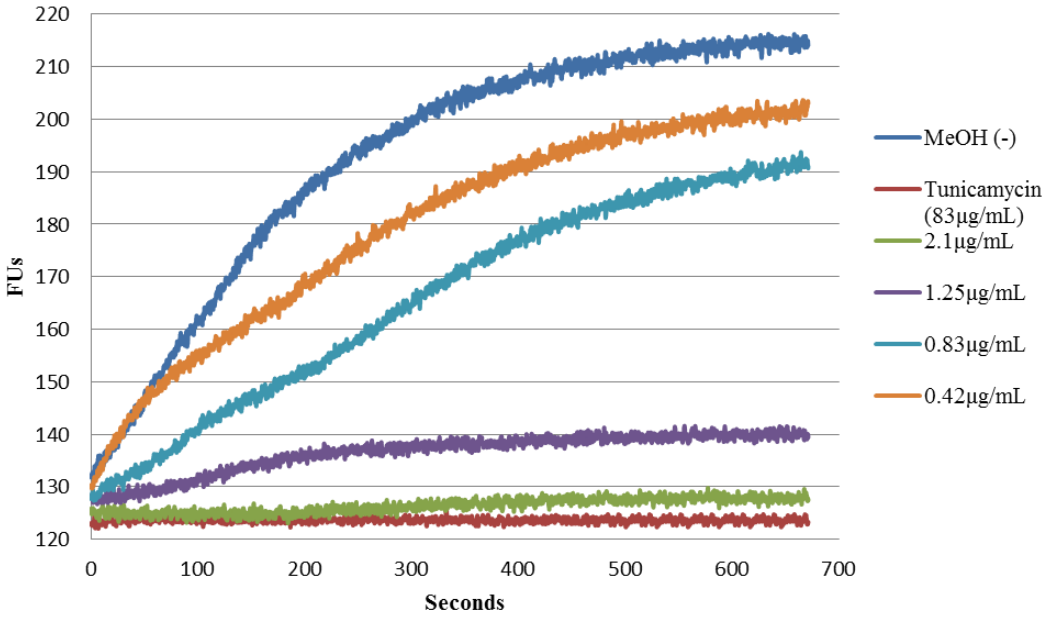


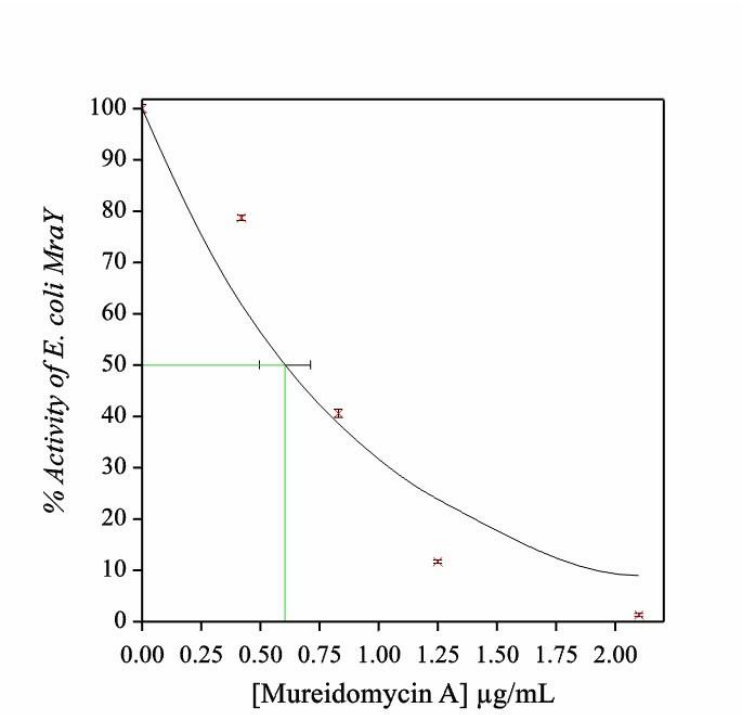

## A3.11 Activity of caparazamycin A against *E. coli* F288L MraY

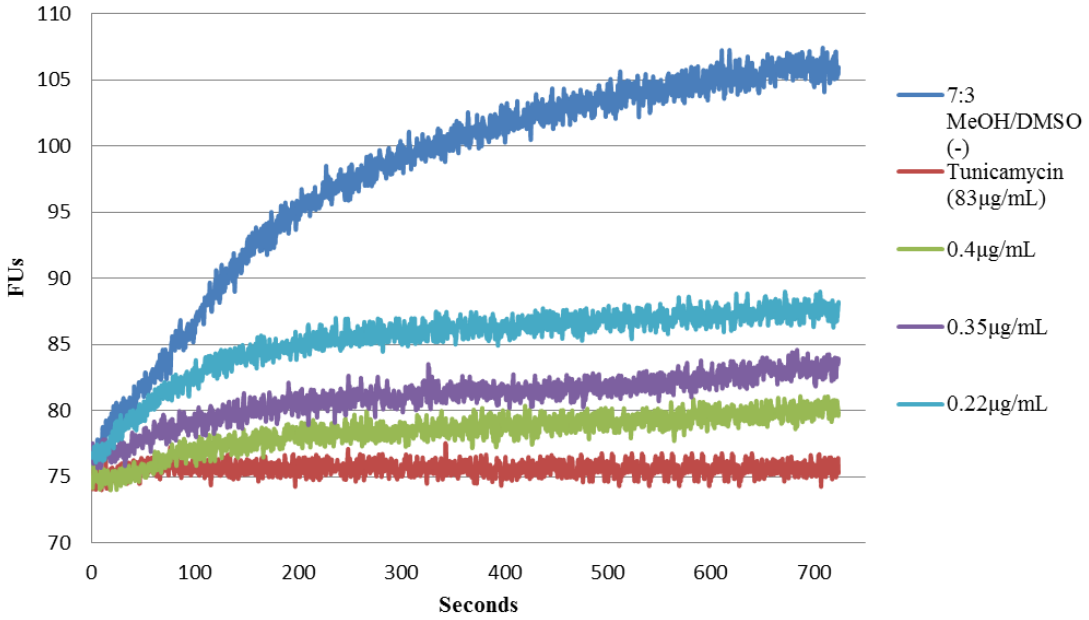


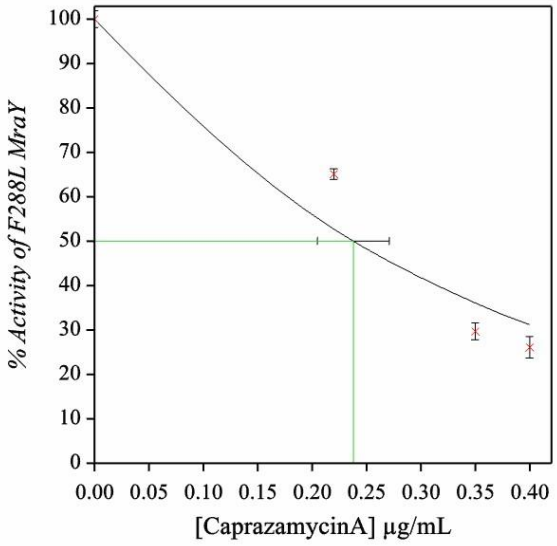

## A3.12 Activity of caparazamycin E against *E. coli* F288L MraY

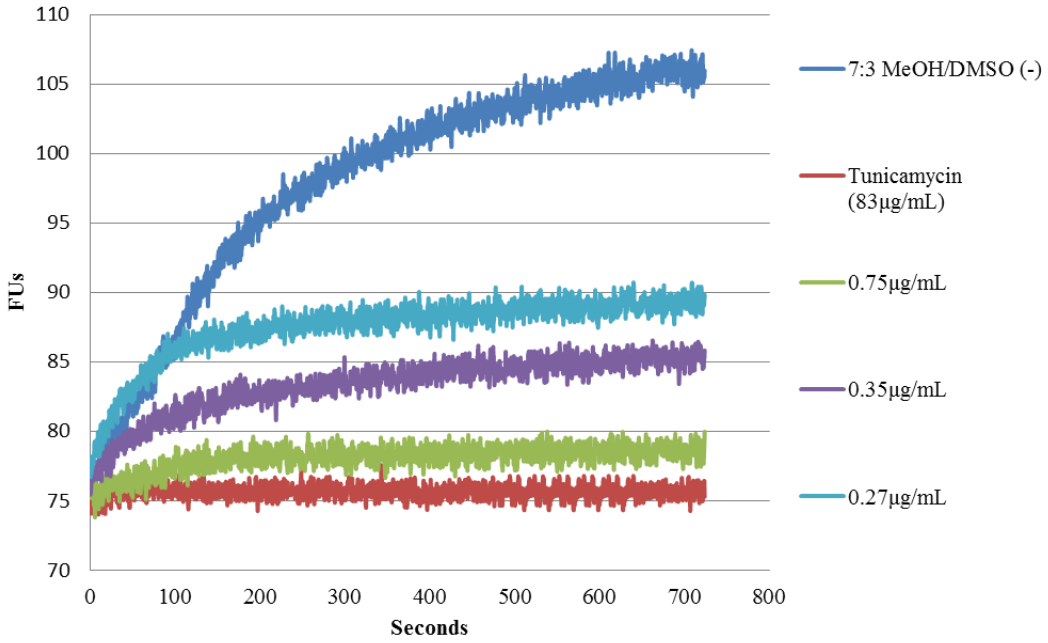


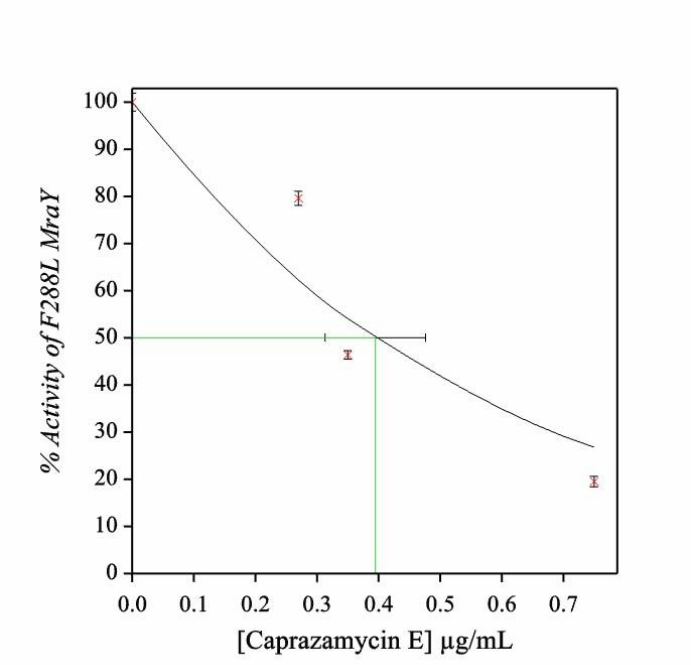

## A3.13 Activity of pacidamycin 1&2 against *E. coli* F288L MraY

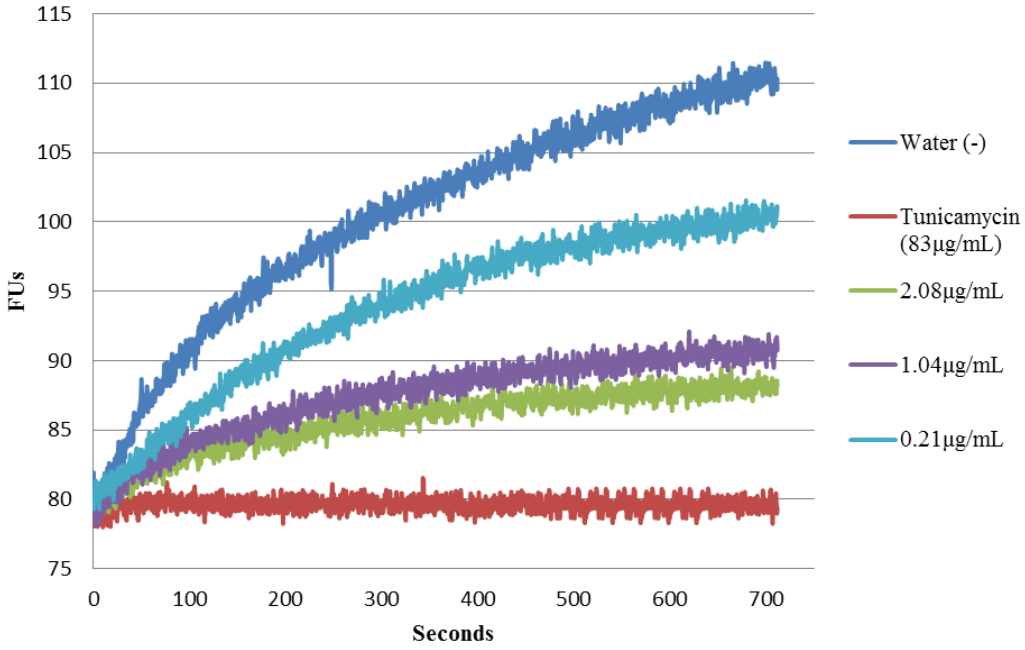


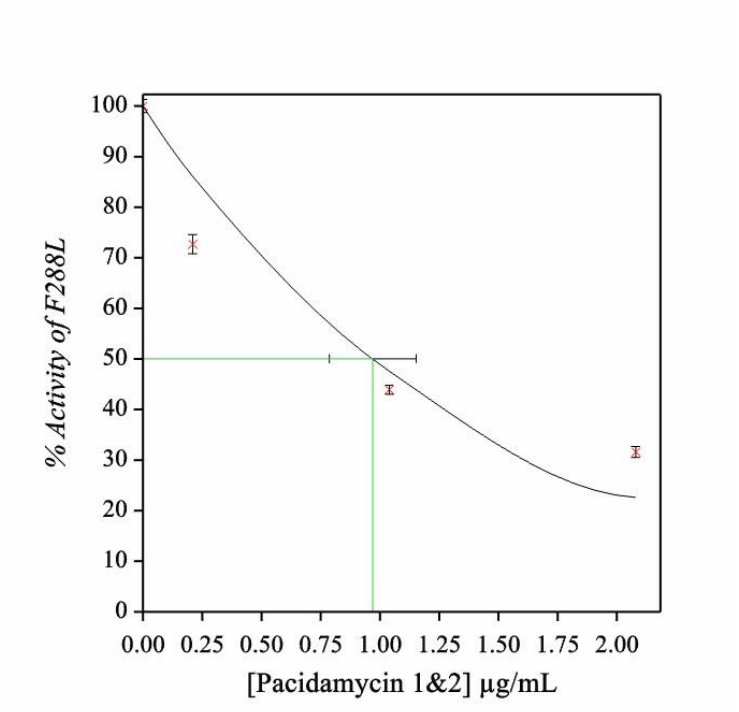

## A3.14 Activity of pacidamycin D against *E. coli* F288L MraY

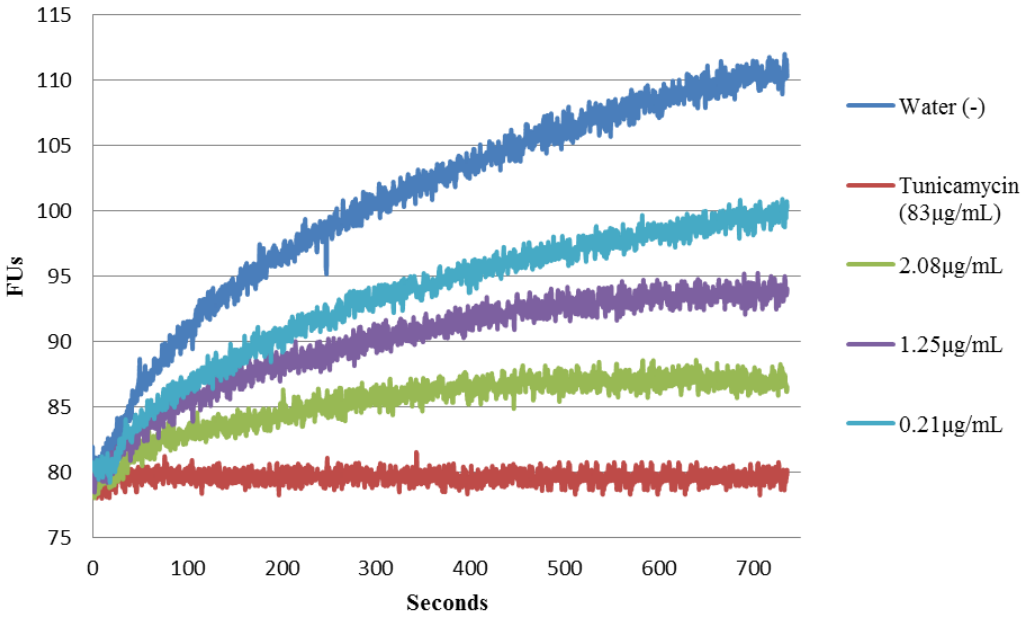


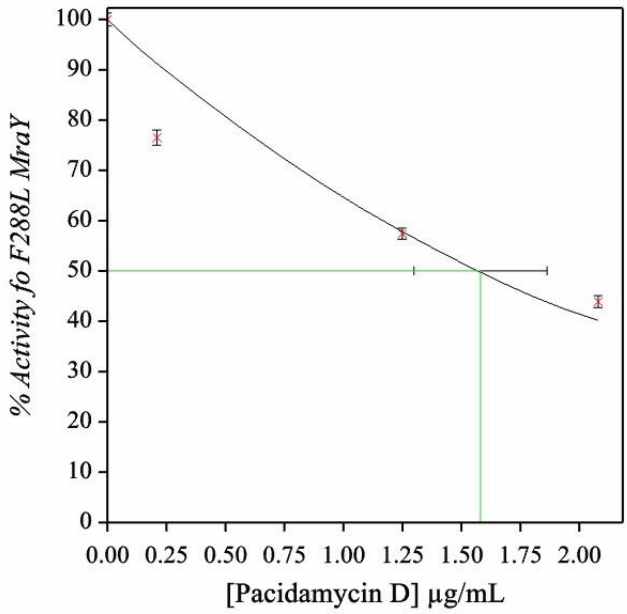

## A3.15 Activity of mureidomycin A against *E. coli* F288L MraY

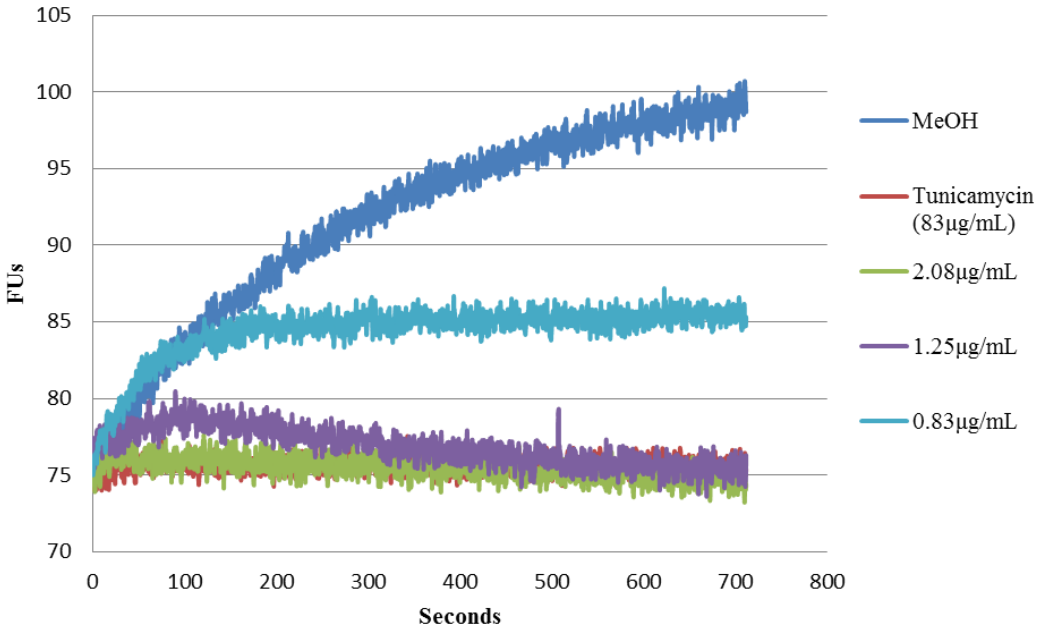


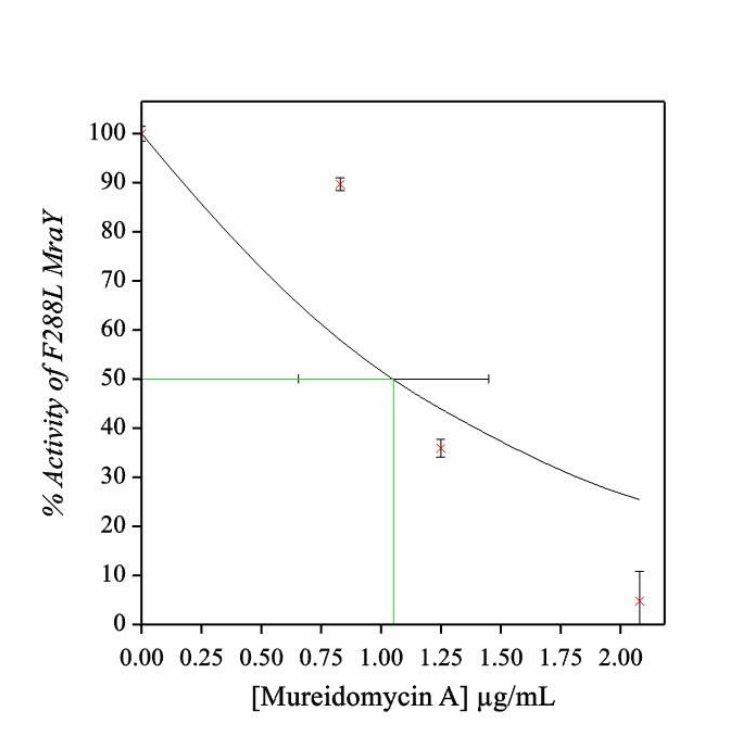

## A3.16 Activity of caparazamycin A against *E. coli* E287A MraY

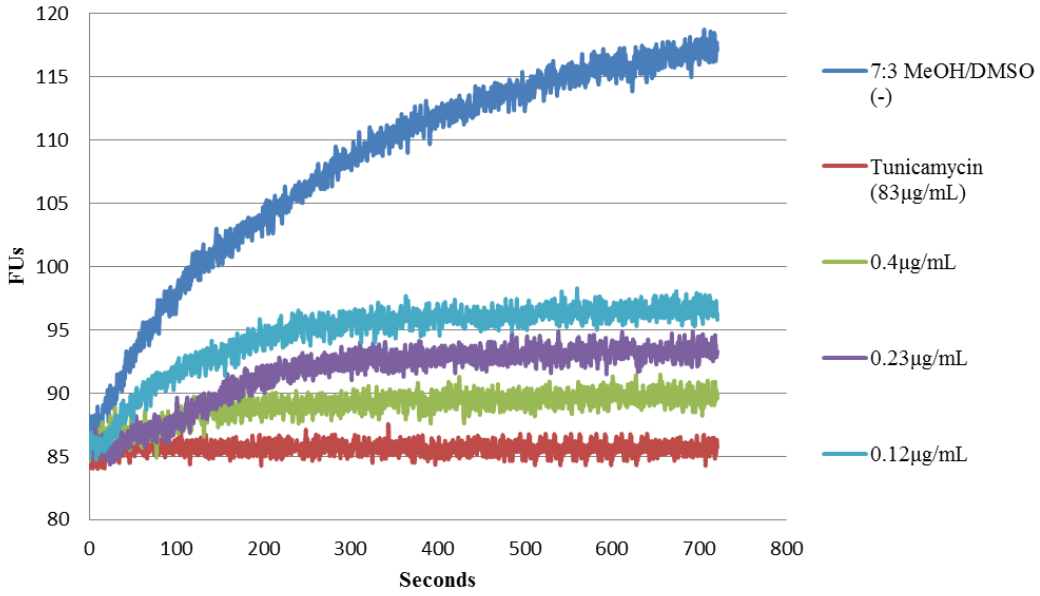


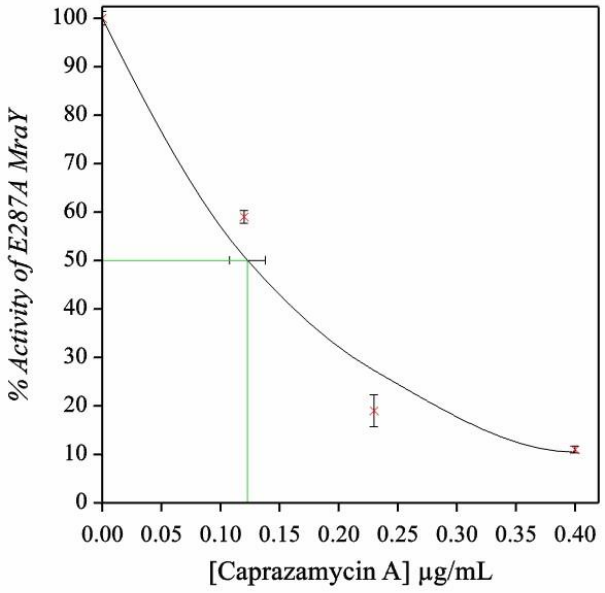

## A3.17 Activity of caparazamycin E against *E. coli* E287A MraY

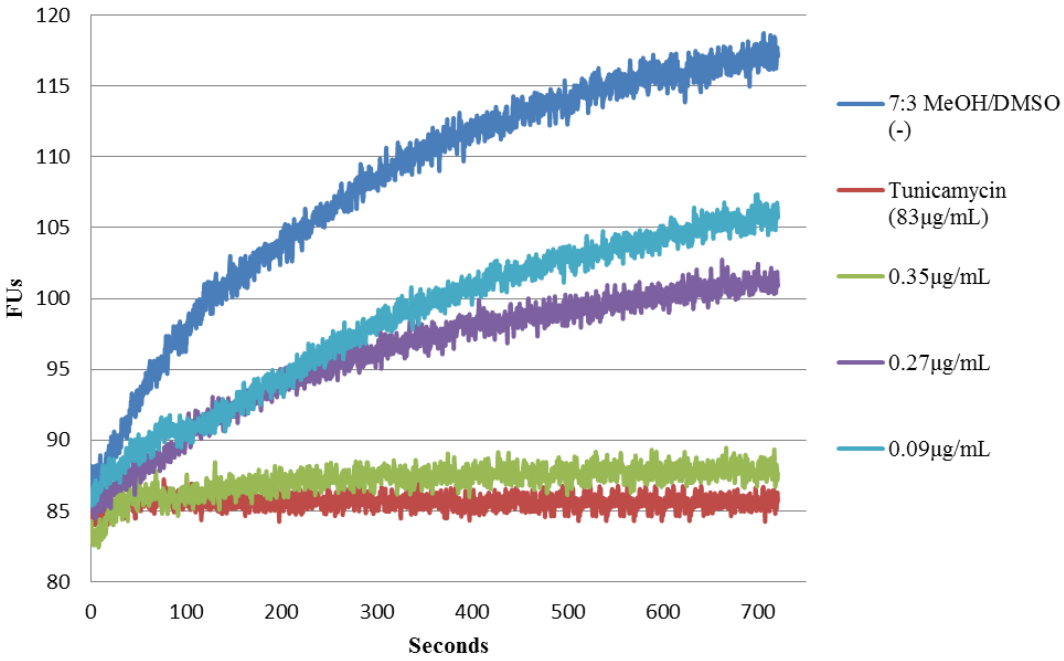


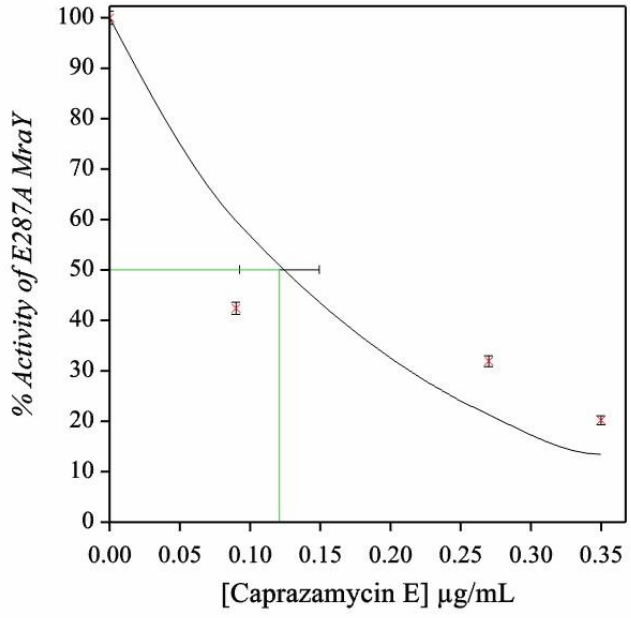

## A3.18 Activity of pacidamycin 1&2 against *E. coli* E287A MraY

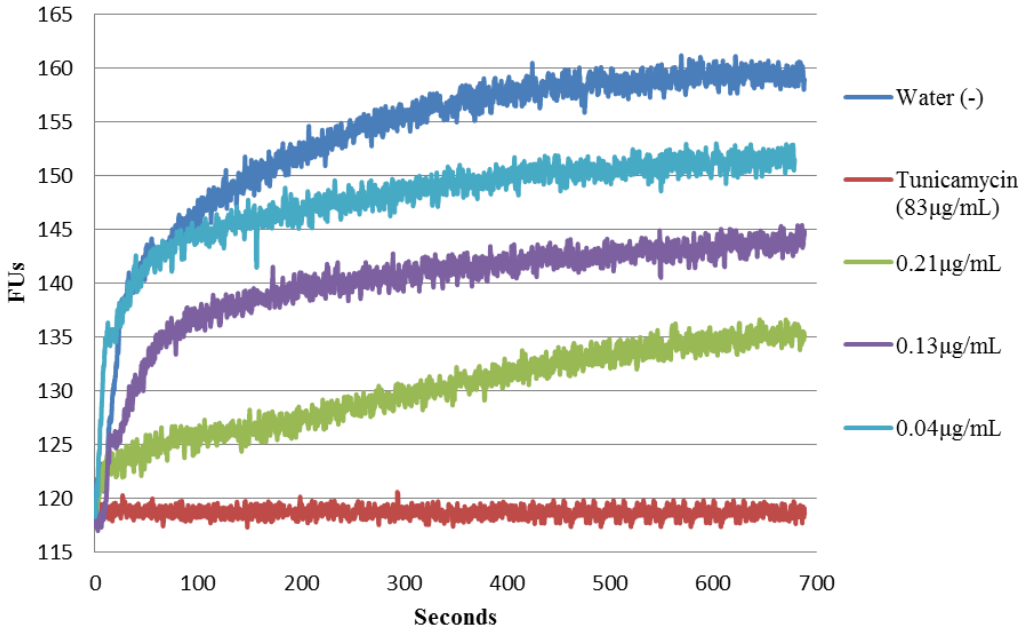


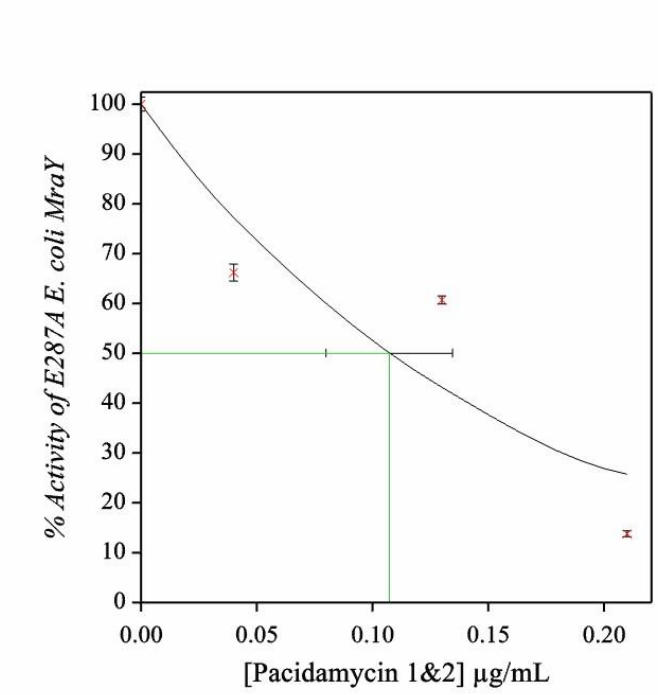

## A3.19 Activity of pacidamycin D against *E. coli* E287A MraY

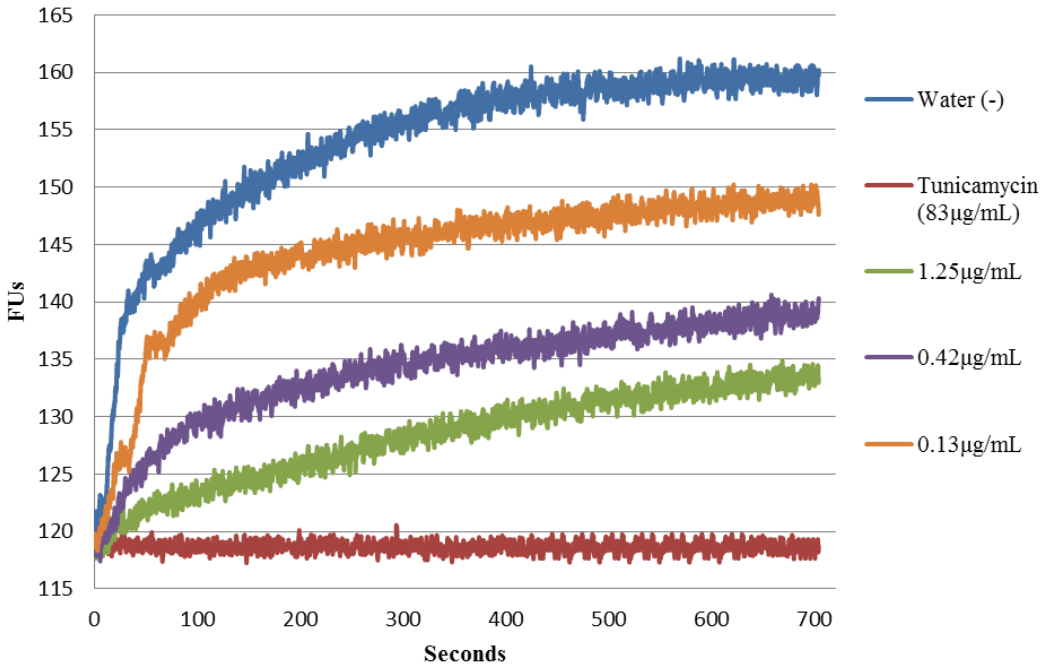


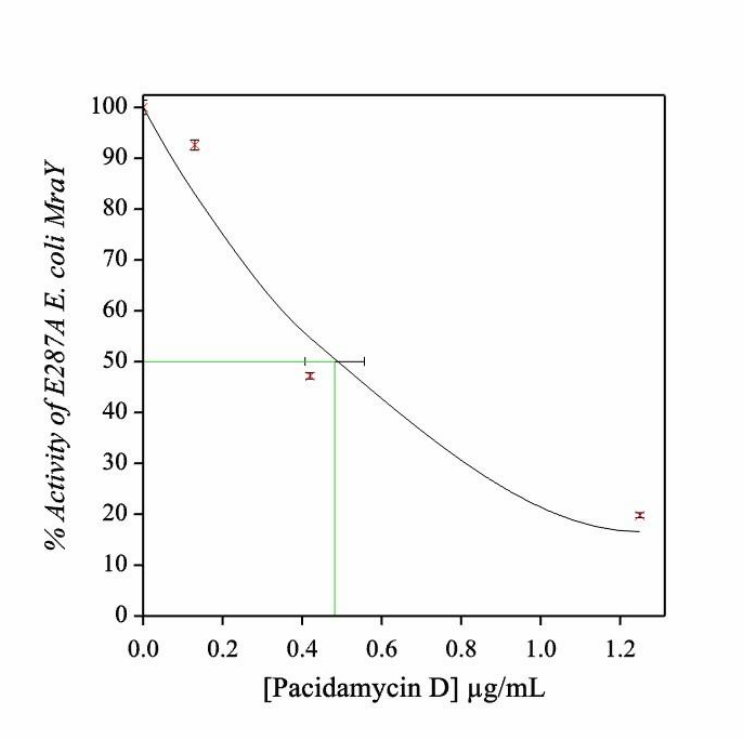

## A3.20 Activity of mureidomycin A against *E. coli* E287A MraY

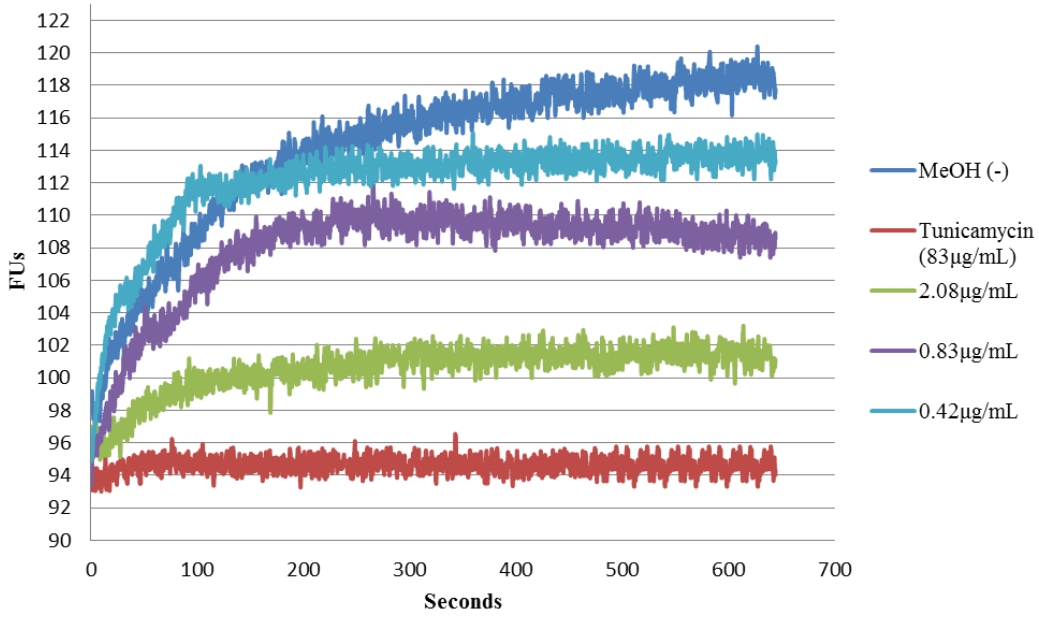


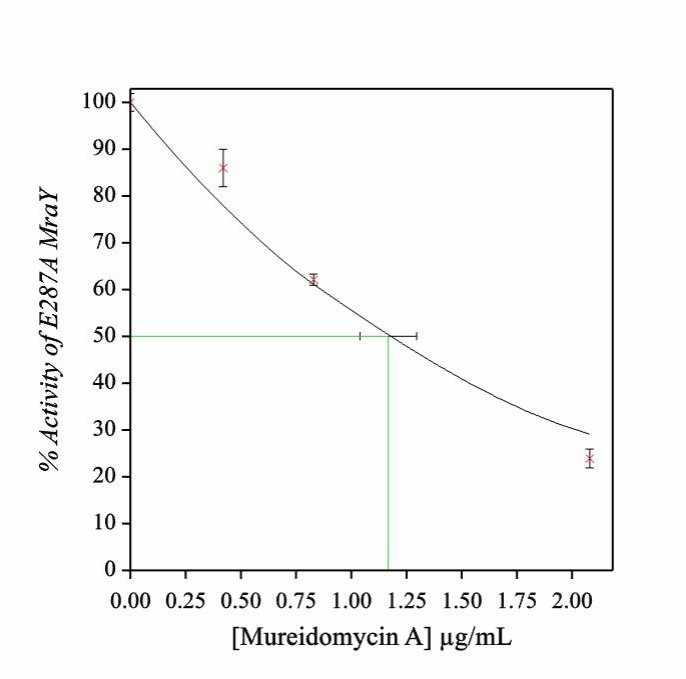

# Appendix 4: NMR spectra of RWXXW peptides

*Compounds which contained solvent peaks were dried further under high vacuum before any biological work was conducted.*

**$^{1}$H-NMR L-Tryptophan methyl ester hydrochloride [17]**

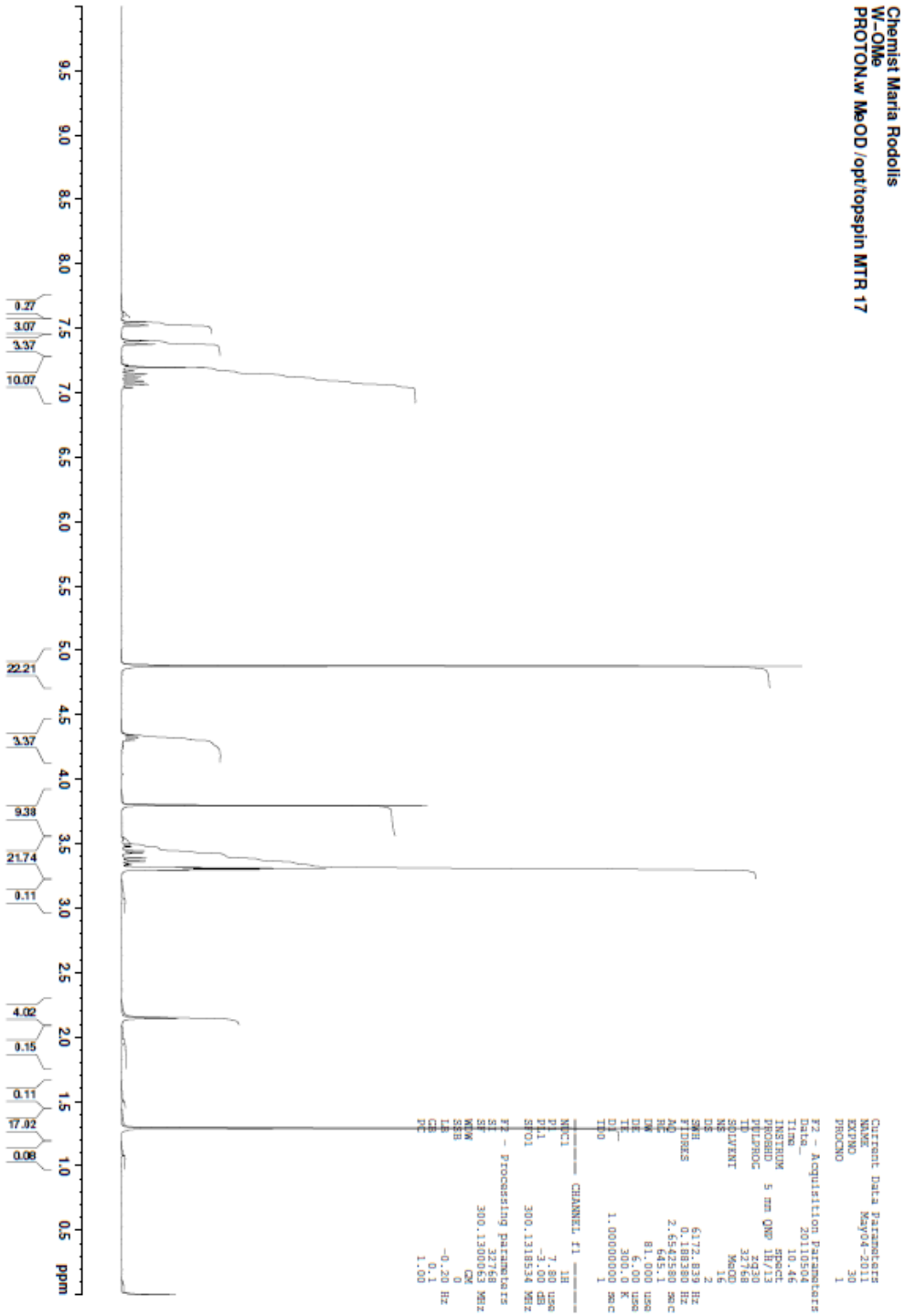

**$^{1}$H-NMR L-Tryptophan octyl ester [18]**

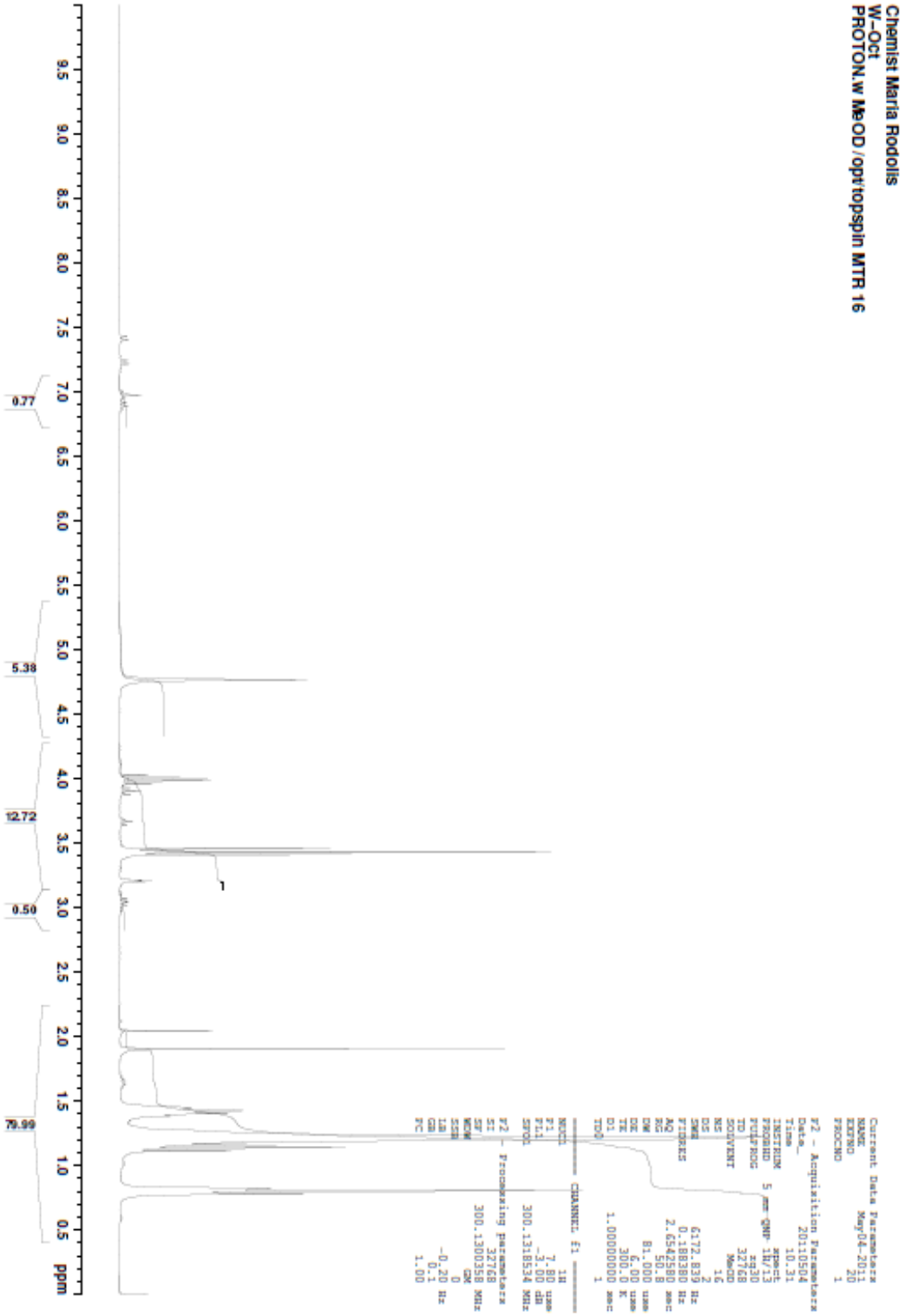

**$^{1}$H-NMR Glycine octyl ester [19]**

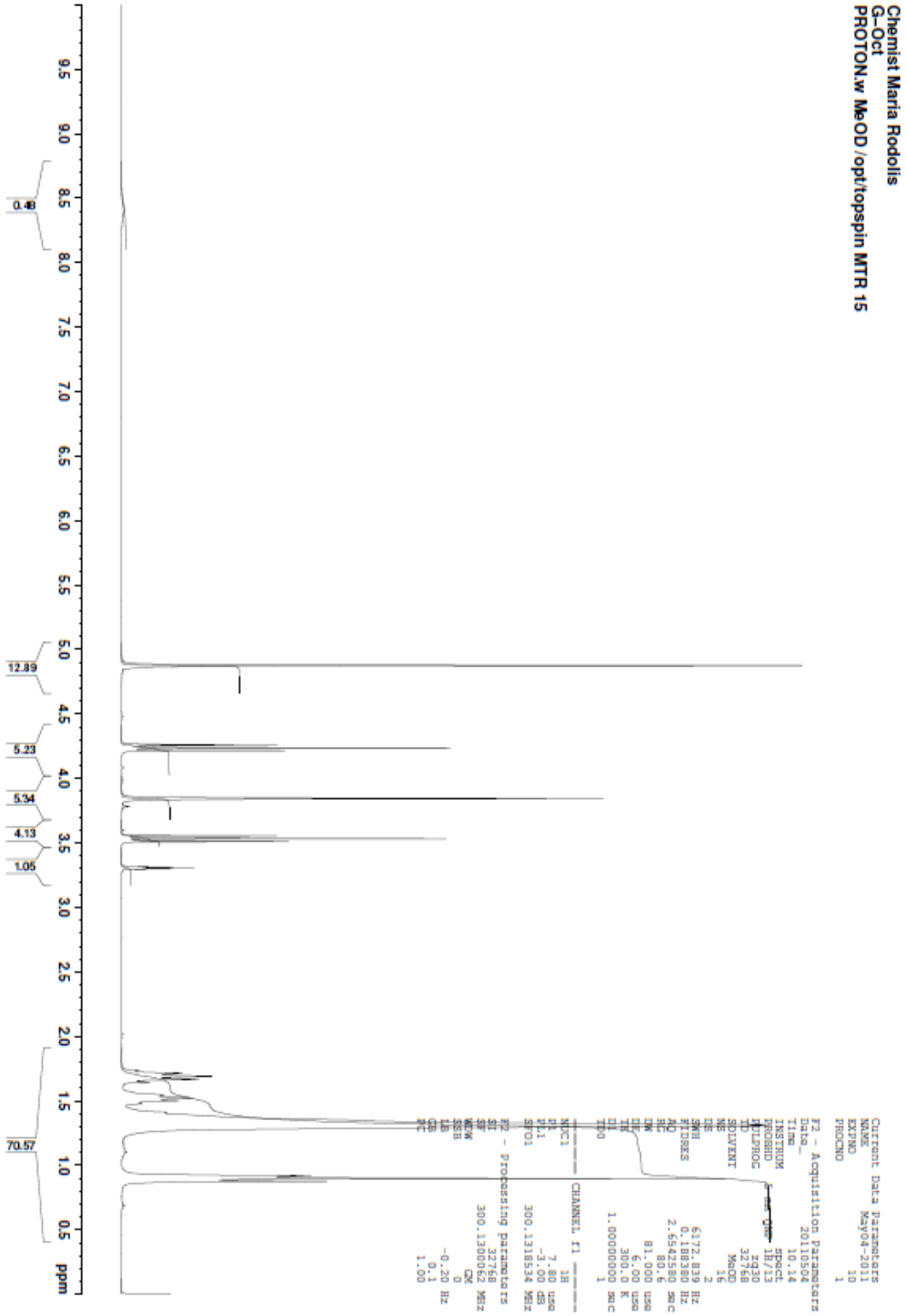

## $^{13}$C-NMR Glycine octyl ester [19]

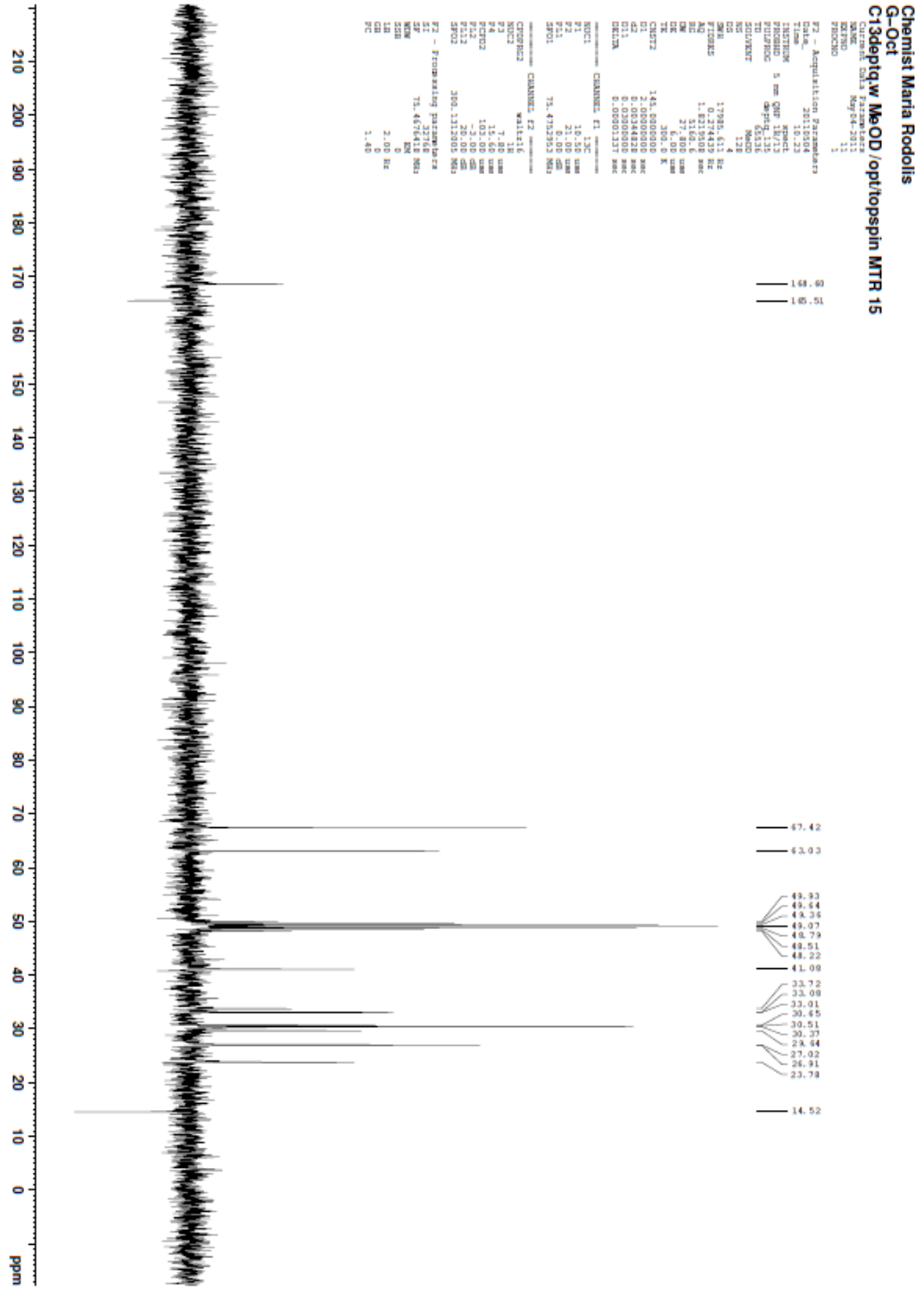

**$^{1}$H-NMR *N*-octanoyl glycine [20]**

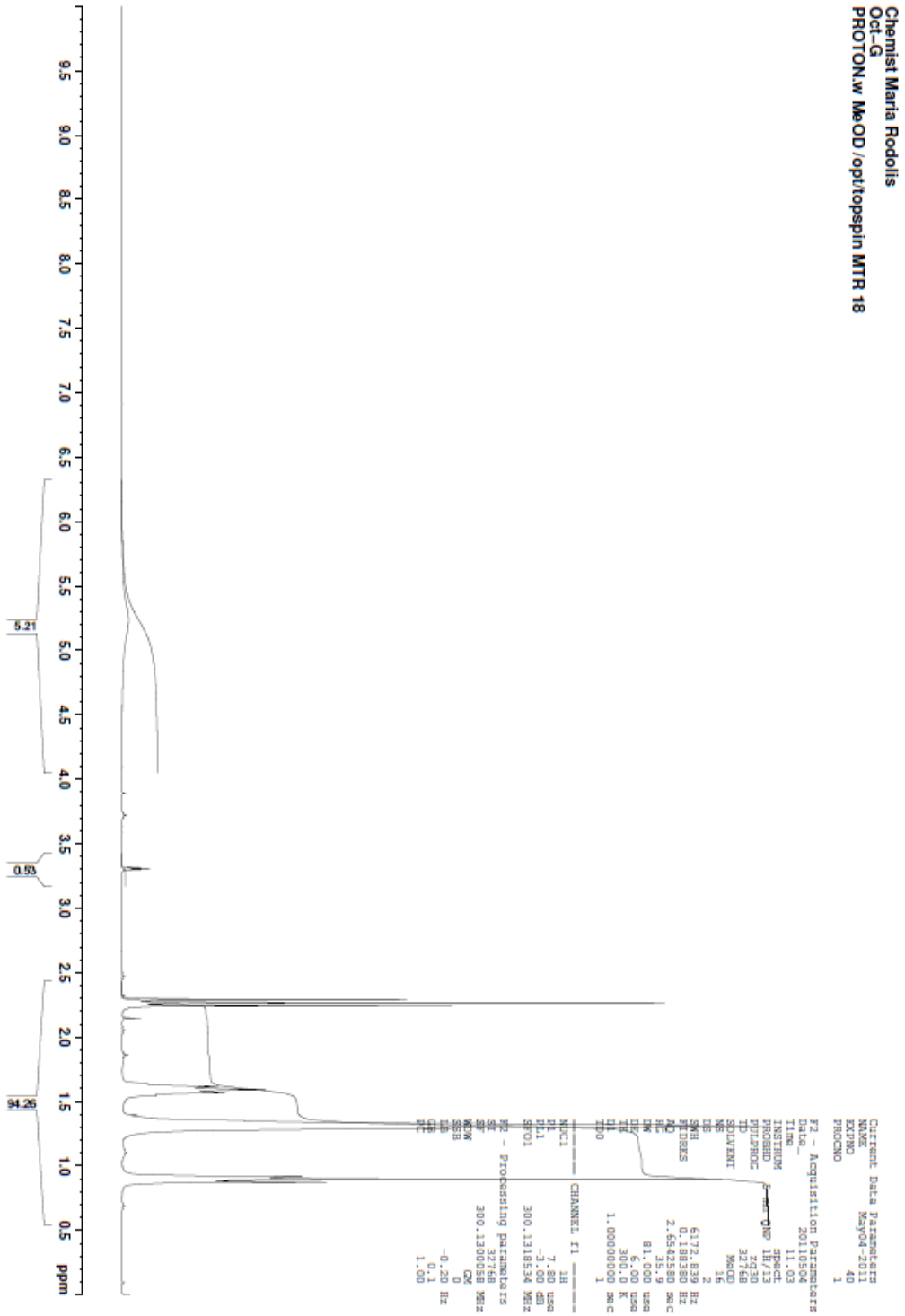

**$^{1}$H-NMR L-Arginyl-L-tryptophan methyl ester; $H_2N$-RW-OMe [1]**

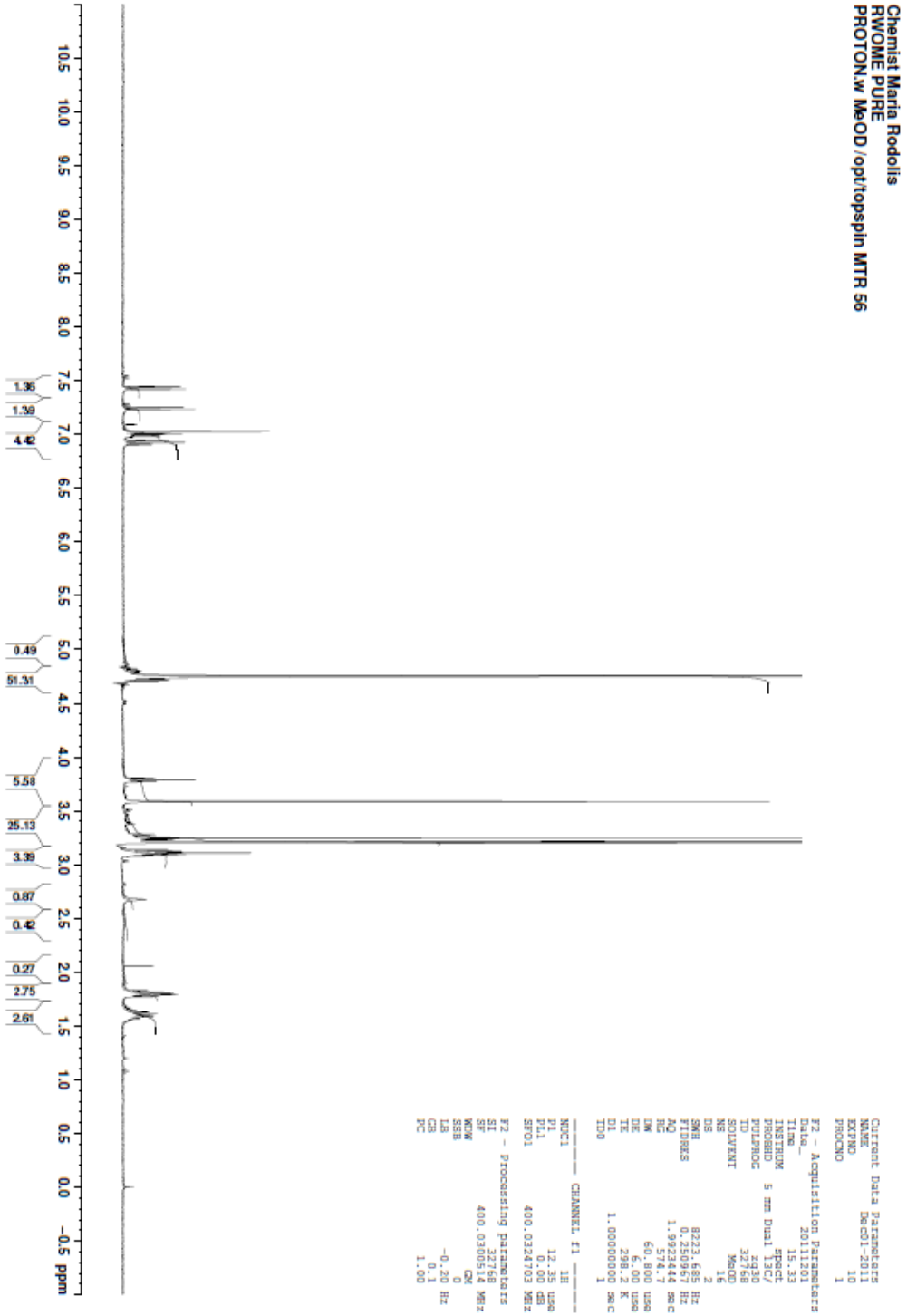

**$^{1}$H-NMR *N*-octanoyl-L-arginyl-L-tryptophan methyl ester; Octanoyl-RW-OMe [2]**

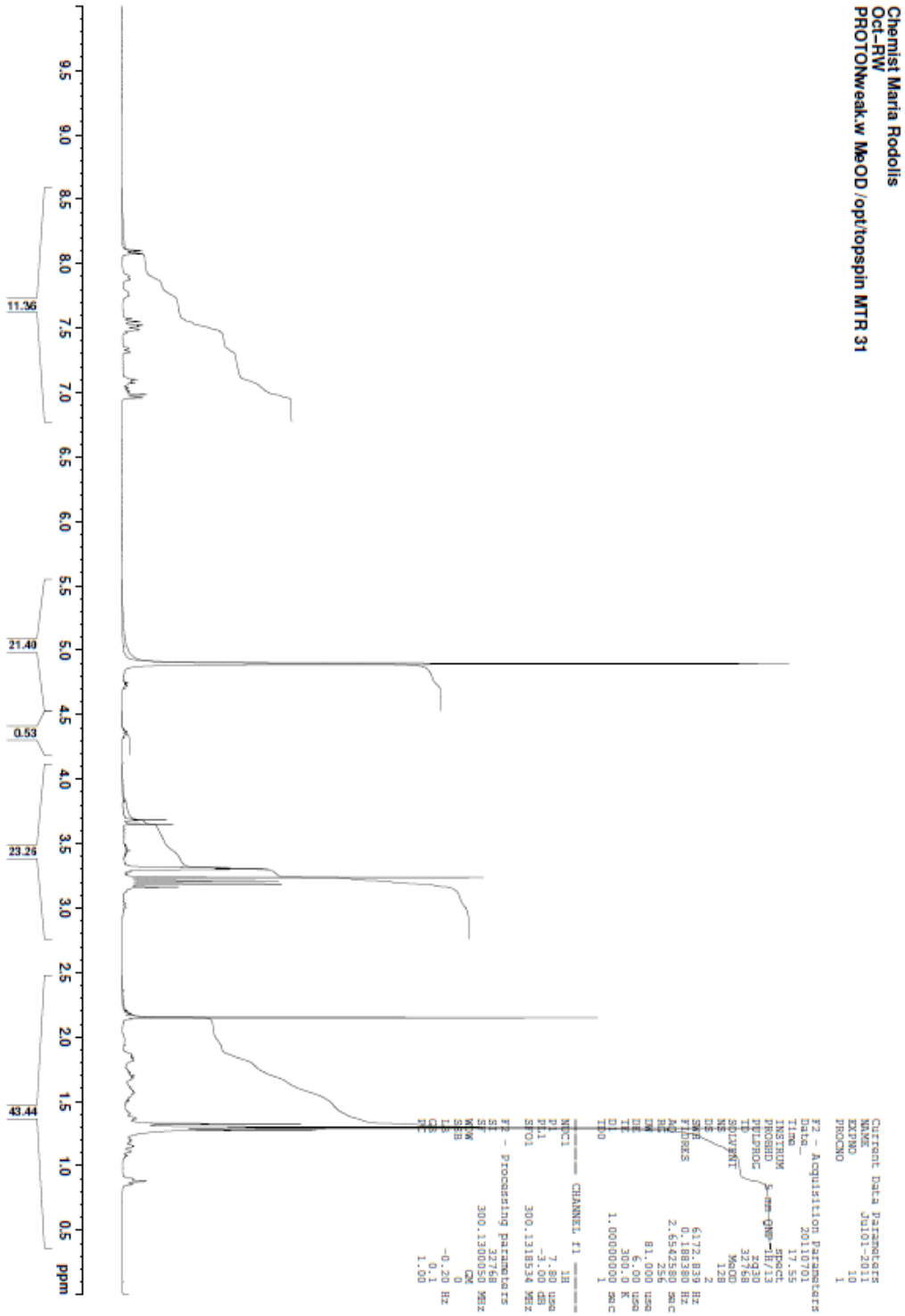

## $^{1}$H-NMR L-Arginyl-L-tryptophan octyl ester; $H_2N$-RW-Oct [3]

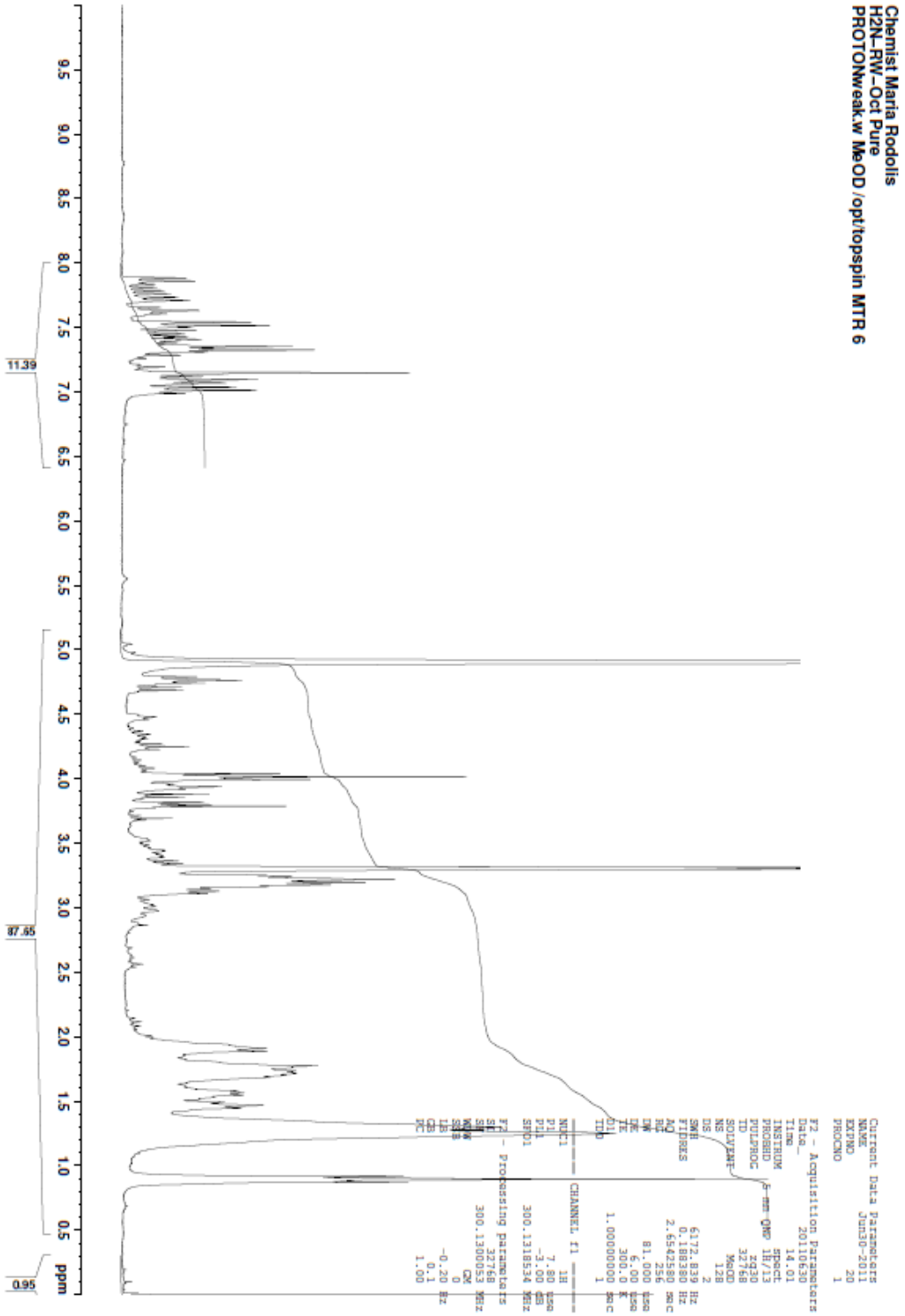

## $^{1}$H-NMR Glycyl-L-tryptophan methyl ester; $H_2N$-GW-OMe [4]

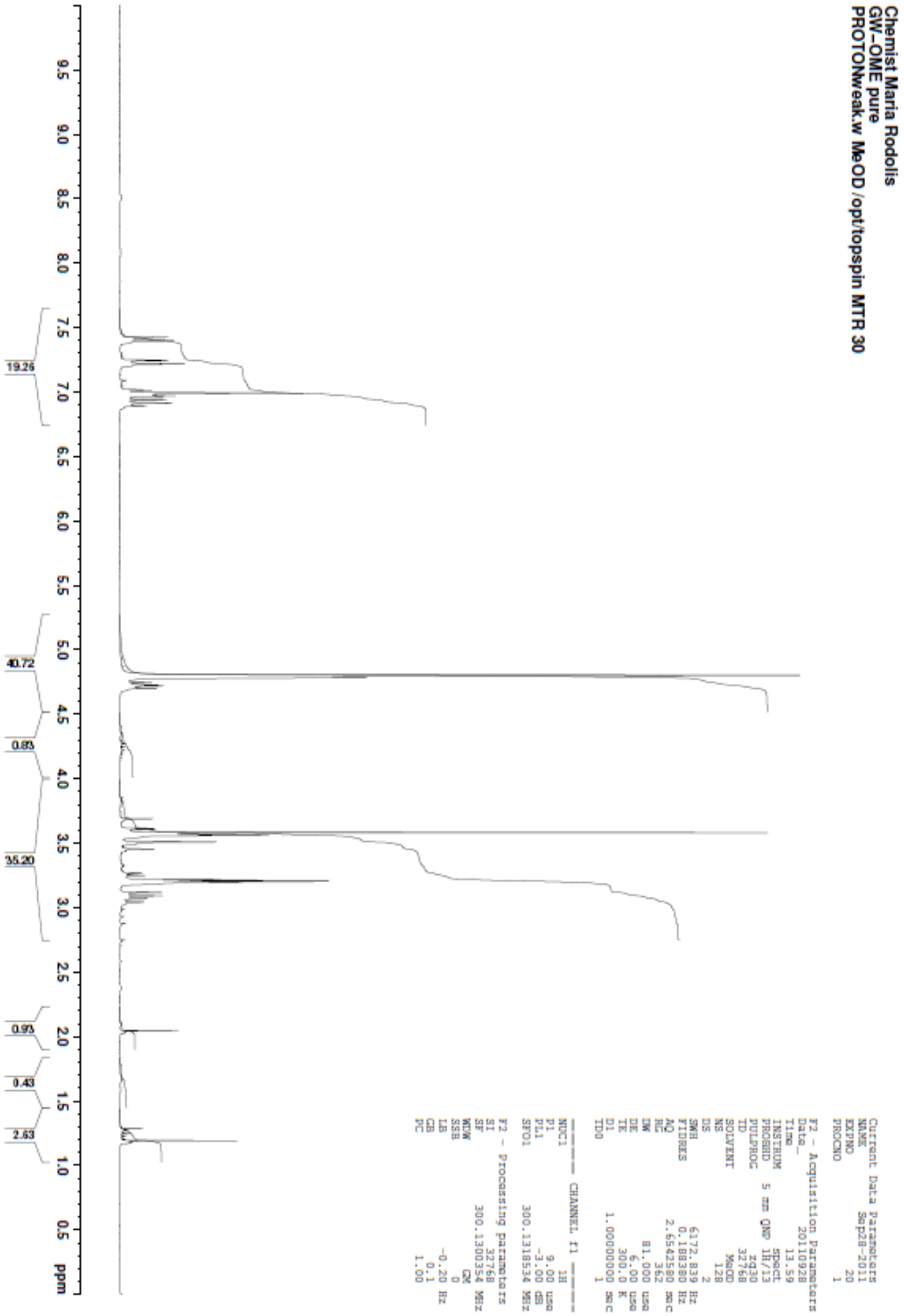

## $^{13}$C-NMR Glycyl-L-tryptophan methyl ester; $H_2N$-GW-OMe [4]

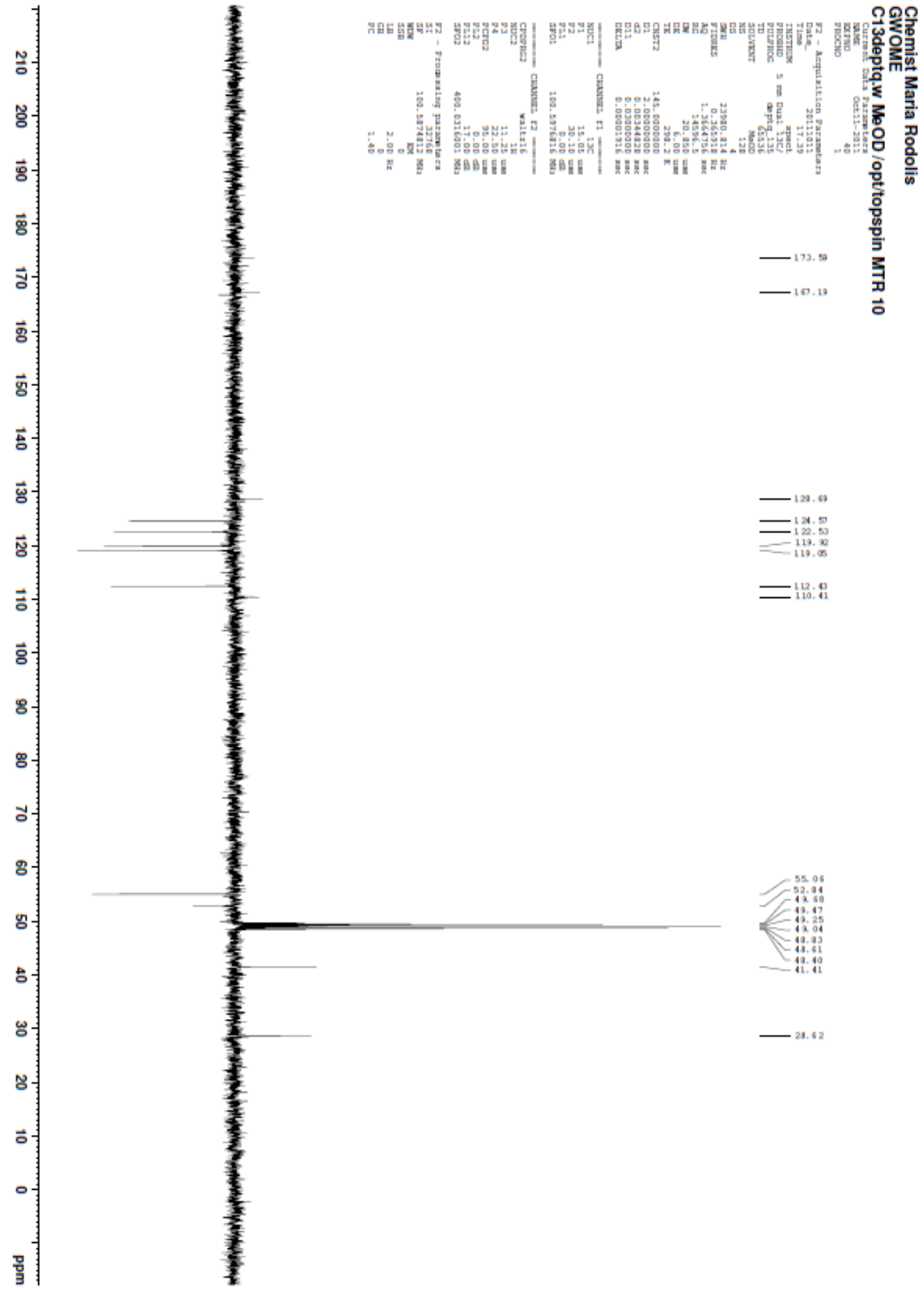

**$^{1}$H-NMR *N*-octanoyl-L-glycyl-L-tryptophan methyl ester; Octanoyl-GW-OMe [5]**

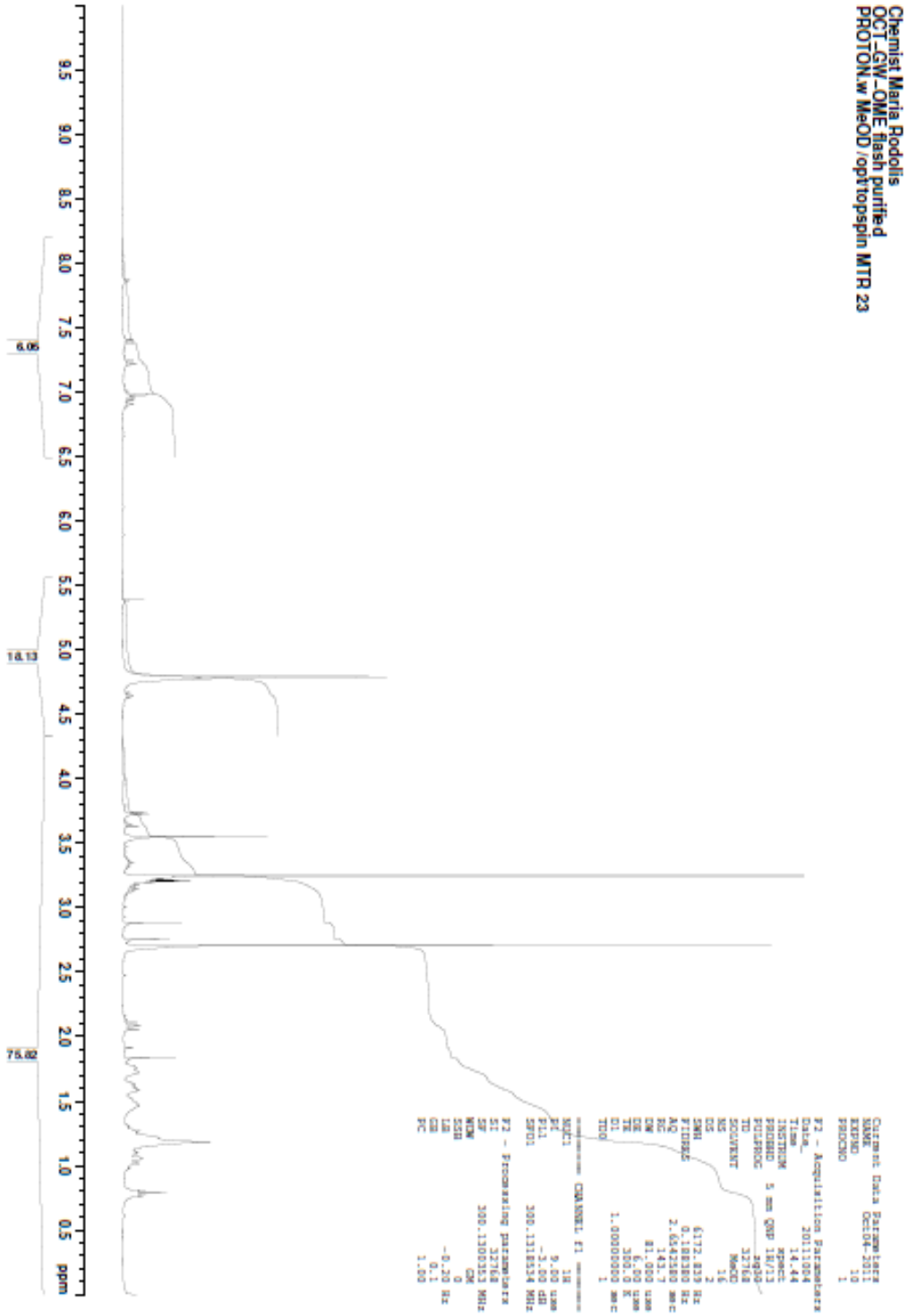

**$^{1}$H-NMR Glycyl-L-tryptophan octyl ester; $H_2N$-GW-Oct [6]**

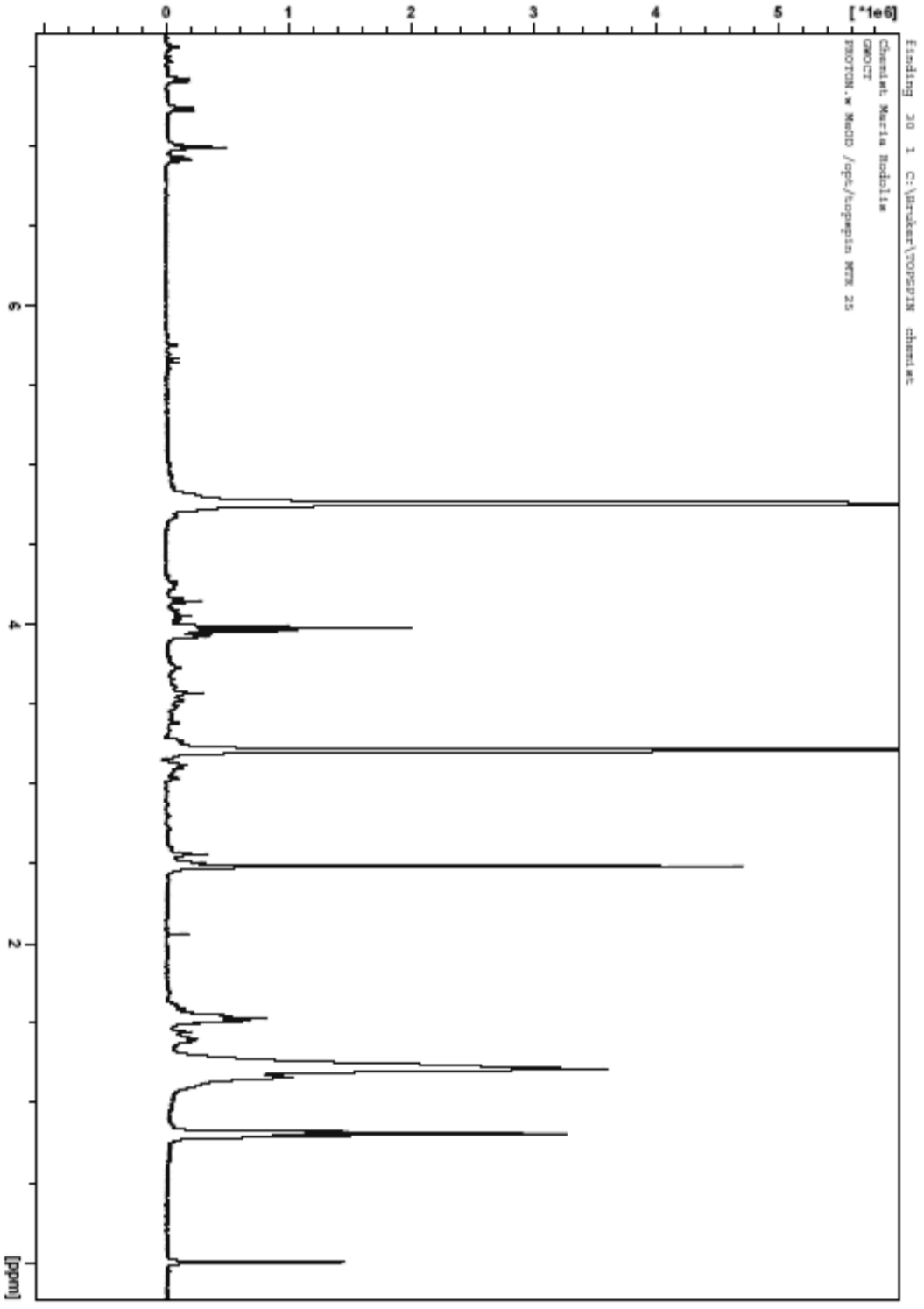

**$^{1}$H-NMR *N*-octanoyl-L-arginyl-glycine; Octanoyl-RG-OH [8]**

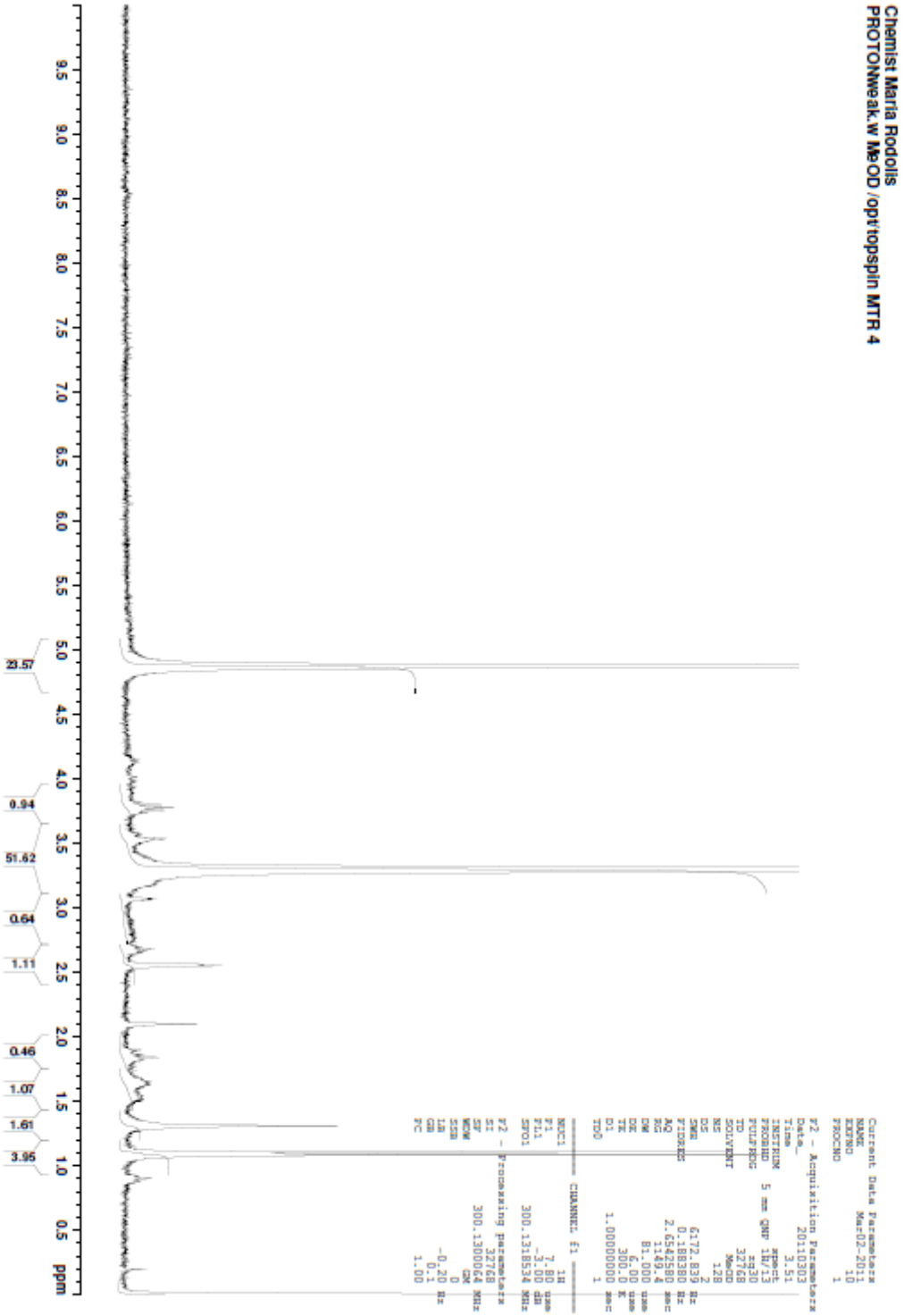

## $^{13}$C-NMR *N*-octanoyl-L-arginyl-glycine; Octanoyl-RG-OH [8]

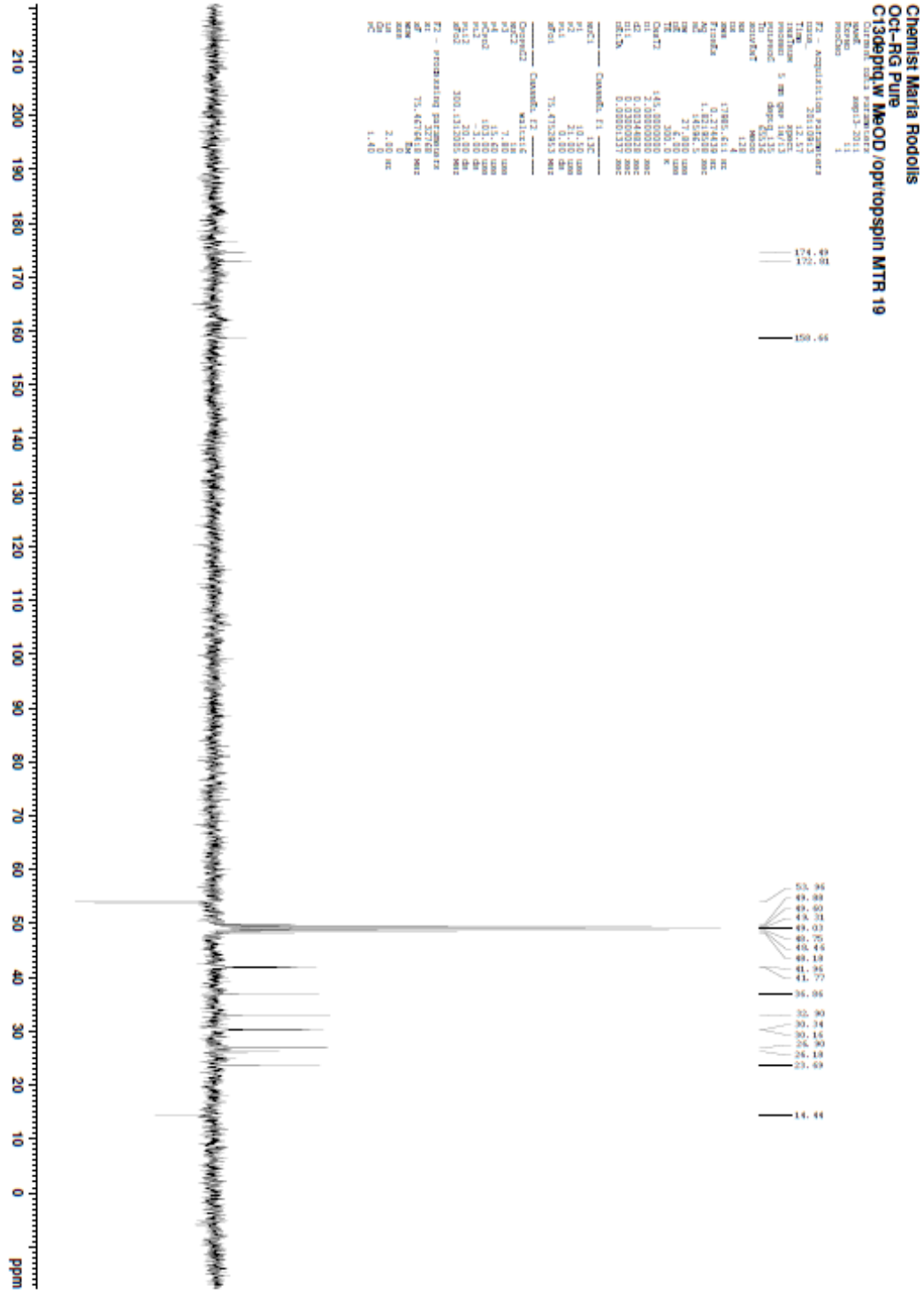

## $^{1}$H-NMR L-Arginyl-glycine octyl ester; $H_2$N-RG-Oct [9]

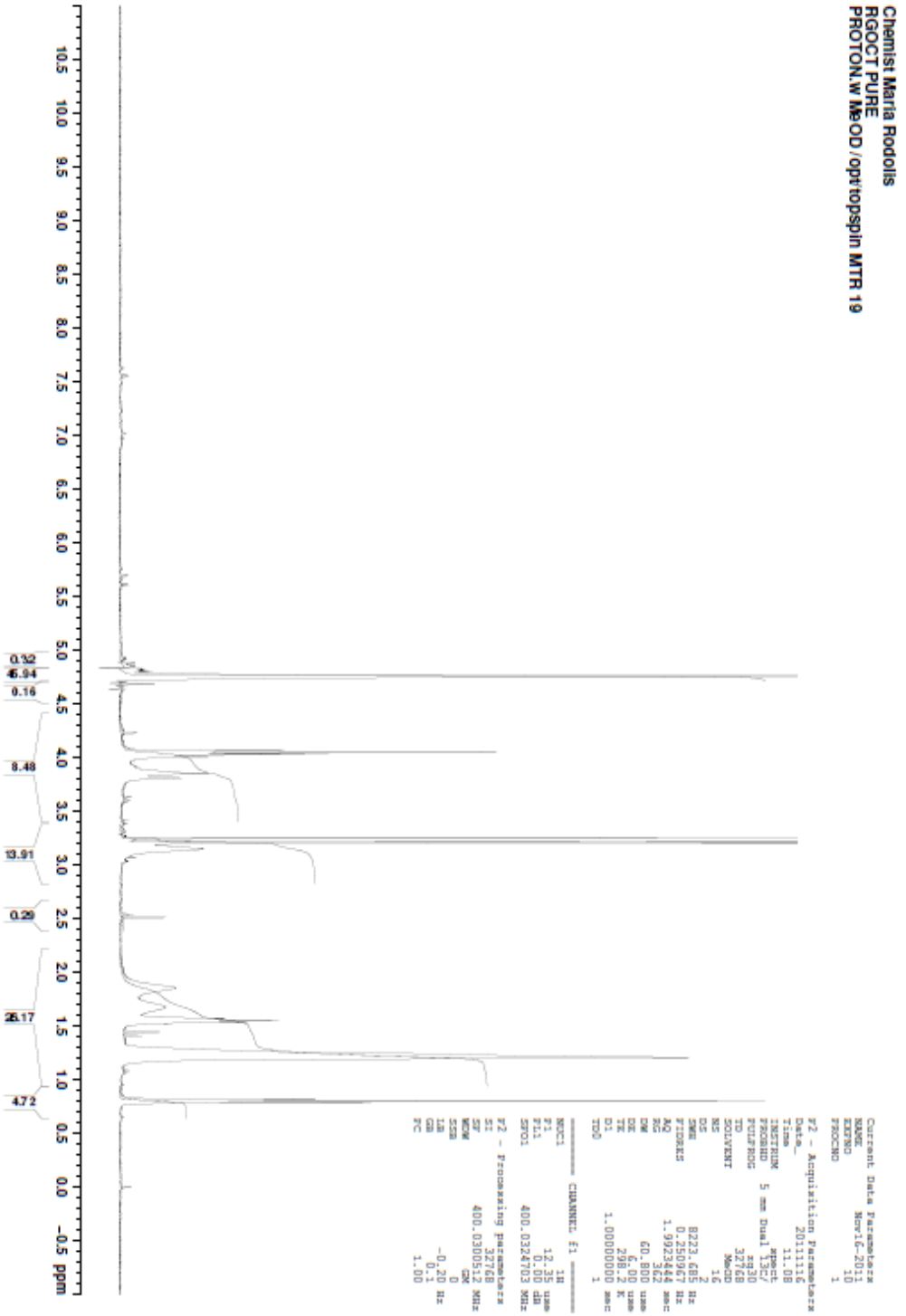

**$^{1}$H-NMR L-Arginyl-glycine; $H_2N$-RG-OH [7]**

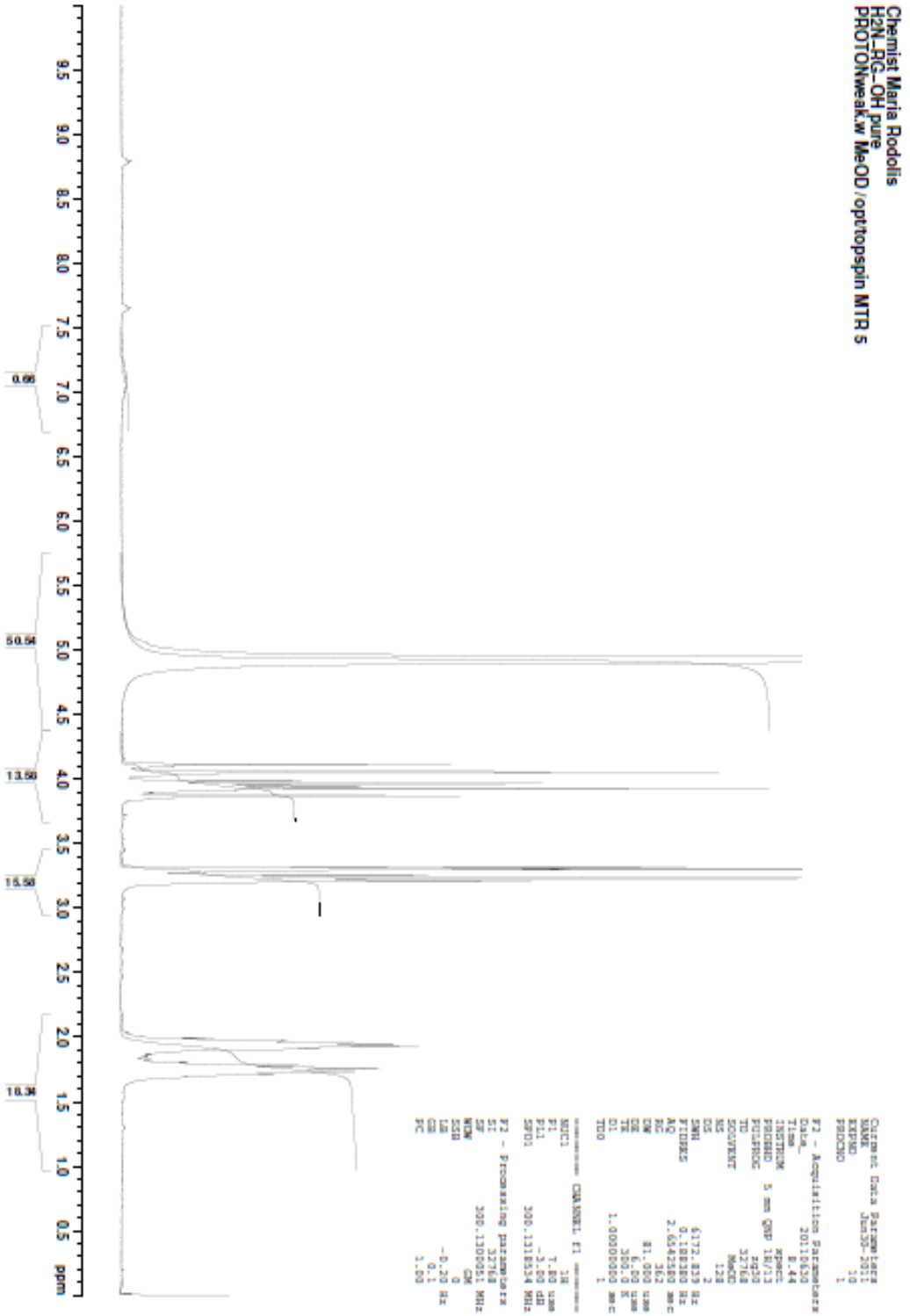

## $^{1}$H-NMR L-Arginyl-L-tryptophyl-glycyl-L-leucinyl-L-tryptophan; RWGLW [10]

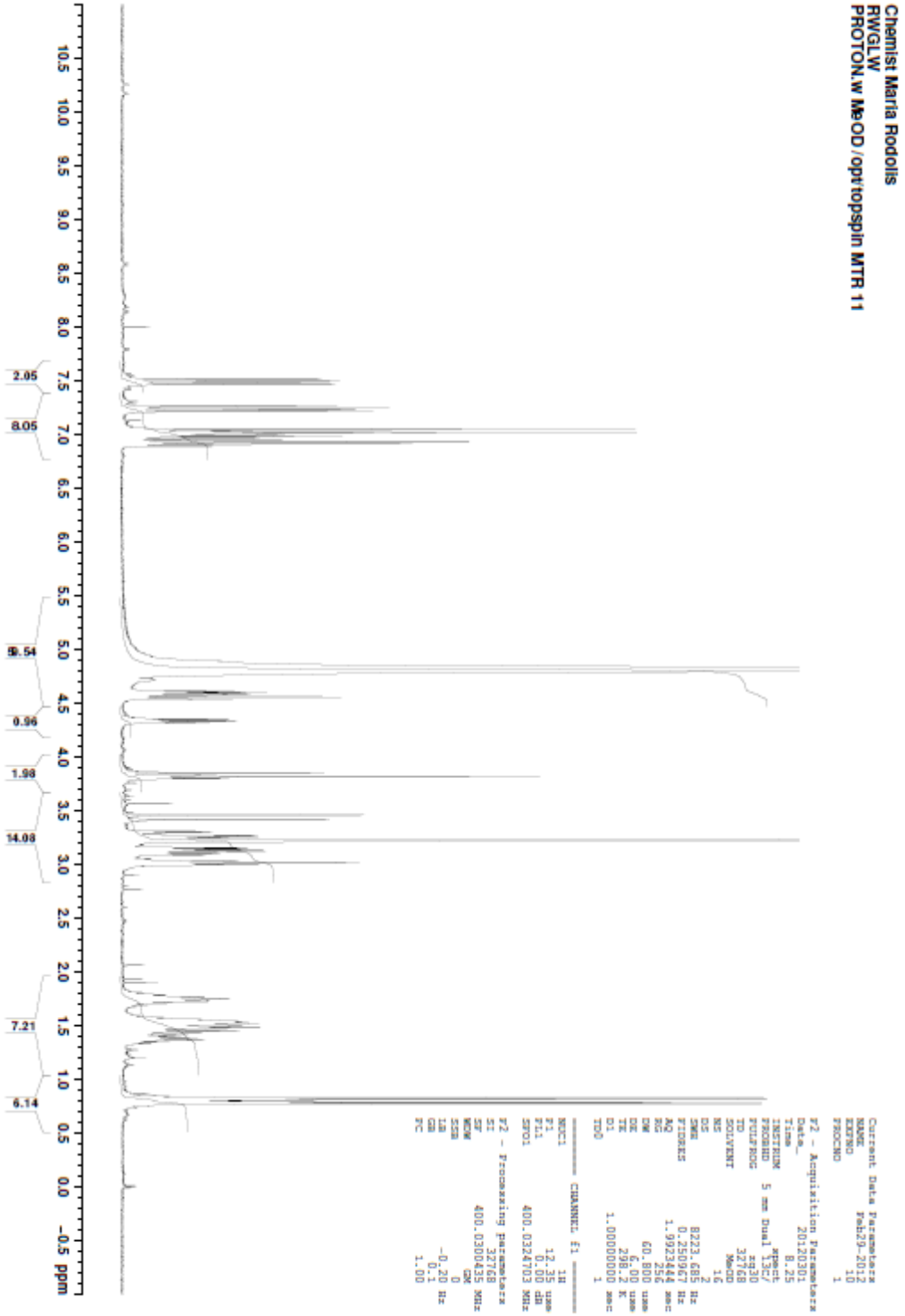

# $^{1}$H-NMR L-Arginyl-glycyl-glycyl-L-leucinyl-L-tryptophan; RGGLW [11]

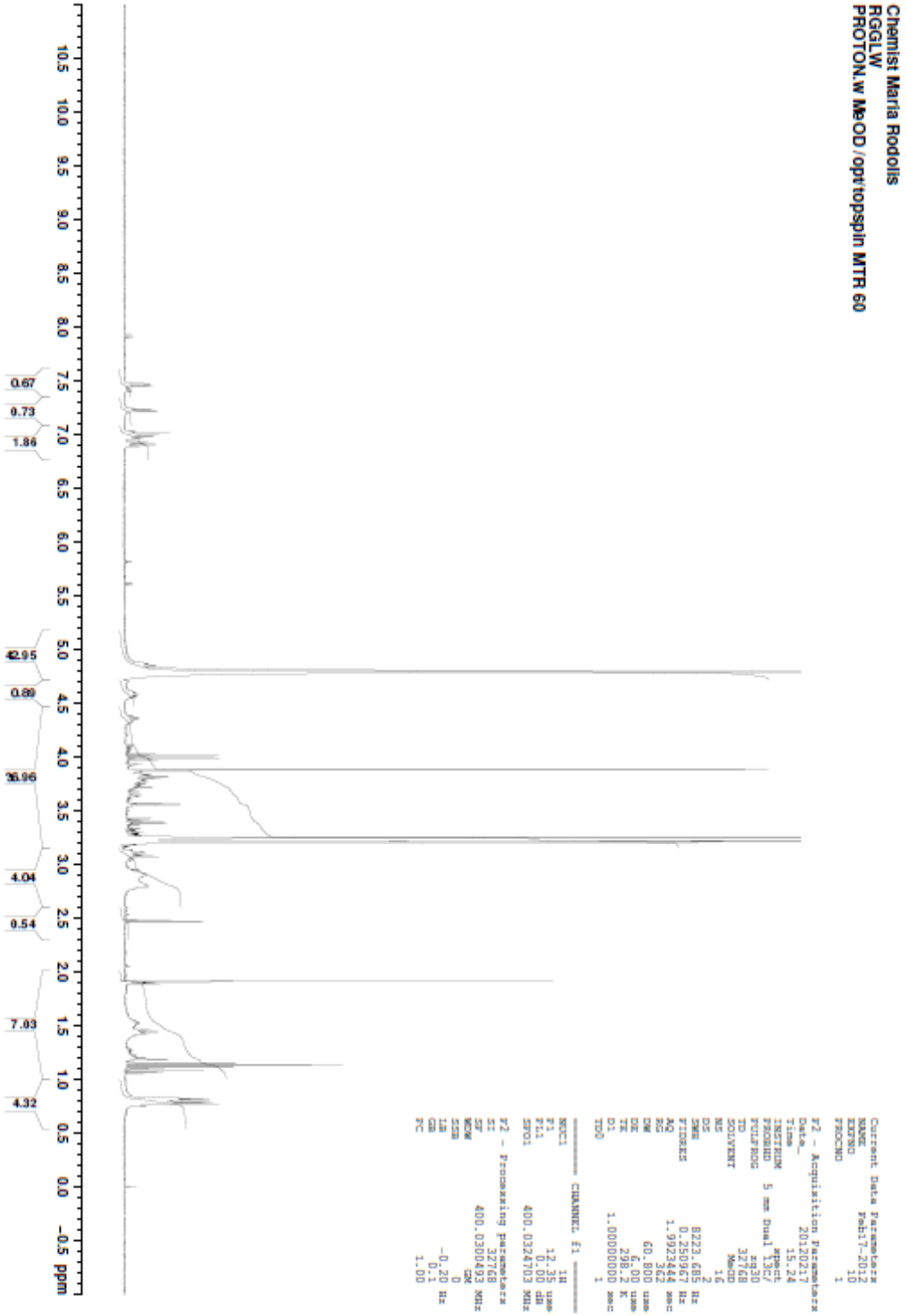

# $^{1}$H-NMR L-Arginyl-L-tryptophyl-glycyl-glycyl-L-tryptophan; RWGGW [13]

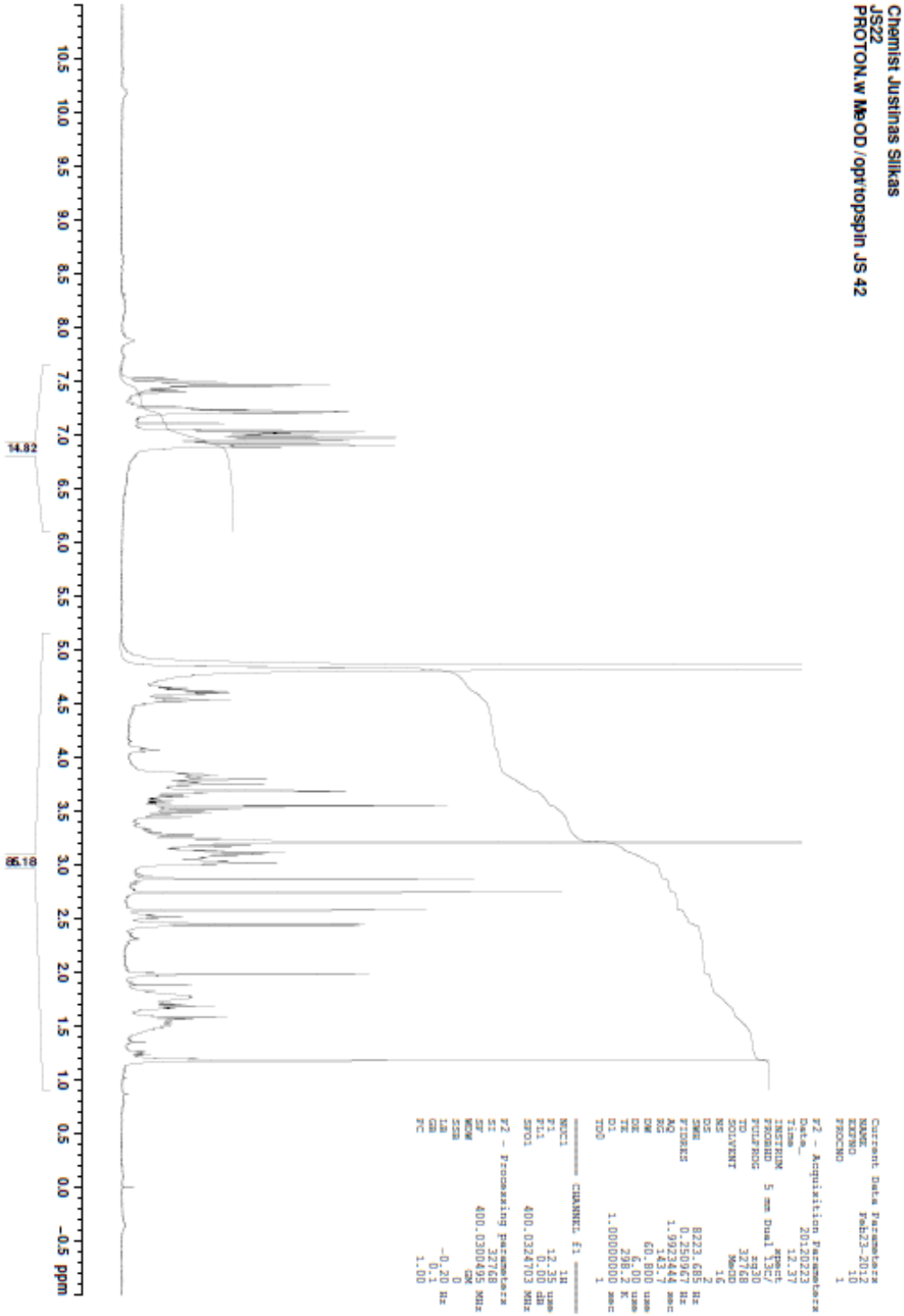

**$^{1}$H-NMR L-Glutamyl-L-histidyl-L-tryptophyl-glycyl-glycyl-glycine; EHWGGG [15]**

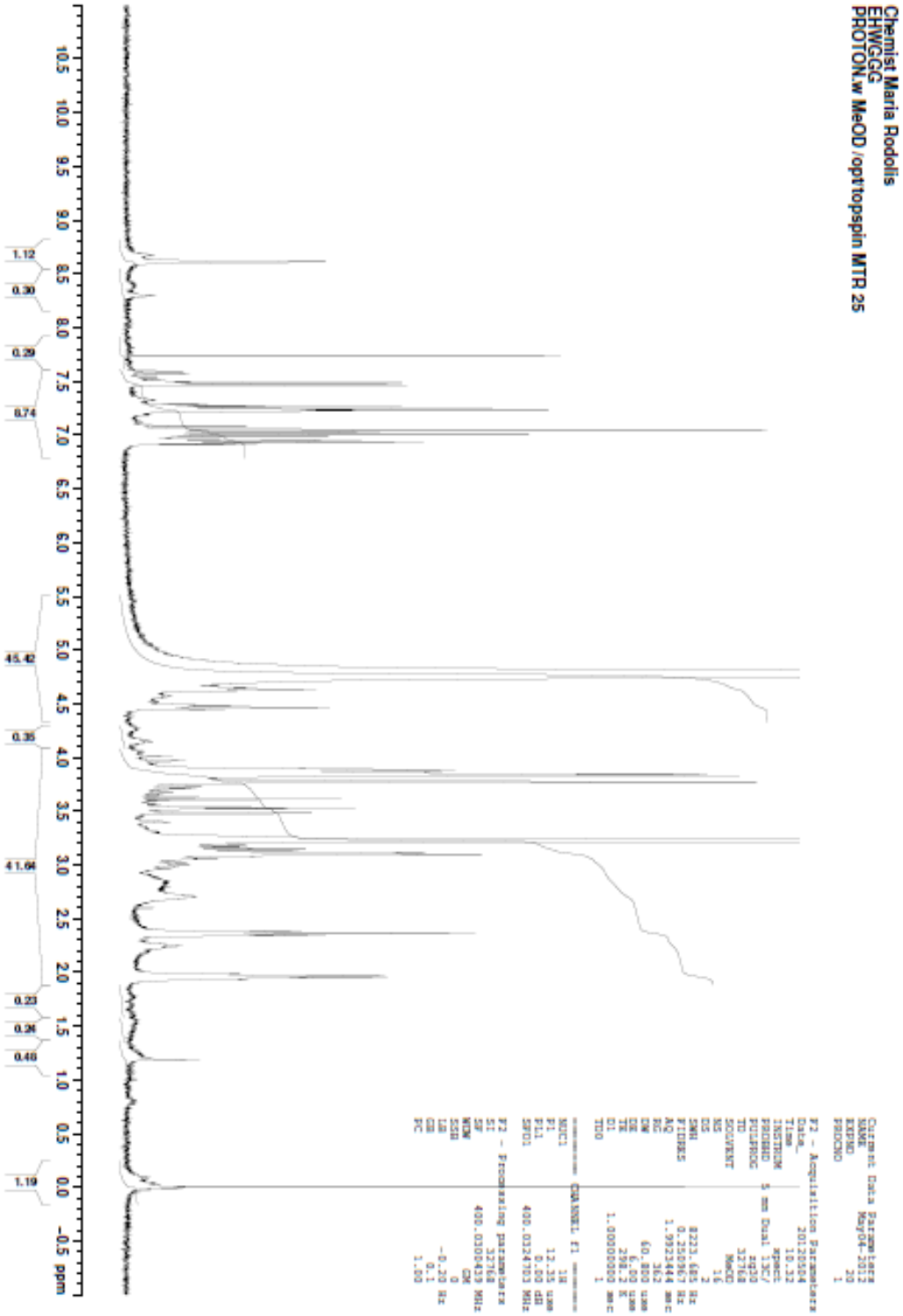

**$^{1}$H-NMR L-Glutamyl-L-arginyl-L-tryptophyl-glycyl-glycyl-L-tryptophan; ERWGGW [16]**

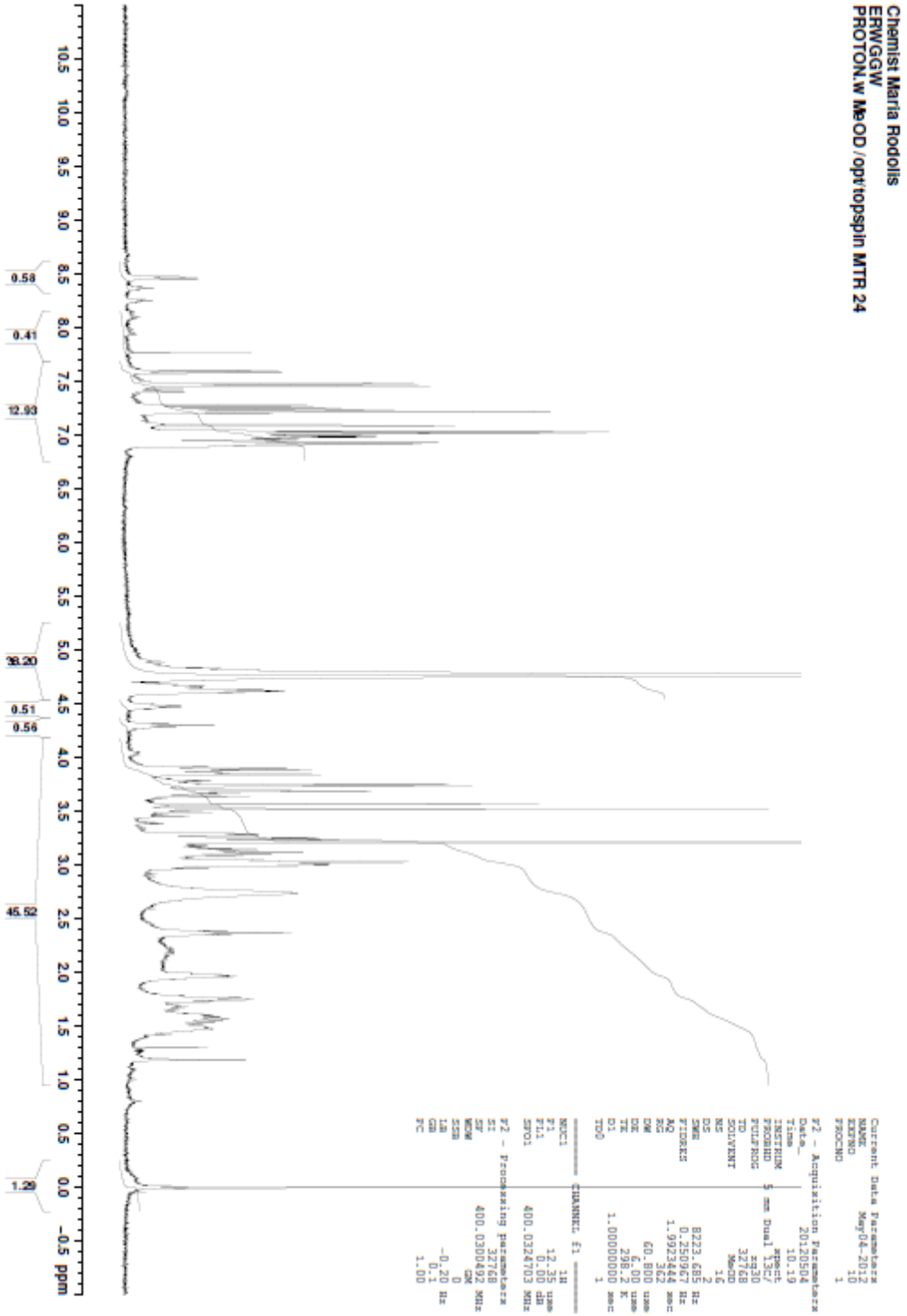

**$^{1}$H-NMR 2',3'-O-Isopropylidene uridine [31]**

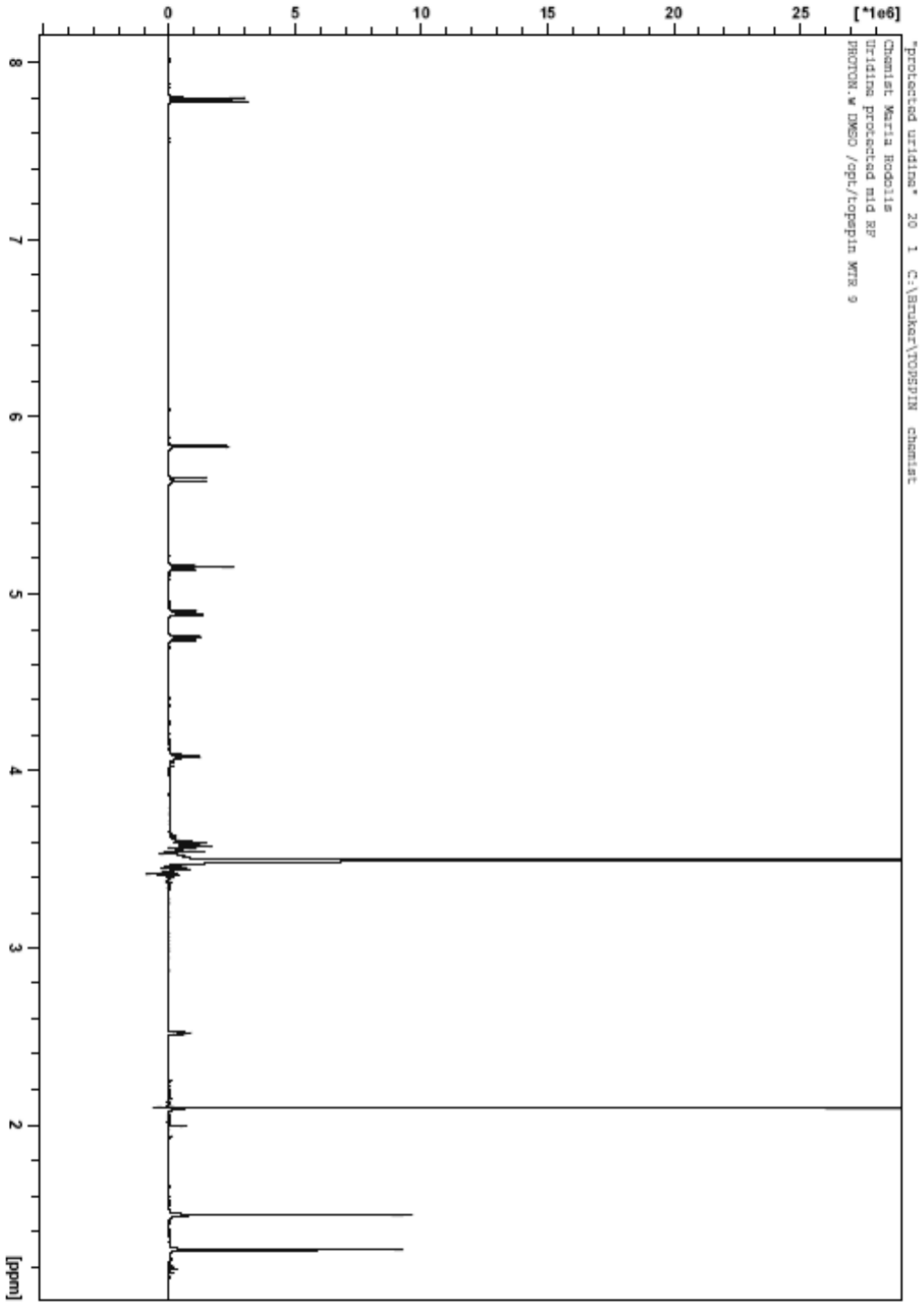

## $^{13}$C-NMR 2',3'-O-Isopropylidene uridine [31]

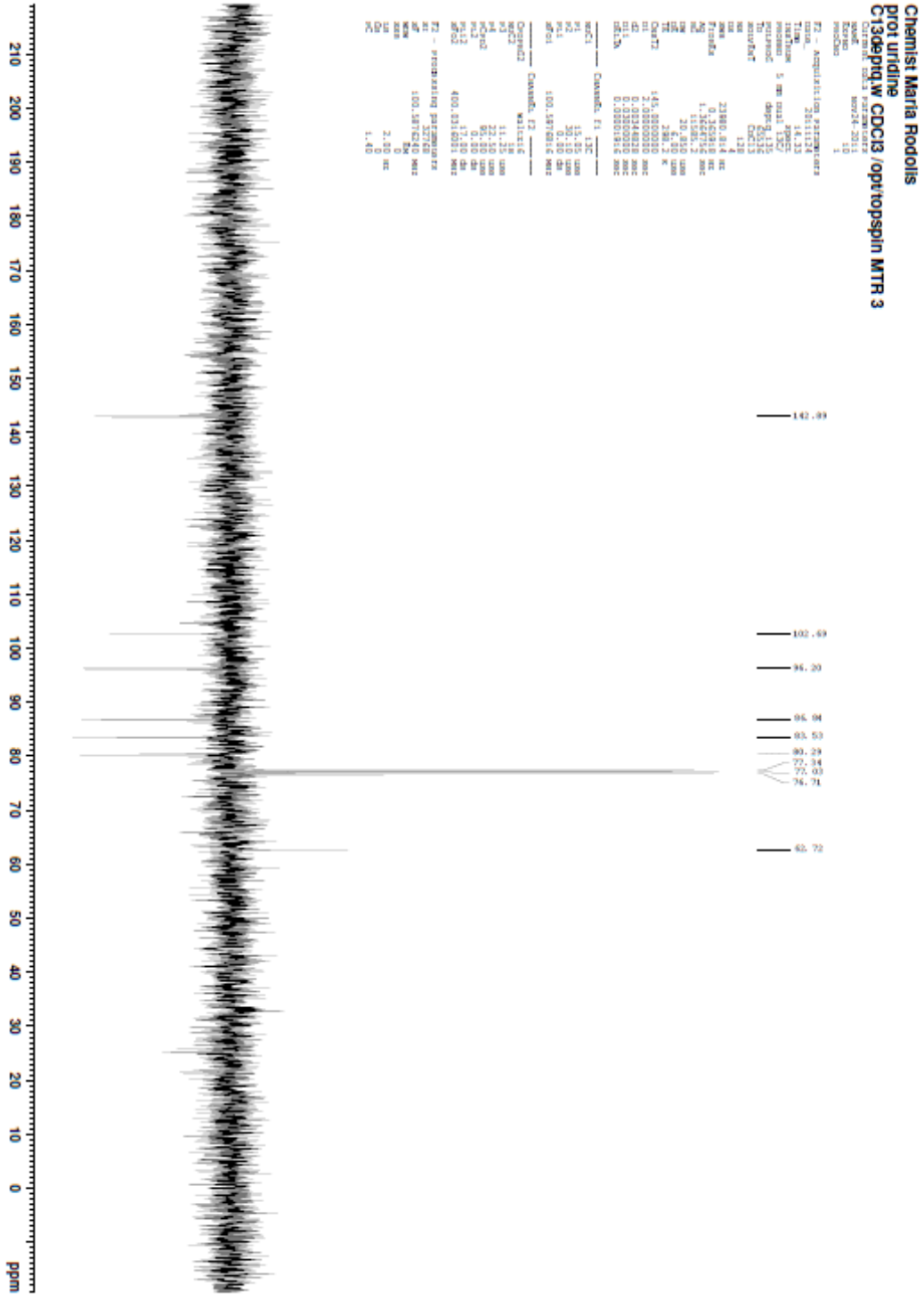

**$^{1}$H-NMR 5'-succinyl-2', 3'-O-isopropylidene uridine [32]**

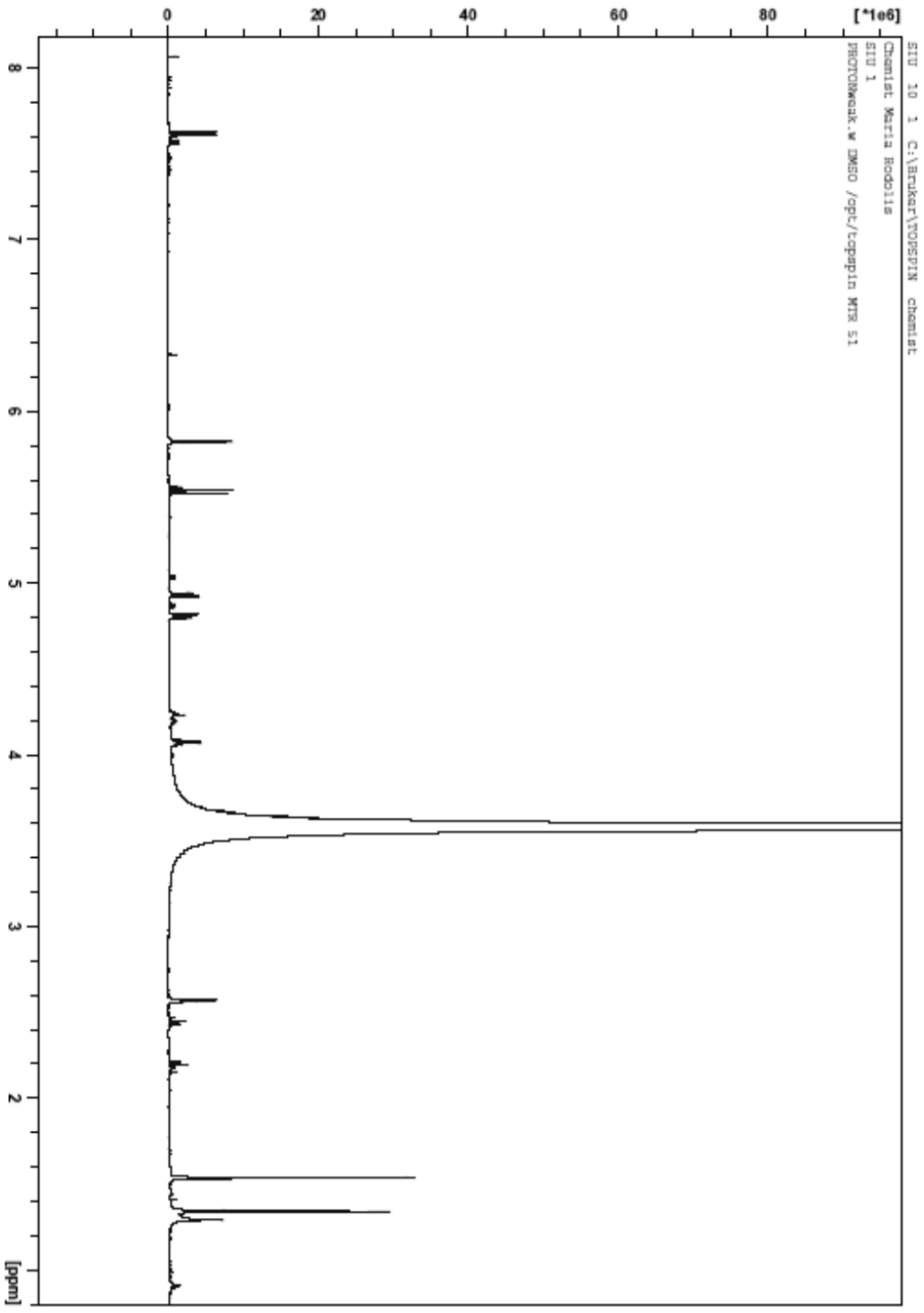

**$^{13}$C-NMR 5'-succinyl-2', 3'-O-isopropylidene uridine [32]**

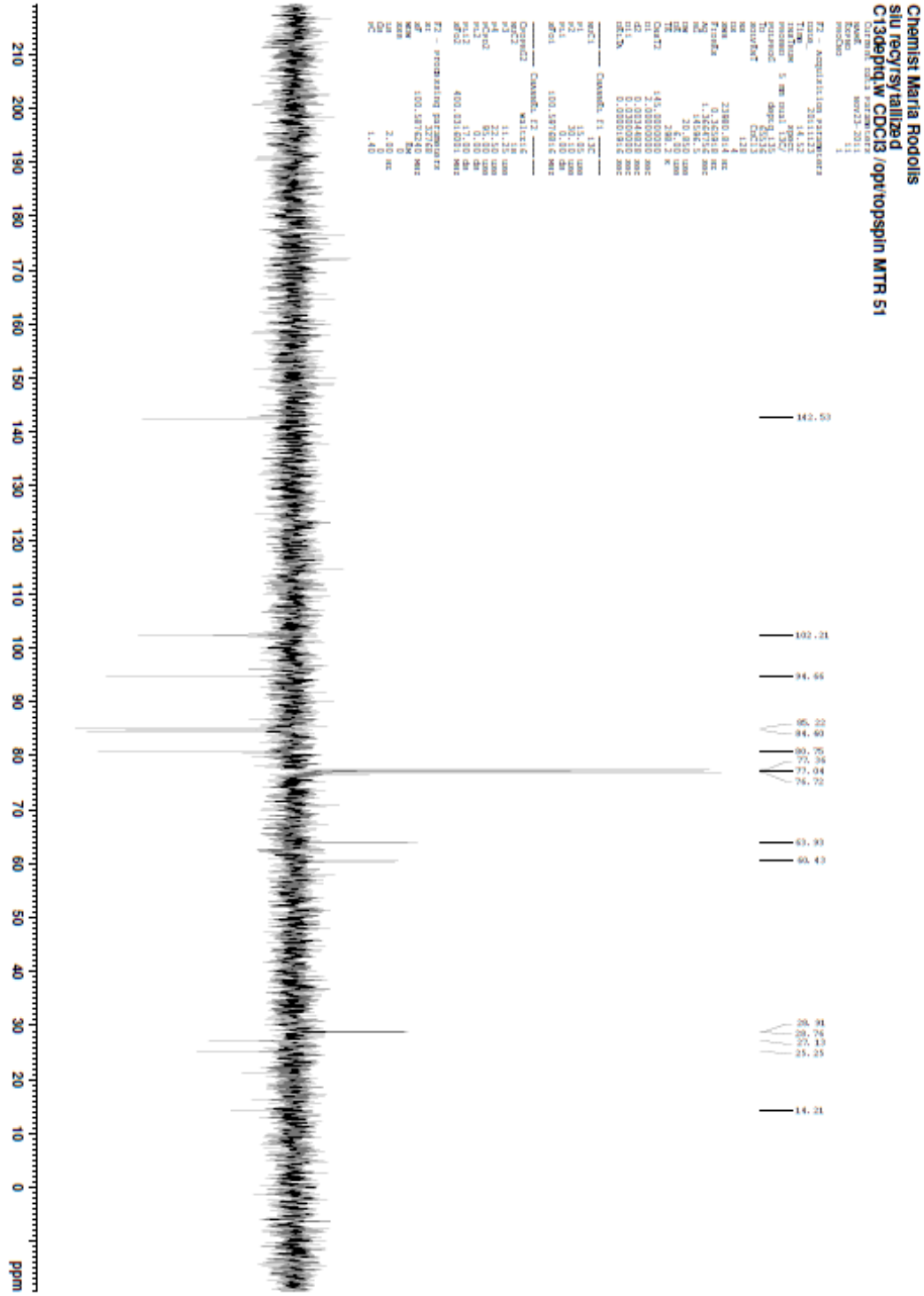

**$^{1}$H-NMR 5'-Succinyl-2',3'-O-isopropylideneuridyl-glycl-glycyl-glycyl-L-arginine [27]**

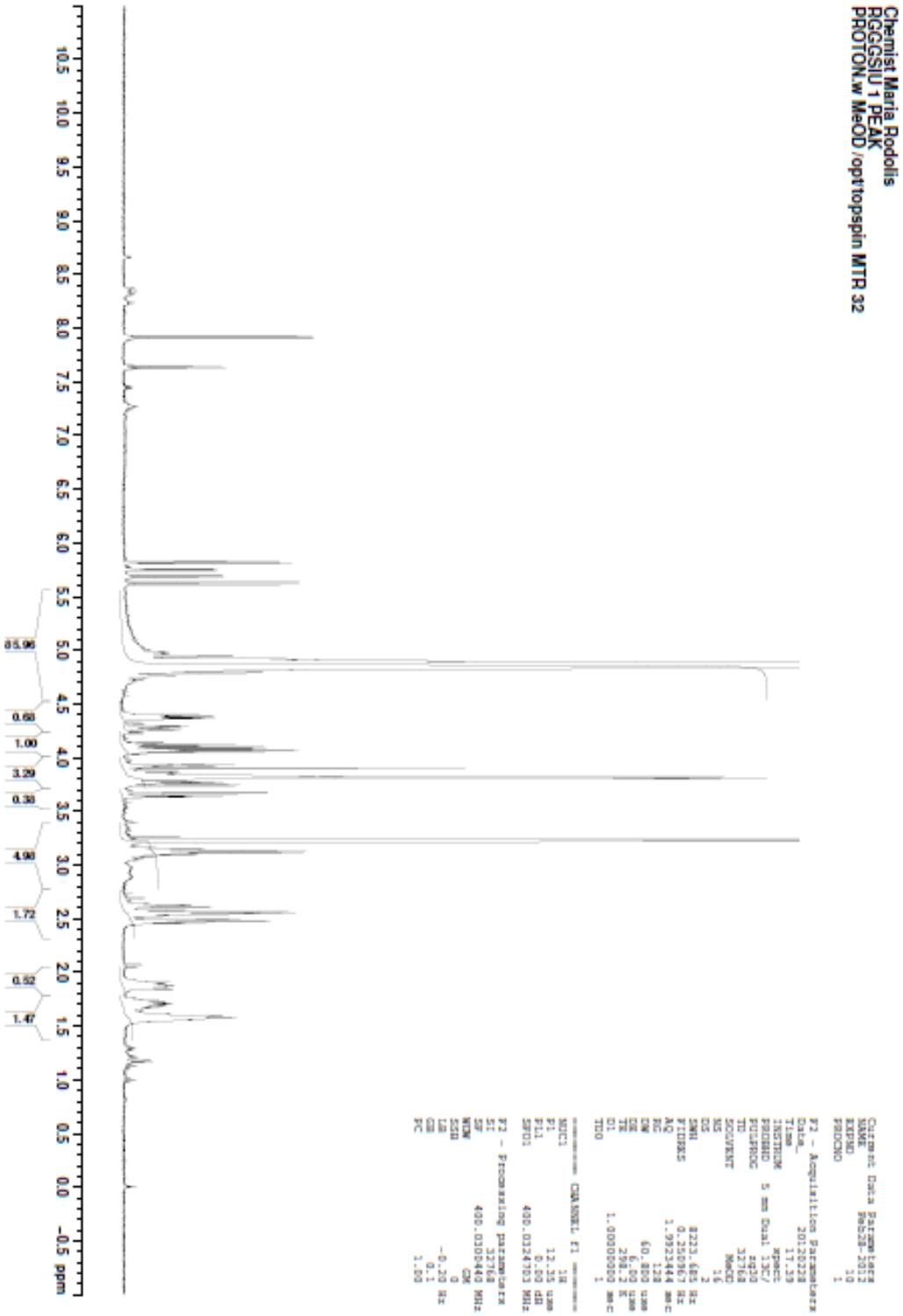

**$^{1}$H-NMR 5'-Succinyl-2',3'-O-isopropylideneuridyl-glycl-glycyl-L-tryptophyl-glycine [28]**

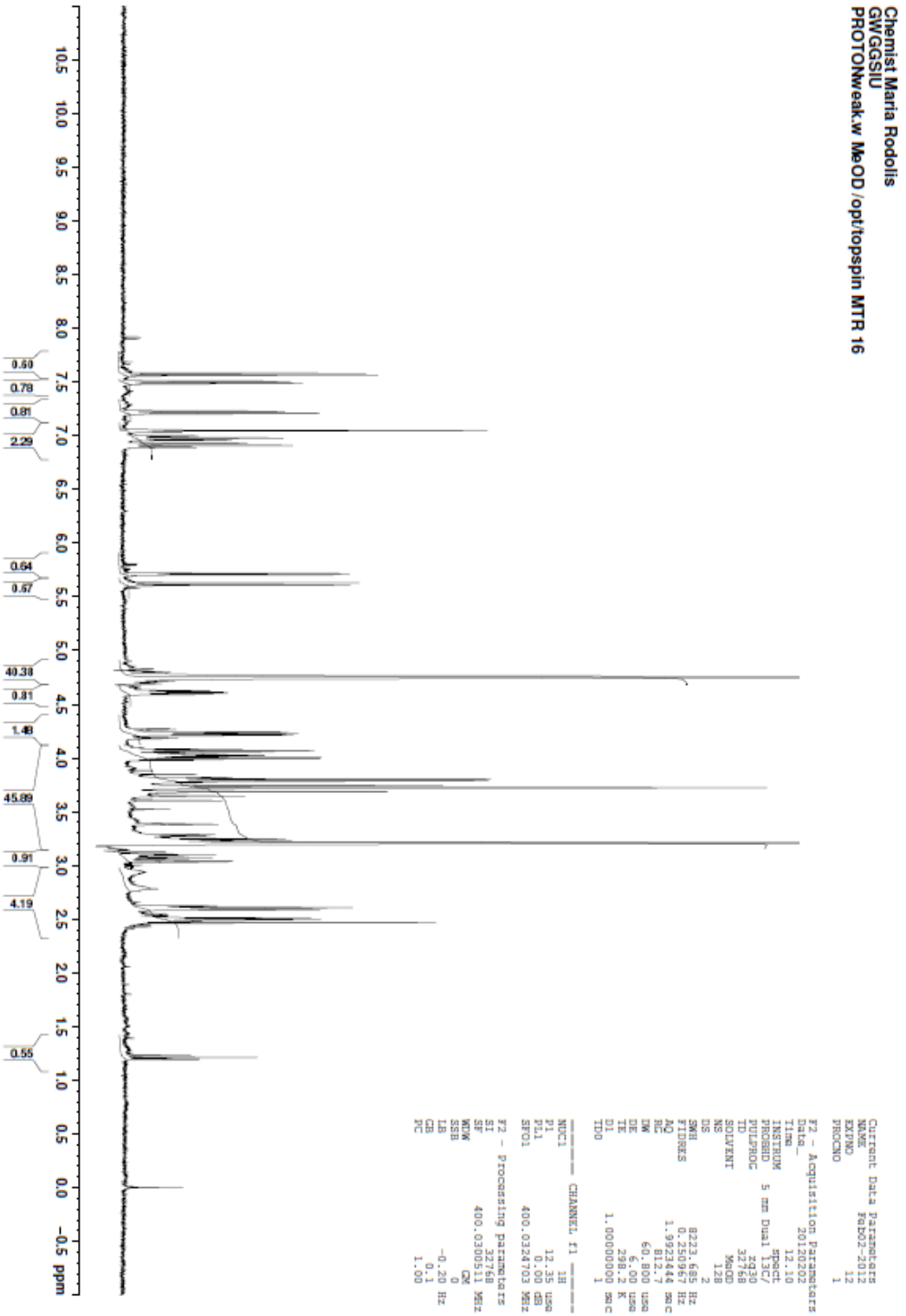

**$^{1}$H-NMR 9*H*-fluoren-9-ylmethyl (2,5-dioxotetrahydrofuran-3-yl)carbamate; *N*-Fmoc-aspartic anhydride [33]**

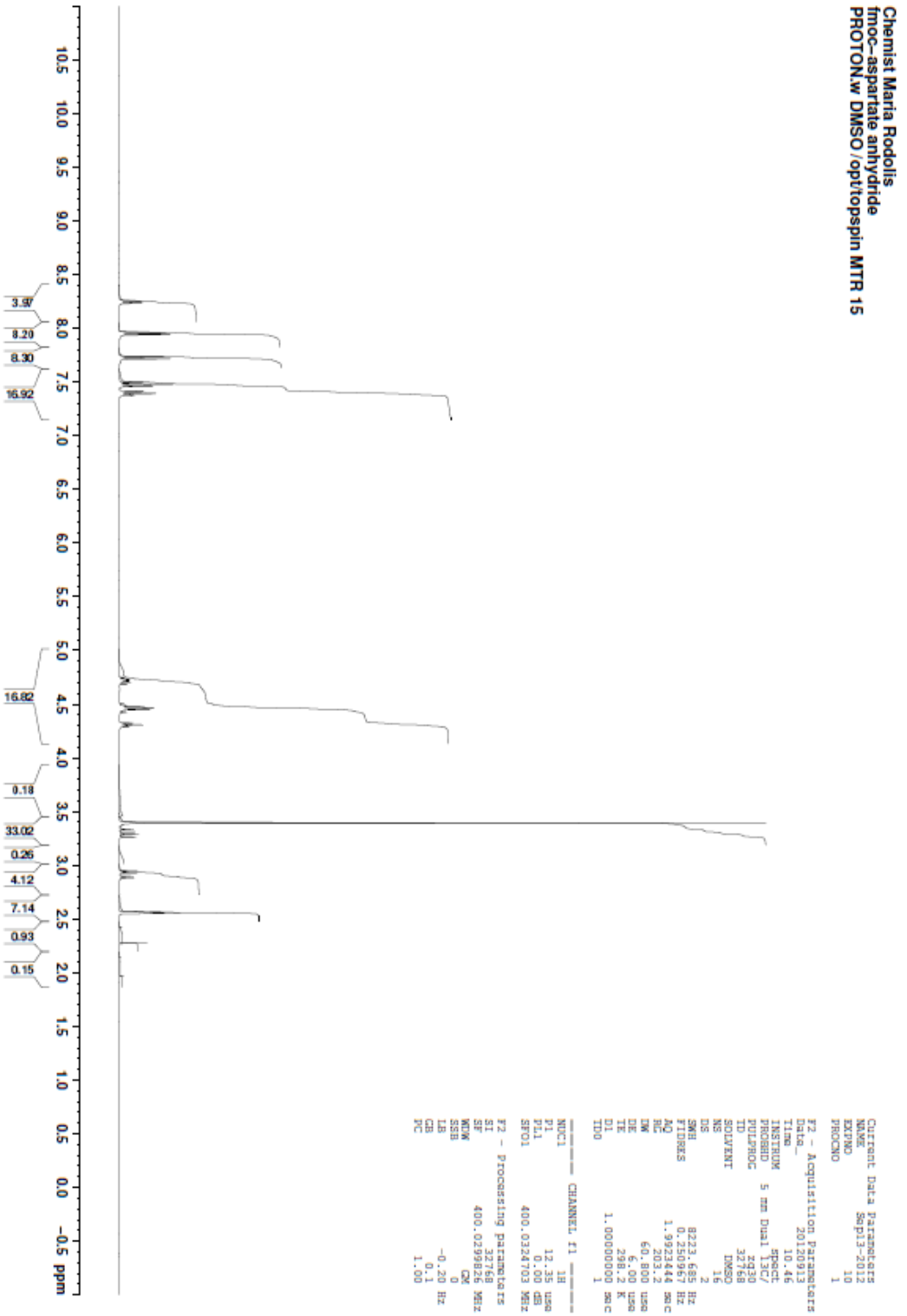

**$^{13}$C-NMR 9*H*-fluoren-9-ylmethyl (2,5-dioxotetrahydrofuran-3-yl)carbamate; *N*-Fmoc-aspartic anhydride [33]**

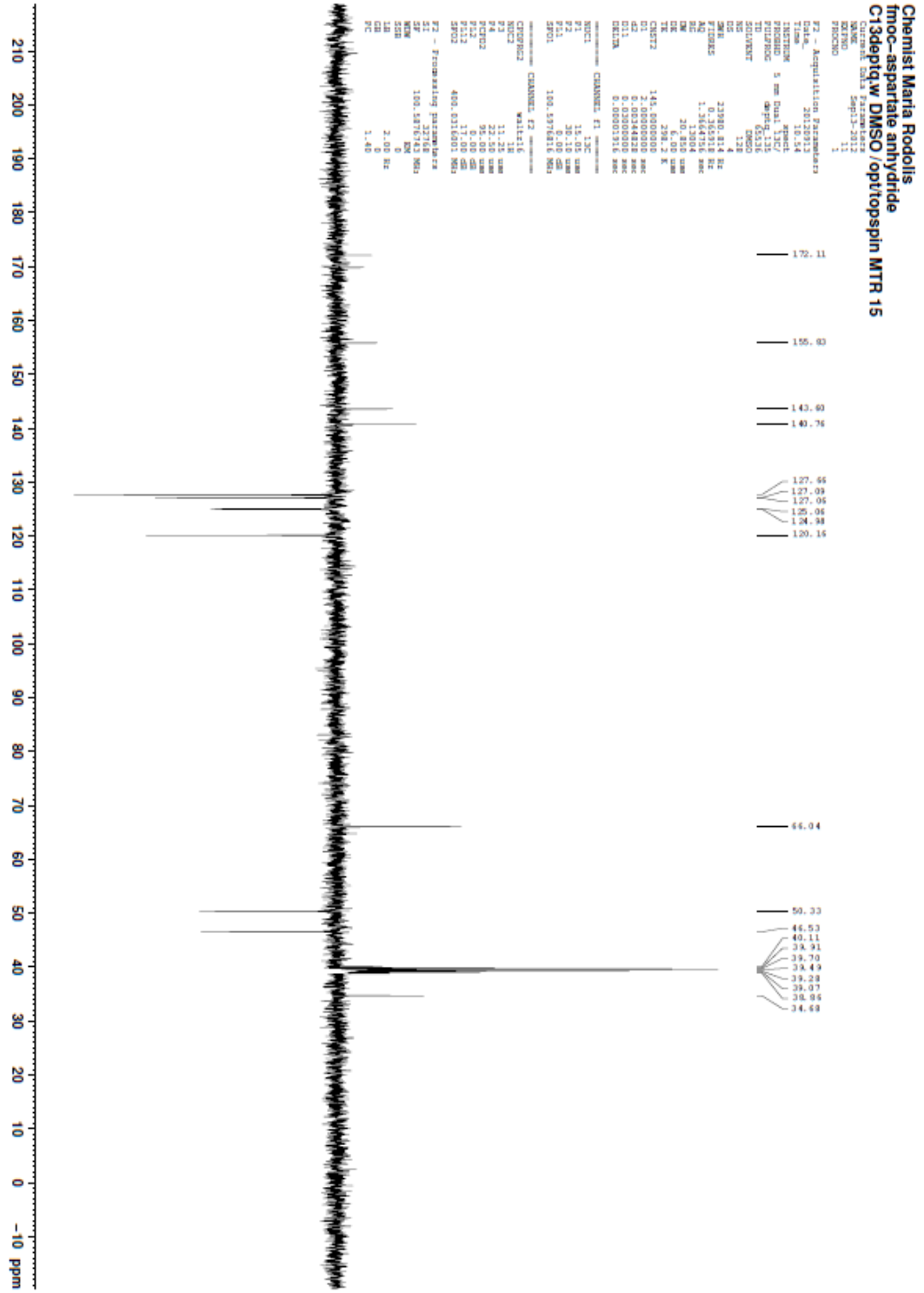

**$^{1}$H-NMR *N*-(9-Fluorenylmethoxycarbonyl)-L-aspartic acid-β-2',3'-O-isopropylidine uridyl ester; FAU-A [34a]**

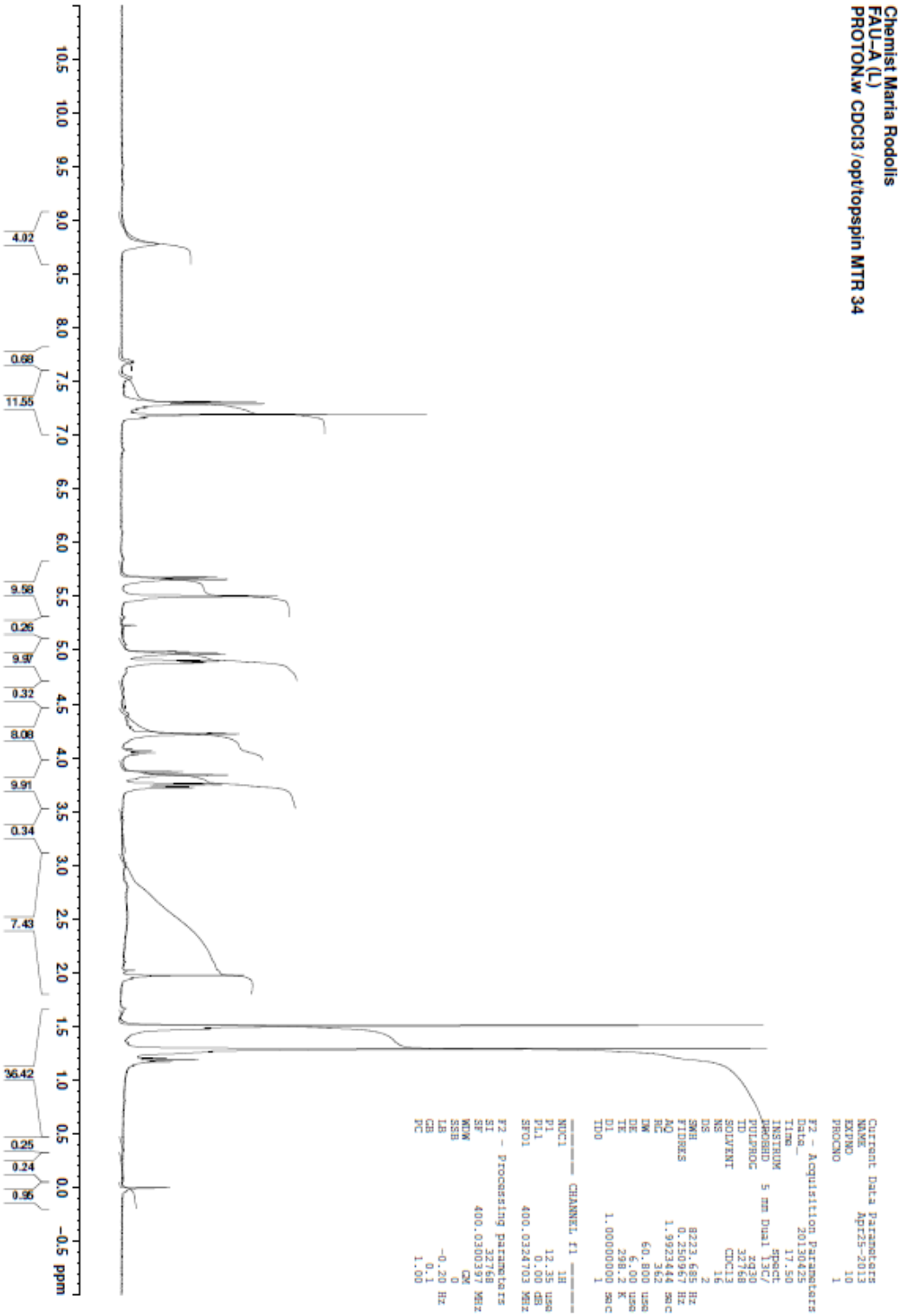

**$^{13}$C-NMR *N*-(9-Fluorenylmethoxycarbonyl)-L-aspartic acid-β-2',3'-O-isopropylidine uridyl ester; FAU-A [34a]**

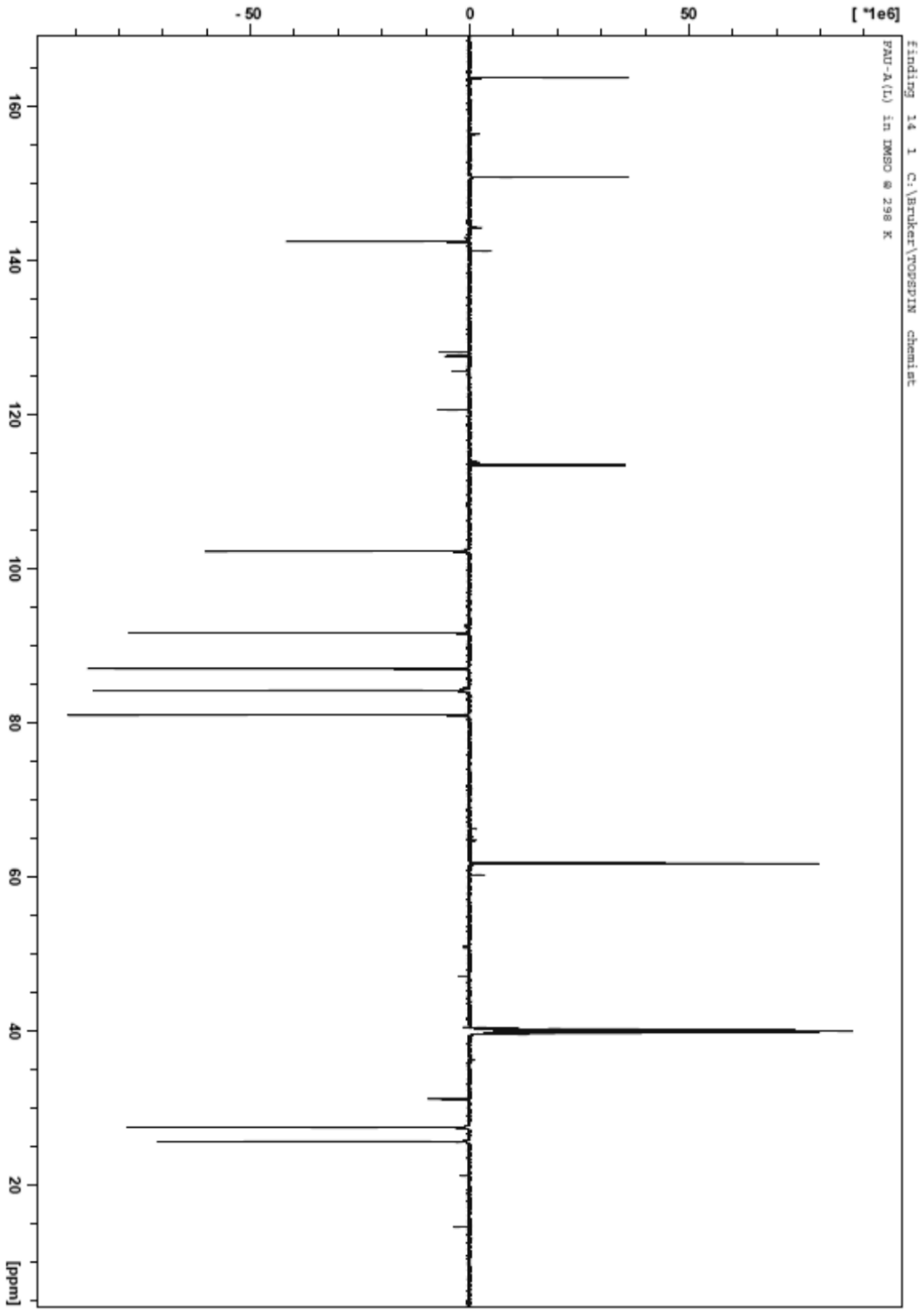

**$^{1}$H-NMR *N*-(9-Fluorenylmethoxycarbonyl)-L-aspartic acid- α -2',3'-O-isopropylidine uridyl ester; FAU-B [34b]**

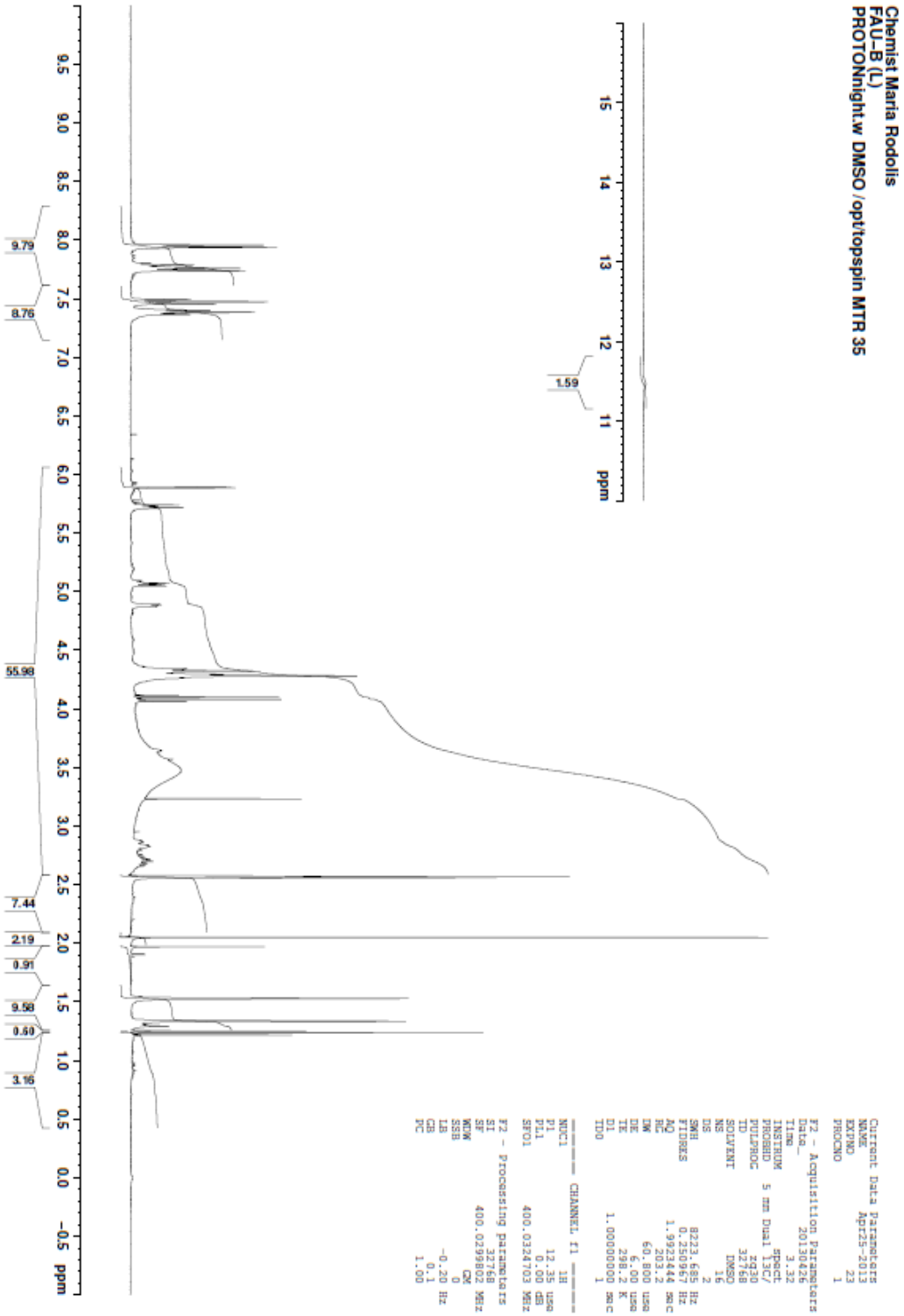

**$^{13}$C-NMR *N*-(9-Fluorenylmethoxycarbonyl)-L-aspartic acid- α -2',3'-O-isopropylidine uridyl ester; FAU-B [34b]**

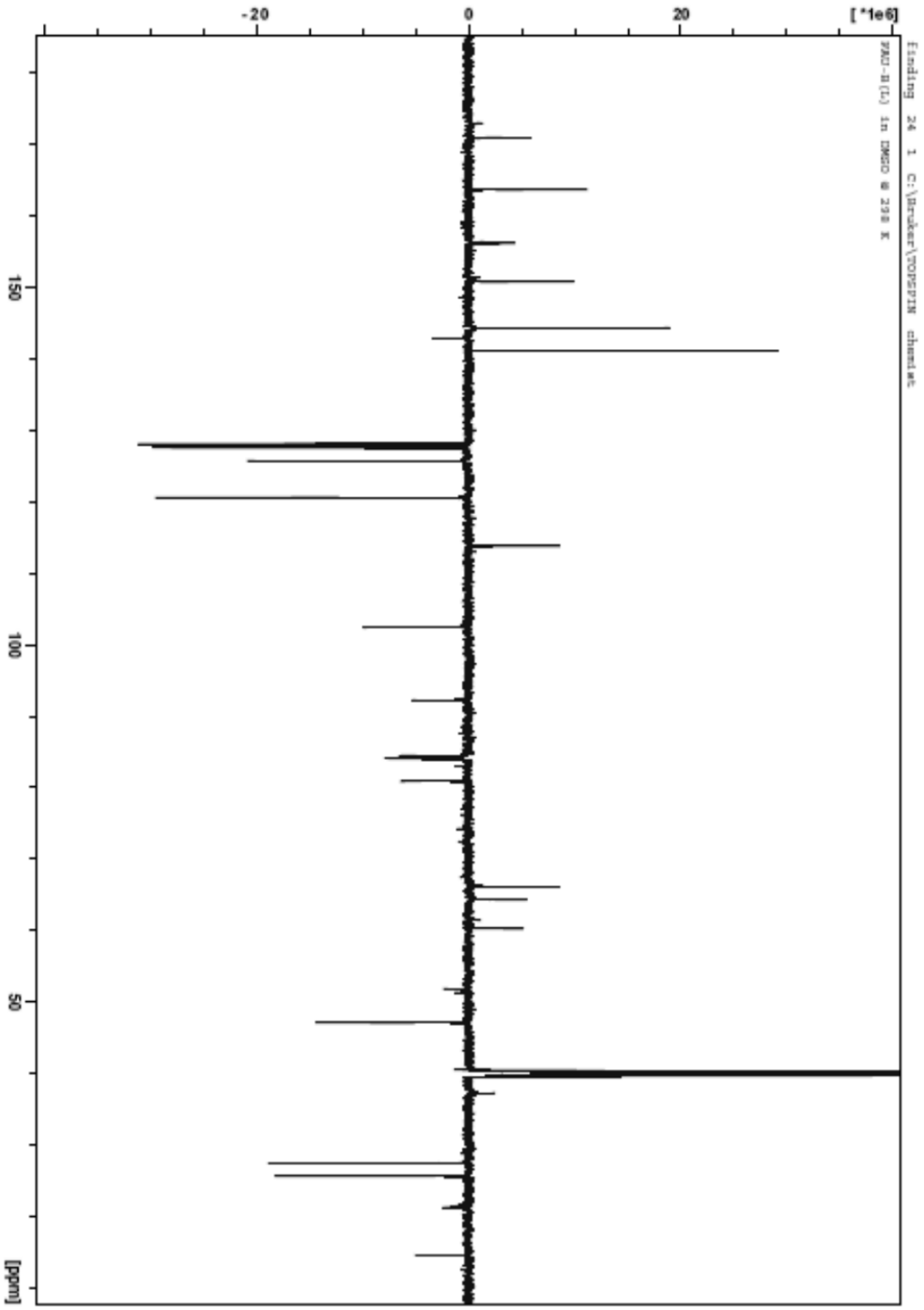

# Appendix 5: UV spectra of purified peptides

**L-Arginyl-L-tryptophyl-glycyl-L-leucinyl-L-tryptophan; RWGLW [10]= 93.4% pure**

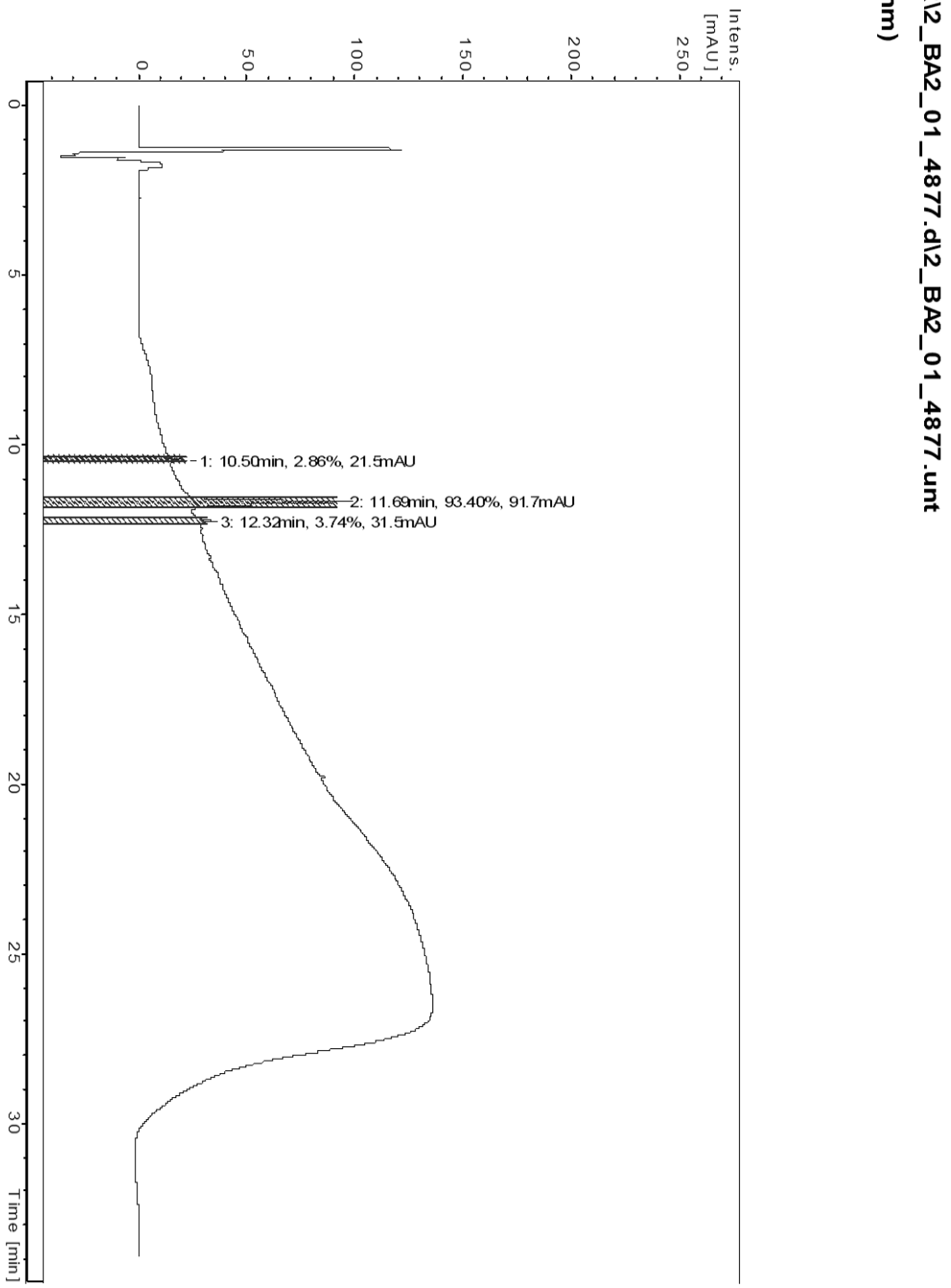

**Glycyl-L-tryptophan octyl ester; $H_2N$-GW-Oct [6] = 98.06% pure**

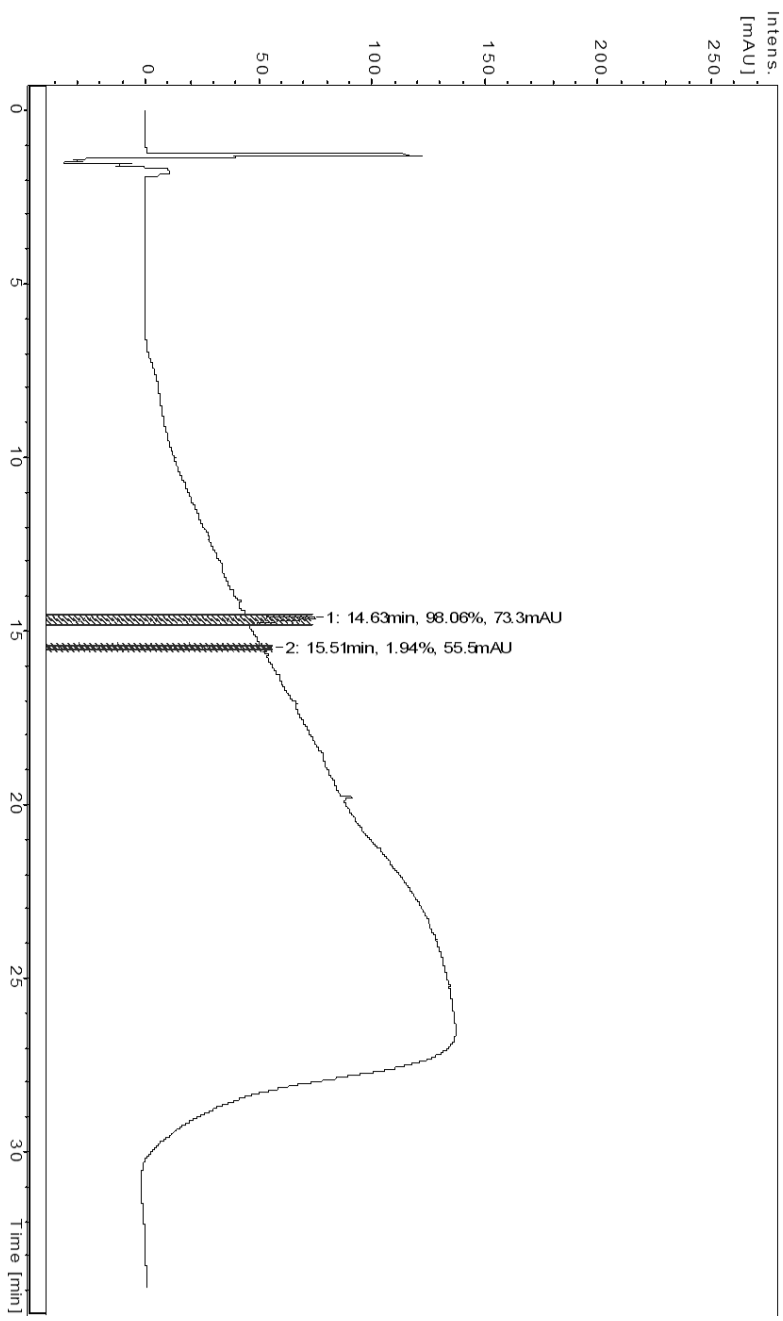

**5'-Succinyl-2',3'-O-isopropylideneuridyl-glycl-glycyl-glycyl-L-arginine [27] = 89.34% pure**

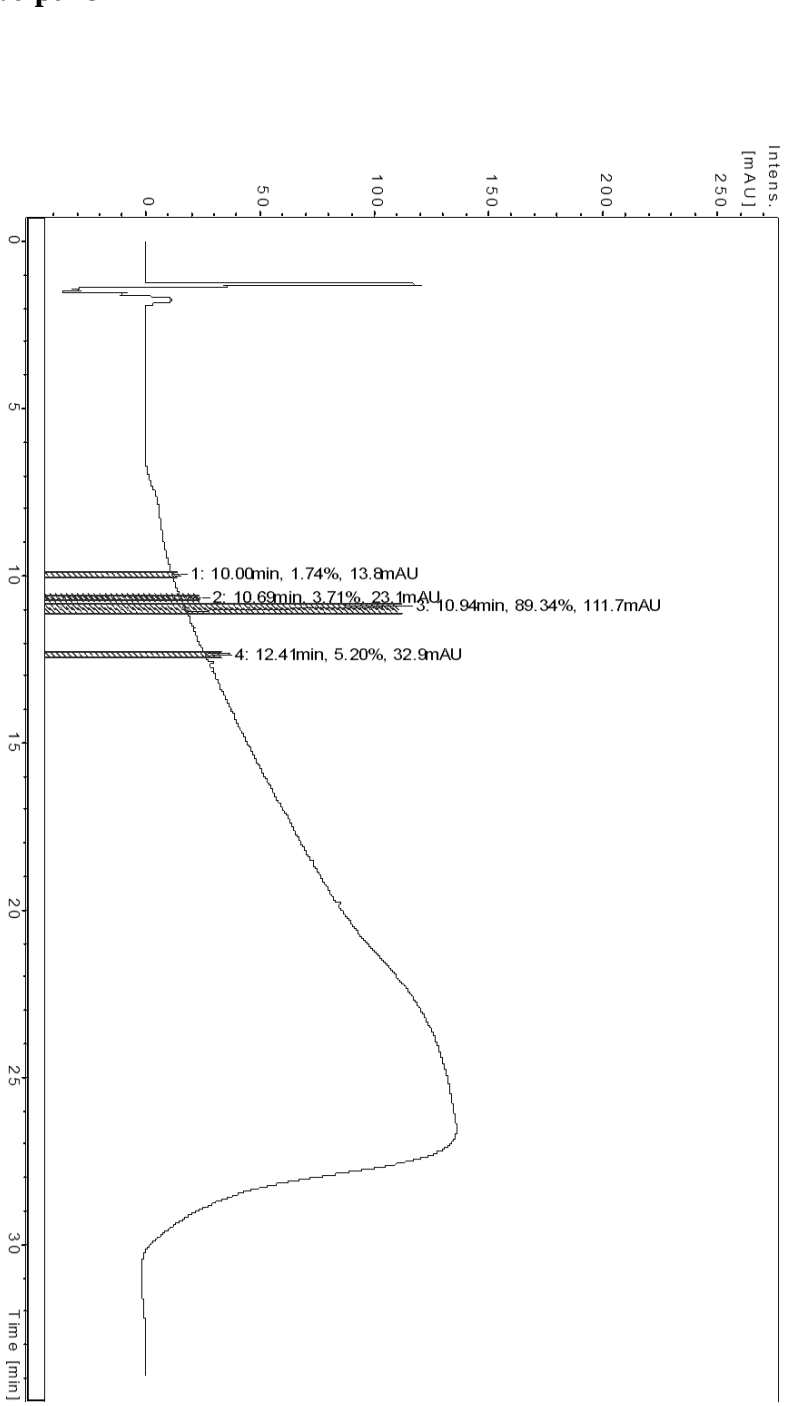

**L-Arginyl-L-tryptophan octyl ester; $H_2N$-RW-Oct [3] = 91.74% pure**